



CALCIUM LOOPING FOR POST-COMBUSTION CO₂ CAPTURE IN THERMAL POWER PLANTS

Sudá de Andrade Neto

Dissertação de Mestrado apresentada ao Programa de Pós-graduação em Planejamento Energético, COPPE, da Universidade Federal do Rio de Janeiro, como parte dos requisitos necessários à obtenção do título de Mestre em Planejamento Energético

Orientador(es): Alexandre Salem Szklo

Pedro Rua Rodriguez Rochedo

Rio de Janeiro

Março de 2020

CALCIUM LOOPING FOR POST-COMBUSTION CO₂ CAPTURE IN THERMAL
POWER PLANTS

Sudá de Andrade Neto

DISSERTAÇÃO SUBMETIDA AO CORPO DOCENTE DO INSTITUTO ALBERTO
LUIZ COIMBRA DE PÓS-GRADUAÇÃO E PESQUISA DE ENGENHARIA DA
UNIVERSIDADE FEDERAL DO RIO DE JANEIRO COMO PARTE DOS
REQUISITOS NECESSÁRIOS PARA A OBTENÇÃO DO GRAU DE MESTRE EM
CIÊNCIAS EM PLANEJAMENTO ENERGÉTICO

Orientadores: Alexandre Salem Szklo

Pedro Rua Rodriguez Rochedo

Aprovada por: Prof. Alexandre Salem Szklo

Prof. Pedro Rua Rodriguez Rochedo

Prof. Bettina Susanne Hoffmann

Prof. Thiago Fernandes de Aquino

RIO DE JANEIRO, RJ - BRASIL

MARÇO DE 2020

Neto, Sudá de Andrade

Calcium Looping for post-combustion CO₂
capture in thermal power plants / Sudá de Andrade
Neto – Rio de Janeiro: UFRJ/COPPE, 2020.

XIV, 183 p.: il.; 29,7 cm.

Orientadores: Alexandre Salem Szklo

Pedro Rua Rodriguez Rochedo

Dissertação (mestrado) – UFRJ/ COPPE/
Programa de Planejamento Energético, 2020.

Referências Bibliográficas: p. 153-183.

1. Captura de Carbono. 2. Looping de Cálcio. 3.
CCS. I. Szklo, Alexandre Salem *et al.* II.
Universidade Federal do Rio de Janeiro, COPPE,
Programa de Planejamento Energético. III. Título.

Agradecimentos

Aos meus orientadores Alexandre Szklo e Pedro Rochedo. Alexandre, além de ser uma das pessoas mais geniais que já tive o prazer de conhecer, foi quem me incentivou a abordar este tema e me orientou com imenso profissionalismo, paciência e dedicação. Não bastasse o brilhantismo como professor, é alguém que possui um grande coração e que tem a rara capacidade de saber dosar firmeza e afabilidade com seus alunos. Pedro, mesmo ainda sendo um jovem engenheiro e professor, possui uma bagagem técnica impressionante e teve um papel fundamental não somente na elaboração deste trabalho, mas também em minha trajetória ao longo do mestrado. Em suma, ambos são para mim fonte de inspiração e admiração, e me traz alegria pensar na escolha acertada que fiz ao pedir para que me orientassem. Sem a ajuda deles, não seria possível a realização deste trabalho.

Ao professor Thiago Fernandes de Aquino e à professora Bettina Susanne Hoffmann por aceitarem fazer parte da banca examinadora e pelas sugestões e contribuições que fizeram a este trabalho.

Aos professores do PPE, André Lucena, Roberto Schaeffer, Mauricio Tolmasquim, Marcos Freitas, David Castelo Branco e Emílio La Rovere, que contribuíram muito para minha formação neste período. Também à equipe administrativa do PPE, em particular à Sandrinha, mas também ao Paulo, Fernando e Queila, que sempre estiveram dispostos a atender às minhas demandas e questionamentos com agilidade e boa vontade.

À minha mãe, por tudo. Seu amor e suporte incondicionais me deram a base e a tranquilidade para que eu pudesse cursar o mestrado. À minha irmã, por dividir comigo a aptidão acadêmica e, com isso, por compreender como ninguém minhas dúvidas, angústias e dificuldades. O convívio familiar harmonioso com as duas tornou tudo mais fácil. Ao meu tio Jorge, por sempre torcer por mim. Ao meu pai (*in memoriam*), por estimular minha curiosidade e amor pelo conhecimento.

Aos meus amigos, em especial ao José Ururahy, Igor Cardoso, Carlos Eduardo Arraes, Vinicius Damous, Anna Metne, Livia Vreuls, Fernanda Romano, Gabriel Saramago, Débora Ladeira, Matheus Poggio, Marcos Magnus, Gilberto De Martin,

George Hambling e Julian Aurelle por sempre acreditarem no meu potencial e me apoiarem em todos os momentos.

À Fundação de Amparo à Pesquisa do Estado do Rio de Janeiro (FAPERJ) pelo apoio financeiro em forma de bolsa de estudo e ao IVIG/COPPE pela oportunidade de trabalho que me proporcionou experiência profissional e suporte financeiro.

Resumo da Dissertação apresentada à COPPE/UFRJ como parte dos requisitos necessários para a obtenção do grau de Mestre em Ciências (M.Sc.)

LOOPING DE CÁLCIO PARA CAPTURA DE CO₂ VIA PÓS-COMBUSTÃO EM PLANTAS TERMOELÉTRICAS

Sudá de Andrade Neto

Março/2020

Orientadores: Alexandre Salem Szklo

Pedro Rua Rodriguez Rochedo

Programa: Planejamento Energético

A captura de carbono é uma alternativa importante para reduzir as emissões de CO₂ no setor energético. O *looping* de cálcio (CaL) é um promissor processo de captura que pode ser aplicado em usinas térmicas a combustível sólido existentes, novas e/ou *capture-ready*. Este trabalho investiga o desempenho técnico-econômico de sistemas CaL integrados a usinas térmicas alimentadas com carvão mineral e bagaço de cana-de-açúcar. Estes sistemas foram simulados e comparados com usinas de referência sem captura e com usinas com absorção química usando solvente à base de aminas, atual referência para a rota de pós-combustão. Parâmetros-chave como potencial de remoção de CO₂, redução de custos devido ao aprendizado tecnológico, uso de água, espaço físico necessário e custo nivelado de energia (LCOE) foram analisados. O software IECM foi usado para conduzir as simulações das plantas. Os resultados demonstram que o CaL tem um custo maior, considerando os níveis atuais de maturidade tecnológica, em comparação com as rotas de absorção química. Porém, apresenta vantagens em eficiência térmica, energia extra gerada, emissões específicas e eficiência no uso de água. Além disso, esses sistemas têm potencial para serem mais econômicos no longo prazo, e investimentos em plantas piloto devem ser estimulados para promover o seu aprendizado e permitir a implementação de plantas de grande porte. Estas devem operar com maior flexibilidade operacional e eficiência térmica do que tecnologias mais maduras de captura de CO₂.

Abstract of Dissertation presented to COPPE/UFRJ as a partial fulfillment of the requirements for the degree of Master of Science (M.Sc.)

CALCIUM LOOPING FOR POST-COMBUSTION CO₂ CAPTURE IN THERMAL POWER PLANTS

Sudá de Andrade Neto

March/2020

Advisors: Alexandre Salem Szklo

Pedro Rua Rodriguez Rochedo

Department: Energy Planning

Carbon capture and storage is an important alternative to reduce emissions of carbon dioxide in the energy sector. Calcium looping (CaL) is a promising carbon capture process to be applied to existing, greenfield, and/or capture-ready solid fuel combustion plants. This work investigates the technical and economic performance of CaL systems added to thermal power plants fuelled with coal and sugarcane bagasse. Power plants integrated with CaL were simulated and compared with their correspondent base plant without CO₂ capture and with chemical absorption using amine-based solvent, the benchmark for post-combustion CO₂ capture, as of today. Key parameters such as CO₂ removal potential, cost reduction due to technology learning, water use, added plant footprint, and levelized cost of energy (LCOE) were analyzed. The software IECM was utilized to conduct the plant simulations. Results demonstrate calcium looping is more costly in comparison to the chemical absorption route considering current technology maturity levels, but the assessed system presents competitive advantages in thermodynamic efficiency, electricity surplus, plant-specific emissions, and water use efficiency. Furthermore, CaL systems could be more economical in the future and investments in pilot-size units should be stimulated in the near term to promote learning and allow the implementation of large-scale plants. These plants will likely operate with greater operational flexibility and thermal efficiency than more mature CO₂ capture technologies.

Table of Contents

1. Introduction	1
1.1 Motivation and structure	1
1.2 Objectives.....	8
2. Technical background	10
2.1 Carbon capture and storage (CCS).....	10
2.1.1 Technology options for CO ₂ capture.....	12
2.1.2 Pre-combustion.....	15
2.1.3 Oxy-combustion.....	16
2.1.4 Post-combustion.....	16
2.1.5 High-temperature solid looping cycles.....	19
2.2 Chemical looping techniques overview	22
2.3 Chemical Looping with oxygen carriers	25
2.4 Calcium looping (CaL) for post-combustion CO ₂ capture.....	29
2.4.1 Review on similar work	35
2.4.2 Integration and operational challenges.....	40
2.4.3 Pilot plant experience with CaL systems	47
2.4.4 Relevant feedstock properties	53
3. Modelling of Calcium Looping cycles for post-combustion CO₂ capture	61
3.1 Performance models.....	61
3.1.1 Solid sorbent activity.....	62
3.1.2 Solids mass balance.....	70
3.1.3 Heat (Energy) balance	76
3.1.4 Gases mass balance	80
3.1.5 Heat recovery from CaL process.....	81
3.2 Carbonator and calciner reactor design for fluidized-bed systems	83
3.2.1 Carbonator design	83
3.2.2 Calciner design.....	87
3.2.3 Reactors dimensions.....	92
4. Methods and Data	96
4.1 Methodological Procedure	96
4.2 Feedstock selection criteria.....	98
4.3 System simulation with software Integrated Environmental Control Model (IECM)	103
4.4 Economic performance and cost model for CaL systems	105
4.4.1 Technology readiness level and contingency costs	109

4.4.2	Cost structure of the post-combustion CaL system	113
4.4.3	Summary of financial assumptions	115
4.5	Case study assumptions.....	118
4.5.1	Configuration 1 – Reference plant (without CCS).....	118
4.5.2	Configuration 2 - Large-scale calcium looping carbon capture unit.....	120
4.5.3	Configuration 3 - Large-scale chemical absorption amine-based carbon capture unit	122
5.	Results Analysis	124
5.1	Supercritical CFPP	124
5.1.1	Technical results.....	124
5.1.2	Economic results	128
5.1.3	Water use analysis	131
5.1.4	Plant footprint analysis.....	134
5.2	Comparative analysis for subcritical BFPP	137
5.3	Comparative analysis for subcritical CFPP	140
5.4	Sensitivity analysis	142
5.4.1	Fuel price.....	142
5.4.2	Size.....	143
5.4.3	Capacity factor	144
5.4.4	Contingency factor	145
6.	Conclusions	147
	References	153

List of Figures

Figure 2.1 CCS represents 7% of emissions reductions in the SDS (IEA, 2019a).	10
Figure 2.2 CCS initiatives worldwide by type of separation process. Elaborated by the author based on data obtained from The US Department of Energy (2019c).	13
Figure 2.3 Post-combustion CO ₂ capture general scheme (US NETL, 2019)	17
Figure 2.4. CL processes possible classifications. Elaborated by the author.	21
Figure 2.5. A general scheme for the CLC process. Adapted from Sai et al. (2018).....	25
Figure 2.6 Simplified block diagram for coal direct chemical looping combustion (CLC) process. Obtained from (MUKHERJEE, KUMAR, et al., 2015).....	27
Figure 2.7. Conceptual scheme for the Calcium Looping process used in post-combustion carbon dioxide capture of a PC plant. Obtained from (MANTRIPRAGADA, RUBIN, 2017a).21	
Figure 2.8. Conceptual scheme for of CaL-based post-combustion CO ₂ capture system for a pulverized coal (PC) powerplant. Obtained from (MANTRIPRAGADA, RUBIN, 2017a).....	34
Figure 2.9. Scheme for the integration of a secondary steam cycle into an existing coal-fired plant. Obtained from (ROMANO et al. 2012).	41
Figure 2.10 (Left) Particle size distribution of the circulating sorbent (experimentally measured and simulated) and the fresh limestone during test campaigns at Technische Universität Darmstadt. Obtained from (Haaf et al., 2017). (Right) Cumulative particle size of raw limestone and calciner bed material in steady-state. Obtained from (Dieter et al., 2012).....	45
Figure 2.11 A) Front view of La Pereda pilot plant B) Scheme of the interconnected fluidized reactors. Obtained from (Arias et al., 2017b).....	49
Figure 3.1. A cycle of carbonation and calcination observed by a TGA. Obtained from OZCAN et al. (2013)	68
Figure 3.2 Equilibrium of the calcination and carbonation reactions based on CO ₂ partial pressure. Obtained from Mantripragada and Rubin (2017a).....	69
Figure 4.1. Configuration screen of the IECM with alternatives for user-defined pollutants control technologies. Obtained from IECM version 11.2	103
Figure 4.2. Development of Post-Combustion Capture Processes and relationship with TRL index. Obtained from (Bhown, 2014).	110
Figure 4.3 Calcium Looping Diagram for Post-combustion carbon dioxide capture. Obtained from IECM version 11.2.	120
Figure 4.4 Configuration 3 proposed for amine-based post-combustion capture. Adapted from (Mantripragada et al., 2019b).....	122
Figure 5.1. Net plant efficiency (HHV basis) on the left-axis and plant specific CO ₂ emissions on the right-axis (kgCO ₂ /MWh).....	125
Figure 5.2 Results diagram for CaL plant added to supercritical coal plant (300 MW gross power). Obtained from IECM.	127
Figure 5.3 Capital cost distribution for a FOAK CaL system capture plant (\$/kW-net)	129
Figure 5.4 Breakdown costs of CaL capture system process facilities capital.....	130
Figure 5.5 Water use analysis of carbon capture systems - wet cooling tower	132
Figure 5.6 Effect of fuel price on plant LCOE.....	143
Figure 5.7 (Left) LCOE for different plant sizes for config. 2 and 3. (Right) Total capital requirement with different plant sizes for config. 2 and 3.	144

List of Tables

Table 2.1. Technology Readiness Level (TRL)^a	14
Table 4.1 Coal properties	100
Table 4.2 Biomass properties	102
Table 4.3. Process contingency costs and TRL^a	111
Table 4.4. Project contingency costs and TRL^a	112
Table 4.5. Selected values for contingency costs for the proposed carbon capture units. Elaborated by the author.	113
Table 4.6. Summary of financial assumptions.	117
Table 4.7 Reference plant (no CCS) configuration parameters	119
Table 4.8 Parameters used in the CaL carbon capture unit simulations	121
Table 4.9 Amine-based carbon capture unit configurations	123
Table 5.1. Technical evaluation summary	124
Table 5.2. Config. 2 operational results	127
Table 5.3. Cost results summary (FOAK plants)	128
Table 5.4. Water use results of power plants for wet cooling tower system*	131
Table 5.5. Water use results of power plants for a once-through cooling system	133
Table 5.6 Performance and cost results for subcritical bagasse-fired power plants with and w/o CCS	137
Table 5.7 Operational results for config. 2A (Bio-CaL)	139
Table 5.8 Performance and cost results for subcritical coal-fired power plants with and w/o CCS	140
Table 5.9 Parameters and values assumed for sensitivity analysis	142
Table 5.10 Cost sensitivity analysis for fuel price	142
Table 5.11 Cost sensitivity analysis for plant size	143
Table 5.12 Cost sensitivity analysis for capacity factor	145
Table 5.13 Cost results for NOAK CCS plants	146

List of abbreviations

AGR	Acid gas removal
ASU	Air separation unit
BECCS	Bioenergy carbon capture and storage
BFPP	Biomass-fired power plant
Bio-CaL	Biomass-fired Calcium Looping
CaL	Calcium looping
CCS	Carbon Capture and Storage
CCU	CO ₂ compression unit
CFB	Circulating fluidised bed
CFPP	Coal-fired power plant
EPRI	Electric Power Research Institute
FGD	Flue gas desulphurisation unit
FOAK	First of a kind
GHG	Global greenhouse gas
IPCC	Intergovernmental Panel on Climate Change
IECM	Integrated Environmental Control Model
LCA	Lifecycle Assessment
LCOE	Levelized Cost of Electricity
MEA	Monoethanolamine
NOAK	N th of a kind
PC	Pulverised Coal

Nomenclature

a_1	sorbent deactivation constant/model fitting parameter	-
a_2	sorbent deactivation constant/model fitting parameter	-
$a_{sorbent}$	limestone purity	%
A_{carb}	cross-section area of the carbonator	m^2
A_{calc}	cross-section area of the calciner	m^2
b	residual carrying capacity	-
$C_{CO_2,eq}$	equilibrium CO_2 molar concentration	mol/m^3
C_{CO_2}	actual CO_2 molar concentration	mol/m^3
C_p	solid heat capacity	J/mol
D	diameter of the reactor	M
f_1	sorbent deactivation constant/model fitting parameter	-
f_2	sorbent deactivation constant/model fitting parameter	-
f_a	fraction of particles in the calciner with a residence time lower than required for complete calcination	-
f_{carb}	carbonated sorbent fraction or mean carbonation extent of the particles	-
f_{calc}	calcined sorbent fraction or mean calcination extent of the particles	-
F_0	molar flow of fresh limestone introduced into the calciner	kmol/s
F_R	molar flow of CaO-based particles from calciner to carbonator	kmol/s
$F_{x,1}$	carbonator inlet molar flow stream of component "x"	kmol/s
$F_{x,2}$	carbonator outlet molar flow stream of component "x"	kmol/s
$F_{x,3}$	calciner outlet molar flow stream of component "x"	kmol/s
$F_{x,fluegas}$	molar flow of "x" component in the flue gas entering the carbonator	kmol/s
$F_{x,inlet}$	molar flow of "x" ASU or fuel component entering the calciner	kmol/s
$F_{x,makeup}$	molar flow of "x" component in fresh limestone entering the calciner	kmol/s
$F_{x,purge}$	molar flow of "x" purge component leaving the calciner	kmol/s
$F_{x,product}$	molar flow of "x" component in gaseous products components from the calciner before recycling	kmol/s
$F_{x,r}$	molar flow of "x" recycled gaseous products from the calciner	kmol/s
$F_{x,calciner,out}$	molar flow of "x" component in gaseous products components leaving the calciner	kmol/s
H_{calc}	heat requirement in the calciner	kJ/s
H_{carb}	heat recovered in the carbonator	kJ/s
$H_{fluegas}$	heat recovered in the carbonator flue gas	kJ/s
$H_{CO_2,cool}$	heat recovered in the calciner output gasses	kJ/s
H_l	height of the lean zone	meters
H_t	total height of the reactor	meters

H_d	height of the dense zone	meters
k_{calc}	kinetic constant for the calcination reaction	$m^3/mol.s$
m_{fuel}	mass flow rate of fuel (as-burnt in wet basis)	kg/s
m_{solids}	solids inventory	Kg
MW_i	molecular weight of the “i” component	G
$N_{Ca,carb}$	total number of moles of Ca-based solids in the carbonator	kmol
$N_{Ca,calc}$	total number of moles of Ca-based solids in the calciner	kmol
$N_{solids,carb}$	total moles of solids in the carbonator or carbonator solids inventory	kmol
$N_{solids,calc}$	total moles of solids in the calciner or calciner solids inventory	kmol
r_0	fraction of uncalcined particles	%
r_{calc}	calcination kinetic rate of $CaCO_3$ particles in solid bed	1/s
$r_{ave,calc}$	average calcination rate	1/s
w_i	weight fraction of the component in fuel	%
t_{calc}^*	time required to achieve complete calcination of $CaCO_3$	S
U_g	superficial gas velocity	m/s
V	volume of the reactor	m^3
X_{ave}	average maximum carbonation conversion at the carbonator	-
X_{carb}	actual carbonation conversion at the carbonator	-
X_{calc}	average molar content of $CaCO_3$ conversions in the calciner	-
X_{active}	fraction of CaO available for CO_2 capture	-
y_{CO_2}	molar fraction of CO_2 at the exit of the calciner	-
$y_{CO_2,eq}$	equilibrium molar fraction of CO_2	-
$y_{CO_2,out}$	carbonator outlet molar fraction of CO_2	-
$y_{CO_2,inlet}$	carbonator inlet molar fraction of CO_2	-
$y_{x,3}$	outlet molar fraction of “x” component at the exit of the calciner	-
x_r	fraction of recycled gases to the calciner	%
α	decay constant for solid fractions	1/s
η_{CO_2}	CO_2 capture efficiency in the carbonator	%
$\eta_{CO_2,eq}$	CO_2 capture equilibrium efficiency in the carbonator	%
ρ_{solids}	solids density	kg/m^3
τ_a	active space-time	S
$\tau_{res,carb}$	solids residence time in the carbonator	S
τ	average particle residence time in the calciner	S
$\epsilon_{s,d}$	solids fraction in the dense zone at the bottom of the reactor	-
$\epsilon_{s,l}$	solids fraction in the lean zone	-
ϵ_s^*	asymptotic value of solids fraction in the lean zone	-
Δp	pressure drop in the reactor	Pa

1. Introduction

1.1 Motivation and structure

Global greenhouse gas (GHG) emissions still have not shown significant signs of reduction to stay on track with internationally defined targets to combat climate change (IEA, 2019e, IPCC, 2018b). In 2017, total anthropogenic or man-made annual greenhouse emissions, including those from land-use change, reached a record of 53.5 Gt of CO₂ (OLHOFF, 2018). If only energy-related emissions are considered, the number rose to a historic high of 33.1 Gt CO₂ in 2018 (IEA, 2019e). As emissions accumulate, concentration of CO₂ in atmosphere has reached 407.4 ppm in 2018, representing a major increase since pre-industrial levels, when the value ranged between 180 and 280 ppm (IEA, 2019e).

While discussions among mitigation and adaptation actions take a major role in international political debate (THE ECONOMIST, 2019), the least-cost scenario indicated by the Intergovernmental Panel on Climate Change (IPCC) reveals that GHG emissions in 2030 must be around 25% or 55% lower than in 2017 to avoid, by the end of the century, respectively, 2° C and 1.5° C global average temperature increase (ETC, 2019, IPCC, 2018b). Coal-combustion alone has contributed to over 30% of the 1° C increase in global average annual surface temperature levels compared to around 200 years ago (IEA, 2019e). This makes coal the single largest historic source of global temperature increase. Actually, its utilisation remains significant to the global energy matrix and coal-fired plants exceeded 10 Gt of CO₂ emitted for the first time in 2018 (IEA, 2019e).

Moreover, more than 200 GW in coal-fired power global installed capacity were in construction or planning phase in 2018 (GLOBAL CCS INSTITUTE, 2018b). Currently, the majority of existing plants are found in Asia where the average age is 12 years old. Those coal plants are decades younger than their average economic lifetime, which is around 40 years (IEA, 2019e, SEKAR, PARSONS, *et al.*, 2007). Not only they have decades ahead of carbon emissions to be released in the atmosphere, but the imposition of strong policy regulatory measures, such as carbon taxes, could make future

and existing plants stranded assets before planned return on investment (ROI) is achieved (CALDECOTT, DERICKS, *et al.*, 2015, KEITH, REINELT, 2009).

An important mitigation approach to reduce CO₂ emission in large scale is carbon dioxide capture and storage (CCS¹) (IEA, 2016), which comprises a portfolio of technologies capable of reducing CO₂ emissions released in combustion processes from stationary sources, usually in electricity generation or industrial facilities (GLOBAL CCS INSTITUTE, 2018b). A basic CCS chain involves three steps: to capture or separate a CO₂ stream emitted during combustion or industrial chemical processes; to transport or sequester the CO₂ stream after compression, usually through pipelines; and to permanently store it in an appropriate geologic formation (VERSTEEG, RUBIN, 2012). Historically, captured carbon dioxide was applied to enhanced oil recovery (EOR) (GLOBAL CCS INSTITUTE, 2018b, VERSTEEG, RUBIN, 2019), however, if significant reductions in emissions are aimed, permanent geological storage of CO₂ with no economic value added to it should be further explored (IEA, 2017a).

Despite inherent economic and political challenges faced by CCS systems, several international institutions and technical experts have acknowledged its potential, recognizing it as a necessary part in the multiple efforts to low CO₂ emissions (IEA, 2017b, 2019e, IPCC, 2018a, U.S. DEPARTMENT OF ENERGY/NETL, 2018). With fossil fuel-fired systems expected to remain in the energy mix for the foreseeable future, the importance of CSS will likely increase in the incoming years (HANAK; MICHALSKI, *et al.*, 2018, VERSTEEG, RUBIN, 2012). In addition, if negative emissions need to be reached (WOOLF, LEHMANN, *et al.*, 2016), CCS combined with net negative emissions technologies, such as bioenergy carbon capture and storage (BECCS), or direct air capture (DAC) will also need to be further developed and deployed (ACKIEWICZ, LITYNSKI, *et al.*, 2018, TAMARYN, HILLS, *et al.*, 2017).

Furthermore, CCS systems are identified as an important pathway if more strict constraints to local pollution from fossil-fuel plants remains a global priority (IEA, 2019f). Besides the energy sector, CCS is one of the few mitigation routes capable of deeply decarbonising major industrial sectors, notably cement, steel, iron, fertiliser, and

¹ Alternatively or more broadly called Carbon Capture Utilisation and Storage (CCUS) (FENNELL, ANTHONY, 2015, IEA, 2019d).

petrochemical industries (IEA, 2019c) – i.e., industrial sectors with relevant process emissions.

Thus, in a context of delayed global actions towards climate change, CCS is one of the few and least costly options that could help the global community to reach aimed environmental targets while maintaining current and future combustion-based plants operating (CUI, ZHAO, *et al.*, 2018, KEITH, REINELT, 2009). Then, finding economically feasible low-carbon alternatives to existing or planned power plants, which includes retrofitting these plants with carbon capture units or planning future plants to receive them, is essential in the short and medium-term.

While CO₂ separation processes are considered well-established in the industry and have been operational for decades in natural gas exploration and fertiliser industries (FENNELL, ANTHONY, 2015), only more recently these technologies have also become operational in large-scale facilities in the power sector (GLOBAL CCS INSTITUTE, 2018a, MANTRIPRAGADA, ZHAI, *et al.*, 2019a). Among the three major approaches for carbon capture in power plants, namely post-combustion capture, pre-combustion capture and oxy-combustion capture, the first is seen as the easier to implement in existing plants, as it could be applied as an end-of-pipe process to current or future capture-ready² plants, without radical changes to the original plant configuration (MERSCHMANN, VASQUEZ, *et al.*, 2013, ROCHEDO, 2011, WANG, LAWAL, *et al.*, 2011b). Throughout the last decades, more individual attention has been given to post-combustion via chemical absorption using amine scrubbing, considered a mature and commercially available process (HANAK, BILYOK, *et al.*, 2015b, KANNICHE, LE MOULLEC, *et al.*, 2017, ROCHEDO, 2011, VERSTEEG, RUBIN, 2019).

This chemical separation process consists of using an amine-based liquid, usually monoethanolamine (MEA), as a solvent to absorb carbon dioxide from flue gas at relatively low temperatures, which is done using amine scrubber columns (MARX-SCHUBACH, SCHMITZ, 2019, WANG, LAWAL, *et al.*, 2011a). Then, carbon dioxide is captured once the solvent is regenerated with low temperature steam in a separate reactor, and the two stages are repeatedly cycled. Sorbent regeneration demands an

² Capture-readiness defines the attribute of thermal power plants whose design already provides for the possibility of installing a future carbon capture unit during the plant useful life. The “degree” of capture-readiness may differ from existing and planned plants (MERSCHMANN, VASQUEZ, *et al.*, 2013, ROCHEDO, 2011).

appropriate amount of thermal energy, which is generally attended using a slip stream from the power plant, significantly reducing its net power output and efficiency (CLARENS, ESPÍ, *et al.*, 2016). Amine scrubbing post-combustion has been recently demonstrated in large-scale coal-fired power plants (MANTRIPRAGADA, ZHAI, *et al.*, 2019b).

Regardless of its technology maturity, conventional post-combustion amine-based CO₂ capture still presents important drawbacks and key challenges to overcome, especially regarding the high energy and efficiency penalties imposed to the base plant, the increase in water consumption and withdraw, and the solvent toxicity and degradation (CLARENS, ESPÍ, *et al.*, 2016, FENNELL, ANTHONY, 2015, KANNICHE, LE MOULLEC, *et al.*, 2017, THITAKAMOL, VEAWAB, *et al.*, 2007). On the other hand, the calcium looping process (CaL), also known as calcium carbonate Looping (CCL)³, appears as a promising alternative to amine-based processes as a post-combustion carbon capture system for retrofitting combustion-plants, both in terms of performance and cost (MANTRIPRAGADA, RUBIN, 2014, MARTÍNEZ, I., GRASA, *et al.*, 2013, ROLFE, HUANG, *et al.*, 2018).

Calcium looping (CaL) post-combustion capture is a second-generation technology based on the reversible carbonation reaction of the solid sorbent lime (CaO) with the CO₂ diluted in the flue gas, which is diverted from the stack of a thermal power plant. The solid looping cycle occurs at high temperatures between two main interconnected fluidized bed reactors, the carbonator, where CO₂ has an exothermic reaction with the solid sorbent and is separated from the flue gas stream; and the calciner, where the spent sorbent is regenerated in an endothermic reaction with the aid of external energy provided. The endothermic reaction releases a highly concentrated CO₂ stream, which requires minor post-treatment before it can be compressed and transported (HANAK, BILYOK, *et al.*, 2015a, ROMANO, MARTÍNEZ, *et al.*, 2013).

Some research has been developed so far in modelling, simulating and experimental testing CaL systems at laboratory and demonstration scales (> 1 MW_{th}) and the solution is considered ready to be scaled-up (FENNELL, ANTHONY, 2015, HILZ, HAAF, *et al.*, 2019, ROMANO, MARTÍNEZ, *et al.*, 2012). CaL technological maturity is not in the same stage as conventional amine-based chemical absorption (ZEP, 2017),

³ In this work, the abbreviation CaL is mostly used.

still, such systems could in theory present several benefits over first-generation capture technologies in terms of plant efficiency penalty, lower toxicity, lower sorbent cost, operational flexibility and integration complexity (FENNELL, ANTHONY, 2015, ROLFE, HUANG, *et al.*, 2018).

One of the main advantages of CaL arises from the high-temperature operation of its capture system, between 600°C and 900°C (ROMANO, MARTÍNEZ, *et al.*, 2012). Unlike conventional pre-combustion, post-combustion and oxy-combustion approaches, the high-temperature operation enables a large amount of high-grade heat to be used for additional power generation in a secondary steam cycle (HANAK, BILİYOK, *et al.*, 2015b). Thus, retrofit of combustion-based plants with CaL systems could re-power plant capacity and the generation fleet, while still reducing emissions (FENNELL, ANTHONY, 2015). Potential increase in net power output is reported in the literature to be around 50–80% higher compared to the base plant without CO₂ capture (HANAK, MANOVIC, 2017).

Although CaL systems seem promising in several aspects such as plant integration and energy and water use efficiency (HANAK, BILİYOK, *et al.*, 2015b, MANTRIPRAGADA, RUBIN, 2017b), more systematic comparative analyses with conventional capture processes are needed, combining detailed techno-economic assessment of the capture unit and key impacts on the original plant (MANTRIPRAGADA, RUBIN, 2014). Plant performance in large-scale systems, potential capture and energy costs, water consumption and withdraw, capture plant footprint, and operational flexibility and complexity are some of the aspects regarding CaL systems that have not yet been fully investigated (FENNELL, ANTHONY, 2015, HANAK, MICHALSKI, *et al.*, 2018, MICHALSKI, HANAK, *et al.*, 2019). This is especially valid in Brazil, where only a few studies over CaL systems have been published so far (ÁVILA, MORTARI, *et al.*, 2013, MOORE, KULAY, 2019, SILVA, Juliana Alves da, CHIMENTÃO, *et al.*, 2019).

Therefore, through a technical-economical approach, this work analyses CaL capture unit integration to combustion-based power plants. Results are then compared to post-combustion amine-based capture, seen as the benchmark technology for post-combustion retrofitting. The comparative analysis is done according to pre-determined criteria defined by a proposed methodology, and coal and sugarcane bagasse are considered as feedstocks. The first, due to its still significant relevance in the current

global generation fleet (BP, 2019). The second, due to the foreseeing demand for net negative emissions technologies⁴ (IPCC, 2019, VAN VUUREN, STEHFEST, *et al.*, 2018). Reference combustion-plants are represented by a set of assumptions of typical supercritical and sub-critical steam power cycles.

The work is divided into six chapters. Chapter 1 continues in the next section summarizing the main work objectives. Chapter 2 briefly discusses the demand and general status of CCS worldwide. Next, CO₂ capture methods are presented, classified in pre-combustion, post-combustion, oxy-combustion, or high-temperature solid looping cycles. Suitability of capture methods to new power plants (in greenfield/new-built market applications) or add-on to existing plants (in retrofit market applications) is also introduced, followed by a discussion over technology maturity of the main capture technologies. The chapter also defines chemical looping technologies and introduces the scientific literature on calcium looping systems, describing the technology, its main challenges, and potential benefits. Then, similar work comparing CaL with amine-based capture is reviewed to help identify knowledge gaps in the subject. CaL integration with an original base plant and current pilot plant experience is explored. Other potential applications of CaL and end-use for the purged sorbent are also investigated. Finally, relevant feedstock properties related to CaL systems are introduced.

Chapter 3 explores available and experimentally validated performance models for mass and energy balance in CaL systems for post-combustion applications. Then, reactors' design is presented. The chapter also discusses optimal operational parameters of a standard CaL plant.

Chapter 4 presents the methodology and data applied in this work. The Integrated Environmental Control Model (IECM)⁵ was used to simulate plants with and without capture. The chapter reviews available economic models before setting performance and economic parameters for reference plants with and without carbon capture. The optimal operational parameters for the CaL capture units are selected based on the available

⁴ Also, the important role in the electricity mix played by bagasse sugarcane fired-thermal power plants in Brazil (ANEEL, 2020, EPE, 2019).

⁵ The Integrated Environmental Control Model (IECM) is a simulation software developed by Carnegie Mellon University for the U.S. Department of Energy's National Energy Technology Laboratory (USDOE/NETL). IECM is a well-documented and publicly available model that provides systematic estimates of performance, emissions, cost and uncertainties for preliminary design of thermal power plants with or without CO₂ capture and storage (ZHAI, RUBIN, 2011).

literature discussed in chapters 2 and 3. A method for cost estimation is developed establishing a relation between contingency costs and technology maturity for large-scale carbon capture plants.

Chapter 5 presents the results of the analysis of CaL systems as an option for post-combustion CO₂ capture. Parameters regarding energy penalty, technology readiness level, plant footprint, cost of CO₂ captured and avoided, water consumption and withdrawal, solid residues production, levelized cost of energy, fuel suitability and operational flexibility, among other indicators are discussed. The results for CaL systems are compared with simulated configurations for an amine-scrubbing capture plant and a reference base plant without capture. Sensitive analyses are performed for key parameters such as plant size, fuel cost, cooling system, capacity factor, and contingency costs. Furthermore, qualitative aspects of the integration of CaL to current plants and scale-up challenges are discussed. Finally, chapter 6 presents main research conclusions and findings, and potential future work is proposed.

1.2 Objectives

This work aimed to conduct a techno-economic assessment of calcium looping systems for post-combustion CO₂ capture in combustion-based power plants. Comparisons were made with the state-of-the-art amine-based CO₂ capture process, considered the benchmark technology, in terms of performance and cost. Important knowledge gaps related to the calcium looping technology were identified in aspects such as potential cost reduction due to technology learning, water use⁶, and physical space requirements (see sections 2.4.1 and 2.4.2). Thus, the technologies were also compared regarding these aspects. Applicability, operability, and flexibility of CaL systems added to new or existing fuel-fired thermal plants were also discussed. Possible differences in the use of coal or biomass-fired (represented by sugarcane bagasse feedstock) power plants in CaL systems were also investigated. Experimentally validated performance models and available economic models were reviewed and used to conduct preliminary simulations over supercritical and subcritical steam cycle power plants integrated with CaL.

Furthermore, costs were estimated for first-of-a-kind (FOAK) and Nth-of-a-kind (NOAK) large-scale power plants with CaL and amine-based CO₂ capture based on current and potential technology maturity. The Integrated Environmental Control Model (IECM) software, developed at Carnegie Mellon University, was used as support for the performance and cost estimations. Published data on plant operational variables and cost models for CaL systems were used to calculate thermodynamic efficiency, energy costs (an approach for levelized cost of electricity – LCOE – was used), and costs for CO₂ capture and avoidance. Results for CaL were then compared with amine-based CO₂ capture. Both capture technologies were modelled in similar conditions and on the basis of the same reference base plant without carbon capture.

The captured CO₂ was considered to be compressed, transported, and stored in an appropriate geological formation. Yet, compression, transportation, and storage aspects were considered beyond the scope of this work, and costs and performance variables were assumed based on the literature. The focus of this work was the calcium looping technology applied for post-combustion power plants. Thus, an extensive review of the

⁶ The term “water use” is utilised in this work to generically refer to water withdraw and consumption.

state-of-the-art technology for calcium looping was conducted prior to its evaluation and comparison with amine-based capture.

At the end of this work, the answers for the following questions should be closer to a clarification:

- Is it calcium looping a feasible alternative to CO₂ capture in combustion-power plants compared to benchmark amine-based technology?
- Is it worth to continue with investments, research and development, and construction of calcium looping plants, until the emerging technology reaches a similar technology maturity to current amine-based technology?
- Regarding water use, space, and integration constraints, is the option for calcium looping suitable for retrofitting existing plants and/or for future capture-ready plants?

2. Technical background

This chapter starts by presenting a technical background of CO₂ capture technologies in section 2.1. Then, section 2.2 introduces chemical looping techniques and the differences between calcium looping, which is a specific type of chemical looping, and other chemical looping processes are discussed. Next, section 2.3 briefly describes chemical looping processes that use oxygen carriers. Lastly, section 2.4 introduces and describes the loop cycle of CaO-based systems and reviews similar work. Also, the section discusses calcium looping systems integration with existing power plants, operational challenges, pilot plant experience, and relevant feedstock properties.

2.1 Carbon capture and storage (CCS)

The Paris Agreement provided a framework for stronger international climate action, which will probably increase the application of carbon capture and storage (CCS) (IEA, 2016). In the global effort to provide modern energy services to a growing world population, the Sustainable Development Scenario (SDS)⁷ predicts CCS technologies will play an important role in the incoming future, accounting for 7% of the cumulative emissions reductions globally required until 2040 (see Figure 2.1) (IEA, 2019a). This implies a rapid scale-up of CCS deployment, from around 30 Mt of CO₂ currently captured each year to 2 300 Mt per year by 2040 (IEA, 2019a).

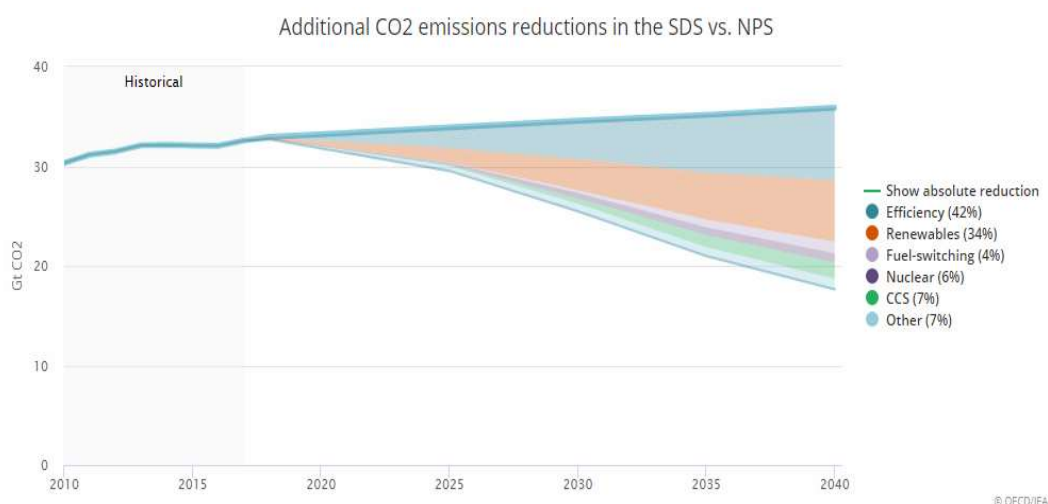


Figure 2.1 CCS represents 7% of emissions reductions in the SDS (IEA, 2019a).

⁷ The Sustainable Development Scenario (SDS) offers a pathway for the global energy system to reach three strategic goals: the Paris Agreement's well below 2°C climate goal, universal energy access and substantial reduction of air pollution (IEA, 2019a).

Even with intense action towards other emissions reduction strategies, such as energy efficiency, reforestation, and wide deployment of renewables (mostly wind and solar), environmental targets might not be reached without the use of CCS technologies (BEN ANTHONY, 2018, IPCC, 2018b). In electric grids, higher penetration of intermittent renewables will eventually require back-up and storage systems to ensure reliability and resilience (GLOBAL CCS INSTITUTE, 2017). Thus, a synergy between renewable energy sources, fossil fuel power and energy storage will be demanded in order of low emission, stable, flexible, and dispatchable generation (HANAK, BILİYOK, MANOVIC, 2016).

Although its meaning encompasses a wide portfolio of technologies, CCS commonly involves three main processes: production of a CO₂ stream of high purity, compression of this stream, and its transportation to a storage site, where CO₂ is usually injected into a stable geological site or utilised for value-added products. Compression, transportation and injection steps present less technical challenges compared to the capture/separation step, which generally represents most of the cost of CO₂ avoided (HOFFMANN, 2010, MANTRIPRAGADA, RUBIN, 2017a, MERSCHMANN, SZKLO, *et al.*, 2016). Transportation is typically assumed to be done via pipeline, but in case of retrofit applications, where construction of pipelines to storage sites might be prohibitively expensive and questionable in terms of public acceptance, transportation via tankers may be considered (VERSTEEG, RUBIN, 2019). While technical barriers of CO₂ transportation and storage appear to be low, its social and political acceptability is not yet clear (INTERCEPT, 2019).

In the capture step, innovation in CCS should target thermal efficiency increase and cost reductions, also expanding the portfolio of available technologies (IEA, 2019f). As CCS becomes internationally seen as a solution to reduce carbon dioxide emissions in stationary sources, its large deployment could also represent a new range of opportunities for an energy sector in transition, as CCS's ability to retrofit plants could help to maintain jobs and economies active while the world changes to a low-carbon future (GLOBAL CCS INSTITUTE, 2018b).

If CCS systems were first applied to natural gas processing facilities, mainly in enhanced oil recovery (EOR) applications (VERSTEEG, RUBIN, 2019), nowadays they are considered for decarbonising not only the power sector but also several other

industries, including cement, iron, steel, fertiliser and paper. In specific industries, such as cement manufacturing, CCS could produce CO₂ capture yields of up to 95% and reduce clinker production process emissions, for which other reduction alternatives are limited (IEA, 2019c). Other low-emission strategies involving CCS include net-negative emissions with bioenergy (BECCS), direct air capture (DAC), and carbon to value projects (C2V) (GLOBAL CCS INSTITUTE, 2018a, HEPBURN, ADLEN, *et al.*, 2019).

New large-scale facilities are starting operation worldwide and the exact number of CCS registered initiatives is dynamic. Thus, databases with frequent updates are the best alternative to track these projects. Some of the open-access global databases with CCS projects are the US NETL database, the Global CCS institute database, the IEA database (only for large-scale facilities), and the MIT-Project (MIT-project was cancelled in 2016 but its database for large-scale CCS projects remains available online) (GLOBAL CCS INSTITUTE, 2020, IEA, 2019a, MIT, 2009, U.S. DEPARTMENT OF ENERGY/NETL, 2019a). In China, a new unit of natural gas processing for use in enhanced oil recovery (EOR) started in 2018, and five new projects are under development in Europe (IEA, 2019e). In other countries where CCS is already stimulated, such as Canada and the US, expansion of carbon tax or credits for CO₂ use and storage are expected to support a new round of investments in the coming years (BENNETT, STANLEY, 2019, GLOBAL CCS INSTITUTE, 2018b).

2.1.1 Technology options for CO₂ capture

The wide range of existing technologies for CO₂ separation and capture from gas streams can be classified according to their gas separation principle. Current main available alternatives are chemical or physical absorption, chemical adsorption, calcium and chemical reversible loops, membranes, and cryogenic separation (VERSTEEG, RUBIN, 2019, ZEP, 2017). These gas separation principles may be applied in different phases of combustion processes (i.e. pre-combustion, post-combustion, and oxy-combustion). Selection of suitable technology and separation phase primarily relies on the type of power or industrial plant and on properties of the gas stream from which CO₂ needs to be separated, especially its volume concentration (vol%), partial pressure, and temperature. While post-combustion capture can be applied as an end-of-pipe technology

and is the most common approach (see Figure 2.2.⁸) (U.S. DEPARTMENT OF ENERGY/NETL, 2019a), CO₂ can also be separated from fuel before combustion, usually through a gasification process combined with a pre-combustion capture system, based on physical absorption. Another common approach is to employ a high purity oxygen stream instead of air for combustion, so an already concentrated CO₂ stream is obtained for later treatment, a process known as oxy-combustion capture (VERSTEEG, RUBIN, 2019).

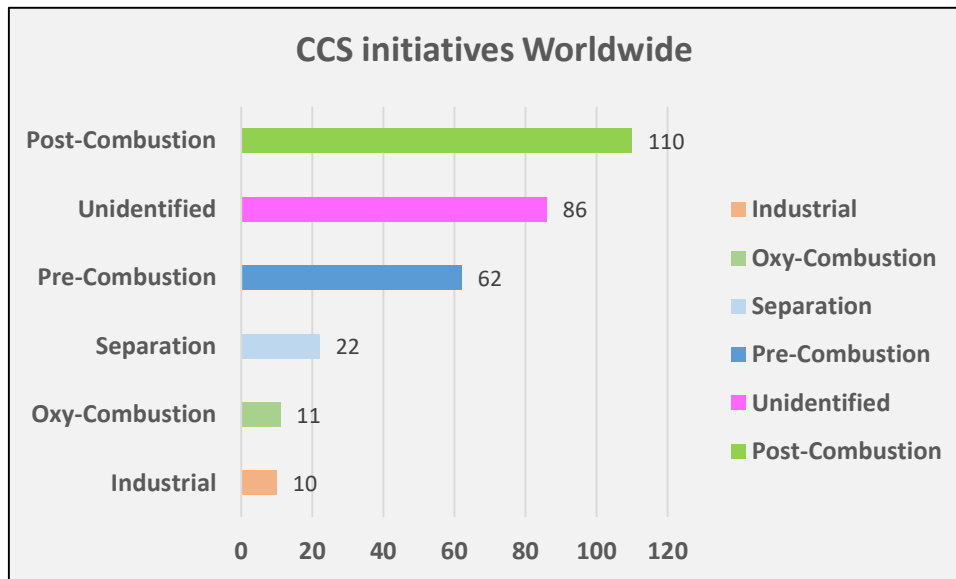


Figure 2.2 CCS initiatives worldwide by type of separation process. Elaborated by the author based on data obtained from The US Department of Energy (2019c).

Although most of the equipment and auxiliary systems required for CCS deployment in power plants are readily available in the energy sector or other industries, power plants with CO₂ capture still struggle to be cost effective at commercial scale, which delays its development. This can be partially explained by the high capital costs of these systems, due to the size of units required to accommodate the flue gas volume, and the efficiency penalty imposed to the base plant, which also affects the levelized cost of energy (LCOE) (HANAK *et al.*, 2015b).

Currently available carbon capture technologies have different maturity stages. They can be broadly labelled as 1st, 2nd, and 3rd generation technologies (IEAGHG,

⁸ Fig 2.2 shows worldwide CCS initiatives among lab, demonstration, pilot and large-scale facilities. Therefore, great part of those initiatives is in preliminary development phases and could not be classified amid the main separation processes, remaining as unidentified. The other databases mentioned do not display CCS facilities by their separation principle consistently.

2014a). Generally, 1st-generation CCS technologies can be considered as technically ready for widespread deployment in the immediate future, although remains scope for improvement in cost, performance, and flexibility (ZEP, 2017). Emerging technologies (2nd and 3rd generation) on the other hand offer significant potential for cost reduction and increased efficiency. Typically, 2nd generation CCS technologies can be considered as late-stage emerging technologies, whilst 3rd generation CCS technologies are usually early-stage emerging technologies (ZEP, 2017).

Another common form of ranking technologies is evaluating its technology readiness level (TRL). TRL is a globally accepted benchmarking tool and has already been used to evaluate CO₂ capture technologies' maturity (IEAGHG, 2014a, ZEP, 2017). The state of development of technologies in TRL is assessed according to a nine-point numeric scale, with nine being the most developed and one the less developed. Table 2.1 displays TRL definitions as applied by The Electric Power Research Institute (EPRI) for use with CO₂ capture processes (FREEMAN, BHOWN, 2011, IEAGHG, 2014a). The following sections further investigate the main capture methods for power generation plants.

Table 2.1. Technology Readiness Level (TRL)^a

Technology Readiness Level (TRL)		
Demonstration	9	Normal commercial service
	8	Commercial demonstration, full-scale deployment in final form
	7	Sub-scale demonstration, fully functional prototype
Development	6	Fully integrated pilot tested in a relevant environment
	5	Sub-system validation in a relevant environment
	4	System validation in a laboratory environment
Research	3	Proof-of-concept tests, component level
	2	Formulation of the application
	1	Basic principles observed, initial concept

^a Based on the Electric Power Research Institute (EPRI) for use with CO₂ capture processes (FREEMAN, BHOWN, 2011, IEAGHG, 2014a).

2.1.2 Pre-combustion

In power generation, pre-combustion CO₂ capture is generally combined with Integrated Gasification Combined Cycle (IGCC) plants. In such a system, a solid fuel such as coal or biomass undertakes a gasification or reforming process at relatively high pressure, which splits the fuel to form, after a series of intermediate processes, a final gas mixture known as syngas, composed mainly by H₂ and CO (FENNELL, ANTHONY, 2015, VERSTEEG, RUBIN, 2019).

The CO₂ also contained in the final mixture is then separated by a physical solvent (currently *Selexol* and *Rectisol* are the main options)(IEAGHG, 2014a, LUIS, 2016), and the H₂-rich stream is used as fuel. The intermediate processes that correspond to CO₂ capture integration in an IGCC plant basically involve two steps: conversion of CO to CO₂ in the water-gas shift reactor; and separation of the CO₂ from the syngas in the acid gas removal unit (AGR).

In recent years, several pilot plants with pre-combustion have been implemented to validate the concept, but crucial developments are still required, especially in the improvement of gasification and oxygen production processes, better integration of water-gas shift reactor, and further development of AGR unit and gas turbine (as gas turbines employed should be suitable for firing H₂ rich syngas) (VERSTEEG, RUBIN, 2019). The performance of pre-combustion CO₂ capture depends on the cumulative performance of all integrated units inside the IGCC plant (from gasification to gas turbine operation) and so it is not limited to the performance of the separation AGR unit alone.

Moreover, pre-combustion capture currently faces barriers in its overall capital expenditure (CAPEX), which is still high mainly due to requirements of a pressurised operation (FENNELL, ANTHONY, 2015). Nevertheless, the conventional pre-combustion CO₂ removal process could be considered as the 1st-generation technology with a TRL close to 9 (IEAGHG, 2014a). Finally, this capture approach is more often seen as an alternative to greenfield plants instead of brownfield/retrofit ones, due to the number of technical changes and replacements needed to adapt and equip an existing plant (ROCHEDO, 2011).

2.1.3 Oxy-combustion

In oxy-combustion or oxyfuel combustion method, solid fuel is burned in a modified burner with almost pure oxygen, previously separated from nitrogen in an air separation unit (ASU). The oxygen used in combustion acts as an oxidant and results in exhaust gases mainly consisting of CO₂ and water, which produces a relatively pure CO₂ stream after condensation, enabling an easier purification of the CO₂ product stream and a lower efficiency penalty compared to amine scrubbing post-combustion (HANAK *et al.*, 2015b; ROLFE *et al.*, 2017).

Part of the exhaust gases is usually recycled in the burner inlet to dilute the oxygen stream, preventing excessive flame temperatures from damaging the burner with local hotspots (FENNELL, ANTHONY, 2015). Several key areas of development exist within the technology and include, besides reducing its high capital costs, further development of the boiler, gas turbine, and burner, as well as achieving a lower efficiency penalty, particularly in the ASU (VERSTEEG, RUBIN, 2019).

The technology is considered of 1st generation but with a lower TRL than pre-combustion benchmarking IGCC with Selexol, reaching a TRL between 6 and 7 points (IEAGHG, 2014a, KANNICHE, LE MOULLEC, *et al.*, 2017). Regarding capture-readiness, the oxy-combustion approach is more often seen as a CO₂ capture process for new combustion-based plants, as the modification of the burner imposes technical and economic challenges to adapt existing plants (ROCHEDO, 2011).

2.1.4 Post-combustion

Post-combustion capture usually offers some advantages, as existing combustion power systems can still be used without drastically changing the original plant, which generally makes it easier for such systems to be implemented as a retrofit option or add-on to current plants (KANNICHE, LE MOULLEC, *et al.*, 2017, WANG, LAWAL, *et al.*, 2011b). The main goal in post-combustion is to concentrate the CO₂ stream after it is generated during combustion, when large amounts of nitrogen originally from the air are found in the flue gas, as shown in the scheme in Fig. 2.3 (U.S. DEPARTMENT OF ENERGY/NETL, 2019b).

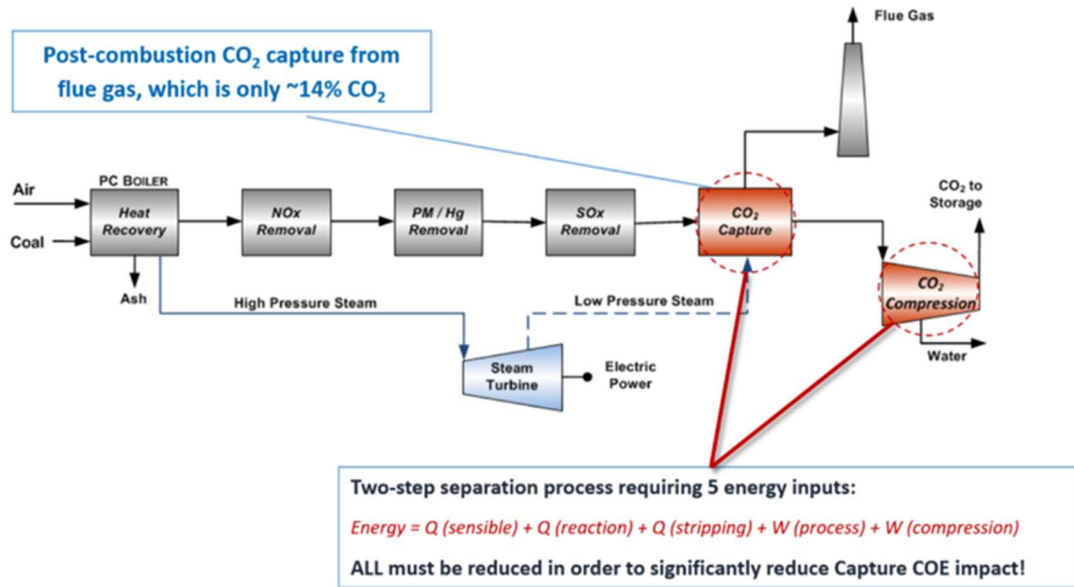


Figure 2.3 Post-combustion CO₂ capture general scheme (US NETL, 2019)

The conventional approach is to use a liquid chemical solvent, usually amine-based, and chemically absorb the CO₂ from flue gas into the liquid carrier in a continuous scrubbing system. The absorption solvent is regenerated by increasing its temperature or reducing its pressure to break the absorbent-CO₂ bond. High capture rates, around 90% of the flue gas, are possible with commercially-available chemical absorption systems, mainly configured with amine and ammonia-based carriers. Chemical absorption post-combustion capture with amines is considered a first-generation technology with operating demonstration/first-of-a-kind (FOAK) commercial systems, with a TRL close to 9 (IEA, 2019c, IEAGHG, 2014a).

In the US NETL CCS database, among 67 active projects worldwide (or on-going facilities) reported for carbon dioxide capture and storage, 21 of them, which represents 32%, use post-combustion with amine-based capture, more than any other capture technology (U.S. DEPARTMENT OF ENERGY/NETL, 2019a). Regarding large-scale active plants (> 50 MW), amine-based post-combustion systems contribute with two of the most representative coal-fired power plants: the Petra Nova plant, in Texas, US, with a 240 MW slip stream from a 610 MW unit; and Boundary Dam, in Saskatchewan, Canada, capturing CO₂ from a 115 MW power plant (MANTRIPRAGADA, ZHAI, *et al.*, 2019a). If potential projects are considered (under planning, in development, or construction phase), post-combustion with amines represents at least 20% of future units (U.S. DEPARTMENT OF ENERGY/NETL, 2019a).

Therefore, also in accordance with the available literature (CLARENS *et al.*, 2016; FENNELL AND ANTHONY, 2015; HANAK *et al.*, 2015b; IEAGHG, 2014b; KANNICHE *et al.*, 2017; VERSTEEG AND RUBIN, 2019), amine-based chemical absorption systems can be seen as the most mature and benchmarking capture technology. Already tested in commercial scale (MANTRIPRAGADA, ZHAI, *et al.*, 2019b), is the conventional option for retrofitting current combustion-based power plants or future capture-ready plants (KRZEMIENÍ, WIĘCKOL-RYK, *et al.*, 2013, ROCHEDO, COSTA, *et al.*, 2016, ROCHEDO, 2011).

The selection for amine-based technologies might be explained due to its effectiveness compared to other alternatives for dilute CO₂ streams, typical of coal combustion flue gas, which ranges from 10-15%_{vol} of CO₂ (U.S. DEPARTMENT OF ENERGY/NETL, 2019b, VERSTEEG, RUBIN, 2019). Additionally, those systems are similar to other end-of-pipe environmental control units already operational in power plants and the process requires low temperatures and pressures. Major efforts are being made worldwide to improve this process due to its potential role in global CO₂ abatement (LUIS, 2016). Recent research has focused on optimizing the process of amine-absorption using either the conventional solvent MEA (Econamine process) or more advanced amine processes such as Econamine FG+ or Cansolv (CLARENS, ESPÍ, *et al.*, 2016, HANAK, ANTHONY, *et al.*, 2015, LUIS, 2016, ROCHEDO, COSTA, *et al.*, 2016).

However, some problems might occur while linking the technology to an operational power plant (HANAK *et al.*, 2015a; KRZEMIENÍ *et al.*, 2013). Firstly, the process is energy-intensive and the energy, usually in the thermal form, is required mainly for solvent regeneration. Overall energy requirements (or parasitic loads) causes a substantial efficiency penalty to the base plant that varies from 7% to 15%, depending on the original plant cycle and the solvent applied (CLARENS, ESPÍ, *et al.*, 2016, HANAK, ANTHONY, *et al.*, 2015, HANAK, BILİYOK, *et al.*, 2015b, KANNICHE, LE MOULLEC, *et al.*, 2017). Then it reduces net power output and increases the levelized costs of energy. The chemical absorption cycle also faces significant solvent losses due to acidic impurities in the gas stream, so a solvent make-up stream is needed and disposal of degraded products may cause environmental and health issues (HANAK *et al.*, 2015b; U.S. DEPARTMENT OF ENERGY/NETL, 2019c; VERSTEEG; RUBIN, 2019).

In addition, power plants with amine-based capture require large water volumes, mainly in steam form. This extra water requirement could cause an increase in the original

plant consumption of up to 120% (MERSCHMANN, VASQUEZ, *et al.*, 2013), which could be a constraint to implement amine-based plants in some regions where access to water resources is limited. Operational flexibility of the base plant once the amine-based system is added is another concern (U.S. DEPARTMENT OF ENERGY/NETL, 2019b, ZEP, 2017), as this feature is increasingly required by thermal power plants (CRIADO, ARIAS, *et al.*, 2017).

When the amine-based process is analysed from a lifecycle perspective, its adoption results in extra environmental effects related to solvent production, use, and regeneration. Solvent production, for example, includes extra CO₂ emissions during the Haber–Bosch process (AZZI, WHITE, 2016, CASTELO BRANCO, MOURA, *et al.*, 2013, HURST, COCKERILL, *et al.*, 2012, LUIS, 2016). Solvent regeneration after absorption is also an indirect source of emissions, as a combustion process is typically needed to provide the extra energy supply. Finally, the environmental impacts associated with the toxicity and waste disposal of the solvent have to be considered (LUIS, 2016). Therefore, the generalized use of amine-based chemical absorption for CO₂ capture should be a point of concern if its global application happens to be the main strategy (LUIS, 2016). According to the US. Department of Energy, research and development of amine-based systems should focus on advanced solvents, resistant to flue gas impurities (U.S. DEPARTMENT OF ENERGY/NETL, 2019b), as well as novel concepts, such as hybrid technologies that incorporate the key attributes required for retrofit applications.

Ultimately, research and development of other CO₂ capture processes for retrofit into existing and future capture-ready plants is still worthwhile, and efforts should be aimed at lowering the energy and efficiency penalties while dealing with operational flexibility and water and space restraints, without incurring in significant additional cost (ZEP, 2017).

2.1.5 High-temperature solid looping cycles

Among emerging 2nd-generation technologies for CO₂ capture, high-temperature solid looping systems are promising alternatives for large emissions sources. Even if these technologies are in an earlier stage of development compared with the systems previously mentioned (IEAGHG, 2014b), they are moving fast towards large scale demonstrations and could represent a solution for the efficiency penalties and high costs of CCS systems

based on amines (DIEGO, M. E., ARIAS, *et al.*, 2017, FAN, ZENG, *et al.*, 2012, FENNELL, ANTHONY, 2015, HILZ, HAAF, *et al.*, 2019).

These systems operate in high-temperature levels, leaving significant fractions of the provided energy available for heat integrations to be applied with the power plant, under several possible configurations (HANAK, MICHALSKI, *et al.*, 2018). Heat integration can lead to better thermodynamic performance and higher overall efficiencies than more mature capture technologies. Specifically, in power plants retrofitted with carbonate calcium looping cycles for post-combustion configurations, a secondary steam cycle can be used to increase power output of the existing plant. This permits reducing energy-related emissions significantly while increasing the generation fleet (FENNELL, ANTHONY, 2015).

Capture technologies such as the CaL system belong to a broader group of emerging technologies generally called Chemical Looping (CL) (FAN, ZENG, *et al.*, 2012, MANTRIPRAGADA, RUBIN, 2017a). This group of technologies uses high-temperature solids sorbents to transfer either oxygen (in case of conventional chemical looping) or CO₂ (in case of calcium looping) between two main interconnected reactors operating through repeated looping cycles (FENNELL, ANTHONY, 2015).

Chemical and calcium looping cycles exploit the degree of reversibility and the high reaction rates of certain gas-solid reactions occurring from 600° C to over 1000° C. The operational temperature depends on the type of reactor, carrier, and process. In the most developed versions, with TRL close to 6 (IEAGHG, 2014a), the main reactors use circulating fluidised beds (CFB), a process that closely resembles thermal and mechanical characteristics of mature CFB reactor systems already available at large scale (> 500 MW_{th}) in power and refining sectors (FENNELL, ANTHONY, 2015, ZEP, 2017).

These systems may be incorporated as an add-on to existing plants in tail-end configurations, which is the conventional approach for calcium looping post-combustion systems for pulverized fuel-fired and natural gas combined cycle (NGCC) plants (BERSTAD, ANANTHARAMAN, *et al.*, 2012, HANAK, Dawid P., MICHALSKI, *et al.*, 2018). Likewise, they can be designed as a newly-built/greenfield plants, which is the case of most chemical looping combustion (CLC) configurations. Additionally, integrated gasification combined cycle with chemical looping (IGCC-CL) is usually thought of as a greenfield plant (FENNELL, ANTHONY, 2015, HANAK, MICHALSKI,

et al., 2018). Figure 2.4 below resume market-related classifications of high-temperature looping cycles. In the following sections of chapter 2, more of CL systems are discussed, with a focus on CaL systems for brownfield or capture-ready plants.

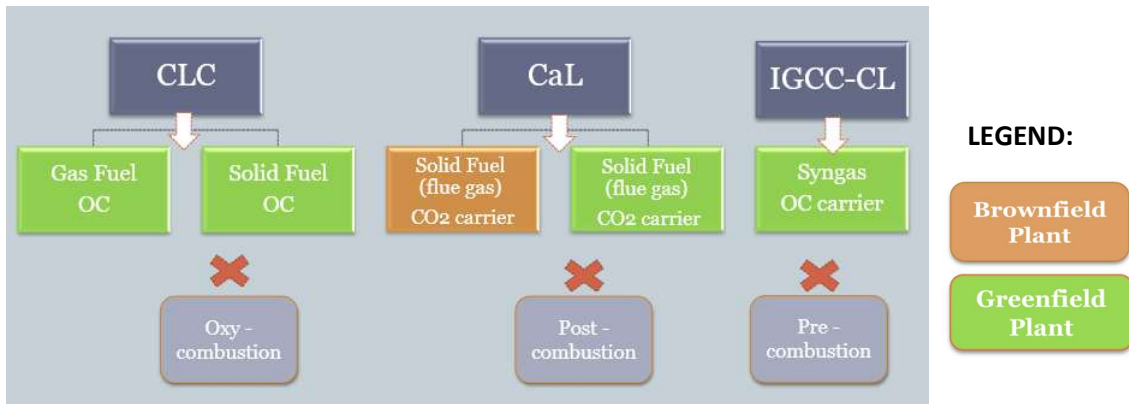


Figure 2.4. CL processes possible classifications. Elaborated by the author.

2.2 Chemical looping techniques overview

Chemical looping techniques are reactions schemes designed for a given reaction in a process system to be decomposed in multiple sub reactions, which are controlled in loops using suitable chemical intermediates. These chemical intermediates react and are regenerated in a self-sustaining medium through the progress of the sub reactions (FAN, ZENG, *et al.*, 2012, MOGHTADERI, 2012). An ideal chemical looping should be capable of minimizing exergy⁹ loss of the overall process, while products generated in the scheme can be separated and handled with greater ease (FAN, 2010, FAN, ZENG, *et al.*, 2012).

Combined with traditional fuels, chemical looping (CL) schemes can be applied in energy conversion systems for power generation with low CO₂ emissions (CAO, PAN, 2006, FAN, LI, *et al.*, 2008, FAN, ZENG, *et al.*, 2012, HU, GALVITA, *et al.*, 2018). Instead of directly converting feedstock, or reactants, into end products - thermal energy, CO₂, and H₂O - a series of cycled chemical reactions are used to generate and separate these same end products (FAN, 2010, MOGHTADERI, 2012). Even if recognized as a potential approach for fuel conversion for over 100 years (FAN, ZENG, *et al.*, 2012), looping materials ineffective reactivity and recyclability have delayed the application of chemical looping processes in a commercial scale. Yet, developments in the last decades have made CL evolve into a promising technique for CO₂ capture (MOGHTADERI, 2012). According to several authors, chemical loops could be more efficient and cost-effective than current commercial capture technologies (FAN, ZENG, *et al.*, 2012, KANNICHE, LE MOULLEC, *et al.*, 2017, MANTRIPRAGADA, RUBIN, 2017a).

For economical operation, some of the key attributes required in CL are: high reactivity at specified temperature and pressure, chemical and physical stability of the looping particles, and favourable equilibrium towards desired products formation (FAN, 2010, MOGHTADERI, 2012). Other requested features include intermediate reactions spontaneity, easy product separation, efficient heat integration, and maximum simplicity

⁹ Exergy can be defined as the maximum amount of usable work extractable from a system during a desired process, leading the system into equilibrium when a reference state is considered. Thermodynamics second law indicates that exergy loss occurs in any given non-ideal process. Although it is not possible to completely eliminate energy degradation, the exergy loss can be minimized using strategic energy management. Then, overall energy conversion efficiency of a given process can be maximized once the largest irreversibility steps are identified (FAN, 2010).

in the chemical looping scheme. Finally, a CL system must employ a low-cost, highly available and efficient chemical carrier to conduct the reactions (FAN, 2010, FAN, ZENG, *et al.*, 2012, FENNELL, ANTHONY, 2015).

These processes can be applied to convert multiple carbonaceous fuels, which can be in solid, gas (CAO, PAN, 2006, ZHAO, ZHOU, *et al.*, 2017), or even in the liquid state (FENNELL, ANTHONY, 2015, RYDÉN, MOLDENHAUER, *et al.*, 2013). In addition to heat and electricity generation, CL systems are capable of processing fuels into diversified products, such as H₂ for fuel cell systems and syngas for posterior chemical synthesis of liquid fuels (FAN, ZENG, *et al.*, 2012, FENNELL, ANTHONY, 2015). CL systems can be classified by the type of looping material, either oxygen or CO₂ carrier (FAN, ZENG, *et al.*, 2012, FENNELL, ANTHONY, 2015). The first type is based on cyclic redox reactions conducted in two or more reactors. At least an air reactor and a fuel reactor are necessary (MUKHERJEE, KUMAR, *et al.*, 2015). Systems with oxygen carriers are generally divided into chemical looping combustion (CLC) process, chemical looping gasification (CLG) process, and chemical looping for hydrogen production process (CLH) (CORMOS, 2014, FAN, ZENG, *et al.*, 2012). The second type of looping system generally employs calcium oxide – CaO - as the CO₂ carrier that conducts cyclic carbonate and calcination reactions occurring in two different reactors, named the carbonator and the calciner. This system is generally called calcium looping (CaL) or Ca-looping process.

Systems using oxygen carriers (OCs) in redox cycles can be integrated into oxy-combustion and pre-combustion CO₂ capture processes, while systems using CO₂ carriers in carbonation cycles can be associated with pre-combustion and post-combustion processes (FAN, ZENG, *et al.*, 2012, PEREJÓN, ROMEO, *et al.*, 2016). As a market strategy, CL processes might be incorporated as an add-on to an existing plant, which is generally the case for CaL post-combustion systems for coal, biomass, and natural gas plants (HANAK, MICHALSKI, *et al.*, 2018). In addition, retrofitting is an option for pre-combustion CL capture in an integrated gasification combined cycle (IGCC-CL) plants (HOFFMANN, 2010). However, IGCC plants are still not fully mature and remain more capital intensive than conventional power generation systems, which can delay or hinder wider deployment of this carbon capture route (FAN, ZENG, *et al.*, 2012), even if the

retrofit itself is maybe simpler than other post-combustion options¹⁰ once the IGCC plants are constructed (FENNELL, ANTHONY, 2015, MANTRIPRAGADA, RUBIN, 2017a, TURNER, IYENGAR, *et al.*, 2019). Lastly, CL systems using OCs are generally conceptualized as greenfield plants, which is the case for most CLC and CLG processes.

¹⁰ This means some capture alternatives may have a greater level of capture-readiness once the base combustion plant is built (lower cost of added CCS and/or layout and operational advantages). Yet, if the combustion plant required for integration with those capture alternatives is significantly more expensive than conventional combustion plants, investors might not take the risk of building these plants in expectation of CCS to be mandatory or economically justifiable.

2.3 Chemical Looping with oxygen carriers

Chemical looping combustion (CLC) technologies for solid and gaseous fuels using oxygen carriers (OCs) combine fuel indirect combustion (nitrogen-free), flexibility, and a concentrated CO₂ stream production with no active gas separation (CAO, PAN, 2006, LYNGFELT, LINDERHOLM, 2017). With the indirect combustion approach, usual energy penalties in CO₂ capture might be avoided, resulting in greater thermodynamic efficiency in the overall energy conversion system (LI, ZENG, *et al.*, 2010, LYNGFELT, LINDERHOLM, 2017). As shown in Figure 2.5, adapted from (SAI, PUNDLIK, *et al.*, 2018), a general CLC process uses a solid metal (Me) or its reduced metal oxide form (Me_xO_{y-1}) as the OC.

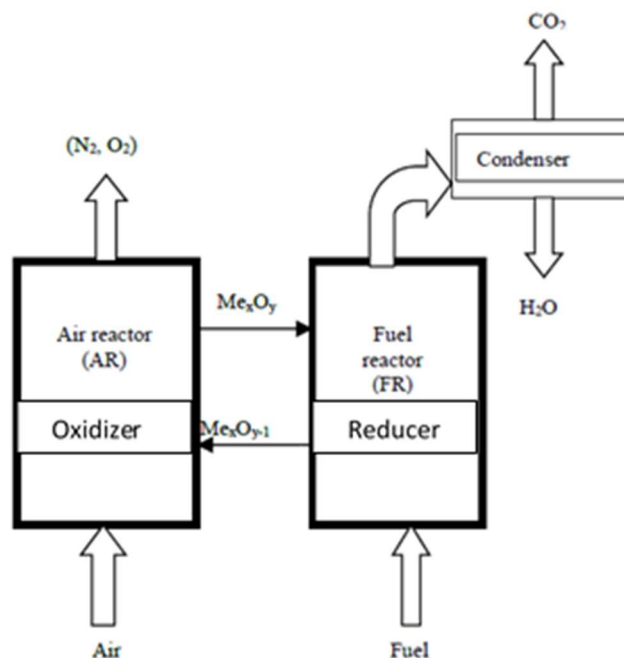
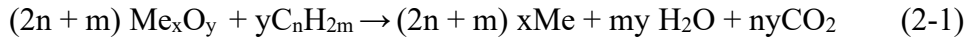


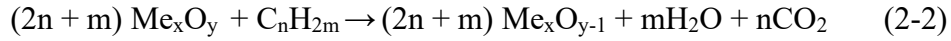
Figure 2.5. A general scheme for the CLC process. Adapted from Sai *et al.* (2018)

The carrier circulates between two interconnected reactors, the reducer (or fuel reactor) and the oxidizer (or air reactor). Within a redox loop, the solid metal (Me) or the reduced metal oxide (Me_xO_{y-1}) reacts with air to form a metal oxide (Me_xO_y) in the oxidizer. In the reducer, the metal oxide (Me_xO_y) previously formed reacts with the carbonaceous feedstock to generate heat and a gas stream of CO₂ and H₂O. The solid metal (Me) is then separated from oxygen and returns to the air reactor to be regenerated and restart the cycle. The gas stream at the exit of the reducer consists of a rich stream of

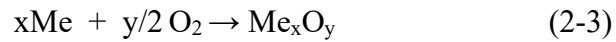
CO₂, which is set ready for compression and sequestration. (CAO; PAN, 2006; SAI *et al.*, 2018). Typical reactions occurring are shown in equations (2-1) to (2-4).



Or



And



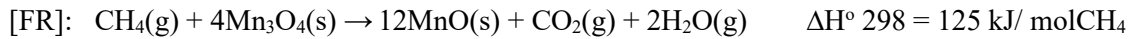
Or



The OC particles are essential to carry both chemical and thermal energy (LI, ZENG, *et al.*, 2010, LYNGFELT, LINDERHOLM, 2017) and might be preheated in a combustor before being sent to the fuel reactor along with the carbonaceous feedstock. Once in the reducer, the OC reacts with the fuel generally in an endothermic reaction while the reaction in the air reactor is highly exothermic in nature (CHENG, QIN, *et al.*, 2018, SAI, PUNDLIK, *et al.*, 2018). Suitable OC is one of the key factors for the successful implementation of CL technology and its performance will govern the feasibility of the process (FAN, 2010). OC requires sufficient and stable oxygen transport capacity over many cycles of oxidation and reduction and enough physical strength to limit particle breakage and attrition. At present, transition metal oxides such as Fe₂O₃, MnO₂, CuO, and NiO are commonly used (RYDÉN, LYNGFELT, *et al.*, 2017, TIAN, NIU, *et al.*, 2018).

In CLC systems, control of pollutants such as NO_x, sulphur oxides and trace metals can be conducted in a more efficient way since the nitrogen-free flue gas generated in the reducer has low volume and CO₂ is not mixed or diluted with nitrogen (CAO, PAN, 2006). Examples of typical reactions occurring in the interconnected reactors are characterized bellow in equations (2-5) to (2-7) (RYDÉN, LYNGFELT, *et al.*, 2017). This example describes a CLC with methane (CH₄) as the feedstock and manganese Mn (II, III) as the OC:

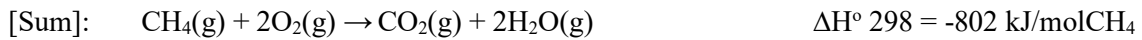
(2-5)



(2-6)



(2-7)



Indeed, actual reactions taking place in CL systems rely on physical properties, reaction thermodynamics, and kinetics of the selected feedstock and OCs (CAO, PAN, 2006). A simplified block diagram of a CLC system using coal as fuel and Fe as the OC is shown in Figure 2.6:

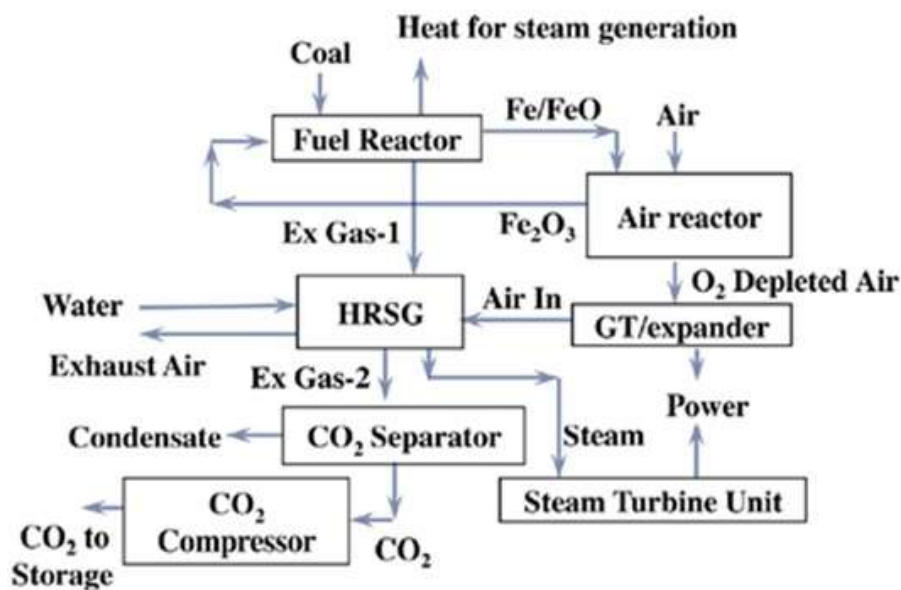


Figure 2.6 Simplified block diagram for coal direct chemical looping combustion (CLC) process. Obtained from (MUKHERJEE, KUMAR, et al., 2015)

Among the units represented in the block diagram above, only fuel and air reactors are not readily available in the industry. However, current research proposes CLC utilises circulating fluidized beds (CFBs), which are already available at a large scale (FENNELL, ANTHONY, 2015). These systems usually aim full fuel energy conversion to increase thermal efficiency and avoid unconverted solid fuels, which might contaminate the reactor. Thus, almost all the carbon content in the feedstock should leave

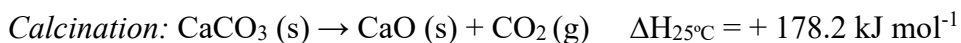
the reducer in the form of CO₂. Following gas clean up and heat recovery, the remaining gaseous product can be directly vented into the atmosphere, with close to zero net CO₂ emission. Primary technical concerns in the reducer are related to low reactivity between fuel and OC, especially with solid fuels due to low solid-to-solid contact efficiency (CAO, PAN, 2006).

In the air reactor or oxidizer is where the OC is regenerated during an exothermic oxidation step that releases heat, further used for power generation (FAN, 2010). The volume of gas flow in the oxidizer is significantly larger than in the reducer because in the first a larger amount of nitrogen is carried in by air (CAO, PAN, 2006). Overall, the net energy release of this system is similar to a conventional combustion system, with reactors temperature in the range of 800-1050°C (RYDÉN, LYNGFELT, *et al.*, 2017).

2.4 Calcium looping (CaL) for post-combustion CO₂ capture

Calcium or Carbonate Looping (CaL) as a post-combustion capture technology was originally proposed about a quart of a century ago by HIRAMA; HOSODA *et al.* (1994) and SHIMIZU, HIRAMA, *et al.* (1999). This chemical looping process is based on the reversible chemical reaction between CO₂ and calcium oxide (CaO). The calcium oxide has the role of solid sorbent or CO₂ carrier, and the cycle occurs by reacting the CO₂ present in the flue gas of an emission stream with solid CaO, forming calcium carbonate (CaCO₃) in a gas-solid reaction. This reaction is known as carbonation and is processed in a reactor called carbonator. After appropriate residence time of particles in the reactor, the partially carbonated CaO leaves the carbonator and is separated from the flue gas with lower CO₂ content by a hot cyclone and loop seals. The loop seals aid the transportation of the solid stream to a regenerator reactor called calciner. At the calciner, the CaCO₃ formed in the carbonator undergoes a calcination reaction that regenerates the CaO sorbent (CLARENS, ESPÍ, *et al.*, 2016). While sorbent is regenerated, calcination produces a relatively concentrated stream of CO₂, suitable for cleaning and compression. Then, after regeneration, the CaO solid rich stream is transferred back to the carbonator to restart the cycle (FENNELL, ANTHONY, 2015, HANAK, MICHALSKI, *et al.*, 2018, MANTRIPRAGADA, RUBIN, 2014, ROLFE, HUANG, *et al.*, 2018). The main intended reversible chemical reaction within the CaL process is represented below in equation 2-8:

(2-8)



The most developed configuration operates under atmospheric pressure and uses two interconnected circulating fluidized beds (CFBs) as the carbonator and the calciner reactors (see Figure 2.7) (DIEGO, ARIAS, *et al.*, 2017, MARTÍNEZ, GRASA, *et al.*, 2013). The carbonator operates at temperatures around 650 °C and its carbonation reaction is exothermic, while the calciner operates with temperatures just above 900 °C and its reaction is endothermic (CLARENS, ESPÍ, *et al.*, 2016, MARTÍNEZ, I., MURILLO, *et al.*, 2011b).

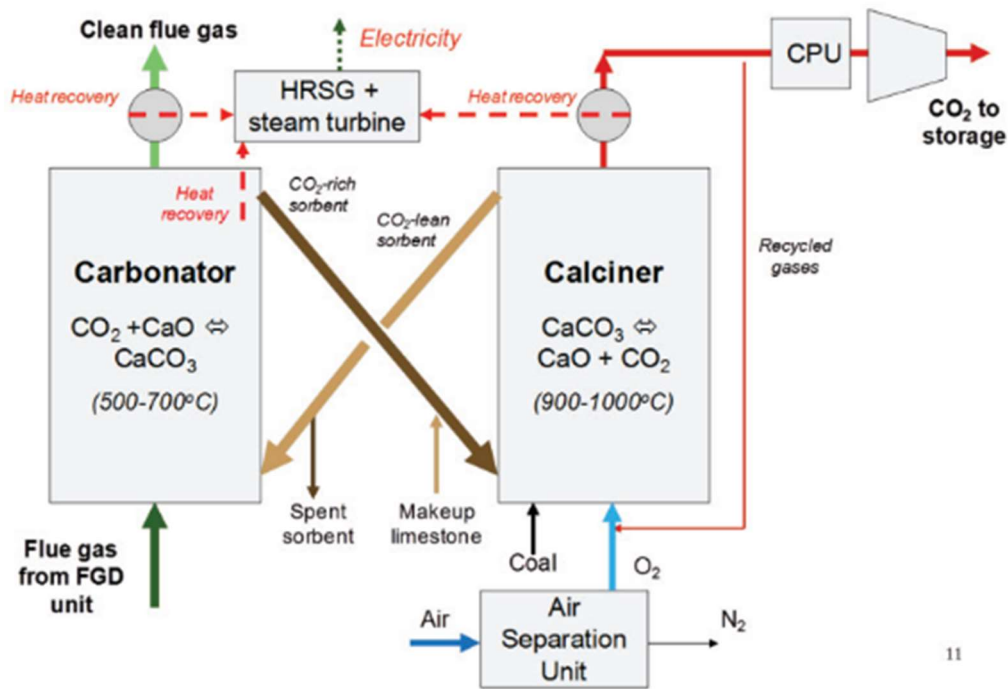


Figure 2.7. Conceptual scheme for the Calcium Looping process used in post-combustion carbon dioxide capture of a PC plant. Obtained from (MANTRIPRAGADA, RUBIN, 2017a).

To maintain the desired operating temperature for the calcination reaction, thermal energy is supplied to the calciner by burning additional fuel, generally coal or biomass at oxy-fuel conditions (DIEGO, ARIAS, *et al.*, 2017, FENNELL, ANTHONY, 2015). The oxy-fuel conditions are necessary to avoid the presence of N₂ in the CO₂-rich environment after the calcination reaction. A fraction of the CO₂ stream leaving the calciner is generally recirculated and reintroduced in the reactor together with the O₂ stream. This is done to ensure a proper volumetric gas flow to fluidize the oxy-combustor and to operate the reactor with the proper fraction of O₂ that avoids hot spots and sorbent sintering (FENNELL, ANTHONY, 2015). The increase in generation capacity of the original plant is done by incorporating a thermal recovery system to the reactors' gas and solid streams with an additional steam cycle, capable of providing supercritical steam at 600 °C and 280 bar (MARTÍNEZ, I., MURILLO, *et al.*, 2011a).

In order to produce the O₂/CO₂ environment needed, an air separation unit (ASU) is required. Although the size of the ASU in a CaL system is about a third of the demanded by a typical oxy-combustion plant to produce the same amount of power (ROMEIO, ABANADES, *et al.*, 2008, SHIMIZU, HIRAMA, *et al.*, 1999), this is the main source of parasitic load in CaL systems (FENNELL, ANTHONY, 2015, HANAK, MICHALSKI,

et al., 2018). The current state-of-the-art ASU technology uses cryogenics distillation units in power plants, and in most cases, requires two to three parallel ASUs with specific power consumption around 200 kWh/tonneO₂ for a 95%vol O₂ (METZ, DAVIDSON, *et al.*, 2005).

Due to the endothermic condition of the calcination reaction and the need to achieve calciner operation high-temperatures for solids arriving from carbonator and recirculated CO₂ stream, there is a great amount of energy required in this reactor, representing 35% to 50% of the total energy introduced in the system, including the existing power plant (DIEGO, MARTÍNEZ, *et al.*, 2015). This energy demand will depend on few process assumptions, such as the type of fuel chosen to be burnt in the reactor (the general assumption is coal) and the flows of fresh sorbent and solid circulation rates considered to achieve a desired CO₂ capture efficiency (ROMANO, MARTÍNEZ, *et al.*, 2012). A reasonable target for capture efficiency with this technology is around 80%-90% (FENNELL, ANTHONY, 2015, ROMANO, MARTÍNEZ, *et al.*, 2012), similar to amine-based capture.

Nevertheless, the energy penalty associated to CaL systems for post-combustion applications is reported to be lower than current amine-based CO₂ capture methods (CORMOS, PETRESCU, 2014, MANTRIPRAGADA, RUBIN, 2017a, MARTÍNEZ, GRASA, *et al.*, 2013). In CaL retrofits to existing plants, efficiency penalties imposed to the base plant are estimated to be mainly between 6 and 8%, and lower values such as 3% are possible (CLARENS, ESPÍ, *et al.*, 2016, MANTRIPRAGADA, RUBIN, 2014, 2017a, ZHANG, SONG, 2019). For greenfield plants, the efficiency penalty is estimated to be even lower since greater heat-integration can be achieved (HANAK, MICHALSKI, *et al.*, 2018, ROMANO, MARTÍNEZ, *et al.*, 2012). This efficient thermodynamic performance is due to the high-grade heat that can be recovered from the exothermic carbonation reaction occurring inside the carbonator and from the high-temperature gas and solid streams leaving both reactors. This high-grade heat is generally used to produce superheated and reheated steam, used to generate additional electricity in a secondary steam cycle, increasing the power plant net output from 50% to almost 90% compared to a base coal-fired power plant (CFPP) without CO₂ capture (HANAK *et al.*, 2015a; HANAK, MANOVIC, 2017; MANTRIPRAGADA, RUBIN, 2014). Since a concentrated and compressed CO₂ stream is aimed prior to transportation, another important parasitic

load is due to the cleaning and compression unit (CCU), required following the exit of the calciner.

Regarding the solid sorbent, natural limestone is the most conventionally used in CaL systems (FENNELL, ANTHONY, 2015), due to the raw material relatively low-cost and global availability (FAN, LI, *et al.*, 2009, JUNK, KREMER, *et al.*, 2014, LASHERAS, STRÖHLE, *et al.*, 2011). Another common option is dolomite, which can be an advantageous alternative to limestone. Further investigation on dolomite is done in the work by VALVERDE *et al.* (2015). However, as this work focus on the standard CaL concept, limestone is considered as the applied solid sorbent. Limestone purity can vary depending on the source, but a conventional value of 92.4% is generally used in models and simulations (MANTRIPRAGADA, RUBIN, 2014).

For sorbents to be viable in such applications they must have high selectivity, adequate absorption kinetics, adequate mechanical strength, and stable absorption level over repeated cycles (BUTLER, 2014). Lime-based sorbents have all of these qualities, except for stable absorption over multiple cycles. This is one of the CaL process key issues, as the sorbent activity decays after a certain number of carbonation-calcination cycles (FENNELL, ANTHONY, 2015). The reduction in sorbent carrying capacity after multiple cycles is a result of sintering, attrition, and sulphation (formation of CaSO_4). Thus, to maintain steady sorbent conversion in the carbonator and compensate for inert accumulation, elutriation of fines, and the gradual loss of sorbent capture capacity due to the increasing number of carbonation/calcination cycles, spent sorbent needs to be partially replaced by the make-up of fresh sorbent (DEAN, BLAMEY, *et al.*, 2011, FENNELL, ANTHONY, 2015, VALVERDE, SANCHEZ-JIMENEZ, *et al.*, 2015).

Sorbent make-up stream is counter-balanced with a reasonable amount of spent sorbent that is purged as waste disposal. Differently from the waste disposal of amine-based components, at least a part of the purged sorbent in the CaL system may be reused for cement production, steelmaking, and other industries (PEREJÓN, ROMEO, *et al.*, 2016). This synergy, mainly with cement manufacture where the purged sorbent can be used as clinker, is considered another possible advantage of this process, increasing profitability and enabling simultaneous decarbonisation of both cement and power sectors (DEAN, BLAMEY, *et al.*, 2011, MARTÍNEZ, I., GRASA, *et al.*, 2013). Another alternative for sorbent end-use is ocean liming, which can reduce lifecycle emissions of

the overall system (HURST, COCKERILL, *et al.*, 2012). Alternative uses of spent sorbent, including ocean liming, steelmaking, and flue gas desulphurization are further explored by FENNELL and ANTHONY (2015).

The use of CaL systems to decarbonize the cement industry instead of power plants is beyond the scope of this work, still, such application is promising as other alternatives for decarbonizing the cement sector are restricted. The subject has recently been investigated by various authors (ARIAS, ALONSO, *et al.*, 2017, GARDARSDOTTIR, DE LENA, *et al.*, 2019, HORNBERGER, SPÖRL, *et al.*, 2017, OZCAN, BOCCIARDO, *et al.*, 2013, SPINELLI, MARTÍNEZ, *et al.*, 2017, VOLDSUND, GARDARSDOTTIR, *et al.*, 2019).

Apart from process heat and electricity, it is also possible to use CaL cycles to produce hydrogen, by enhancing the water-gas shift reaction (DEAN, BLAMEY, *et al.*, 2011, FENNELL, ANTHONY, 2015). By using careful thermodynamic integration, parts of the H₂ production process can yield high efficiencies with integrated CaL CO₂ capture (FENNELL, ANTHONY, 2015). Application of the CaL cycle in pre-combustion to generate hydrogen is discussed by DEAN *et al.* (2011) and HANAK *et al.* (2018b).

It is important to note that relevant developments have been made in the last decade with CaL demonstrations on the MW scale (HANAK, MICHALSKI, *et al.*, 2018). Particularly, the 1.0 MW_{th} unit in Darmstadt, the 1.7 MW_{th} unit in Oviedo (La Pereda power plant), and the 1.9 MW_{th} unit at the Industrial Technology Research Institute (ITRI), in Taiwan, are the most representative facilities. These pilot plants will be further discussed in following sections. The CaL concept has been developing rapidly not only due to the construction of new test facilities, but also because of new correlations for process modelling and sorbent performance. The most studied configuration integrates the CaL system as a retrofit to an existing coal-fired power plant (CFPP)

(HANAK, MICHALSKI, *et al.*, 2018). Figure 2.8 shows the schematic of the CaL-based post-combustion CO₂ capture system integrated with a pulverized coal (PC) powerplant.

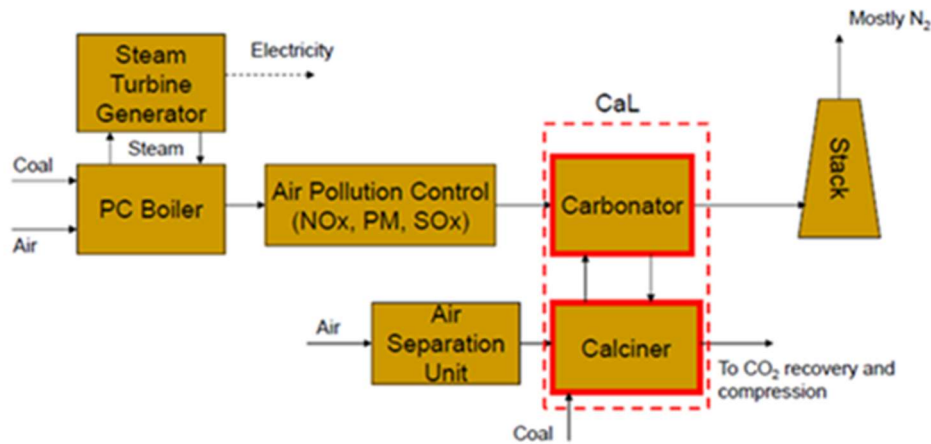


Figure 2.8. Conceptual scheme for of CaL-based post-combustion CO₂ capture system for a pulverized coal (PC) powerplant. Obtained from (MANTRIPRAGADA, RUBIN, 2017a)

Recent developments in the research area focus on reducing the energy penalty, particularly O₂ consumption in the calciner. One of the alternatives to provide heat for sorbent regeneration is by heating the solids leaving the carbonator with indirect heat exchangers fed with the heat recovered from the solids and gas streams exiting the calciner (MARTÍNEZ, I., GRASA, *et al.*, 2013). This is known as the indirect calcination process (OZCAN, D. C., BOCCIARDO, *et al.*, 2013). Indirect heat can be supplied also by a combustor via solid heat carriers, heat transfer walls, or heat pipes (HANAK, MICHALSKI, *et al.*, 2018). Other advanced designs propose eliminating the need of a pure O₂ stream, and by consequence of the ASU, by integrating the CaL with another chemical loop combustion system, in order to use the exothermic reduction of the oxygen carrier CuO with a fuel gas as the heat supply to regenerate the sorbent in the calciner (MARTÍNEZ, I., GRASA, *et al.*, 2013).

Indeed, further improvement in energy and efficiency penalty can be achieved via increasing the degree of heat integration of the entire system, which can be done through the application of a systematic heat exchanger network (HEN) analysis, considered an industrial standard to optimise heat utilization within a system (HANAK, MICHALSKI, *et al.*, 2018). Another possibility is utilising a secondary power cycle of higher thermal efficiency than a supercritical steam cycle. (HANAK., MANOVIC, 2017). A review of

alternative configurations for efficiency improvement of CaL systems can be found in the works by HANAK *et al.* (2018b), (2015a) and FENNELL and ANTHONY (2015).

2.4.1 Review on similar work

Few studies, to the authors' knowledge, have been published so far dealing with technical and economical comparisons between calcium looping and amine-based CO₂ capture technologies for post-combustion configurations. One of the first analyses was performed by HURST *et al.* (2012). Their work examines lifecycle greenhouse gas emissions of a 500 MW_e gross power output supercritical pulverised coal-fired power plant (CFPP), retrofitted with post-combustion calcium looping (CaL) and off-shore geological storage of the CO₂ product stream. Results for the power plant with CaL, which is boosted to 700 MW_e net power output with the addition of the capture unit, were compared with amine-based capture using MEA solvent and a pulverised-coal (PC) plant with no capture. Both plants had the same net power output of the CaL integrated plant and all three configurations followed the same lifecycle assessment (LCA) model. Technical-modelling of the CaL integrated plant, including sorbent degradation and mass and heat balances, is described to calculate material input and output flows. Modelling was based on previous work by LI *et al.* (2008). CaL parameters were set to give the highest net electrical output possible, whilst maintaining solids inventories and circulation rates at sensible levels, similar to commercially operated circulating fluidized bed combustors (CFBC) (HURST, COCKERILL, *et al.*, 2012).

The CaL plant modelled had an overall CO₂ capture rate of 89.4% for a carbonator capture efficiency of 78%, resulting in an efficiency penalty of 6.4% points over a PC plant with no capture (with the same net power output). In the case of a PC plant with a 90% CO₂ capture rate using the MEA method, the efficiency penalty undergoes a de-rating of 8.3%. Additionally, while CaL repowered the base plant by 40%, MEA de-rated the base plant by 29% (HURST, COCKERILL, *et al.*, 2012). The LCA conducted demonstrated that the emission intensity of a CFPP with CaL is worthy of comparison with chemical absorption using amine-based MEA-solvent (values of 229 gCO_{2e}/kWh and 225 gCO_{2e}/kWh were found, respectively). The negative impact of increased coal demand and transportation is outweighed by the effects of increased power and efficiency. Moreover, there is still significant potential for specific emissions reduction in CaL systems if re-carbonation of purged sorbent is considered. Lifecycle emission (LCE)

reductions when spent sorbent is disposed of in landfills, ocean, or used as a feedstock for cement production were estimated. Results for some of these options exhibited potential for zero LCEs in cases where the net plant output is still acceptable, and efficiency is higher than an equivalent PC plant with MEA. The study concluded, from a lifecycle perspective, that CaL systems can significantly outperform MEA-based carbon capture. While the advantages of CaL regarding lower energy penalty, potential to repower the power plant, and mitigated risks for technology scale-up¹¹ are pointed out, no economic comparison was conducted (HURST, COCKERILL, *et al.*, 2012).

In the work by MANTRIPRAGADA and RUBIN (2014), a techno-economic assessment of a CaL system for post-combustion CO₂ capture at a PC power plant is performed. The results for the CaL system were compared in terms of technical performance and cost with a similar power plant with conventional amine-based (MEA solvent) CO₂ capture. Both plants were designed to capture 90% of the CO₂ from the flue gas for further transport and storage. The amine-based plant was modelled using the IECM software, while the performance model for the CaL plant is described based on previous studies¹². Costs were calculated based on results of the performance model and to reflect first-of-a-kind (FOAK) commercial estimates, using values for project and process contingency factors following standard guidelines for cost estimation of emerging technologies (RUBIN, SHORT, *et al.*, 2013). The base PC plant had a gross power output of 650 MW_e and met all the new source performance standards (NSPS) for pollution control. Gross power output of the integrated PC + CaL plant increased to 1,275 MW_e with a net power output of 1060 MW_e. Net plant efficiency was 36% (HHV basis), against 39% of the base plant without CCS, which configures an efficiency penalty of around 3% points. This value is compared to the efficiency penalty of 11% of the MEA-based process imposed on the same base plant (28% HHV). Despite the superior performance and lower efficiency penalty, the CaL-based CO₂ capture process was more capital intensive and led to significant increases in plant capital cost and levelized cost of electricity (LCOE) over the base plant and the PC + MEA-based plant. However, it is suggested that assumptions for a mature technology, with lower process contingency costs, would bring capital costs and LCOE closer to the MEA-based process. Total capital cost and LCOE

¹¹ Due to the utilization of circulating fluidized bed (CFB) boilers, for which significant industrial experience exists at the scales required (HURST, COCKERILL, *et al.*, 2012, ZHENG, YAN, 2013).

¹² However, the model proposed is similar to the one currently available for CaL post-combustion systems in IECM (MANTRIPRAGADA, RUBIN, 2017b).

of the integrated PC + CaL power plant was estimated as 5218 \$/kW-net¹³ and 136 \$/MWh, respectively. These values were significantly superior to those of the plant without capture, which had a total cost and LCOE of 1922 \$/kW-net and 57 \$/MWh, respectively. On the other hand, the MEA-based plant (considered with the same net power output of 1060 MW_e) exhibited values of 2961 \$/kW-net and 92 \$/MWh for total capital cost and LCOE, respectively, with the same economic assumptions applied (MANTRIPRAGADA, RUBIN, 2014).

HANAK *et al.* (2015b) developed a model for a CaL process integrated to a reference 580 MW_e gross output supercritical CFPP. A secondary steam cycle was also modelled for thermal recovery of the high-grade heat originated from the CaL process. The optimal fresh sorbent make-up rate¹⁴ and O₂ content in the fluidising gas inside the calciner are discussed and a parametric study is performed by varying these parameters based on available data from the literature. The authors claim there is a trade-off between the process thermodynamic performance and its economics regarding the optimisation of the sorbent make-up rate. Results for the CaL systems were compared with plants using amine scrubbing retrofits considering 90% total capture rate (for the overall plant¹⁵). The efficiency penalty imposed on the base plant with the CaL retrofit was 6.7–7.9% and compared favourably in relation to the MEA scrubbing retrofit, which had an efficiency penalty of 9.5%. Scenarios for CaL systems using biomass, coal/biomass mixtures, and natural gas to supply heat for the calciner were also evaluated. It was concluded that the limestone make-up rate should be higher for high-ash fuels (such as coal) and lower for low-ash fuels (biomass and natural gas) so the plants can have similar solid looping rates and, therefore, reasonable sizes for the reactors.

When a biomass-fired calciner was used, the integrated system (CFPP + CaL) became a negative emitter of CO₂, as the ratio between the CO₂ captured in the system and the CO₂ generated in the system was 155%. Due to the CO₂-neutral character of the woody biomass applied, the integrated system has potential to operate as a CO₂-negative system, regardless of the CO₂ capture level of 71.1% in the carbonator/absorber.

¹³ Original costs were displayed in 2012 constant dollars and were brought to 2017 constant dollars based on the CEPCI (Chemical Engineering Plant Cost Index), available on Jenkins (2018). This calculation procedure is adopted throughout this work.

¹⁴ The rate between fresh sorbent make-up and solid looping rate on a molar basis.

¹⁵ Total CO₂ capture rate considers the amount of CO₂ captured from the flue gas by the carbonator (79,6% mass basis) and the amount of CO₂ captured from the calcination reaction in the calciner (100% of the oxy-combusted extra fuel in mass basis).

Moreover, the retrofit with CaL was found to be less complex than chemical absorption as it does not require major changes to the layout and the operation of the existing CFPP. Finally, the study concluded the CaL system would result in two times higher net power output compared with chemical solvent scrubbing alternatives for the same base plant (HANAK, BILYOK, *et al.*, 2015b). This is an important advantage of CaL over more mature amine-based CO₂ capture technologies, as power plant operators and energy planners could focus on increasing the system capacity to meet growth in electricity demand and, in parallel, reduce overall CO₂ emissions.

CLARENS *et al.* (2016) also conducted a life cycle assessment (LCA) comparison between CaL and amine-based chemical absorption technologies, both configured as retrofit post-combustion units with a 90% capture rate of the overall system. A subcritical coal-fired power plant was considered as the reference plant without capture, with a 500 MWe gross power output. The amine-based capture plants were modelled with two solvents, namely: Econamine (conventional type of MEA solvent) and Econamine FG+ (advanced amine solvent). Amine-based solvents were selected for comparison with CaL due to their well-established utilisation in industry. However, high energy costs, solvent degradation and subsequent equipment corrosion were some of the difficulties reported for the implementation of these systems in large-scale CCS systems. Then, the CaL process was proposed as a CO₂ capture alternative (CLARENS, ESPÍ, *et al.*, 2016). System boundaries covered the capture processes from the extraction of raw materials to the production and delivery of electricity to the grid. CO₂ capture and compression were considered, while transportation and storage were not included within scope. The IECM software v6.4.2 was used to model and simulate the coal power plant without capture and the amine-based plants. The CaL plant, on the other hand, was modelled based on studies reported in the available literature. The calciner and carbonator operational temperatures were set at 950 °C and 650 °C, respectively. Deactivated CaO (or purged sorbent) was considered as a recyclable product. Results for impact in several environmental categories showed both technologies were responsible for reducing climate change impacts. Finally, the study concluded that the CaL process is an environmentally viable option compared to chemical absorption, though further optimization and analyses are needed, especially when environmental credits from deactivated CaO are not considered. Economic performance of the assessed alternatives was not investigated.

In a more recent paper by MANTRIPRAGADA and RUBIN (2017b), technical and economic aspects were considered in the capture technology comparison. A performance model was developed for the post-combustion CaL cycle applied to a PC power plant. The CaL system was designed to capture 90% of the CO₂ in the flue gas of the base plant, with a total (base plant + CaL) net power output of 550 MW_e. The system was compared to a base plant integrated with an amine-based system (using Econamine FG+ as solvent) with the same net power output of 550 MW_e. For cost calculations, the same contingency (indirect) cost factors were used for both CO₂ capture technologies, assuming a moderately mature process. Thus, study results were considered to represent a future mature plant. It demonstrated CaL systems, even if thermodynamically more efficient, are more capital-intensive, with the overall cost of plants (capital and LCOE) greater than the amine-based technology. The efficiency penalty was around 3% against 11% of the amine-based system, while costs were 4265 \$/kW-net for total plant capital cost and 116 \$/MWh for LCOE. Values for the amine-based system assuming the same economic parameters were respectively 3418 \$/kW-net and 104 \$/MWh. In the same work, a chemical looping¹⁶ system for a pre-combustion configuration was investigated and compared to a conventional pre-combustion capture technology. While in this work CaO-based sorbent was not considered for pre-combustion capture, a modified configuration of the calcium looping process for pre-combustion undertakes a lifecycle comparison against conventional pre-combustion in KURSUN *et al.* (2014).

Finally, a comparison review of CO₂ capture technologies was presented by KANNICHE *et al.* (2017). The review focused on the most mature technologies, which were compared based on the following evaluation criteria: technology maturity; net efficiency loss¹⁷; cost of CO₂ avoided; operability, flexibility and risk levels (qualitative analysis); market application (if the technology is suitable for retrofit and/or newly built plants); technology advantages and gaps; and environmental issues. The study concludes that amine-based post-combustion technology remains the best reference/benchmark for the short and medium-term. Additionally, the study claims that innovative technologies such as chemical looping have the potential to reduce capture costs in comparison to amine-based plants, but may not have their development guaranteed up to industrial-scale

¹⁶ Calcium looping is considered a specific type of chemical looping, which is a more broader term (FAN, ZENG, *et al.*, 2012).

¹⁷ The same as efficiency penalty, i.e. the difference between the power-plant net efficiency with and without CCS.

if are not suitable to retrofit. Nevertheless, the study did not evaluate CaL systems for post-combustion configurations.

2.4.2 Integration and operational challenges

In retrofit applications, energy sources from a CaL system can be integrated into an existing power cycle to produce additional power output (MARTÍNEZ, I., MURILLO, *et al.*, 2011b). Highly integrated systems, to minimize the energy penalty, can include modifications in the operation conditions of the original plant (MARTÍNEZ, I., MURILLO, *et al.*, 2011b). The option to produce extra steam for the existing primary cycle requires a tight thermal integration that can limit operational flexibility (ROMANO, MARTÍNEZ, *et al.*, 2012, ROMEO, ABANADES, *et al.*, 2008), and/or include modifications in turbines and water heaters. Several studies on heat integrations of the CaL system with the existing primary cycles heat are reviewed in HANAK *et al.* (2015a).

Instead of using the power cycle of the original plant, integration of the energy released from the CaL system into a new steam cycle, decoupled from the existing power plant, is the usual option considered (HANAK, MICHALSKI, *et al.*, 2018, MARTÍNEZ, MURILLO, *et al.*, 2011b, ROMANO, MARTÍNEZ, *et al.*, 2012). Without involving major modifications on the original plant performance, the option for a CaL system with a new efficient secondary steam cycle makes the system act as an extra oxy-fired plant (see figure 2.9). In this configuration, the only integration between the existing power plant and the CO₂ capture plant is the flue gas exiting the boiler and diverted from the stack, entering the carbonator with a temperature around 180 °C (LARA, ROMEO, 2017). This integration allows the CaL cycle and integrated secondary steam cycle to operate more independently of the primary steam cycle. Additionally, this integration can avoid delays in terms of start-up and shutdown of the primary cycle, as reported for amine-based technologies (MARX-SCHUBACH, SCHMITZ, 2019).

Among several configurations for CaL, the retrofit option is seen as the most ready-to-use in the short to medium term (ABANADES, ARIAS, *et al.*, 2015, ROMANO, MARTÍNEZ, *et al.*, 2012). Furthermore, the concept of repowering a power plant or a generation fleet while strongly reducing its emissions, as CO₂ capture rates of 90% are

possible, is an important advantage of this process considering the wide deployment of large-scale plants.

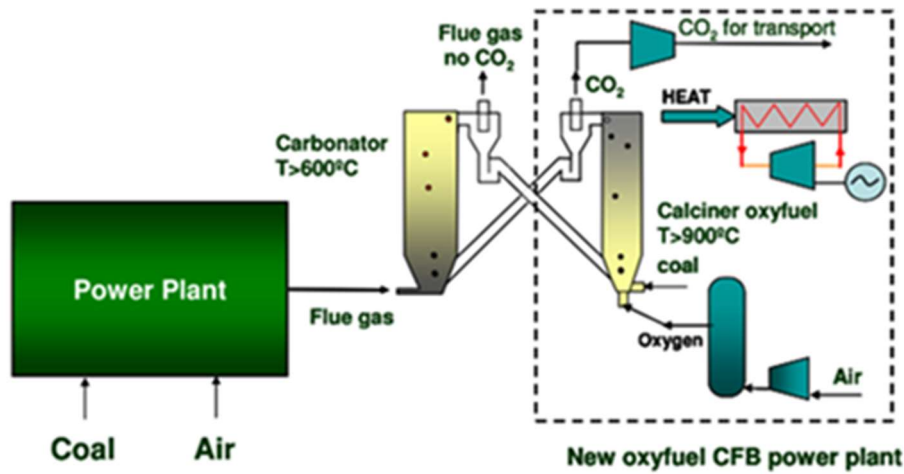


Figure 2.9. Scheme for the integration of a secondary steam cycle into an existing coal-fired plant. Obtained from (ROMANO *et al.* 2012).

Considering a supercritical pulverised coal (PC) as the existing plant, HANAK *et al.* (2015b) investigated the integration of the CaL system as a retrofit. The study claims the retrofit configuration does not require major adjustments to the layout and operation of the existing plant. Compared to chemical scrubbing technologies, the authors considered CaL systems retrofit as a less complex and more flexible capture method, as it does not necessarily follow the operation of the original power plant with a steam requirement like amine-based alternatives, which usually demand steam extraction for solvent regeneration between the intermediate and the low-pressure turbine (IP/LP) (FENNELL, ANTHONY, 2015; HANAK *et al.*, 2015b; MARX-SCHUBACH, SCHMITZ, 2019).

Capture technologies require the ability to adapt to scenarios with large load changes, as in an energy mix with high share/penetration of renewables. In terms of operational flexibility, CaL systems could take advantage of solids circulation at high temperatures between reactors for storing thermal and chemical energy. Concepts for flexible operation of the full CCS with CaL plant in scenarios of variable loads have been studied and proposed (CORMOS, SIMON, 2015, HANAK, BILYOK, MANOVIC, 2016, LARA, ROMEO, 2017). CaL system offers potential to be scaled up with the flexibility currently required, using alternatives such as calcining during low demand periods and carbonating during high power demand periods (ARIAS, CRIADO, *et al.*,

2014), and/or using piles of sorbent CaO/CaCO₃ for energy storage (ASTOLFI, DE LENA, *et al.*, 2019, CRIADO, ARIAS, *et al.*, 2017). The possibility of storing the Ca-based sorbent to buffer the operation at different loads and exploiting its potential as a thermochemical storage medium may lead to advantages with respect to chemical absorption (MARTÍNEZ, GRASA, *et al.*, 2016, PILLAI, SURYWANSHI, *et al.*, 2019). Even though flexible Ca-based post-combustion processes are still in initial stages of R&D, it offers potential for scale-up, as technologies for storing, handling, and circulating large flows of CaO and derived materials can be considered mature (ABANADES, ARIAS, *et al.*, 2015).

Yet, the additional power produced through the secondary cycle designed for the CaL system may be restricted to water and space constraints, which is rarely discussed in the open literature. In most studies, an independent secondary water-steam cycle for heat recovery is considered (ABANADES, ARIAS, *et al.*, 2015, YANG, ZHAI, *et al.*, 2010). The need for a secondary heat recovery steam generator (HRSG) and an associated cooling system greatly increases water consumption and withdrawal. Even though the specific water use (m³/kWh) of chemical scrubbing technologies are possibly higher (GLOBAL CCS INSTITUTE, 2016, MERSCHMANN, VASQUEZ, *et al.*, 2013), which means less efficiency in water use compared to CaL, the last will likely use greater water volumes. Obviously, water constraints will depend on the water availability in the region of the existing plant and the choice for the type of cooling system among the standard options such as once-through, recirculating or wet cooling tower and dry cooling (GLOBAL CCS INSTITUTE, 2016, HOFFMANN, SZKLO, *et al.*, 2014). This subject will be further investigated in chapter 5 with the water use results from the proposed plant simulations.

Regarding space constraints, even if there is available land adjacent to the plant site, there may not be enough space around the existing units to which the capture plant must be connected. Costly rearrangements due to very long solids and flue gas conveyors affect more CaL systems than amine scrubbing, as this last must be cooled before entering the scrubbing system (BUI, DOWELL, 2019, HILLS, SCEATS, *et al.*, 2020). If minimum plant footprint estimates for CaL systems have not yet been published, the calculations for oxy-combustion, which require similar equipment (e.g. an ASU and an oxy-fired CFB boiler), could help to estimate CaL systems land requirement compared to other post-combustion alternatives. Amine-based systems can have more than three times the land

requirement of oxy-fuel plants for power plants over 700 MW_e net output (FLORIN, FENNELL, 2011). The work by FLORIN; FENNELL (2011) reviewed the available literature on space requirements of carbon capture plants. In the work by HILZ *et al.* (2019), where the space of a 20 MW_{th} demonstration CaL plant is calculated, the area occupied by the interconnected reactors is about half of the area of oxygen supply, coal delivery, and CO₂ purification unit. This subject is further investigated in chapter 5 where a plant footprint analysis of the CaL plant is conducted based on reactors cross-section area and literature values from (FLORIN, FENNELL, 2011).

ROMEO *et al.* (2008) emphasises the lack of exotic material requirements in CaL systems, and the strong knowledge background for analogous key processes and units involved, such as CFB boilers, advanced steam cycles, and ASU. These components have their own development path, which can facilitate CaL plants to gain maturity compared to other emerging capture technologies. Still, other technical aspects about the operation of the interconnected circulating fluidized bed (CFB) with the solid looping circulation of Ca-based particles must be addressed. A CFB is a fluidized bed system that includes a riser and a down-comer with the solid particles circulating between them (GRACE, CHAOUKI, *et al.*, 2016). As will be further seen in chapter 3, in CaL systems the riser is operated in a fast fluidization regime, with solids carried over from the top and returned to the bottom of the riser through a standpipe, via feeding or control device. Important operating variables include both gas and solids circulation flow rate.

CFB systems have been widely used in the petrochemical industry with fluid catalytic cracking (FCC) units and in the power industry with coal combustion. Depending on the process application, the operating conditions can be significantly different. In coal combustion, superficial gas velocity and solids flow rates are typically 5–8 m/s and less than 40 kg/m²·s, respectively (GRACE, CHAOUKI, *et al.*, 2016). On the other hand, FCC uses gas velocities of 15-20 m/s and solids flow rates above 300 kg/m²·s (GRACE, CHAOUKI, *et al.*, 2016). Common disadvantages and challenges of operating CFBs are: *backmixing* of solid particles; losses of particles due to entrainment, very tall vessels required, nonuniform gas distribution and by-pass, and particle attrition.

As fluidized bed reactors should provide a good mixture and large surface area, particle attrition is seen as an important parameter that affects the performance of the reactor due to the elutriation of particles and change in particle size distribution (HAAF, M., STROH, *et al.*, 2017). The attrition phenomena can be defined as the degradation of

bed material that leads to change in size and number of particles in the system as a result of mechanical, thermal, and chemical stresses that emerge in and between the particles during operation (HAAF, M., STROH, *et al.*, 2017, SCALA, CHIRONE, *et al.*, 2013). Sorbent attrition is influenced by factors like particle porosity, particle size of fresh sorbent, material hardness, particle velocity, and exposure time. The attrition rate peaks when fresh sorbent is introduced and decays to a stationary attrition rate level when steady-state is achieved (HAAF, M., STROH, *et al.*, 2017). Sorbent attrition of limestone in fluidized bed reactors has been researched in numerous works and is further discussed by SCALA *et al* (2013), MONTAGNARO *et al.* (2010), ALONSO *et al.* (2018), COPPOLA *et al.* (2012), and DIETER *et al.* (2014). Natural limestone generally exhibits high porosity and relatively low hardness compared to other materials generally used in fluidized bed systems (DIETER, BIDWE, *et al.*, 2014). Thus, experimental campaigns are essential to address this potential bottleneck.

In the experiments conducted in La Pereda 1.7 MW_{th} pilot plant, attrition problems and malfunctioning of cyclones during certain experiments were reported in continuous operation (DIEGO, ARIAS, *et al.*, 2017). Sorbent attrition was also addressed in the work by HAAF *et al.* (2017), where a model for a steady-state of the CaL process, developed using ASPEN PLUSTM, incorporates particle attrition in an empirical approach, as well as the loss of fine particles as entrained throughout the cyclones (HAAF, M., STROH, *et al.*, 2017). The values simulated for particle size distribution (PSD) and attrition effects were in good agreement with experimental data obtained in long-term testing at the 1 MW_{th} pilot plant at Technische Universität Darmstadt (see Figure 2.10). At the 200 kW_{th} Stuttgart pilot plant, attrition was also monitored in several experimental campaigns. After two days of operation, the sorbent is considered to be in a steady-state as the whole bed inventory has been exchanged several times (DIETER, BIDWE, *et al.*, 2014). A particle size average reduction of 70 μm in the mean diameter d_{50} of the fresh limestone particles was measured, reducing from 420 to 350 μm (see Figure 2.10) (DIETER, HAWTHORNE, *et al.*, 2012). Results based on the dust filtered from both flue gas streams over the experimental campaign exhibited an average sorbent loss of less than 3 wt.% (and during several hours of less than 2 wt.%) of the total solid inventory per hour. These values are lower than the required make-up ratios to maintain sorbent activity, so attrition and bed material loss were not considered critical for CaL operation with the specific limestone tested (Swabian Alb A) (DIETER, BIDWE, *et al.*, 2014). Limestones

with lower hardness will show higher attrition tendencies. However, preliminary results with weaker limestones have shown that CaL operation is possible if proper attention to plant operation is given, specially through reduction of thermal and mechanical stresses using lower fluidization velocities and minimum calcination temperatures (DIETER, BIDWE, *et al.*, 2014, FENNELL, ANTHONY, 2015).

The majority of the fine material is found in the calciner flue gas, which indicates that the thermal stress of calcination and the mechanical stress in the cyclones are the main sources of attrition. The initial calcination of the fresh limestone is responsible for a significant part of the overall amount of attrition. Therefore, in order to limit attrition and avoid operational issues such as fines deposition in the system, cyclones, and fluidization nozzles should be carefully designed (DIETER, BIDWE, *et al.*, 2014, FENNELL, ANTHONY, 2015).

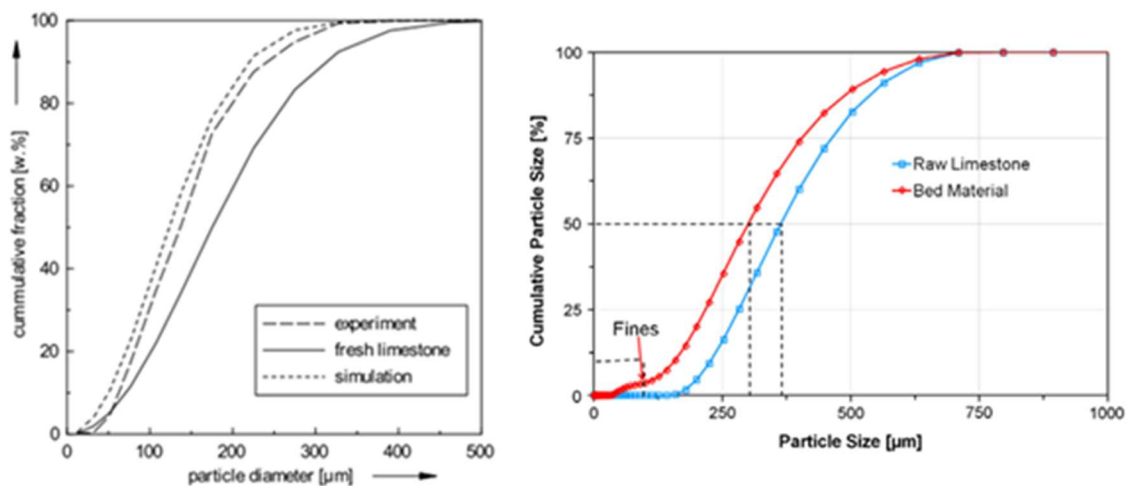


Figure 2.10 (Left) Particle size distribution of the circulating sorbent (experimentally measured and simulated) and the fresh limestone during test campaigns at Technische Universität Darmstadt. Obtained from (Haaf *et al.*, 2017). (Right) Cumulative particle size of raw limestone and calciner bed material in steady-state. Obtained from (Dieter *et al.*, 2012)

According to KNOWLTON (2000), process plants which involve the reaction of gases and solids are difficult to operate. Among the more complex of these processes are the ones incorporating a fluidized bed reactor and/or a solid recycle transport system, which is the case for CaL systems. Operational problems occur both in starting up and maintaining the plant operating continuously (KNOWLTON, 2000). Difficulties of operating those plants have been surveyed by MERROW (1984), who discovered in his study with 37 solids processing plants that the majority of performance problems

(characterized as problems that caused the plant to be off-line for one week or more) were caused by non-chemical problems. The study also found that 94% of the plants had experienced some kind of performance problem (MERROW, 1984). The most common problems reported were solids transfer failures, followed by mechanical equipment failures, plugging of reactors by solids, and handling of fines and dust. Solids processing plants operated on average at 64% of the design capacity in the first year of operation, while the industry average for non-solids operating plants was between 90% and 95%. It was also reported that solids processing plants take a longer time to start-up than plants not using solids. If 2.5 months was the actual start-up time for liquid/gas plants, the start-up time for plants processing raw solid material was 18 months (KNOWLTON, 2000). Start-up planning was also considered a problem for solids processing plants, as actual start-up times were over two to three times longer than what was originally agreed (KNOWLTON, 2000).

Several techniques have been developed to help reducing start-up and operation problems in fluidized-solids recycle systems reacting and transporting solids. According to KNOWLTON (2000), two of the most important alternatives to verify potential problems in commercial large-scale systems processing solids are cold models and pilot plants. Cold models are built models (of the entire plant or just a section of it) based on a commercial plant and operated at ambient temperature. Cold models can be used to simulate a plant on large-scale and help to solve problems occurring in the actual high-temperature unit. They are useful as can be constructed of clear plastic material that allows for visual observation of solids movement in the flow system, helping to identify solids flow patterns and stagnant regions. They are also relatively inexpensive and can be constructed in a relatively short time (KNOWLTON, 2000).

Pilot plants, on the other hand, are useful tools used for scaling up a process to a larger unit. Pilot plants also help to solve performance problems and improve the operation of an existing unit and are relevant when operation at exact process conditions is required. Pilot plant size is an important aspect of its design, since if the plant is too small, problems may arise from wall effects (slugging, excess friction, etc.) and if the pilot plant is too large, costs may be prohibitive (KNOWLTON, 2000).

2.4.3 Pilot plant experience with CaL systems

Pilot-scale demonstrations are essential to collect parameters required for the design, operation, and techno-economic analysis of CaL systems at commercial scale (FAN, ZENG, *et al.*, 2012). Through the successful operation of various pilot plants at the MW_{th} scale, sustained by long-term tests in recent years, the feasibility of the CaL process and its readiness for further scale-up has been confirmed (HAAF, STROH, *et al.*, 2017, HAAF, HILZ, *et al.*, 2018). This section focuses on the progress of CaL process testing at pilot-scale, to gather valuable data of design and operational development for validation of performance models. Lab-scale plants differentiate from pilot-scale plants usually by the size and heating source, with the former in the low kilowatt range and using external heating sources such as electrical heating systems. Pilot-scale facilities, on the other hand, are larger in scale (around the 1 MW_e range) and the process heat is usually generated by the combustion of fuel inside the calciner/regenerator (BHOWN, 2014, FENNELL, ANTHONY, 2015).

CaL systems lab-scale facilities were fundamental to develop the basis for the pilot-scale plants and a review of these facilities can be found in several works (FENNELL, ANTHONY, 2015; HANAK *et al.*, 2014; HANAK *et al.*, 2015a). In particular, important lab-scale facilities worldwide are: the 30 kW_{th} in Oviedo, Spain, at The Instituto Nacional del Carbón –Consejo Superior de Investigaciones Científicas (INCAR-CSIC) (ALONSO, ARIAS, *et al.*, 2018); the 75 kW_{th} in Ottawa, Canada, at CANMET (FAN, ZENG, *et al.*, 2012); the 10 kW_{th} in Stuttgart, Germany, at the IFK in University of Stuttgart (DIETER, BIDWE, *et al.*, 2014); and the 25 kW_{th} in Cranfield, UK, at the Combustion and CCS Centre in Cranfield University (ERANS, JEREMIAS, *et al.*, 2017). These facilities use two interconnected CFBs or a CFB with a bubbling fluidized bed (BFB) as reactors and loop seals and/or cone valves to control sorbent circulation. Other two important lab-facilities are: the 120 KW_{th}, in Ohio, United States, at Ohio State University; and the 3 KW_{th}, in Hsinchu, Taiwan, at ITRI. These two follow a different calciner principle and use a rotary kiln, as commonly applied in cement applications for clinker production (FENNELL, ANTHONY, 2015; HANAK *et al.*, 2014; HANAK *et al.*, 2015a). The most representative pilot-scale plants are further described.

2.4.3.1 INCAR-CSIC – La Pereda 1.7 MW_{th} pilot plant

Using the experience gained through operating the 30 kW_{th} unit, as well as the industrial expertise for large-scale CFB combustors, INCAR-CSIC decided to build the 1.7 MW_{th} pilot-plant in 2009 in agreement with several partners: ENDESA (which coordinated the project), Foster Wheeler, and HUNOSA (owner of the CFPP linked to the pilot plant). They had R&D support from University of Stuttgart (IFK), Lappeenranta University, Imperial College, and the University of Ottawa and CANMET-ENERGY. The plant was commissioned in 2011 and entered operation in 2012 under the scope of the project called *CaOling*, partly funded by the European Union 7th Framework Programme (ENDESA, 2013; HANAK *et al.*, 2015a; SACRISTÁN, 2014). In 2017, the plant had more than 3100 hours of stable operation in fulfilment of three European projects (ARIAS, DIEGO, *et al.*, 2017).

La Pereda demonstration facility receives a small fraction or slip stream (about 1%) of the flue gas generated from a nearby 50 MW_e CFB boiler at the HUNOSA power plant, located in Asturias, northern Spain. Flue gas from the power plant is blown to the carbonator with a fan. The test rig consists of two main reactors designed as CFBs and interconnected by loop seals, which are designed in order to control internal solids circulation and exchange among reactors (see figure 2.11). The carbonator operates around 650 °C with recorded CO₂ removals between 40% and 95% (ARIAS, DIEGO, *et al.*, 2017, FENNELL, ANTHONY, 2015). To achieve near full sorbent conversion, the calciner operates with calcination temperatures of 20 to 30 °C above the equilibrium concentration temperature of the calcination reaction. In oxy-combustion conditions, the plant is operated with O₂ over 5%.vol at the exit of the calciner for high coal combustion efficiency. Retractable heat exchangers or water-cooled bayonet tubes allow for heat removal and temperature control in the carbonator, with an adjustable cooling area (DIEGO, ARIAS, *et al.*, 2017, FENNELL, ANTHONY, 2015, HANAK, ANTHONY, *et al.*, 2015). The range of operating conditions and the main variables involved during test campaigns are available in ARIAS *et al.* (2013).

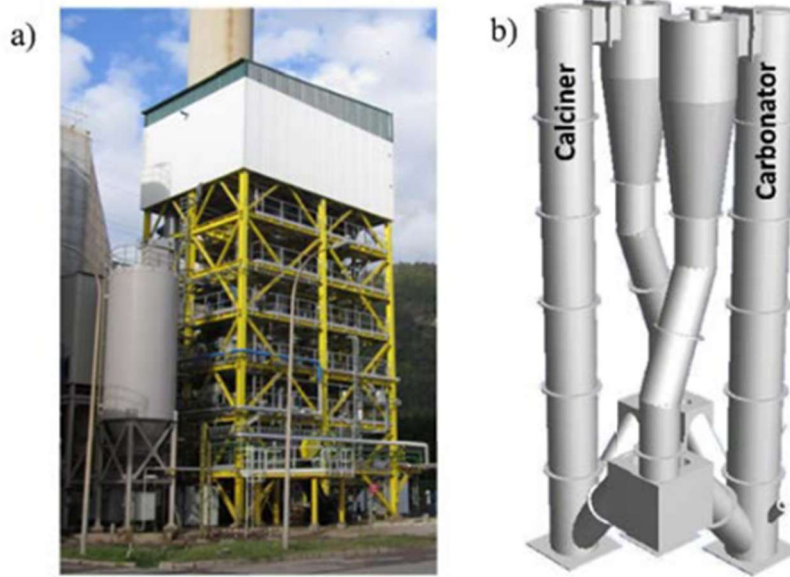


Figure 2.11 A) Front view of La Pereda pilot plant B) Scheme of the interconnected fluidized reactors. Obtained from (Arias et al., 2017b).

The two interconnected CFB reactors have both heights of 15 m and internal diameters of 0.65 and 0.75 m for the carbonator and the calciner, respectively. The diameters were selected to achieve gas velocities between 3 m/s and 6 m/s, which are similar to those encountered in industrial CFBs (SÁNCHEZ-BIEZMA, BALLESTEROS, *et al.*, 2011). While the carbonator is fluidized using the flue gas from the power plant, coal and limestone are fed to the calciner from two independent silos by a feeding system. They are mixed before entering the calciner reactor, which can operate under air or oxy-firing conditions, using a mixture of O₂ and CO₂ from gas storage tanks (DIEGO, ARIAS, *et al.*, 2017, FAN, ZENG, *et al.*, 2012). With CO₂ entering the calciner from storage tanks, no recirculation of the flue gas in this reactor is used. Both reactor exits are equipped with high-efficiency cyclones. The carbonator cyclone separates the flue gas from the partially carbonated solids while the calciner cyclone separates the concentrated CO₂ stream from the calcined sorbent at the oxy-fired CFB combustor. The solids fall into double loop seals which are operated with BFBs to enable control of solid circulation. Part of the solids in each loop seal is circulated internally to maintain desired operational conditions and stability of the CFB system, while the rest of the solids are transported towards the other reactor. Results of the test facility confirm the feasibility of the process for further scale up to a 30 MW_{th} plant if the system is operated with proper sorbent inventory and activity. Actual CO₂ capture in the carbonator was achieved close to the equilibrium value at a given temperature, e.g above 90% at 660 °C. Moreover, an

SO₂ capture rate of more than 95% was achieved (HANAK, ANTHONY, *et al.*, 2015). More results from the 1.7 MW_{th} test facility can be found in ARIAS *et al.* (2017b, 2013) and SÁNCHEZ-BIEZMA *et al.* (2013).

2.4.3.2 Institute of Energy Systems and Technology at Technische Universität (TU) Darmstadt – 1 MW_{th} pilot plant

The 1 MW_{th} TU Darmstadt pilot plant was erected and commissioned in 2011 at Darmstadt University of Technology, Germany. The pilot plant comprises two interconnected CFB reactors with a screw conveyor (for transport from carbonator to calciner) and loop seal (from calciner to carbonator) in the solid looping mechanism (FENNELL, ANTHONY, 2015, STRÖHLE, JUNK, *et al.*, 2014). The solids transfer between the CFBs by a screw conveyor differs from other pilot plants. In a commercial-scale unit, as large volumes of solids and variant loads will be transferred between the reactors due to changes in the power plant load, screw conveyors will not be a mechanically efficient alternative (HANAK, ANTHONY, *et al.*, 2015). The carbonator is 8.66 m in height and 0.6 m in internal diameter and it is equipped with internal bayonet cooling tubes at the top of the reactor for temperature control. The calciner is 11.35 m in height and has an internal diameter of 0.4 m. The entire system, including circulation ducts, has a refractory lining to minimise heat loss (HANAK, ANTHONY, *et al.*, 2015, STRÖHLE, JUNK, *et al.*, 2014). Both reactors are equipped with components of industrial CFB systems at a semi-industrial scale, including start-up burners, heat exchangers, and bag filters (HILZ, HAAF, *et al.*, 2019). The sorbent dosing system adds continuous fresh limestone to the carbonator, instead of the calciner as in other pilot plants. This configuration is claimed to reduce fuel and O₂ consumption in the calciner (STRÖHLE, JUNK, *et al.*, 2014). A combustion chamber provides the coal flue gas for the carbonator. Coal is fired with the oxygen-enriched recirculated flue gas (a recirculation unit is attached to the calciner) under oxy-fuel conditions. The fuel is continuously fed to the calciner by a gravimetric dosing system (HELBIG, HILZ, *et al.*, 2017). The flue gas and the CO₂ product stream are subsequently cooled down in the heat exchangers, and then cleaned from fly ash in fabric filters (HANAK, ANTHONY, *et al.*, 2015).

First test campaigns had no internal recirculation, which was changed in a second configuration where the lower loop seal was replaced by a cone valve. In 2019, the pilot plant had successfully been operated for more than 3,900 hours in a wide range of

operating conditions, achieving steady-state operation in gas and sorbent phases (HILZ, HAAF, *et al.*, 2019). Investigation on fuel influence has shown that the amount of ash in the circulating sorbent stream is significantly affected by the particle size of the coal fired in the calciner (HILZ *et al.*, 2018). The industrial size feasibility of the CaL process was considered proven after over 1219 hours of steady-state CO₂ capture with capture rates up to 94 % (HELBIG, HILZ, *et al.*, 2017). The experience with this plant is serving as basis to a planned scale-up to a 20 MW_{th} plant. The facility is also used for chemical looping combustion tests (HAAF, HILZ, *et al.*, 2018, HILZ, HAAF, *et al.*, 2019, JUNK, KREMER, *et al.*, 2014).

2.4.3.3 Institute of Combustion and Power Plant Technology at University of Stuttgart (IFK) – 200 kW_{th} pilot plant

The 200 kW_{th} pilot plant was commissioned in 2010 and designed for maximum operating flexibility to enable experiments with different concepts for solid circulation and fluidization regimes. The plant includes a CFB calciner operating in the fast fluidisation regime interconnected with two CFB carbonators, one operating under a fast fluidisation regime and the other in a turbulent regime (DIETER, BIDWE, *et al.*, 2014). The turbulent carbonator presence is justified to enable a more flexible flue gas load. Operational velocities are between 4-6 m/s for the two reactors in the fast regime and between 1-4 m/s for the carbonator reactor in the bubbling/turbulent regime (FENNELL, ANTHONY, 2015). The design involving two symmetric CFBs in the fast fluidisation regime has two loop seals with cone valves in the solid circulation system for independent control of the looping ratios (DIETER, HAWTHORNE, *et al.*, 2012, DIETER, BIDWE, *et al.*, 2014, HANAK, ANTHONY, *et al.*, 2015). The calciner is 10 m in height and 0.021 m internal diameter and is equipped with a staged oxidant supply for oxy-combustion of solid fuel. The staged oxidant supply allows for a uniform temperature profile in the reactor and operations with wood pellets reached 50%vol of O₂ without the presence of hot spots. Flue gas recirculation in the calciner is implemented to simulate realistic conditions, even if the firing system is designed to support operations with up to 70%vol of O₂. The fast-fluidised CFB carbonator has 10 m in height and 0.023 m in internal diameter, while the turbulent carbonator has 6 m in height and 0.033 m in internal diameter. The temperature in the carbonator fluctuates between 620-650°C with the designed temperature of 650°C only observed in the bottom dense region. Still, temperature reduction in the upper part had a minor effect on the carbonator efficiency,

indicating most of the reaction occurs in the dense region (HANAK, ANTHONY, *et al.*, 2015, HANAK, MANOVIC, *et al.*, 2014). Up to 2015, the pilot plant had operated for 1400 h, of which 700 h in carbon capture mode (FENNELL, ANTHONY, 2015).

2.4.3.4 Industrial Technology Research Institute (ITRI) – 1,9 MW_{th} pilot plant

Based on experience with the 3 kW_{th} unit, a 1,9 MW_{th} pilot plant was fully constructed in 2013 at the ITRI, Taiwan, for CO₂ capture from cement plants flue gases. In contrast to most of the CaL pilots in operation, which are based on CFB or BFB reactor systems, this pilot plant is the attempt to design and operate the calciner as a rotary kiln unit. This configuration is beneficial for investigating integration opportunities between the power and cement industries (CHANG, CHEN, *et al.*, 2014b, HANAK, ANTHONY, *et al.*, 2015).

The pilot plant removes a tonne of CO₂ per hour from the Hualien cement plant flue gas, whose concentration is more than 15 vol. % of CO₂. The solids transportation is done via a pneumatic conveying link. The carbonator is a bubbling fluidized bed and has a diameter of 3.3 m and a height of 4.2 m. The rotary kiln calciner has a diameter of 0.9 m and a length of 5m. The system was designed for and has operated with CO₂ capture levels higher than 85%. Heat for calcination is provided through direct oxy-combustion of diesel oil in the rotary kiln calciner, which requires flue gas recirculation for temperature control. The accumulated time of unit operation in a fully-continuous looping test is more than 300 hours. The plant is considered an important milestone for the future construction of a 30 MW_{th} demonstration plant (CHANG, CHEN, *et al.*, 2014a, FENNELL, ANTHONY, 2015, HANAK, ANTHONY, *et al.*, 2015).

2.4.4 Relevant feedstock properties

The scientific literature usually focuses on evaluating CaL systems added to coal-fired plants (ARIAS, B., DIEGO, *et al.*, 2013, ARIAS, Borja, DIEGO, *et al.*, 2017, SÁNCHEZ-BIEZMA, PANIAGUA, *et al.*, 2013, STRÖHLE, JUNK, *et al.*, 2014). There are important differences between using solid fossil fuels and biomass for electricity and heat generation. Among chemical and physical-mechanical fuel properties, the more relevant for combustion in boiler or oxy-combustor reactors are: heating value, moisture content, ash content, contaminant content (mainly nitrogen, sulphur, and chlorine contents), material grindability, and bulk density. A proximate analysis can be used in a preliminary evaluation of fuel chemical properties. Proximate analysis is composed of fixed carbon, volatile matter, ashes, and moisture. The fixed carbon content represents the amount of material left over after the removal of the volatile matter. The volatile matter content, which is primarily represented by combustible gases, represents the tendency for fuel ignition (HOFFMANN, 2010) and is usually greater in biomass than coal (CENTENO-GONZÁLEZ, LORA, *et al.*, 2017). Ash content represents the inorganic material that forms ashes when burned, which needs to be ultimately removed from the system. Relevant characteristics of ashes are its melting temperature and fouling properties. The temperature and melting behaviour of ashes depend on their composition, which greatly differs for biomass and coal, and is also different intra fuels – i.e. between different coals and biomasses (HOFFMANN, 2010). High moisture content affects the net yield of the process and the fuel heating value, with more heat required for water evaporation. Depending on the boiler and fuel, moisture content limits need to be specified to ensure satisfactory fuel conversion (HOFFMANN, 2010).

The heating value determines how much heat can be generated by a given amount of fuel. In the case of a calciner or boiler, the heating value influences the amount of fuel that needs to be fed into the system to obtain the desired operating temperature. Therefore, it impacts the design and size of the combustion system. High carbon and hydrogen contents contribute to an increase in the heating value, while high oxygen content decreases it (HOFFMANN, 2010). Biomass generally has a lower heating value relative to coal as it has less carbon and more oxygen in its composition (KHAN, DE JONG, *et al.*, 2009).

Fuel contaminants content is an important parameter to measure how flue gases and solid waste (ashes) needs to be treated. Flue gas and solid waste can be reused and/or

discharged (HOFFMANN, 2010). Some fuel contaminants cause unwanted emissions or make the combustion process more difficult by damaging the system. The nitrogen content has a direct effect on the formation of HCN and N₂O, compounds that form NO_x in combustion conditions, one of the main causes of acid rain. Sulphur can form SO_x compounds and needs to be removed for the same reasons as NO_x. Sulphur content is lower in biomass compared to most coals. Besides, chlorine compounds, can cause fouling, participate in corrosion processes, and lead to HCl emissions (JANTTI, 2012). Chlorine corrosion is often accelerated by alkaline components in the fuel (BASU, 2015). This contaminant participates in different combustion-related problems and is one of the most important elements with regard to feedstock behaviour (BASU, 2015, KHAN, DE JONG, *et al.*, 2009).

Physical-mechanical properties define how the fuel can or should be prepared for the combustion process. One of the most important physical-mechanical properties for combustion is grindability. The grindability describes material behaviour in the mill process. A relatively good grindability means that the material fragments with low energy consumption and presents a uniform grain size. Fibrous materials such as biomass typically consume more energy than porous materials such as coal (HOFFMANN, 2010). The advantage of using pulverised fuel is the increase in specific surface area, increasing combustion efficiency. Thus, reactors that work with pulverized material achieve a higher load capacity with smaller installations. Grain size uniformity is also important in reactors that operate with bulk material in order to obtain homogeneous operating conditions. A heterogeneous distribution in bed material could cause failures in aeration, which leads to problems in temperature control (HOFFMANN, 2010). Bulk density is also important considering heating value and transportation of biomass.

In relation to coal, fuel properties depend on formation conditions of incomplete decomposed organic matter, including: temperature, pressure, original biomass, and formation time. Coal is generally classified into four coal classes: anthracite, bituminous, sub-bituminous, and lignite (HOFFMANN, 2010). Fixed carbon content and heating value tend to decrease from anthracite to lignite, while the volatile material and moisture contents increase. Based on these characteristics, anthracite and bituminous coal are considered nobler classes or high-rank, and sub-bituminous and lignite coal are considered low-rank. Low-rank coal generally has a higher content of ash, sulphur, and contaminants. A CaL system equipped with oxy-fired CFB calciner can process a wide

variety of fuels of different qualities, however, differences mainly in the sulphur content can change sorbent activity. This is due to the sulphation reaction that occurs with priority in the reactor, altering sorbent make-up and looping rates. The influence of inert solids and sulphur content on the design of CaL systems fuelled with coal was investigated by (DIEGO, ARIAS, *et al.*, 2013). It was found that the impact on CaL performance is greater due to the sulphur inlet rather than the ash or inert inlet. The work confirmed that when operating with low make-up flows, the carbonator efficiency shows high sensitivity to the composition of the coal added to the calciner and the SO₂ content in the flue gas (DIEGO, ARIAS, *et al.*, 2013). The work by (HE, QIN, *et al.*, 2017) particularly investigated the influence of coal-derived ash in the CaL process. The findings point out that the impact of ash are of concern even though the inhibition of the CO₂ sorption could be minimised by careful selection of the coal used (HE, QIN, *et al.*, 2017). Therefore, it can be derived that it could be a limiting factor for the application of CaL systems to use certain coals with high sulphur and ash content. This is especially relevant considering the Brazilian coal, which has high ash and sulphur content (EPE, 2017). Co-combustion with biomass could be an alternative to deal with the high sulphur content of some coals.

At the same time, the CaL system could also work as an SO₂ capture plant, as is possible to capture high rates of the sulphur present in the fuel, at the expense of an increase in limestone consumption, avoiding SO_x emissions (ABANADES, ARIAS, *et al.*, 2015). On the other hand, amine-based systems require an FGD unit downstream of the process (and possibly an SO₂ polisher set to 10 ppm downstream of the scrubber), to keep solvent consumption and cost at reasonable values (METZ, DAVIDSON, *et al.*, 2005), as the cost of the amine-based solvent is comparatively high.

Volatile matter influences coal reactivity and sub-bituminous and lignite have higher reactivity than nobler coals. Typical moisture content is below 20 wt% for bituminous coal, between 20 and 30 wt% in sub-bituminous coal, and up to 45 wt% for lignite (HOFFMANN, 2010). Regarding grindability, high-rank coal is generally harder than sub-bituminous coal or lignite. Considered a high-value material, anthracite is not normally used in power generation systems. Bituminous coal is generally used for coal-fired plants, followed by sub-bituminous and lignite (FOOT, ZOELLE, *et al.*, 2015, MANTRIPRAGADA, ZHAI, *et al.*, 2019b).

On the other hand, biomass presents lower energy density (heating value) and greater moisture content and material heterogeneity (IEAGHG, 2011, ZHAO, ZHOU, *et al.*, 2017). These differences can lead to modifications particularly in the feeding system, boiler design, burner configuration, and pre-treatment stages (IEAGHG, 2011). The main options for pre-treatment stages for biomass include sizing, drying, washing, palletisation, and torrefaction, as well as combinations of some of them (CARBO, ABELHA, *et al.*, 2016, MACIEJEWSKA, VERINGA, *et al.*, 2006). The costs of pre-treatment may be compensated by the ease in operating the fuel during handling, storage, transportation, feeding, and controlled combustion (BAHADORI, ZAHEDI, *et al.*, 2014, MACIEJEWSKA, VERINGA, *et al.*, 2006).

The common disadvantages of biomass for combustion processes include: the heterogeneity concerning ash content; seasonal feedstock availability; high alkaline content; low ash melting point; low bulk density; and uncertain transportation and pre-treatment costs (ZHAO, ZHOU, *et al.*, 2017). The low ash melting point is due to greater levels of alkali compounds such as potassium (K) and sodium (Na), which react with flue gases and bed material (silica or sand) by forming eutectics compounds. This leads to less efficient thermal systems since steam cycle temperature must be limited or the eutectic compounds will contribute to operational problems such as bed agglomeration, corrosion, and fouling in boilers and circulating fluidized bed combustors (CFBCs) (AMEC FOSTER WHEELER ENERGIA OY, 2015, ARJUNWADKAR, BASU, *et al.*, 2016, KHAN, DE JONG, *et al.*, 2009). Other components such as Mg and Ca can increase ash melting temperature (KHAN, DE JONG, *et al.*, 2009). These and other ash-related problems of biomass such as alkali-induced slagging (ash fusion) are further investigated in the work by NIU *et al.* (2016).

In addition, pulverising solid biomass to feed the boiler is more difficult due to its fibrous character, which makes disintegration an energy-intensive process. The pulverised biomass material is often more cohesive, leading to conveying problems in pneumatic systems and, therefore, additional costs caused by the need for a more specified feeding system (BERGMAN, BOERRIGTER, *et al.*, 2002, HOFFMANN, 2010). In short, the pulverised untreated biomass requires higher gas velocity in its pneumatic conveying system to achieve the same mass loading as coal (CARBO, ABELHA, *et al.*, 2016). Finally, to guarantee a more steady fuel supply on a year-round basis, fuel storage is necessary and should also have a different approach for biomass compared to coal,

since the first is more susceptible to water-induced and mechanical degradation, being able to change its moisture content, energy value and dry matter content due to its microbiological activity and degradation processes (RENTIZELAS, 2016). Biomass should be stored protected from water exposure, typically below 12 wt% of moisture content so that the risk of biological decay is diminished (CARBO, ABELHA, *et al.*, 2016). At the same time, a moisture content below 2 wt%, increases the risk of self-heating, fire, and/or explosion (CARBO, ABELHA, *et al.*, 2016). The most suitable biomass storage method depends on key factors such as the type of biomass, its shape and size, quantity and volume, regional weather conditions, end-use, transportation distance, etc (RENTIZELAS, 2016). Open-air storage, covered with and without climate control, and steel or concrete bins and silos are some of the available methods (RENTIZELAS, 2016).

Due to economic reasons associated with its supply chain, storage, and operational processes, large scale dedicated biomass thermal plants (over 100 MWe) have not been extensively deployed¹⁸ in the past, with most of the proposed solutions aimed at significantly introducing biomass in the electricity sector focused in co-firing it with coal in existing power plants (DAI, SOKHANSANJ, *et al.*, 2008, LIVINGSTON, MIDDLEKAMP, *et al.*, 2016, OZCAN, ALONSO, *et al.*, 2014). Co-firing up to 20% biomass with coal is technically feasible with relatively modest modifications on the existing system (DAI, SOKHANSANJ, *et al.*, 2008). Higher mixing ratios, in turn, can cause more difficulties in fuel preparation, milling stages, boiler capacity, and ash utilization, which can reveal a need for a dedicated biomass infrastructure (MACIEJEWSKA, VERINGA, *et al.*, 2006, OZCAN, ALONSO, *et al.*, 2014). Generally, the feedstock price and the high operational costs associated (fuel collection, storage, transportation, and pre-treatment) are important drawbacks for the wide deployment of large-scale dedicated biomass-fired power plants (BFPPs) (XU, YANG, *et al.*, 2020). In short, large-scale dedicated biopower units impose inherent logistical challenges and are roughly viable in a range from 25 to 100 MWe (HETLAND, YOWARGANA, *et al.*, 2016). Thus, dedicated biomass-fired thermal plants are typically smaller and more dispersed than thermal plants fuelled with coal (XU, YANG, *et al.*, 2020), which implies

¹⁸ One of the largest operating biomass-fired fluidised bed system is located in Polaniec, Poland and delivers 205 MWe (447 MWth) to the grid (ERIKSSON, TIMO, *et al.*, 2015).

on a negative effect on the economies of scale of these systems, especially if the application of CCS is considered (IEAGHG, 2011).

On the other hand, aside from being a carbon-neutral fuel and reducing net emission of greenhouse gases compared to coal (SAIKAEW, SUPUDOMMAK, *et al.*, 2012, XU, YANG, *et al.*, 2020), biomass direct combustion usually generates lower content of certain pollutants, such as sulphur and mercury, and has lower ash content than coal (ZHAO, ZHOU, *et al.*, 2017). When co-fired with high-sulphur coal, reductions in NO_x and SO_x emissions can be achieved (OZCAN, ALONSO, *et al.*, 2014, SCHOLARSARCHIVE, LIN BAXTER, *et al.*, 2005).

Regarding fuel properties influence in CaL systems, the ash content of a given feedstock is of great importance to the complexity of the removal facilities and can also be responsible for modifying design parameters in order to maintain reasonable solid looping circulation rates (HANAK, BILYOK, *et al.*, 2015b). In CaL systems, feedstock ashes will arguably be removed in solid-state after incomplete burn in the calciner, most likely using dry ash reactors and specified particle removal facilities.

In terms of the reported experiences with CaL and biomass, solid biomass direct combustion with *in situ* CO₂ capture by CaO in a 300 kW_{th} circulating fluidized bed facility was experimentally validated in continuous mode (ALONSO, DIEGO, *et al.*, 2014). The system concept relies on the higher reactivity of biomass over coal, which allows for effective combustion around 700 °C in air at atmospheric pressure. In such conditions, CaO particles are fed into the fluidized bed combustor (which plays the role of carbonator combustor), and react with the CO₂ generated during biomass combustion (ALONSO, DIEGO, *et al.*, 2014). Wood pellets are used as biofuel (ALONSO, DIEGO, *et al.*, 2014, OZCAN, ALONSO, *et al.*, 2014). A dedicated large-scale (>100 MWe) similar version of this system was proposed and modelled by (OZCAN, 2014). The process is compared to conventional biomass-air-fired and biomass-oxy-fired power plants. It has demonstrated to be capable of achieving 84% overall CO₂ capture rate with an energy penalty of 5% when a proper heat exchanger network (HEN) is designed with the support of a pinch analysis (OZCAN, 2014, OZCAN, ALONSO, *et al.*, 2014). OZCAN *et al.* (2014) point out the similarity of a biomass-fired CaL system with commercial coal-based CFB power plants, which enables one to evaluate in detail the costs of electricity and CO₂ avoided. Considering carbonator and calciner interconnected

reactors are erected as CFBs, following (HAAF, HILZ, *et al.*, 2018, HILZ, HAAF, *et al.*, 2019), is useful, as CFB fuelled with biomass has already achieved commercial level (AMEC FOSTER WHEELER ENERGIA OY, 2015, JANTTI, 2012, NUORTIMO, ERIKSSON, *et al.*, 2017). However, there is still continuous effort to deal with specific biomass-related problems. Typical problems while operating CFBs with biomass are fouling on furnace walls and convection surfaces, combined or not with corrosion, bed agglomeration, slagging, and chlorine emissions (AMEC FOSTER WHEELER ENERGIA OY, 2015, KHAN, DE JONG, *et al.*, 2009). As previously mentioned for conventional energy conversion systems, the presence in the feedstock of elements such as Si, K and Na, and also Cl, is specifically responsible for causing ash fouling, slagging and other problems in CFBs systems (NIU, TAN, *et al.*, 2016).

In the work by MARTÍNEZ *et al.* (2018), the calciner of a CaL system retrofitted in an existing subcritical coal-fired power plant is fired with woody biomass so that the full system achieves a negative emission factor – i.e. the entire system becomes carbon-negative including the existing coal power plant retrofitted with the CaL capture system (MARTÍNEZ, ARIAS, *et al.*, 2018). This carbon-negative potential for existing coal-fired plants using a biomass-fired calciner is also defended by HANAK *et al.* (2015) (HANAK, BILYOK, *et al.*, 2015b).

The use of a pure oxygen environment in a CFB biomass boiler could bring problems associated with the high fuel reactivity, and extremely high temperatures could be reached close to the oxidant injection ports, creating hot spots (MARTÍNEZ, ARIAS, *et al.*, 2018). The high temperatures may also cause melting and vaporization issues associated with the biomass ashes, leading to bed agglomeration (MARTÍNEZ, ARIAS, *et al.*, 2018). However, the oxy-fired calciner of a CaL system could reduce some of these problems due to the absence of heat transfer surfaces within the reactor (only the carbonator has an integrated heat exchanger in a CaL standard configuration), which would ultimately avoid the corrosion problems in the heat exchanger tubes (KHAN, DE JONG, *et al.*, 2009, MARTÍNEZ, I., ARIAS, *et al.*, 2018). Additionally, large circulation of CaO as the bed material within the reactor may greatly reduce agglomeration problems caused by the high alkali content in biomass ashes (MARTÍNEZ, I., ARIAS, *et al.*, 2018).

Results reported in the work by HANAK *et al.* (2015) (HANAK, BILYOK, *et al.*, 2015b), simulating coal and biomass-fired calciners for post-combustion CaL plants,

have shown that the increase in net power output is higher for high-ash fuels like coal in typical sorbent make-up rates (lower than 5%) and calciner higher oxygen content (higher than 30%vol in wet basis). The opposite is true for higher sorbent make-up rates, favouring low-ash fuels (biomass feedstock), though, under such conditions, high solid circulation and larger equipment would increase the costs and make the system design unattractive. For optimized performance parameters, a value of 2% for the make-up ratio was used for the biomass-fired calciner, and 4% for the coal-fired. The distinct values for make-up rate were selected so the systems would result in similar total solid looping rates considering the different ash and sulphur contents, ensuring reasonable sizes for the reactors (HANAK, BILİYOK, *et al.*, 2015b). Thus, one can derive those biomass-fired calciners or Bio-CaL systems, when compared to coal CaL systems, will likely require reduced circulation of solids between the reactors, which translates into reduced thermal input and lower temperatures to achieve the same calcination efficiency (HANAK, BILİYOK, *et al.*, 2015b, MARTÍNEZ, I., ARIAS, *et al.*, 2018).

PILLAI *et al.* (2019) (PILLAI, SURYWANSHI, *et al.*, 2019) evaluated dedicated biomass-fired power plants using organic Rankine cycles (ORC) integrated with CaL carbon capture and supplied by sugarcane bagasse in both the calciner and base plant. Two CaL configurations, including the conventional single loop and a second-generation double loop, were analysed due to the abundant availability of limestone in countries like India and China. The study indicated that for the same energy input from biomass combustion, the energy and exergy penalties of the conventional CaL were less than 2%, compared to the stand-alone system without carbon capture (without compression, that accounted for around more 4%) while of the double CaL, more thermally efficient, was around 0.1% (PILLAI, SURYWANSHI, *et al.*, 2019).

Therefore, as the use of CFBs for CaL systems enables more flexibility in feedstock selection, the main differences between a conventional CaL using coal and a Bio-CaL system are more evident in pre-treatment stages, including more plant footprint for pre-treatment equipment. Thus, minor modifications in the interconnected reactors that compose the CaL system are required in a Bio-CaL system if lower thermal efficiencies and capture rates, compared to the standard coal case, are considered acceptable.

3. Modelling of Calcium Looping cycles for post-combustion CO₂ capture

In this chapter, values are discussed for key operational parameters based on available models and experimental data. The chapter is mainly focused on the mass and energy balances and fluidization regimes of a standard CaL system for post-combustion CO₂ capture. In section 3.1, performance models are presented and the subsections follow detail sorbent activity mechanism and mass and energy balances. In section 3.2 reactor design of the CaL system is investigated based on the literature review.

3.1 Performance models

A performance model for a CaL system should be able to calculate the amount of limestone and fuel needed to achieve a desired CO₂ capture efficiency under specified operating conditions. Results from a performance model should include impacts on the base power plant efficiency, emissions, and resource requirements (MANTRIPRAGADA, RUBIN, 2014). Energy and mass balances of solids and gases across all components, as well as requirements of main reactors and other equipment, are also calculated. In addition, the potential heat recovered and extra power generated should be estimated (MANTRIPRAGADA, RUBIN, 2014, 2017a). Usually, a dual CFB reactor system is considered. In the last decade, several published works have attempted to model the performance of CaL processes based on a dual CFB reactor system (HAAF, M., STROH, *et al.*, 2017, MARTÍNEZ, GRASA, *et al.*, 2013, ROMANO, 2012, STRÖHLE, LASHERAS, *et al.*, 2009). More recently, various authors developed models using ASPEN PLUSTM software (HAAF, M., STROH, *et al.*, 2017, HAAF, HILZ, *et al.*, 2018, HANAK, BILİYOK, *et al.*, 2015a, MOORE, KULAY, 2019) or Aspen Hysys[®] (MARTÍNEZ, I., ARIAS, *et al.*, 2018, MARTÍNEZ, I., MURILLO, *et al.*, 2011b).

The performance models presented in the following sections are a review of the work of several authors. Yet, most of the equations described are essentially based in the technical document by MANTIPRAGADA, RUBIN (2017a), as this report follows the calculation procedure of the Integrated Environmental Control Model (IECM) software, which is used in this study for plant simulations in chapter 4. The software simulates a power plant with an integrated CaL cycle for post-combustion CO₂ capture

(MANTRIPRAGADA, RUBIN, 2017b). The software is introduced and its utilization is justified in chapter 4. Some of the design parameters (or input variables) considered in the model are: CO₂ capture efficiency in the carbonator, degree of carbonation and calcination, limestone purity, ratio of make-up CaCO₃ molar flow, recirculating sorbent molar flow, among others.

3.1.1 Solid sorbent activity

The use of solid sorbents for post-combustion CO₂ capture can offer some advantages over conventional aqueous solvent-based processes, including reduced regeneration energy requirements, due to significantly lower heat capacity (U.S. DEPARTMENT OF ENERGY/NETL, 2019b). Sorbents with the ideal properties will provide relatively high absorption capacity (or reactivity), quantified by kg CO₂ absorbed/kg sorbent, and the best kinetics for the CO₂ absorption process. A high absorption capacity for both forward and reverse reactions, along with faster kinetics, allow for lower solids circulation, lower sorbent make-up, and smaller reactors, all of which lead to lower capital and operational costs (FAN, ZENG, *et al.*, 2012). Other properties of an ideal sorbent include: low risk for health and safety, low sorbent attrition and fragmentation, low tendency for agglomeration and sintering, low cost, and high-availability (FENNELL, ANTHONY, 2015).

In CaL systems, the sorbent carrying activity is one of the most important parameters to design and operate the cycle, as it sets limits on the calcium inventory and solid circulation rates to achieve high CO₂ capture efficiencies (DIEGO, ARIAS, *et al.*, 2017). It is known that the activity of a calcined natural limestone particle decreases with the increasing number of cycles until it reaches a residual capacity (FENNELL, ANTHONY, 2015, RODRÍGUEZ, ALONSO, *et al.*, 2010). After multiple cycles, the residual capacity of CaL systems remains between 7.5-10% mol CO₂/mol CaO (FENNELL, ANTHONY, 2015, GRASA, ABANADES, 2006).

Sorbent deactivation can be partially explained by a sintering-induced change in the morphology of CaO derived from limestone that occurs after a few cycles. Nanostructured grains turn into large micrometre-sized grains, accompanied by a reduction in pore volume which diffusion-limits the carbonation reaction. Still, predetermined average sorbent activity can be maintained by replacement of some of the

recirculating sorbent with fresh sorbent, as previously mentioned. Spent sorbent is purged to avoid the accumulation of inert CaO, fines, ashes, and CaSO₄ in the system (DIEGO *et al.*, 2013). Many sources of natural limestone worldwide have enough reactivity to sustain large scale plants, maintaining large purge and make-up rates, of hundreds of tonnes per hour (FENNELL, ANTHONY, 2015).

Several semi-empirical models have been proposed to express the maximum sorbent conversion rate as a function of the number of carbonation/calcination cycles (DIEGO, ARIAS, *et al.*, 2017, GRASA, ABANADES, 2006, LI, CAI, *et al.*, 2008). The model proposed by GRASA, ABANADES (2006) is one of the most commonly used in CaL process performance (HANAK, MANOVIC, 2016) and it is demonstrated by equation 3-1:

(3-1)

$$X_N = \frac{1}{\frac{1}{1 - X_R} + kN} + X_R$$

Where X_N is CaO conversion in an N^{th} cycle, X_R is the residual CaO conversion, and k a deactivation constant. The value of 0.52 for k is representative for many limestones and under many conditions, but can vary from 0.28 to 1.96. X_R represents residual conversion and is usually set to a realistic value of 0.075. (FENNELL, ANTHONY, 2015, RODRÍGUEZ, ALONSO, *et al.*, 2010). The predictions based on the semi-empirical model presented in equation (3-1) have been relatively accurate for a wide range of limestones, particle sizes, and CO₂ partial pressures (HANAK, MANOVIC, 2016, HANAK, ANTHONY, *et al.*, 2015).

As a result of multiple cycles in continuous operation, the CaL system solids inventory is composed of a mixture of particles that have undergone a different number of carbonation-calcination cycles. Therefore, sorbent particles have different CO₂ carrying capacities and the activity of the inventory can be characterized by an average CO₂ carrying capacity known as X_{ave} . The X_{ave} in a continuous large-scale CaL plant should adequately represent CaO particles lifetime (DIEGO, ARIAS, *et al.*, 2017).

The methodology to represent X_{ave} proposed by RODRÍGUEZ *et al.* (2010) and also used by DIEGO *et al.* (2017) takes into account the partial conversion of particles in the carbonator-calciner cycles and assumes operating conditions for a typical CaL system, which comprises: limited residence time in the reactors, low CO₂ partial pressure in the

carbonator, high CO₂ concentration in the calciner and moderate calcination temperature. Under these assumptions, X_{ave} can be calculated as a function of the “age” of the sorbent N_{age} , which means the actual number of full carbonation-calcination cycles that each individual particle has undergone in the system (RODRÍGUEZ *et al.*, 2010). Thus, assuming the carbonator and calciner to be perfectly mixed reactors (ALONSO, RODRÍGUEZ, *et al.*, 2009), the X_{ave} of the sorbent can be calculated utilizing the following expression (RODRÍGUEZ *et al.*, 2010):

$$X_{ave} = \sum_{N_{age}=1}^{N_{age}=\infty} r_{N_{age}} X_{N_{age}} \quad (3-2)$$

Where $X_{N_{age}}$ represents the maximum CO₂ carrying capacity of the particles after N_{age} complete carbonation-calcination cycles. To calculate $r_{N_{age}}$, a mass balance of the carbonator loop was carried out in the work by RODRÍGUEZ *et al.* (2010). The work estimates the fraction of particles, r_N , that have cycled the system N times. This mass fraction is a function of the solids circulation rate F_R , which is the molar flow of CaO-based particles¹⁹ arriving at the carbonator from the calciner, and fresh limestone make-up molar flow, F_0 , as described by equation 3-3 presented below (RODRÍGUEZ, ALONSO, *et al.*, 2010).

$$r_N = \frac{F_0 F_R^{N-1}}{(F_0 + F_R)^N} \quad (3-3)$$

The F_0/F_R ratio represents the make-up flow over the recirculating sorbent molar flow and is often regarded as a key performance parameter (HANAK, MANOVIC, 2016, HANAK, ANTHONY, *et al.*, 2015, RODRÍGUEZ, ALONSO, *et al.*, 2010). The value for this parameter varies from 1-5% in the literature (CLARENS, ESPÍ, *et al.*, 2016, HANAK, BILYOK, *et al.*, 2015b, MARTÍNEZ, MURILLO, *et al.*, 2011a, ROMANO, MARTÍNEZ, *et al.*, 2012, ROMEO, ABANADES, *et al.*, 2008, YANG, ZHAI, *et al.*, 2010), and a realistic value is closer to 2% in more recent works considering coal-fired plants (FENNELL, ANTHONY, 2015, HAAF, HILZ, *et al.*, 2018, MARTÍNEZ, ARIAS, *et al.*, 2018). The analysis by HANAK *et al.* (2015) of the F_0/F_R ratio in the 1-5% range,

¹⁹ In the form of CaO, CaCO₃ and CaSO₄ (MARTÍNEZ, I., ARIAS, *et al.*, 2018)

revealed that the net thermal efficiency and net power output were the highest at low F_0/F_R ratios. However, such operation requires larger equipment, and thus, a trade-off between economic and thermodynamic performance of the system is required. For an optimal design, balance between the capital costs and operational revenue has to be considered (HANAK, BILİYOK, ANTHONY, *et al.*, 2016, HANAK, BILİYOK, *et al.*, 2015a). Also, the selection of the fuel utilized in the calciner, due to different ash and sulfur contents, influences the choice for the F_0/F_R parameter and the size of the CaL process units, and has considerable impact on the net thermal efficiency and the net power output of the integrated system.

Then, $r_{N_{age}}$ is the fraction of particles that have experienced N_{age} cycles and is calculated as follows. For more details see RODRÍGUEZ *et al.* (2010):

$$r_{N_{age}} = \frac{(r_0 + (F_0/F_R))f_{carb}^{N_{age}-1}f_{calc}^{N_{age}}}{\left(\frac{F_0}{F_R}\right) + f_{carb}f_{calc}}^{N_{age}} \quad (3-4)$$

In the above equation $r_{N_{age}}$ depends on the fraction of uncalcined particles, r_0 , and the fractional carbonation and calcination conversions, f_{carb} and f_{calc} , respectively, which can be defined by the following equations (RODRÍGUEZ *et al.*, 2010):

$$r_0 = \frac{F_0(1 - f_{calc})}{F_0 + F_R f_{calc}} \quad (3-5)$$

$$f_{carb} = \frac{X_{carb} - X_{calc}}{X_{ave} - X_{calc}} \quad (3-6)$$

$$f_{calc} = \frac{X_{carb} - X_{calc}}{X_{carb}} \quad (3-7)$$

Where X_{carb} and X_{calc} are the average molar content of CaCO_3 conversions of the solids leaving the carbonator and calciner reactors, respectively. Full conversions are not achieved in the carbonator or the calciner (RODRÍGUEZ, ALONSO, *et al.*, 2010), and the degrees of calcination f_{calc} and carbonation f_{carb} in each reactor can be seen as design parameters for an aimed capture efficiency and sorbent carrying capacity. For the

carbonated sorbent fraction f_{carb} , a value of 0.7 is commonly specified (HANAK, BILİYOK, *et al.*, 2015a, b, MICHALSKI, HANAK, *et al.*, 2019), though a higher value of 0.8 was used in MANTRIPRAGADA, RUBIN (2014). For the degree of calcination or calcined sorbent fraction f_{calc} , a value of 0.95 is used in several works (HANAK, BILİYOK, *et al.*, 2015a, MANTRIPRAGADA, RUBIN, 2014, MICHALSKI, HANAK, *et al.*, 2019). YLATALO *et al.* (2013) claim that achieving almost full calcination at the lowest possible temperature reduces costs by minimizing oxygen and fuel consumption (YLÄTALO, PARKKINEN, *et al.*, 2013).

As it is difficult to determine an explicit solution for the infinite sum in equation (3-2) when using equation (3-1), the semi-empirical correlation proposed by LI *et al.* (2008) in equation (3-8) can be used, since it approaches equation (3-1) as a geometric progression (LI, CAI, *et al.*, 2008).

(3-8)

$$X_{N_{age}} = a_1 f_1^{N_{age}+1} + a_2 f_2^{N_{age}+1} + b$$

Where a_1 , f_1 , a_2 , f_2 , and b are sorbent fitting constants that can be calculated using a $X_{N_{age}} \times N_{age}$ curve, obtained with thermogravimetric analysis (TGA) equipment. The constants in equation (3-8) are determined for a particular sorbent and no particular reference to their physical meaning was made (except for b , which represents the residual carrying capacity X_R in equation 3-1). This semi-empirical model was found to successfully predict the decay in the conversion of limestone and other sorbents such as dolomite, provided the fitting parameters were known (HANAK, ANTHONY, *et al.*, 2015).

For the limestone used during tests with TGA equipment reported in DIEGO *et al.* (2017), the fitting constants are $a_1 = 0.1619$, $f_1 = 0.9590$, $a_2 = 0.8196$, $f_2 = 0.7066$ and $b = 0.1075$. In the work by Rodríguez *et al.* (2010), slightly different values for the fitting constants are used: $a_1 = 0.1045$, $f_1 = 0.9822$, $a_2 = 0.7786$, $f_2 = 0.7905$ and $b = 0.07709$. These last constants were applied and compared to equation (3-1), which found a regression square coefficient higher than 0.99, meaning $X_{N_{age}}$ in equation (3-8) represents virtually the same deactivation curve as the one expressed by equation (3-1).

Finally, by combining equations (3-2), (3-4) and (3-8), and calculating the limit of the infinite sum of the geometric series, one can obtain an expression similar to

equation (3-9) below, which allows estimating the maximum average CO₂ carrying capacity of the sorbent. This parameter is a function of the make-up flow of fresh limestone F_0 , the circulation rate of calcium solids between the reactors F_R , calcination and carbonation fractional conversion (f_{calc} and f_{carb}) and sorbent parameters (a_1 , f_1 , a_2 , f_2 , and b):

$$X_{ave} = (F_0 + F_R r_0) f_{calc} \left(\frac{a_1 f_1^2}{F_0 + F_R f_{calc} f_{carb} (1 - f_1)} + \frac{a_2 f_2^2}{F_0 + F_R f_{calc} f_{carb} (1 - f_2)} + \frac{b}{F_0} \right) - \frac{F_s}{F_0} \quad (3-9)$$

The term F_s/F_0 is included to account for the deactivating effect of sulphur, by assuming the molar content of sulphur F_s , captured from the flue gas entering the carbonator and from the fuel fed to the calciner, reacts only with the fraction of CaO particles which are active for CO₂ capture. Therefore, equation (3-9) allows estimating the maximum average sorbent conversion that can be reached in the carbonator. The practical average activity will depend on the sorbent degree or extent of carbonation and calcination (MANTRIPRAGADA, RUBIN, 2014). The actual conversion fraction can be seen as equivalent to rich and lean-loading in the solvent scrubbing technologies, and are based on the carbonator and the calciner performance, using the following expressions (MANTRIPRAGADA, RUBIN, 2014):

$$X_{carb} = \frac{f_{carb}}{1 - (1 - f_{carb})(1 - f_{calc})} X_{ave} \quad (3-10)$$

$$X_{calc} = (1 - f_{calc}) X_{carb} \quad (3-11)$$

Although there is little experimental information available on the evolution of sorbent activity in steady-state systems, the average CO₂ carrying capacity of the sorbent was monitored at a relevant scale in La Pereda 1.7 MW_{th} pilot plant (ARIAS, B., DIEGO, *et al.*, 2013). Results have shown that the decay in the CO₂ carrying capacity during the operations campaigns was consistent with the deactivation trends observed during

standard TGA tests, and the model described in this section can be used with reasonable precision if the calciner is operated at conditions far from the equilibrium curve of CO_2 on CaO , and residence time of particles in the reactor is kept to a minimum to reduce their chance of experiencing multiple carbonation-calcination cycles. (ARIAS, DIEGO, *et al.*, 2013, DIEGO, ARIAS, *et al.*, 2017)

The reaction between CaO and CO_2 occurs in two distinct stages, an initial fast-reaction stage and a slower-reaction stage, as illustrated in figure 3.1. First stage occurs within a few minutes and is kinetically controlled. Second stage is slower and diffusion-controlled by a CaCO_3 product layer. The formation of a non-porous carbonate product layer makes the inward diffusion of CO_2 more difficult. Since CaCO_3 has a higher molar volume than CaO , plugging of pores is inevitable during reaction (FAN, ZENG, *et al.*, 2012).

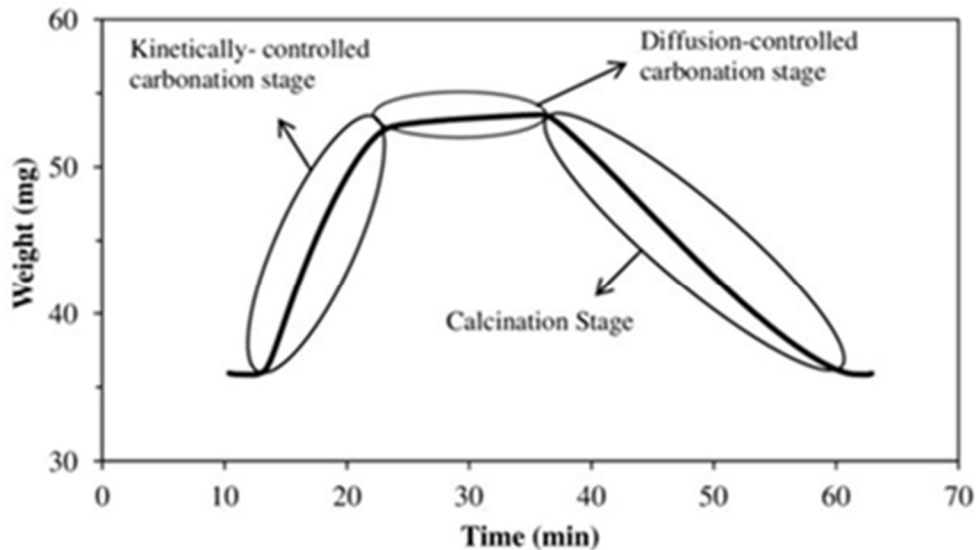


Figure 3.1. A cycle of carbonation and calcination observed by a TGA. Obtained from OZCAN *et al.* (2013)

Thus, the decrease in reactivity and cyclability of CaO can be attributed to the deteriorating morphological properties due to sintering and surface porous structure rearrangement. For those reasons, only the first stage of the reaction should be considered for commercial application, which facilitates the use of more compact reactors. (FAN, ZENG, *et al.*, 2012).

As previously mentioned, the calcination reaction is endothermic and occurs at a higher temperature than carbonation under typical conditions. Reaction temperatures are dependent upon the partial pressure of CO_2 and can be lowered through a dilute gas or

under sub-atmospheric conditions (FAN, ZENG, *et al.*, 2012). As it can be seen in Figure 3.2 (MANTRIPRAGADA, RUBIN, 2017b), the carbonation reaction will only take place below the temperature corresponding to the equilibrium partial pressure of CO₂. It is generally agreed that the ideal operating temperature is approximately 650 °C in the carbonator reactor, considering carbonation reactions kinetics and equilibrium limitations (HAAF, HILZ, *et al.*, 2018). For calcination, reaction temperature also depends on CO₂ partial pressure and type of sorbent fed to the calciner. In pure CO₂ atmospheric pressure, complete calcination occurs for temperatures above 900°C for dolomite and limestone. Even though higher operating temperatures favours reaction kinetics, it starts inducing greater sorbent sintering, decaying CO₂ capture efficiency, and increasing the need for fresh sorbent (HANAK, MICHALSKI, *et al.*, 2018). Values just above the equilibrium temperature of 900°C are ideal to ensure accelerate kinetics and almost full calcination in the calciner (DIEGO, MARTÍNEZ, *et al.*, 2015, JUNK, KREMER, *et al.*, 2014). Therefore, optimal operational window of CaL systems needs to counter-balance reactions kinetics and mechanical constraints.

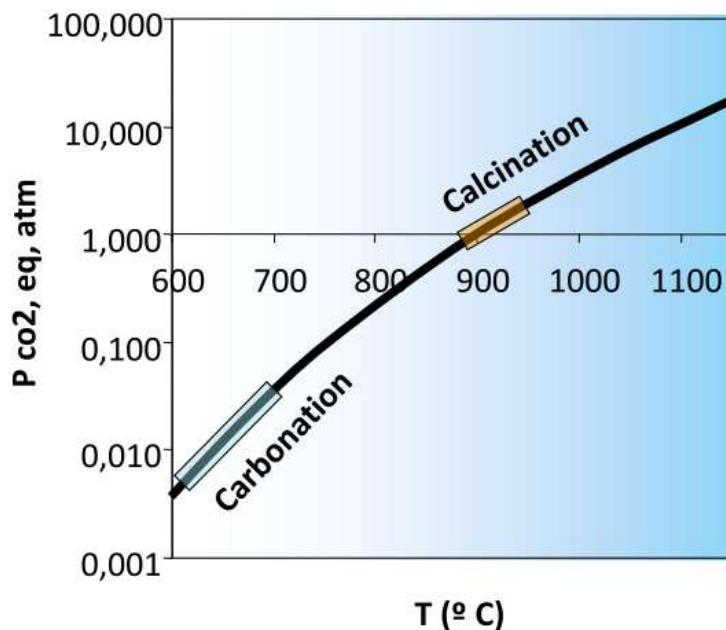


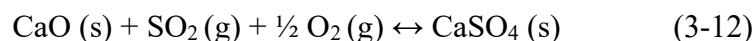
Figure 3.2 Equilibrium of the calcination and carbonation reactions based on CO₂ partial pressure. Obtained from Mantripragada and Rubin (2017a).

Synthetic and enhanced materials (mainly through doping, thermal and chemical treatment) have been proposed as an alternative for natural limestone or dolomite, in order to increase CO₂ uptake during carbonation/calcination cycles (FENNELL, ANTHONY, 2015, MORENO, 2017). Additionally, CaO reactivation methods, aimed at effectively

recovering sorbents capture capacity, may also be a strategic improvement, with hydration being one of the reactivation mechanisms that has shown promising results (FAN, ZENG, *et al.*, 2012, PAWLAK-KRUCZEK, BARANOWSKI, 2017). Another reactivation mechanism is extended carbonation in a separate third reactor (FENNELL, ANTHONY, 2015, MARTÍNEZ, I., ARIAS, *et al.*, 2018). However, reactivation methods and synthetic and enhanced materials usually present a higher cost and their development is still in initial phases. For these reasons, this work focuses on the standard CaL cycle, with the use of natural limestone as sorbent.

3.1.2 Solids mass balance

Important objectives of a mass balance in CaL cycles are to calculate the amount of sorbent circulating between the reactors and the sorbent inventory required for designed capture efficiency. In large-scale plants, inventory of solids circulating within reactors is much higher than in loop seals (between reactors) (DIEGO, MARTÍNEZ, *et al.*, 2015). CaO reacts not only with CO₂ in carbonation (equation 2-8), but also with any residual SO₂ (which was not captured in a previous flue gas desulphurisation (FGD) unit in the existing plant) by forming CaSO₄ in a sulphation reaction, as shown in equation (3-12). In fact, SO₂ reacts with CaO more readily than CO₂. For this reason, a fraction of sorbent equivalent to the amount of residual SO₂ in flue gas and sulphur in the calciner fuel is assumed to be unavailable for CO₂ capture. Then, besides the unreacted CaO, both CaCO₃ and CaSO₄ coexist in the recirculating solids streams. Another solid component present in the recirculating sorbent is ash originated from the oxy-combustion of carbonaceous fuel in the calciner (MANTRIPRAGADA, RUBIN, 2014).



As CaSO₄ is more stable and does not dissociate into CaO and SO₂ under calcination operating conditions, the solid it is usually treated as inert along with ash and limestone impurities (MANTRIPRAGADA, RUBIN, 2014).

Carbonator solids inlet flows:

The inlet streams are identified with the subscript “1” and outlet streams with the subscript “2”. Parameters with “F” represent molar flows. The inlet solid streams for the carbonator contains CaO, uncalcined CaCO₃, impurities in limestone (considered inert),

CaSO₄, and ash. Molecular weight of sorbent impurities is assumed to be equal to that of CaCO₃ (MANTRIPRAGADA, RUBIN, 2014). As demonstrated in equation (3-12), one mole of SO₂ reacts with one mole of CaO. Thus, the molar flow of CaO available for carbonation entering the carbonator might be represented by the following equation:

(3-13)

$$F_{CaO,available} = F_{CaO,1} - F_{SO_2,flue\ gas}$$

Maximum conversion of $F_{CaO,available}$ is limited by X_{ave} , defined in equation (3-9), and dependent upon the activity of recirculated sorbent and the amount of fresh sorbent input. The actual conversion fraction of CaO in the carbonator, in turn, is represented by X_{carb} , defined in equation (3-10), and depends on the designed degrees of carbonation and calcination. As presented in equation (2-8), one mole of CaO reacts with one mole of CO₂ to form one mole of CaCO₃. Therefore, the amount of CaCO₃ that is formed in the carbonator is equal to the amount of CO₂ captured, as presented below in equation (3-14):

(3-14)

$$\begin{aligned} F_{CaCO_3,carbonated} &= \eta_{CO_2} F_{CO_2,fluegas} = X_{carb} F_{CaO,available} \\ &= X_{carb} (F_{CaO,1} - F_{SO_2,flue\ gas}) \end{aligned}$$

Where η_{CO_2} represents the CO₂ capture rate/efficiency in the carbonator and $F_{CO_2,fluegas}$ represents the molar flow of CO₂ in the flue gas entering the carbonator. From equation (3-14), the inlet molar flow of CaO can be revealed in terms of the following input variables:

(3-15)

$$F_{CaO,1} = \frac{\eta_{CO_2} F_{CO_2,fluegas}}{X_{carb}} + F_{SO_2,flue\ gas}$$

Considering X_{calc} is the fraction of CaCO₃ in the inlet sorbent flow, inlet molar flow of CaCO₃ can be expressed as:

(3-16)

$$F_{CaCO_3,1} = \frac{X_{calc}}{1 - X_{calc}} F_{CaO,1}$$

Then, fresh sorbent molar flow (CaCO₃ make-up) can be calculated as follows, based on the input parameter F_0/F_R :

$$F_{CaCO3,makeup} = \frac{F_0}{F_R} (F_{CaO,1} + F_{CaCO3,1}) = \frac{\frac{F_0}{F_R}}{1 - X_{calc}} F_{CaO,1} \quad (3-17)$$

The equation (3-17) above considers that $F_0 = F_{CaCO3,makeup}$ and $F_{CaO,1} + F_{CaCO,1} = F_R$. Equations for molar flow inlets of CaSO₄ and ash in the carbonator will be found later. When limestone purity $a_{sorbent}$ is taken into account, equations for inert make-up and sorbent make-up develop as follows:

$$F_{inert,makeup} = \frac{1 - a_{sorbent}}{a_{sorbent}} F_{CaCO,makeup} \quad (3-18)$$

$$F_{sorbent,makeup} = \frac{1}{a_{sorbent}} F_{CaCO3,makeup} \quad (3-19)$$

Carbonator solids outlet flows or calciner solids inlet flows:

The molar flow of CaCO₃ leaving the carbonator is composed by the uncalcined molar flow that entered plus the molar flow of CaCO₃ formed inside the carbonator:

$$\begin{aligned} F_{CaCO3,2} &= F_{CaCO3,1} + F_{CaCO3,carbonated} = F_{CaCO3,1} + \eta_{CO} F_{CO2,flue\ gas} \\ &= F_{CaCO,1} + X_{carb} (F_{CaO,1} - F_{SO2,flue\ gas}) \end{aligned} \quad (3-20)$$

As one mole of SO₂ in the flue gas forms one mole of CaSO₄:

$$F_{CaSO4,2} = F_{CaSO4,1} + F_{SO2,flue\ gas} \quad (3-21)$$

The other inert is ash from the calciner and sorbent impurities, and can be represented as follows:

$$F_{as,2} = F_{ash,1} \quad (3-22)$$

(3-23)

$$F_{inert,2} = F_{inert,1}$$

The last solid stream to be accounted for in the carbonator is the outlet stream of CaO. As one mole of CaO in the inlet forms one mole of CaCO₃ and one mole of SO₂ in the flue gas consumes one mole of CaO, the following equation, derived from equation (3-20), represents this molar flow:

(3-24)

$$F_{CaO,2} = F_{CaO,1} - F_{CaCO_3,carbonate} - F_{SO_2,flue\ gas} = F_{CaO,1} - F_{CaCO_3,2} + F_{CaCO_3,1} - F_{SO_2,flue\ gas} = (1 - X_{carb})(F_{CaO,1} - F_{SO_2,flue\ gas})$$

Calcliner outlet solid flows:

The inlet streams are identified with the subscript “2” and outlet streams with the subscript “3”. CaO is formed in the calciner by calcination of CaCO₃ that comes from the carbonator and the make-up flow. The SO₂ from the oxy-combusted fuel also consumes CaO. Thus, the molar flow of CaO that leaves the calciner can be represented with the following equation:

(3-25)

$$F_{CaO,3} = F_{CaO,2} + F_{CaO,calcined} - F_{SO_2,oxy} \\ = F_{CaO,2} + (F_{CaCO_3,2} + F_{CaCO_3,makeup} - F_{CaCO_3,3}) - F_{SO_2,oxy}$$

By its definition, X_{calc} can be represented as:

(3-26)

$$X_{calc} = \frac{F_{CaCO_3,3}}{F_{CaCO_3,3} + F_{CaO,3}} = \frac{F_{CaCO_3,1}}{F_{CaCO_3,1} + F_{CaO,1}}$$

Thus, $F_{CaO,3}$ can be derived as:

(3-27)

$$F_{CaO,3} = F_{CaO,1} + (1 - X_{calc})(F_{CaCO_3,makeup} - F_{SO_2,oxy} - F_{SO_2,flueg})$$

From equation (3-26) and (3-27):

$$\begin{aligned}
 F_{CaCO_3,3} &= \frac{X_{calc}}{1 - X_{calc}} F_{CaO,3} \\
 &= \frac{X_{calc}}{1 - X_{calc}} F_{CaO,1} + X_{calc}(F_{CaCO_3,makeup} - F_{SO_2,oxy} - F_{SO_2,fluegas})
 \end{aligned}
 \tag{3-28}$$

As presented in equation (3-16) the term $\frac{X_{calc}}{1 - X_{calc}} F_{CaO,1}$ is equal to $F_{CaCO_3,1}$. Then, if complete calcination occurs and $X_{calc} = 0$, there will be no flow of $CaCO_3$ out of the calciner and $F_{CaCO_3,3}$ will equal 0. To account for all components, flows for ash and $CaSO_4$ can be calculated as follows:

$$F_{CaSO_4,3} = F_{CaSO_4,2} + F_{SO_2,oxy} = F_{CaSO_4,1} + F_{SO_2,fluegas} + F_{SO_2,oxy}
 \tag{3-29}$$

$$F_{CaSO_4,3} = F_{CaSO_4,2} + F_{SO_2,oxy} = F_{CaSO_4,1} + F_{SO_2,fluegas} + F_{SO_2,oxy}
 \tag{3-30}$$

$$F_{ash,3} = F_{ash,2} + F_{ash,oxy} = F_{ash,1} + F_{ash,oxy}
 \tag{3-31}$$

$$F_{inert,3} = F_{inert,2} + F_{inert,makeup} = F_{inert,1} + F_{inert,makeup}$$

Purge solid flows:

As purge flows are usually taken from the calciner outlet streams, the molar flow rates of purges will be the difference between flow rates of calciner outlet “3” and carbonator inlet “1”. Thus:

$$F_{CaO,purge} = F_{CaO,3} - F_{CaO,1} = (1 - X_{calc})(F_{CaCO_3,makeup} - F_{SO_2,oxy} - F_{SO_2,fluegas})
 \tag{3-32}$$

$$F_{CaCO_3,purge} = F_{CaCO_3,3} - F_{CaCO_3,1} = X_{calc}(F_{CaCO_3,makeup} - F_{SO_2,oxy} - F_{SO_2,fluegas})
 \tag{3-33}$$

$$F_{CaCO_3,purge} = F_{CaCO_3,3} - F_{CaCO_3,1} = X_{calc}(F_{CaCO_3,makeup} - F_{SO_2,oxy} - F_{SO_2,fluegas})
 \tag{3-34}$$

$$F_{CaSO_4,purge} = F_{CaSO_4,3} - F_{CaSO_4,1} = F_{SO_2,oxy} + F_{SO_2,fluegas}
 \tag{3-35}$$

$$F_{ash,purge} = F_{ash,3} - F_{ash,1} = F_{ash,oxy}$$

(3-36)

$$F_{inert,purge} = F_{inert,3} - F_{inert,1} = F_{inert,makeup}$$

Purge molar flows equations for CaSO₄ and ash confirm the mass balance of the complete system, as sulphur from flue gas and oxy-combustion goes out through purge, as well as ash coming from oxy-combustion. Considering purge is taken from calciner outlet streams “3”, the fraction of different solid streams in the total flow will be equal for streams “1”, “3” and “purge”, which means the following equation is valid:

(3-37)

$$\frac{F_{CaSO4,1}}{F_{CaCO3,1}} = \frac{F_{CaSO4,purge}}{F_{CaCO3,purge}}$$

Thus, combining equations (3-16), (3-33) and (3-34), equation (3-37) can be derived as:

(3-38)

$$F_{CaO,1} = \frac{F_{CaO,1}}{1 - X_{calc}} \frac{(F_{SO2,fluegas} + F_{SO2,oxy})}{(F_{CaCO3,makeup} - F_{SO2,oxy} - F_{SO2,fluegas})}$$

In a similar way, $F_{ash,1}$ and $F_{inert,1}$ can be expressed as:

(3-39)

$$F_{ash,1} = \frac{F_{CaO,1}}{1 - X_{calc}} \frac{(F_{ash,oxy})}{(F_{CaCO3,makeup} - F_{SO2,oxy} - F_{SO2,fluegas})}$$

(3-40)

$$F_{inert,1} = \frac{F_{CaO,1}}{1 - X_{calc}} \frac{(F_{inert,makeup})}{(F_{CaCO3,makeup} - F_{SO2,oxy} - F_{SO2,fluegas})}$$

Therefore, total flow of solids at the carbonator inlet can be calculated as follows:

(3-41)

$$\begin{aligned} F_{total,1} &= F_{CaO,1} + F_{CaCO3,1} + F_{CaSO4,1} + F_{ash,1} + F_{inert,1} \\ &= \frac{F_{CaO,1}}{1 - X_{calc}} \left(1 + \frac{F_{SO2,oxy} + F_{SO2,fluegas} + F_{inert,makeup} + F_{ash,oxy}}{F_{CaCO3,makeup} - F_{SO2,oxy} - F_{SO2,fluegas}} \right) \end{aligned}$$

To solve this equation, the variables $F_{SO2,oxy}$ and $F_{ash,oxy}$ have to be known. However, these variables depend on the amount of fuel burnt in oxy-combustion, which

relies upon the heat requirement of the calciner, and, as a consequence, the heat balance of the calciner needs to be solved. The next section calculates these variables.

3.1.3 Heat (Energy) balance

The energetic loop of the capture process for the proposed retrofit configuration should consider the energy supplied to the calciner from the additional fuel and the exothermic reaction occurring in the carbonator. Heat input to the calciner should be sufficient to heat the inlet streams up to the calcination temperature - between 900 and 950 °C - and supply thermal energy for the calcination reaction. Calciner inlet streams include the solid streams from the carbonator, the solid stream of sorbent make-up, and recycled flue gases (MANTRIPRAGADA, RUBIN, 2014, 2017b). The recycled flue gas is needed despite the endothermic calcination reaction taking place in the calciner because high O₂ contents can lead to local hot-spots²⁰ and enhance sorbent sintering in the reactor (HANAK, BILİYOK, *et al.*, 2015b). Considering the reaction heat is supplied by oxy-combustion of a fuel, the following equation can be used to account for this heat requirement:

$$H_{calc} = \frac{m_{fuel} HHV_{fuel}}{\eta_{comb}} \quad (3-42)$$

Where H_{calc} is the heat requirement of the calciner and can be represented in kJ/s, m_{fuel} is the mass flow rate of fuel (kg/s as-burnt in wet basis), HHV_{fuel} is the fuel higher heating value and η_{comb} is the efficiency of the oxy-combustion. The variable m_{fuel} can be expressed in terms of the molar contents of its constituents, as follows:

$$m_{fuel} = F_i \left(\frac{MW_i}{w_i} \right) \quad (3-43)$$

²⁰ The state-of-the-art CaL configuration assumes that, similarly to oxy-fuel combustion systems, the CO₂-rich stream leaving the calciner needs to be recycled to moderate the temperatures inside calciner and avoid hot-spots, which ultimately leads to increased heat requirement in the system. Few studies have proposed steady state operation with no flue gas recirculation and/or 100%vol O₂ concentration or minimum flue gas recycling, with O₂ concentration higher than 75%vol in the gas stream entering the calciner (EUROPEAN COMMISSION, 2019; HANAK *et al.*, 2018a). Results of these studies report temperatures within the calciner operation range and potential for significant reductions in specific capital cost and cost of energy, though further development is necessary.

Where F_i is the inlet molar flow of a component "i" (C, S, H₂, ash, and others), MW_i is the molecular weight of the components and w_i is the weight fraction of the component in fuel²¹, obtained from the ultimate analysis data of the fuel in a wet basis. Inlet molar flow rates of fuel components can be expressed in terms of equation (3-42), as follows:

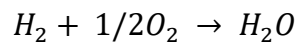
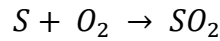
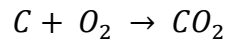
$$F_{C,inlet} = \left(\frac{H_{calc}}{HHV_{fuel}} \right) \left(\frac{w_C}{12} \right) \quad (3-44)$$

$$F_{S,inlet} = \left(\frac{H_{calc}}{HHV_{fuel}} \right) \left(\frac{w_S}{32} \right) \quad (3-45)$$

$$F_{H_2,inlet} = \left(\frac{H_{calc}}{HHV_{fuel}} \right) \left(\frac{w_{H_2}}{2} \right) \quad (3-46)$$

$$F_{as ,inlet} = \left(\frac{H_{calc}}{HHV_{fuel}} \right) \left(\frac{w_{as}}{MW_{ash}} \right) \quad (3-47)$$

The following main reactions, apart from calcination and sulphation reactions already presented in equations (2-8) and (3-12), respectively, take place in the oxy-combustion calciner:



Accounting for the number of moles in those reactions, the amount of O₂ that needs to enter the calciner can be expressed as:

$$(3-49)$$

²¹ The fuel supplied to the calciner can be coal, biomass, natural gas, etc.

$$F_{O_2,inlet} = (1 + x_a) (F_{C,inlet} + F_{S,inlet} + \frac{1}{2}F_{H_2,inlet})$$

Where x_a represents the excess oxygen for oxy-combustion. A value of 2 vol% (dry basis) for x_a is used in HILZ *et al.* (2019), while 2.5% is used in HANAK *et al.* (2016a). A typical ASU will have an inlet molar flow of N_2 dependent on the value of $F_{O_2,inlet}$, as the following equation express:

(3-50)

$$F_{N_2,inlet} = \left(\frac{0.05}{0.95}\right)F_{O_2,inlet}$$

Considering the solid mass balance and the reactions in (3-48), the gaseous products flow rates from the calciner can be expressed as the following equations, assuming no NO_x is formed:

(3-51)

$$F_{CO_2,product} = F_{CaCO_3,calcined} + F_{C,inlet}$$

$$F_{H_2O,product} = F_{H_2,inlet}$$

$$F_{N_2,product} = F_{N_2,inlet}$$

$$F_{SO_2,product} = 0$$

$$\begin{aligned} F_{O_2,product} &= F_{O_2,inlet} - \left(F_{C,inlet} + \frac{3 F_{S,inlet}}{2} + \frac{1}{2}F_{H_2,inlet}\right) \\ &= x_a \left(F_{C,inlet} + \frac{1}{2}F_{H_2,inlet}\right) + \left(x_a - \frac{1}{2}\right) F_{S,inlet} \end{aligned}$$

A fraction of the gaseous products of the calciner is recycled, in order to moderate the temperature in the oxy-combustion reactor. Thus, a part of the heat requirement goes into heating the recycled stream, rich in CO_2 . First works on CaL systems accounted for no recirculation (ROMANO *et al.* 2012) and a part of recent works also claim the possibility of using a rich-oxygen environment in the calciner (above 75% vol) (PARKKINEN, MYÖHÄNEN, *et al.*, 2017) or even no recirculation (ERANS, JEREMIAS, *et al.*, 2017, HANAK, ERANS, *et al.*, 2018). This is justified by the fact CaL systems will have large amounts of relatively cold particles introduced to the calciner as well as heat absorbed by the calcination reaction, which would permit higher oxygen

inlet concentrations than conventional oxy-combustion boilers (HAAF, HILZ, *et al.*, 2018).

However, the standard CaL concept currently defines values for the percentage of gas fraction recirculated close to 60% at 900 °C, so the calciner environment will have an oxygen concentration of 30 vol%, similar to oxy-combustion conditions. (HAAF, HILZ, *et al.*, 2018). Recycling of around 60% of the gas stream exiting the calciner is also proposed by MARTÍNEZ *et al.* (2013) to achieve an oxygen inlet concentration of 25 vol%. The recycled stream is identified with the “r” subscript and x_r is the fraction of recycled gases. If values for x_r and x_a are assumed, all recycled gas flows can be expressed in terms of known parameters and H_{calc} . Then, the molar flow rates of gases in the recycled stream can be derived as the following equations:

$$(3-52)$$

$$F_{CO_2,r} = \frac{x_r}{1 - x_r} \left(F_{CaCO_3, calcined} + \frac{H_{calc}}{HHV_{fuel}} \frac{w_C}{12} \right)$$

$$F_{H_2O,r} = \frac{x_r}{1 - x_r} \left(\frac{H_{calc}}{HHV_{fuel}} \frac{w_{H_2}}{2} \right)$$

$$F_{O_2,r} = \frac{x_r}{1 - x_r} \left(\frac{H_{calc}}{HHV_{fuel}} \right) \left(x_a \left(\frac{w_C}{12} + \frac{w_{H_2}}{4} \right) + \left(x_a - \frac{1}{2} \right) \left(\frac{w_S}{32} \right) \right)$$

$$F_{N_2,r} = \frac{x_r}{1 - x_r} \left(\frac{H_{calc}}{HHV_{fuel}} \right) \left(1 + x_a \right) \left(\frac{w_C}{12} + \frac{w_{H_2}}{4} + \frac{w_S}{32} \right)$$

The heat balance can be calculated by the specific heats of gases and solids entering and leaving the calciner and the formation of CaO reaction enthalpy. The calciner heat requirement, neglecting the flow of ash, can be expressed as (CLARENS, ESPÍ, *et al.*, 2016, MANTRIPRAGADA, RUBIN, 2017b):

$$(3-53)$$

$$H_{calc} = F_{CaCO_3, calcined} h_{CaCO_3} + \left(F_{CaO,2} C_{p,CaO} + (F_{CaCO_3,2} + F_{inert,2}) C_{p,CaCO_3} \right. \\ \left. + F_{CaSO_4,2} C_{p,CaSO_4} \right) \Delta T_{calc-carb} + \frac{F_{CaCO_3, makeup}}{a_{sorbent}} C_{p,CaCO_3} \Delta T_{calc-makeu} \\ + \sum F_{i,r} C_{p,i} \Delta T_{calc-r}$$

Where C_p stands for the solids heat capacity and can be expressed in $J mol^{-1}$, F represents the molar flow rates and can be expressed in mol/s, $\Delta T_{calc-carb}$ is the temperature

difference between the calciner and the carbonator, $\Delta T_{\text{calc-makeup}}$ is the temperature difference between the calciner and the fresh sorbent and $\Delta T_{\text{calc-r}}$ is the temperature difference between the calciner and recycled stream. Finally, h_{CaCO_3} is the calcination reaction heat of CaCO_3 at a specified temperature (which can also be expressed in J mol^{-1}).

From equation (3-53) above, $F_{\text{CaCO}_3, \text{calcined}}$, F_{CaSO_4} and $F_{\text{CO}_2, r}$ depend on $F_{\text{SO}_2, \text{oxy}}$. However, $F_{\text{SO}_2, \text{oxy}}$ is the same as the term $F_{S, \text{inlet}}$ defined in equation (3-45) and can be written in terms of H_{calc} and HHV_{fuel} . The same is true for $F_{\text{ash, oxy}}$, which is equal to $F_{\text{ash, inlet}}$, defined in equation (3-47). Thus, all parameters in the above equation are known and H_{calc} can be calculated (MANTRIPRAGADA, RUBIN, 2017b). Now, it is possible to calculate the mass balance of gases in the CaL system.

3.1.4 Gases mass balance

Carbonator outlet:

For the carbonator outlet, the molar flow of CO_2 depends on the design parameter of capture efficiency in the carbonator, or η_{CO_2} . The molar flow of O_2 is consumed by the molar flow of SO_2 in the flue gas, as the following equations express. All other gases molar flows do not change:

$$\begin{aligned} F_{\text{CO}_2, 2} &= (1 - \eta_{\text{CO}_2}) F_{\text{CO}_2, \text{fluegas}} \\ F_{\text{O}_2, 2} &= F_{\text{O}_2, \text{fluegas}} - F_{\text{SO}_2, \text{fluegas}} \end{aligned} \quad (3-54)$$

Calciner outlet:

For the calciner outlet, assuming no NO_x is formed, the molar flow of gases can be derived from previous equations for recycled and inlet gases, as follows:

$$\begin{aligned} F_{\text{CO}_2, \text{calciner, out}} &= \frac{1}{1 - x_r} (F_{\text{CaCO}_3, \text{calcined}} + F_{C, \text{inlet}}) \\ F_{\text{H}_2\text{O}, \text{calciner, out}} &= \frac{1}{1 - x_r} F_{\text{H}_2, \text{inlet}} \\ F_{\text{O}_2, \text{calciner, out}} &= \frac{1}{1 - x_r} \left(x_a \left(F_{C, \text{inlet}} + \frac{1}{2} F_{\text{H}_2, \text{inlet}} \right) + \left(x_a - \frac{1}{2} \right) F_{S, \text{inlet}} \right) \end{aligned} \quad (3-55)$$

$$F_{N2,calciner,out} = \frac{1}{1 - x_r} F_{N2,inle}$$

The CO₂-rich product stream of the calciner is then the sum of the flow rates above multiplied by $1 - x_r$ and can be expressed as:

$$\begin{aligned} F_{calciner,stream} &= (1 - x_r) (F_{CO2,calciner,out} + F_{H2O,calciner,out} + F_{O2,calciner,out} \\ &+ F_{N2,calciner,out}) \end{aligned} \tag{3-56}$$

3.1.5 Heat recovery from the CaL process

There is a large amount of high-grade heat recoverable in the CaL plant, and steam can be generated in the heat recovery steam generator (HRSG) and sent to the secondary steam cycle to increase the power output of the integrated CCS system (HANAK, BILYOK, ANTHONY, *et al.*, 2016). The reaction heat from carbonation is usually directly recovered from the carbonator with an integrated heat exchanger. The usual design assumption is that water runs through the heat exchanger, which is placed inside the carbonator, and helps maintain a steady carbonator temperature while producing steam for power generation. Likewise, flue gas stream leaving the carbonator and CO₂-rich product stream leaving the calciner are at high-temperatures, and thus have latent heat extracted by the cooling system (CLARENS, ESPÍ, *et al.*, 2016, FENNELL, ANTHONY, 2015).

These three high-grade heat streams can work as economizer, evaporator, superheater, reheater, or feedwater heaters depending on their temperature levels (ZHANG, SONG, 2019). Pinch method or exergy analysis can be used to achieve an optimum configuration for heat integration (ROMEO, *et al.* 2010). There are also three low-grade heat streams in the system that can be used: the purge flow, the heat from the intercoolers in CO₂ compression, and the heat from the intercoolers in the ASU compression step (ZHANG, SONG, 2019).

In preliminary analyses, the amount of energy recovered might be obtained as a fraction of the energy supplied to the calciner (CLARENS, ESPÍ, *et al.*, 2016). More specifically, the heat released in the carbonator H_{carb} is a combination of carbonation reaction heat and solids and gas high-temperature streams entering and leaving the reactor

in steady-state. For this reason, the amount of heat from these three sources can be calculated as follows:

$$\begin{aligned}
 H_{carb} = & (F_{CO_2,2} - F_{CO_2,fluegas})h_{CO_2} + (F_{CaO,2} - F_{CaO,1})h_{CaO} \\
 & + (F_{CaCO_3,2} - F_{CaCO_3,1})h_{CaCO_3} \\
 & + (F_{N_2,fluegas}C_{p,N_2} + F_{O_2,fluegas}C_{p,O_2} + F_{H_2O,fluegas}C_{p,H_2O} \\
 & + F_{CO_2,fluegas}C_{p,CO_2})\Delta T_{25-fluega} \\
 & + (F_{CaO,1}C_{p,CaO} + F_{CaCO_3,1}C_{p,CaCO_3} + F_{CaSO_4,1}C_{p,CaSO} \\
 & + F_{ash,1}C_{p,ash})\Delta T_{25-calc} \\
 & + (F_{N_2,2}C_{p,N_2} + F_{O_2,2}C_{p,O_2} + F_{H_2O,2}C_{p,H_2O} + F_{CO_2,2}C_{p,CO_2} \\
 & + F_{CaO,2}C_{p,CaO} + F_{CaCO_3,2}C_{p,CaCO_3} + F_{CaSO_4,2}C_{p,CaSO} \\
 & + F_{ash,2}C_{p,ash})\Delta T_{carb-25}
 \end{aligned}
 \tag{3-57}$$

In addition, assuming the flue gas is cooled up to 50°C in an external heat exchanger, before being redirected to the stack, heat recovered in this stream can be calculated as:

$$H_{fluegas} = (F_{N_2,2}C_{p,N_2} + F_{O_2,2}C_{p,O_2} + F_{H_2O,2}C_{p,H_2O} + F_{CO_2,2}C_{p,CO_2})\Delta T_{carb-50}
 \tag{3-58}$$

Finally, one can calculate the heat recovered from the cooling of the calciner output gases up to a recycle steam temperature. The temperature of the recycled stream can be assumed as 120°C (MANTRIPRAGADA, RUBIN, 2017b):

$$\begin{aligned}
 H_{CO_2,cool} = & (F_{N_2,calc,out}C_{p,N_2} + F_{O_2,calc,out}C_{p,O_2} + F_{H_2O,calc,out}C_{p,H_2O} \\
 & + F_{CO_2,calc,out}C_{p,CO_2})\Delta T_{calc-120}
 \end{aligned}
 \tag{3-59}$$

The steam power generated from the heat recovered depends on the steam cycle heat rate HR_{steam} . Assuming all heat streams presented above can be integrated into a new steam cycle, the steam power generated can be calculated as the equation below:

$$ST_{power} = (-H_{carb} + H_{fluegas} + H_{CO_2,cool})/HR_{steam}
 \tag{3-60}$$

3.2 Carbonator and calciner reactor design for fluidized-bed systems

This section provides details for reactors' design and operation, which are further used to calculate solids inventory and system costs. As seen in previous sections, CaL systems should be designed and operated with the pair of reactors carbonator and calciner and their interconnections. These interconnections should facilitate solids flow between reactors and effective flue gas separation at atmospheric pressure. The reactors are usually seen as CFBs, and the interconnections are generally designed as non-mechanical valves known as loop-seals, while cyclones are responsible for the solid-gas separation. Therefore, this section will discuss available reactor models including key parameters on thermodynamics, deactivation mechanism, and kinetics.

3.2.1 Carbonator design

Several studies, including experimental and analytical, have dealt with the subject of carbonator design, including the works by RODRIGUEZ *et al.* (2011), CORMOS AND SIMON (2013), DIEGO *et al.* (2015), ORTIZ *et al.* (2015), ROMANO (2012), HAAF *et al.* (2017) and LASHERAS *et al.* (2011). In the work by ROMANO *et al.* (2012), previous studies are reviewed and carbonator models are compared based on the following modelling steps: particle conversion, sorbent carrying capacity/decay, hydrodynamic regime of the reactors, hydrodynamic model, particles size distribution, criteria for reactor designing and inclusion of sulphur and ash effects (ROMANO *et al.*, 2012).

Particle conversion was briefly discussed in section 3.1.1. According to more recent kinetic models, the carbonation reaction takes place in two stages with different reaction rates. A first regime chemically-controlled, where the reaction occurs at the highest velocity, and a second regime diffusion-controlled, limited by the CaCO₃ product layer thickness increase (ALONSO, RODRÍGUEZ, *et al.*, 2009, ROMANO, 2012). Equations for sorbent carrying decay were also discussed in section 3.1.1 and, for a carbonator model to be accurate, must take into account the real age of the CaO particles in the system N_{age} , which represents the number of cycles that particles require to achieve a conversion equal to their carrying capacity. This parameter depends on particle residence time in the reactors (ROMANO *et al.*, 2012). In more recent works, the hydrodynamic regime of the carbonator is based on CFBs. Although some of the first

studies considered the carbonator as a bubbling fluidized bed (BFB) (SHIMIZU, HIRAMA, *et al.*, 1999), it was found that the fast fluidization regime is more appropriate considering needed reactions residence time (CORMOS, SIMON, 2013, RODRIGUEZ *et al.*, 2011, ROMANO, 2012).

Regarding hydrodynamic models, some works have used semi-predictive models based on simple thermodynamics and have considered the carbonator to be perfectly and instantaneously mixed for the solids, or a continuous stirred-tank reactor (CSTR) and plug-flow for the gas phase (ALONSO, RODRÍGUEZ, *et al.*, 2009, DIEGO., MARTÍNEZ, *et al.*, 2015, RODRIGUEZ, ALONSO, ABANADES, 2011). These works often consider the carbonator as a stoichiometric reactor, with all reactions in equilibrium (HANAK, ANTHONY, *et al.*, 2016). Other works have used a semi-predictive core-annulus model with an upper lean and a lower dense region based on the approach for CFBs (LASHERAS, STRÖHLE, *et al.*, 2011, ROMANO, 2012). For particle size, a uniform particle diameter is often considered, which is justified since non-uniformity does not affect kinetics and absorption capacity (GRASA, ABANADES, 2006).

The review by HANAK *et al.* (2015a) also summarizes recent carbonator models and points out the one developed by ROMANO (2012) as the most advanced currently available. This semi-predictive model considers the effect of reaction kinetics, reactor hydrodynamics, and the influence of sulphation and ash accumulation in the system. It can also estimate the residence time of solids in the reactor, an important parameter in reactor design along with residence-time-distribution (RTD) curves (HANAK, ANTHONY, *et al.*, 2015, ROMANO, 2012).

On the other hand, the work of RODRIGUEZ *et al.* (2011) presented the result of several experimental campaigns and investigated carbonation efficiency and “active space-time” τ_a , which can be roughly defined as the residence time of active CaO particles in the carbonator, given by the following equation:

$$\tau_a = \frac{N_{Ca,carb} X_{active}}{F_{CO_2,inlet,fluegas}} \quad (3-61)$$

Where, $N_{Ca,carb}$ is the total number of moles of Ca-based solids (CaO and CaCO₃) in the carbonator and $X_{active} = X_{ave} - X_{carb}$, which is the fraction of CaO which is still available for CO₂ capture. The relationship between carbonator efficiency η_{CO_2}

(normalized over equilibrium efficiency) and active space-time can be expressed in linear form for τ_a , in seconds, as in the technical report by MANTRIPRAGADA, RUBIN (2017a):

$$\frac{\eta_{CO}}{\eta_{CO,eq}} = 1 - e^{-\frac{\tau_a}{14.04}} \quad (3-62)$$

To calculate the carbonator solids inventory, a perfectly mixed reactor is assumed (MANTRIPRAGADA, RUBIN, 2017a), which means the composition everywhere in the reactor is the same as the exit composition for both solids and gases. Then, carbonator capture efficiency can be expressed in terms of inlet and outlet mole fractions of CO₂ as follows:

$$\eta_{CO} = \frac{y_{CO_2,inlet} - y_{CO_2,out}}{y_{CO_2,inlet}(1 - y_{CO_2,out})} \quad (3-63)$$

Equilibrium molar fraction of CO₂ depends on operating temperature and pressure and is given by the following equation proposed by BARKER (1973) and used in other works (ALONSO, RODRÍGUEZ, *et al.*, 2009, MARTÍNEZ, GRASA, *et al.*, 2013):

$$y_{CO_2,eq} = \frac{10^{7.07 - \frac{8038}{T}}}{P} \quad (3-64)$$

Where T is temperature (in K) and P is pressure (in atm). For CaL applications, P = 1 atm. As pressure and temperature of the carbonator are known, the equilibrium CO₂ mole fraction can be calculated. From this point, $\eta_{CO,eq}$ can also be calculated (by replacing the value of $y_{CO_2,out}$ in equation 3-63 by $y_{CO_2,eq}$) and substituted in the equation for active space-time. The actual capture efficiency is a design parameter. Hence, active space-time required to achieve a desired CO₂ capture at a particular temperature and pressure is given by the following equation:

$$\tau_a(s) = \frac{14.04}{\ln\left(1 - \frac{\eta_{CO_2}}{\eta_{CO_2,eq}}\right)} \quad (3-65)$$

From the equation above, the number of moles of CaO and CaCO₃ inside the carbonator N_{Ca} can be calculated by reorganizing equation (3-61). The other solids present in the reactor are CaSO₄ and ash. With the assumption of a perfectly mixed reactor, the mole fractions of these inside the carbonator are the mole fractions at the exit, as follows:

$$y_{CaSO_4} = F_{CaSO_4,2}/F_{total,2} \quad (3-66)$$

$$y_{as} = F_{as,2}/F_{total,2}$$

Total moles of solids in the carbonator, or solids inventory, can then be calculated as:

$$N_{solids,carb} = \frac{\tau_a F_{CO_2,inlet,fluegas}}{X_{active} (1 - y_{CaSO_4} - y_{as})} \quad (3-67)$$

Thus, solids residence time in the carbonator can be calculated as follows:

$$\tau_{res,carb} = \frac{N_{solids,carb}}{F_{total,1}} \quad (3-68)$$

Therefore, with the equations above, the total mass and volume of the solids inventory can be calculated once the molecular weights and specific volumes of the chemical components are known.

The operational experience and results in the 1 MW_{th} scale at TU Darmstadt showed the influence of solid looping ratio and active space-time in carbonator capture efficiency (HILZ, HAAF, *et al.*, 2019). In the work by HILZ *et al.* (2019), active space-time is defined by the specific carbonator inventory (in kg/m²) and the make-up flow rate. For $\tau_{res,carb} = 42s$, specific carbonator inventory was in the range of 400–500 kg/m² and the make-up rate $F_O/F_{CO_2,fluegas}$ was around 0.1 molCa/molCO₂. For these values, carbonator capture efficiency was below 80% even for high values of solid looping ratio $F_R/F_{CO_2,fluegas}$.

A higher active space-time of 68s was achieved with 600–700 kg/m² and 0.17 molCa/molCO₂, and capture efficiency surpassed 90% for higher solid looping ratios.

Even higher active space-time of 89s achieved 90% of capture efficiency even with low solid looping ratios, by operating with 700–950 kg/m² with 0.1-0.18 mol Ca/molCO₂. The results demonstrated the influence of solid looping ratio decrease with increasing active space-time (HILZ, HAAF, *et al.*, 2019).

3.2.2 Calciner design

The oxy-fired CFB combustion reactors are considered an enabling technology for CaL, with its own developing path as a major oxy-fuel combustion capture technology for power generation (MARTÍNEZ, I., GRASA, *et al.*, 2013). The choice for this technology in CaL systems has been dominant due to the need for a large supply of thermal energy to the system and current commercial application of CFB oxy-combustors in the industry up to the 400 MW_e scale (FENNELL, ANTHONY, 2015). The thermal power requirement in the calciner is between 30% and 50% of the total energy introduced into the whole system, including the existing power plant (DIEGO, MARTÍNEZ, *et al.*, 2015, SHIMIZU, HIRAMA, *et al.*, 1999).

Calciner design and its operational window influences not only the fraction of CaCO₃ regenerated and entering the carbonator, which is the amount of CaO newly formed that will further react with CO₂ in the carbonator, but also the degree of sorbent deactivation, which affects sorbent CO₂ carrying capacity (DIEGO, MARTÍNEZ, *et al.*, 2015, MARTÍNEZ, GRASA, *et al.*, 2013). As reported by MARTÍNEZ *et al.* (2013), large-scale CaL systems will have to deal with a trade-off between achieving the lowest CaCO₃ content in the solids leaving the calciner, which is equivalent to reach high calcination conversion of CaCO₃ at a concentrated CO₂ atmosphere, and the requirements of this high calcination conversion, such as greater heat demand, high temperatures and low CO₂ partial pressures (MARTÍNEZ, I., GRASA, *et al.*, 2013). High temperatures in a steady-state will need to be moderated with increased recirculation of the CO₂ stream to minimize sorbent deactivation by sintering and to avoid ash-related problems. Therefore, substantial contributions to heat demand in the calciner are associated with heating the recirculated CO₂ stream and the inert solids flowing from the carbonator up to calciner temperature. In the end, the energy consumption in the calciner will be higher as the temperature set for the calciner increases (MARTÍNEZ, I., GRASA, *et al.*, 2013)

Based on early investigations on sorbent performance (DIEGO, MARTÍNEZ, *et al.*, 2015, GRASA, ABANADES, 2006), an upper limit of 950 °C is pointed as reasonable

to avoid these problems, but lower values will have benefits such as a less energy-demanding, more compact and lower-cost reactor (DIEGO, MARTÍNEZ, *et al.*, 2015).

The works by DIEGO *et al.* (2015) and HANAK *et al.* (2015a) summarized several attempts on modelling the calciner with different degrees of prediction. YLÄTALO *et al.* (2013) proposed an elaborated 3-D oxy-fired calciner model using computational fluidizing dynamics (CFD). The authors combined fundamental mass and energy balance equations and empirical correlations for describing chemical reactions and output solid flows. Still, they concluded that a simplified 1-D model produced similar results to those obtained with the more detailed 3-D model regarding parameters such as solids inventory. Unlike other calciner models, the model proposed by FANG *et al.* (2009) accounted for the reactor hydrodynamics using the model K-L (the same presented in the carbonator model section), which divides the reactor into two regions (FAN, LI, *et al.*, 2009, HANAK, ANTHONY, *et al.*, 2015).

The semi-predictive model by MARTÍNEZ *et al.* (2013) is based on simple hydrodynamics and a steady-state overall mass balance of the calciner. It is considered a simplified model to calculate solids inventory (DIEGO, MARTÍNEZ, *et al.*, 2015, HAAF, STROH, *et al.*, 2017, MANTRIPRAGADA, RUBIN, 2017b). It includes a realistic kinetic description of the calcination reaction for highly cycled particles and can be compared with more elaborate methods when necessary. The model is in line with the one previously described for the carbonator, following the same simple fluid dynamic assumptions for the solid and gas phases: instantaneous and perfectly mixed solids and complete combustion of the fuel at the entrance of the reactor. With the relatively fast combustion process taking place at the bottom of the reactor and a large impact of the CO₂ recycling, the perfectly mixed atmosphere is considered a reasonable assumption, as concentration along the reactor will be close to the CO₂ concentration at the exit of the calciner (DIEGO, MARTÍNEZ, *et al.*, 2015). This model was validated against experimental results in the 1 MW_{th} pilot testing plant at TU Darmstadt (HAAF, STROH, *et al.*, 2017).

Calciner solids inventory

In the conditions proposed in the work by MARTÍNEZ *et al.* (2013), the mass balance in the calciner can be expressed as follows (DIEGO, MARTÍNEZ, *et al.*, 2015, HANAK, ANTHONY, *et al.*, 2015, MARTÍNEZ, GRASA, *et al.*, 2013):

(3-69)

$$F_{CO_2,calcined} = N_{Ca,calc} r_{calc} = (F_{CaO,2} + F_{CaCO_3,2} + F_{CaCO_3,makeup})(X_{ave} - X_{calc})$$

Where $F_{CO_2,calcined}$ is the molar flow of CO_2 in the calciner as a result of the calcination reaction (equal to $F_{CaCO_3,calcined}$), r_{calc} is the calcination kinetic rate and $N_{Ca,calc}$ is the number of moles of CaO and $CaCO_3$ inside the calciner. To define the calcination kinetic rate, the expression proposed by FAN *et al.* (2009), based on a grain model and TGA experiments, can be applied to $CaCO_3$ particles that have experienced several calcination and carbonation cycles:

(3-70)

$$r_{calc} = \frac{d(X_{carb} - X_{calc})}{dt} = k_{calc} \left(1 - \frac{X_{carb} - X_{calc}}{X_{carb}}\right)^{\frac{2}{3}} (C_{CO_2,eq} - C_{CO_2})$$

Where k_{calc} is the kinetic constant for the calcination reaction, which is calculated by an Arrhenius approach (HAAF, STROH, *et al.*, 2017), $C_{CO_2,eq}$ is the equilibrium CO_2 molar concentration and C_{CO_2} is the actual molar concentration of CO_2 . Calcination in CaL systems is generally considered to be a fast chemically-controlled reaction if the equilibrium conditions are met in the oxy-fuel CO_2 -rich atmosphere, with the particles having an average diameter of less than 2 mm (YLÄTALO, PARKKINEN, *et al.*, 2013). By integrating equation (3-70), it is possible to obtain the time required to achieve complete calcination of $CaCO_3$ (HAAF, STROH, *et al.*, 2017):

(3-71)

$$t_{calc}^* = \frac{3(X_{carb})}{k_{calc} (C_{CO_2,eq} - C_{CO_2})}$$

As a consequence of the calcination model validation through experimental trials, MARTÍNEZ *et al.* (2013) determined that the calcination rate can be considered constant and independent of the $CaCO_3$ content of the particles (MARTÍNEZ, I., GRASA, *et al.*, 2013). Particles leaving the carbonator with modest $CaCO_3$ content will tend to calcine in much shorter times than fresh limestone particles entering the calciner from the make-up flow $F_{CaCO_3,makeup} = F_O$. Given the majority of particles inside the calciner will present a $CaCO_3$ content close to X_{carb} , as the typical F_O/F_R ratio of CaL systems is low, the average calcination rate can be expressed as:

(3-72)

$$r_{ave,calc} = \frac{X_{ave}}{t_{cal}^*} = \frac{k_{calc} (C_{CO_2,eq} - C_{CO_2})}{3} \text{ for } t < t_{calc}^*$$

$$r_{ave,calc} = 0 \text{ for } t \geq t_{calc}^*$$

Following the work of MARTÍNEZ *et al.* (2013) and considering the average particle residence time in the calciner, the fraction of particles that have a residence time lower than the time required for complete calcination is estimated as:

(3-73)

$$f_a = 1 - e^{-\frac{t_{calc}^*}{\tau}}$$

Where τ is the average particle residence time in the calciner, which can be defined as follows:

(3-74)

$$\tau = \frac{N_{Ca,calc}}{F_{CaO,2} + F_{CaCO_3,2} + F_{CaCO_3,makeup}}$$

Assuming ideal gases, the mole fraction of CO₂ in the calciner outlet gases can be defined as a function of molar concentration as follows:

(3-75)

$$C_{CO_2,eq} - C_{CO_2} = (y_{CO_2,eq} - y_{CO_2}) \frac{p}{RT}$$

Where p is the calciner pressure in Pa, T is the temperature in K and $y_{CO_2,eq}$ was previously defined in equation (3-64), but now is calculated for the calciner. The value of y_{CO_2} for the calciner can be derived from equation (3-56) as:

(3-76)

$$y_{CO_2} = \frac{F_{CO_2,calciner,out}}{(F_{CO_2,calciner,out} + F_{H_2O,calciner,out} + F_{O_2,calciner,out} + F_{N_2,calciner,out})}$$

According to the procedure detailed by MARTINEZ *et al.* (2013) and using the definitions above, the extent of calcination f_{calc} , which was defined as the fraction of CaCO_3 calcined in the reactor and previously described in section 3.1.1, can finally be expressed as follows:

$$f_{calc} = \frac{f_a}{\ln\left(\frac{1}{1-f_a}\right)} = \frac{1 - e^{-\frac{t_{calc}^*}{\tau}}}{\frac{t_{calc}^*}{\tau}} \quad (3-77)$$

For different values of $\frac{t_{calc}^*}{\tau}$, f_{calc} was plotted and the exponential function that fits the curve can be defined by the following expression (MANTRIPRAGADA, RUBIN, 2017b):

$$\frac{t_{calc}^*}{\tau} = 2.179 \ln\left(\frac{0.9933}{f_{calc}}\right) \quad (3-78)$$

Considering f_{calc} is a design variable, $\frac{t_{calc}^*}{\tau}$ can be calculated and substituted in the following equation for estimation of the solid inventory of Ca-based particles:

$$N_{Ca,calc} = \frac{3(F_{CaO,2} + F_{CaC,2} + F_{CaCO3,makeup})}{k_{calc}(y_{CO2,eq} - y_{CO2})\left(\frac{p}{RT}\right)} \frac{1}{\left(\frac{t_{ca}^*}{\tau}\right)} \quad (3-79)$$

Therefore, for a given calciner efficiency f_{calc} , the total solids inventory necessary in the calciner can be calculated with a similar approach used in the carbonator, considering the mole fractions of ash and CaSO_4 at the exit of the calciner:

$$N_{solids,calc} = \frac{N_{Ca,calc}}{1 - y_{CaSO4,3} - y_{as,3}} \quad (3-80)$$

Hence, for known values of molecular weight and density, total mass and volume inside the calciner can be estimated similarly to what was done with the carbonator. As a result of the equations above, for a given pressure and temperature, higher solid inventories are needed for higher values of f_{calc} , which leads to a higher solid residence

time of the CaCO₃ particles in the calciner. This implies working at temperatures of around 900 °C with reasonable specific solid inventories around 600-800 kg/m², corresponding to 1-3 min of residence time. These conditions are enough to achieve a calciner efficiency of 95% under a CO₂ concentration close to 80 vol%, which is typical of an oxy-fired boiler (DIEGO, M.E., MARTÍNEZ, *et al.*, 2015).

Finally, working around 15-20 °C above the equilibrium temperature associated with the CO₂ partial pressure is enough to obtain calciner efficiencies as high as 95% (DIEGO, M.E., MARTÍNEZ, *et al.*, 2015). Experimental results obtained from the 1.7 MW_{th} pilot plant in La Pereda have validated, with reasonable precision, the predictions made by the presented model (ARIAS, B., DIEGO, *et al.*, 2013).

3.2.3 Reactors dimensions

One of the aims of reactor design is to calculate the volume of reactors in order to estimate capital costs and pressure drop. As assumed in the last sections, both carbonator and calciner operate as a CFB reactor in a fast fluidization regime (CORMOS, SIMON, 2015, STRÖHLE, LASHERAS, *et al.*, 2009). A typical CFB has a dense lower zone and lean upper zone to account for the varying solid distribution within the riser (HAAF, M., STROH, *et al.*, 2017, HANAK, ANTHONY, *et al.*, 2015, KUNII, LEVENSPIEL, 1997). The solids fraction in the dense zone at the bottom of the reactor is a fairly constant value and can be identified as $\varepsilon_{s,d}$, while the solids fraction in the lean zone, identified as $\varepsilon_{s,l}$, undergoes an exponential decay with height towards an asymptotic value of ε_s^* as described in the following equation (CORMOS, SIMON, 2013, LASHERAS, STRÖHLE, *et al.*, 2011, MANTRIPRAGADA, RUBIN, 2017b):

$$\varepsilon_{s,l} = \varepsilon_s^* + (\varepsilon_{s,d} - \varepsilon_s^*)e^{-\alpha H_l} \quad (3-81)$$

Where α is the decay constant and H_l is the height of the lean zone. According to experimental data, α is determined by $\alpha U_g = \text{constant}$, where U_g is the superficial gas velocity. The value of α is <1 and superficial gas velocities will range between 3-7 m/s, with a realistic value close to 5 m/s (CORMOS, SIMON, 2015, HILZ, HAAF, *et al.*, 2019, LYNKFELT, LECKNER, 2015, STRÖHLE, LASHERAS, *et al.*, 2009). Typical values for αU_g are then between 2-4 s⁻¹, but it can be assumed as 3.0 s⁻¹

(MANTRIPRAGADA, RUBIN, 2017b, OZCAN, 2014, ROMANO, 2012, STRÖHLE, LASHERAS, *et al.*, 2009). Based on these assumptions, α can be calculated.

The volume fraction of solids in the dense region $\varepsilon_{s,d}$ ranges from 0.06 to 0.22, but can realistically be set to 0.15 (CORMOS, SIMON, 2015, KUNII, LEVENSPIEL, 1997, OZCAN, 2014, ROMANO, 2012), while ε_s^* can be set to 0.01 (ROMANO, 2012). These values are typical of fast fluidization regimes (KUNII, LEVENSPIEL, 1997, LASHERAS, STRÖHLE, *et al.*, 2011). Then, the average volume of solids in the lean zone can be estimated by (LASHERAS, STRÖHLE, *et al.*, 2011):

$$\varepsilon_{s,l} = \varepsilon_s^* + \frac{(\varepsilon_{s,d} - \varepsilon_s^*)}{\alpha(H_t - H_d)} \quad (3-82)$$

Where H_t is the total height of the reactor and H_d is the height of the dense zone. Thus, $H_t - H_d = H_l$.

H_t is in the order of meters, probably more than 10 meters for large-scale applications and up to 40 meters (EUROPEAN COMMISSION, 2019, ROMANO, 2012). The average lean zone solids fraction $\varepsilon_{s,l}$ can be estimated as 0.015 (MANTRIPRAGADA, RUBIN, 2017b). Hence, considering this model, total solids inventory of a reactor can be estimated based on the following equation (ROMANO, 2012):

$$m_{solids} = \rho_{solids}A(\varepsilon_{s,d}H_d + \varepsilon_{s,l}(H_t - H_d)) \quad (3-83)$$

Where ρ_{solids} is the solids density and A is the reactor cross-section area. ROMANO (2012) assumes a constant value for the ratio H_t/D of 3, being D the diameter of the reactor in meters. However, considering the wide variation in H_t/D for CFB boilers, this constant is not assumed by MANTRIPRAGADA, RUBIN (2017a). Instead, the authors assume that for solids flow rates in typical CFB applications, the ratio H_t/H_d varies between 4 and 7, but is most likely around 5. Solids inventory can then be expressed as:

$$m_{solids} = \frac{\rho_{solids}AH_t}{(H_t/H_d)} (\varepsilon_{s,d} + \varepsilon_{s,l}(H_t/H_d - 1)) \quad (3-84)$$

Where AH_t is the volume of the reactor V , which can now be expressed as:

$$V = \frac{m_{solids}(H_t/H_d)}{\rho_{solids}(\varepsilon_{s,d} + \varepsilon_{s,l}(H_t/H_d - 1))} \quad (3-85)$$

Also, the pressure drop in Pa in the reactors is calculated as:

$$\Delta p = \frac{m_{solids} \times 9.81}{A} \quad (3-86)$$

Cross-section area A in m^2 can be calculated from gas flow rates and superficial gas velocity as follows (LYNGFELT, LECKNER, *et al.*, 2001, MANTRIPRAGADA, RUBIN, 2012):

$$A_{carb} = \frac{F_{fluegas,in} \times 22.4(T_{carb} + 273.15)}{(P_{carb} \times 273.15 \times U_g)} \quad (3-87)$$

$$A_{calc} = \frac{(F_{O_2,in} + F_{recycle}) \times 22.4(T_{calc} + 273.15)}{(P_{calc} \times 273.15 \times U_g)} \quad (3-88)$$

With the above equations, reactor diameter D can be estimated. Maximum reactor inner diameter is set to 8 m by FAN (2010) since is a possible size for a CFB combustor riser. If the calculated D is greater than 8 meters, the gas flow is divided into multiple reactors.

However, larger cross sections A for the reactors are reported in several related works. LYNGFELT, LECKNER (2015) estimates cross-sections areas up to 198 m^2 for CFB and CLC-CFB reactors for a 5.4 m/s gas velocity, corresponding to a reference 1000 MW_{th} (around 400 MW_e) CFB boiler based on the actual dimensions of the Lagisza 460 MW_e plant (LYNGFELT, LECKNER, 2015). In LASHERAS *et al.* (2011), a 1052 MW_e reference plant is considered to be equipped with two carbonate looping units that divide the flue gas into two cleaning paths to reach the top of the CFB carbonator with 1163 m^3/s of volume flow rate and 80% carbonator capture efficiency. The simulation supposes a superficial gas velocity of 6 m/s at the top of the reactor and a cross-sectional area of 194

m^2 for a reactor height set to 30 m (LASHERAS, STRÖHLE, *et al.*, 2011, STRÖHLE, LASHERAS, *et al.*, 2009).

In ROMANO (2012), an example is given for a volumetric flow of $700 \text{ m}^3/\text{s}$ to be treated in a single carbonator, which roughly corresponds to a flue gas flow rate from a $600 \text{ MW}_{\text{th}}$ air-blown boiler. The CFB carbonator operates at $650 \text{ }^\circ\text{C}$ with a superficial velocity of 5 m/s and would require 140 m^2 in cross-section area (or $D = 13.4 \text{ m}$) for a height of 40 m (ROMANO, 2012). In the work of DIEGO *et al.* (2014), where a CFB recarbonator is designed, cross-sections of the carbonator and calciner, operating with a superficial gas velocity around 5 m/s , are considered to be in the order of 200 m^2 . This value is comparable to the cross-section of a CFB combustor for a power plant of $1000 \text{ MW}_{\text{th}}$ (DIEGO, ARIAS, *et al.*, 2014). In the work by MARTÍNEZ *et al.* (2018), a standard post-combustion scheme is defined for a PC subcritical power plant of 365 MW_e ($1014 \text{ MW}_{\text{th}}$ referred to the LHV of the thermal coal input) with 90% capture efficiency in the carbonator. The cross-sections of the carbonator and calciner are respectively 175.6 m^2 and 196.7 m^2 , assuming a superficial gas velocity of 5 m/s at the reactor outlet (MARTÍNEZ, I., ARIAS, *et al.*, 2018).

In the end, the cross-section area affects the investment cost, and the smallest cross-section area is desired. However, this leads to a higher gas velocity, which, in turn, is limited by entrainment of bed material and required residence time (LYNGFELT, LECKNER, *et al.*, 2001). At the same time, multiple parallel vessels operating at high temperatures are also challenging to operate.

4. Methods and Data

This chapter is divided into five subsections. Section 4.1 describes methodological procedure. Section 4.2 discusses feedstock selection criteria. Section 4.3 briefly describes the software used to simulate the technical performance and costs of the power plants with and without capture. In section 4.4, the economics of CaL is discussed and a cost model is proposed for this system. Section 4.5 presents performance assumptions for each configuration simulated -i.e. base power plants with and without capture units. The power plants with capture units are integrated with CaL or amine-based post-combustion systems.

4.1 Methodological Procedure

This study conducted the simulation of thermal power plants with carbon capture units using the IECM (Integrated Environmental Control Model) tool. Simulations were carried out for plants without carbon capture (for reference), named config. 1, and with carbon capture applying calcium looping and amine-based chemical absorption technology, named config. 2 and config. 3, respectively. The simulated base case for the CFPP represents a thermal unit with 300 MW of gross output capacity. In terms of the carbon sink for the captured CO₂, a permanent geological storage route is assumed. The specific location for storage and other aspects regarding the captured CO₂ transportation, which is assumed to be done via pipeline, are defined in general terms.

Although CO₂ transportation and storage are not the focus of this work, the selection of a carbon capture method involves the setting of a pressure at which the almost pure CO₂ stream is obtained. As pipeline transport is considered for distances close to 100-150 km, the output pressure of the capture stage should be set at around 120 atm (DA SILVA, CARVALHO, *et al.*, 2018, PAULO, SZKLO, *et al.*, 2016, TAGOMORI, CARVALHO, *et al.*, 2018). In that case, CaL configurations will present an extra CO₂ stream to be compressed because of the calcination emission.

To evaluate water use in consumption and withdraw, a wet cooling tower was assumed for the base case. However, simulations with an open cooling system (once-through) were also performed to assess differences in water use caused by the selection of

the water system (ZHAI, RUBIN, *et al.*, 2011). Water use analysis is made using the *Water Life Cycle Assessment* tool of IECM, which accounts for plant water consumption and withdrawal, including water use in chemical production (amine, limestone, and ammonia), plant infrastructure, and operation.

For the type of analysis proposed, it is more important the differences in costs for different capture technologies are accurately assessed, rather than the absolute value of an expected project cost²² (RUBIN, DAVISON, *et al.*, 2015). Thus, “technology-levelling” assumptions are applied to maintain uniformity of basic power plant assumptions (such as plant size, fuel type, capacity factor, and other variables). The main goal is to highlight differences due only to the choice of capture technology configuration. Recommended data to be presented in scientific publications for CCS technology comparison is discussed in (RUBIN, SHORT, *et al.*, 2013b) and it was used as guidance.

²² Therefore, no location factor is applied in this study, which also avoids introducing a source of uncertainty in the estimates.

4.2 Feedstock selection criteria

Among feedstocks with potential to be adopted in CaL systems, two types are particularly investigated in this work: coal, as the most used feedstock in thermal power plants (IEA, 2019g), and biomass, whose application does not yet occur in the same scale as CFPPs²³, but which is relevant in Brazil, especially using sugarcane bagasse (EPE, 2017), that accounts for about 80% of the biomass consumed in the country for electricity generation purposes (ANEEL, 2020).

Biomass is also being supported given the need of achieving net negative CO₂ emission technologies, including BECCS (CONSOLI, 2019, MOREIRA, ROMEIRO, *et al.*, 2016). Even though several types of biomass feedstocks can be used for solid combustion processes, including wood, crop residues (from rice, soy, corn, etc.) or urban and industrial waste, sugarcane bagasse has the further advantage of potential use in more modern/efficient energy conversion systems, including supercritical steam cycles (COELHO JUNIOR, DA SILVA SEGUNDO, *et al.*, 2019, MOORE, KULAY, 2019, PELLEGRINI, DE OLIVEIRA JÚNIOR, *et al.*, 2010, RITTER, 2019). The option for sugarcane bagasse conversion plants associated with CaL systems could also be favoured due to their low alkali content, which makes this biomass residue more likely to stand calcination temperatures above 900 °C without leading to bed agglomeration and fouling problems in the interconnected reactors system (BASU, 2006, 2015).

In addition, sugarcane bagasse is already used in large-scale plants in Brazil, with over 100 MWe of net output capacity (ANEEL, 2020), and present a seasonal complementarity with the dry period of hydroelectric water tanks systems that supply the country's interconnected power system (UNICA, 2018). Therefore, sugarcane bagasse is selected as the biomass feedstock.

For the case proposed, even though sugarcane bagasse does not impose, compared to coal, important material restrictions for solid direct combustion and CaL applications, some of its inherent challenges include the poor transport properties due to the bagasse elongated shape, low bulk and energy density, biodegradation due to residual sugars and spontaneous and unstable combustion (caused by high volatile and moisture content,

²³ While the average size of a coal-fired plant is around 600 MWe in the U.S (FOUT, ZOELLE, *et al.*, 2015) and is even larger for new power plants, only few dedicated biomass-fired power plants worldwide can deliver more than 100 MWe in net power output (NUORTIMO, ERIKSSON, *et al.*, 2017).

respectively). Pre-treatment by torrefaction is proposed to help counter-measure these issues (VALIX, KATYAL, *et al.*, 2017).

Natural gas is another fuel addressed in some works for application with CaL systems, especially considering NGCC plants (BERSTAD, ANANTHARAMAN, *et al.*, 2012, MOORE, KULAY, 2019). However, its utilization in CaL is often regarded as more costly and with lower thermodynamic performance than amine-based systems (BERSTAD, ANANTHARAMAN, *et al.*, 2012, HANAK, MICHALSKI, *et al.*, 2018). Therefore, it is not considered in this work.

Moreover, the full post-combustion CaL system has two inputs of feedstock, one for the base plant and another to fire the calciner. In this work, the same fuel is considered for both feedstock inlets. Notwithstanding, co-firing or mixing of feedstocks in the calciner could also be an advantageous option depending on the power plant location and feedstock availability in the plant region²⁴ (OZCAN, ALONSO, *et al.*, 2014).

Bituminous coal is selected for the coal-fired cases and to fire the calciner in the CFFP with CaL (config. 2) (FOOT, ZOELLE, *et al.*, 2015). The coal source is Appalachian medium Sulfur, as used in (MANTRIPRAGADA, RUBIN, 2014). See Table 4.1 for detailed coal properties. Price of fuel is defined as 49.87 \$₂₀₁₇/tonne in accordance with (MANTRIPRAGADA, RUBIN, 2014). Other input values are derived from IECM (default coal properties for bituminous Appalachian medium sulfur). Sensitivity analyses on the coal price for electricity generation are further performed based on values ranging from 80 to 40\$₂₀₁₇/tonne (IEA, 2019b).

²⁴ For example, the co-firing alternative proposed by HANAK *et al.* (2015) (HANAK, BILYOK, *et al.*, 2015b) uses a mix of 80% coal:20% biomass in the calciner.

Table 4.1 Coal properties

Coal rank	Bituminous
Coal specification	Appalachian Medium Sulphur
Fuel price (\$ ₂₀₁₇ /tonne)	49.87
HHV (MJ/kg)	30.84
Ultimate analysis Composition (weight % as-fired)	
Moisture	5.05
Carbon	73.81
Hydrogen	4.88
Oxygen	5.41
Nitrogen	1.42
Chlorine	0.06
Sulphur	2.13
Ash	7.24
Ash properties (weight% as-fired)	
SiO ₂	54.50
Al ₂ O ₃	17.30
Fe ₂ O ₃	4.50
CaO	10.70
MgO	2.40
Na ₂ O	1.48
K ₂ O	1.11
TiO ₂	0.70
P ₂ O ₅	0.27
SO ₃	7.04
Other	0.00

The IECM software is primarily designed to work with thermal power plants using coal or natural gas as feedstocks, so it was necessary to adapt the feedstock characteristics inputs to run simulations using sugarcane bagasse. Ultimate analysis and ash composition were obtained through the Phyllis2 database of the Energy Research Centre of Netherlands (ECN) (ECN, 2013), and the values as-fired are given on a wet mass basis in table 4.2. The price of sugarcane bagasse should include the costs of planting, harvesting, transportation, storage, and pre-processing. In the Brazilian case considered,

however, the raw material is a by-product available in suitable conditions at the sugarcane mill producing unit (KHATIWADA, LEDUC, *et al.*, 2016, MARQUES, 2011). Thus, the cost of a great part of the production chain, except for pre-processing, may be considered null since the bagasse is a by-product of the process to produce ethanol and sugar from sugarcane²⁵. If the bagasse has to be transported to the production unit, its price could be assumed to be equal to the transportation costs, which according to BASTOS (2011) is around 7 US\$/tonne (US\$ 2017 constant dollars) (BASTOS, 2011).

The typical costs of pre-processing, including milling and drying from 50% to about 10% of moisture content in mass basis were evaluated by (GERBASI, 2013) for a thermochemical route (through gasification) to produce ethanol and higher alcohols from the bagasse residue (GERBASI, 2013). The work was based in a 2011 NREL report (HUMBIRD, DAVIS, *et al.*, 2011), where drying costs for a woody material, from 50% to 10% moisture, are reported altogether with costs of biomass reception, storage, and pre-processing, accounting for a total of 7.27 US\$/tonne (US\$ 2017 constant dollars). Thus, in accordance with (GERBASI, 2013) a conservative price for the bagasse is assumed as 7.27 US\$/tonne after drying or in ready to be burned condition.

²⁵ Another approach to estimate the price of bagasse is suggested by (SILVA, , 2013) and it is based on the opportunity cost of the bagasse for bioelectricity production.

Table 4.2 Biomass properties

Biomass type	Sugarcane Bagasse
Biomass specification	#894
Fuel price (\$ ₂₀₁₇ /tonne)	7.27
HHV (MJ/kg) as-fired	17.02
LHV (MJ/kg)	15.62
Ultimate analysis composition (weight % as-fired)	
Moisture	10.39
Carbon	43.59
Hydrogen	5.26
Oxygen	38.37
Nitrogen	0.14
Chlorine	0.02
Sulfur	0.04
Ash	2.19
Ash properties composition (weight% as-fired)	
SiO ₂	46.61
Al ₂ O ₃	17.69
Fe ₂ O ₃	14.14
CaO	4.47
MgO	3.33
Na ₂ O	0.79
K ₂ O	4.15
TiO ₂	2.63
MnO ₂	0.00
P ₂ O ₅	2.72
SO ₃	2.08
Other	1.39

4.3 System simulation with software Integrated Environmental Control Model (IECM)

The Integrated environmental control model (IECM) is a software program developed by Carnegie Mellon University and mainly used to simulate operations of a range of thermal power generation technologies, such as pulverized coal (PC), natural gas combined cycle (NGCC), integrated gasification combined cycle (IGCC), and oxy-combustion (CMU EPP, 2012). These thermal power plants may be configured with or without CO₂ capture, and several capture technologies can be chosen based on user-defined parameters (MERSCHMANN, VASQUEZ, *et al.*, 2013), as exemplified for the power plant with post-combustion using CaL selected in the configuration screen of the software in Figure 4.1.

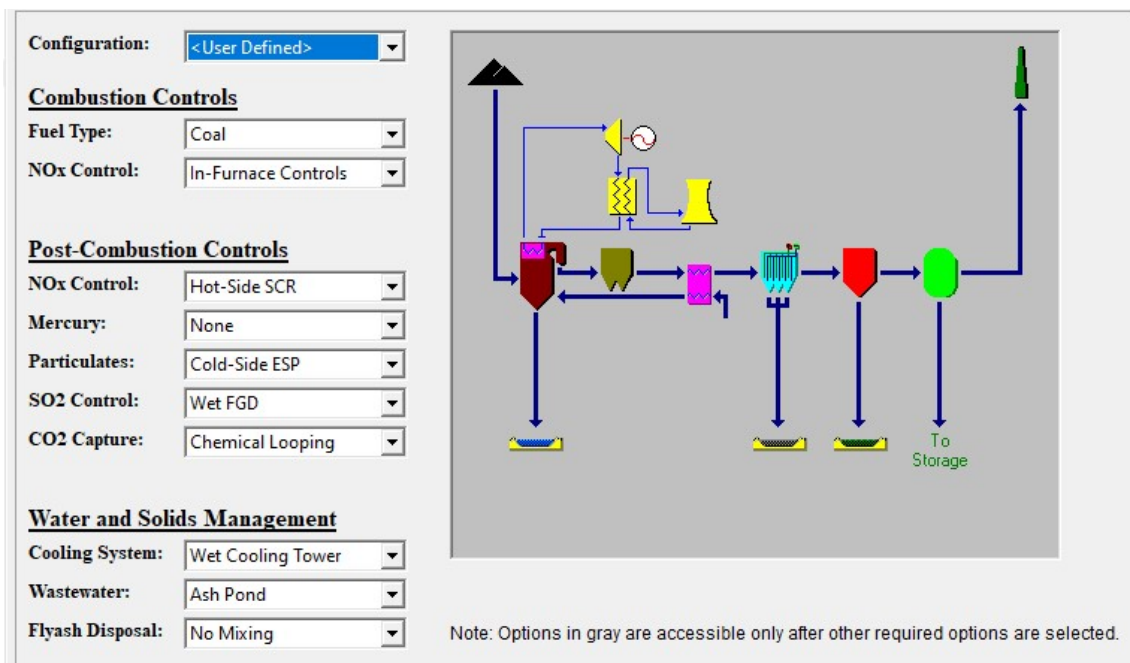


Figure 4.1. Configuration screen of the IECM with alternatives for user-defined pollutants control technologies. Obtained from IECM version 11.2

The simulation tool is based on fundamental mass and energy balance equations and is useful to run preliminary studies, which can indicate specific challenges associated with a power plant and its capture system (such as energy penalties, water consumption and demand, and capture costs) (MERSCHMANN, VASQUEZ, *et al.*, 2013). IECM has been used in recent years for several performance and cost comparison studies between CO₂ capture systems (BUI, FAJARDY, *et al.*, 2017, CLARENS, ESPÍ, *et al.*, 2016, HOFFMANN, 2010, MANTRIPRAGADA, ZHAI, *et al.*, 2019b, MERSCHMANN,

VASQUEZ, *et al.*, 2013, ROCHEDO, 2011, ZHAI, RUBIN, 2011, ZHAI, RUBIN, *et al.*, 2011), including post-combustion CaL systems (MANTRIPRAGADA, RUBIN, 2014, 2017a).

IECM input data includes location and meteorological data, detailed feedstock input (ultimate analysis, HHV, and ash composition); selection of end-of-pipe control technologies (for particulate, SO_x, mercury, and NO_x); and the basic configuration of the thermal power plant, allowing the implementation and simulation of sub, super and ultra-supercritical steam boilers. The simulation model also includes the input of financial assumptions and economic parameters such as equipment costs, labour costs, discount rate, taxes, and the economic lifetime of the plant.

Technical limitations of the input parameters are also indicated by the model, and a reference value is usually displayed. A great advantage relies on the fact that the model calculates not only the overall results of the plant (e.g. input of fuel, emissions, and utilities' consumption), but also the results per component (e.g. composition of the exhaust flow, water consumption, temperature and pressure conditions). This characteristic allows the user to analyse the results and impacts of individual components in the performance, cost, and financial conditions.

The IECM also calculates fuel and other mass flow rates and with this data estimates the size of the equipment needed to meet the designed gross power output. Selected power plant configuration can be analysed to obtain parameters such as the demand for resources (including water, fuel, and limestone), net plant efficiency, net CO₂ emissions intensity (kg/ MWh), plant capital costs (\$/kW-net), CO₂ emissions avoided, levelized cost of electricity (\$/MWh) and costs of CO₂ captured and avoided (\$/tonne) (MERSCHMANN, VASQUEZ, *et al.*, 2013). Different plant configurations and technologies can then be compared on a consistent basis. The IECM model for CaL allows to use the equations defined previously in chapter 3, and then adjust the input data to run user-defined simulations. For these reasons, the software may be considered suitable for the purposes of this study. IECM version 11.2 was used to run the simulations in this work (RUBIN, 2020).

4.4 Economic performance and cost model for CaL systems

Capturing CO₂ always represent extra costs in comparison to conventional power and industrial plants. Hence, large-scale CO₂ capture technologies only make sense in a context of climate change mitigation (FENNELL, ANTHONY, 2015). Yet, current CCS technologies such as MEA scrubbing and oxy-combustion still need to strongly reduce their associated costs as they represent an average increase of 60% to 80% in electricity costs for PC power plants (RUBIN, DAVISON, *et al.*, 2015, TURNER, IYENGAR, *et al.*, 2019). Among the CCS chain process, the capture step accounts for roughly 80% of total CCS costs, which are higher for retrofit scenarios and first-of-a-kind (FOAK) plants (RUBIN, DAVISON, *et al.*, 2015). Regarding an emerging technology such as CaL systems, the data supporting economic feasibility remains limited in the open literature (MICHALSKI, HANAK, *et al.*, 2019). The lack of data is even more evident considering Bio-CaL applications.

Economics of CaL systems is usually assessed using the levelized cost of electricity (LCOE) approach (MANTRIPRAGADA, RUBIN, 2014, MICHALSKI, HANAK, *et al.*, 2019), presented in equation (4-1). The LCOE depends on the following parameters: total capital requirement (TCR), net power output of the power plant (MW), capacity factor (CF), fixed charge factor (FCF), fixed operating and maintenance cost (FOM), specific fuel cost (SFC), specific variable operating and maintenance cost (VOM) and net power plant heat rate (HR). This method is simple to be implemented and is broadly used to evaluate the economic performance of several clean energy systems.

(4-1)

$$LCOE = \frac{(TCR \times FCF) + FOM}{MW \times CF \times 8760} + VOM + (SFC) \times (HR)$$

Recent review studies on the economics of CaL concepts indicate that CaL retrofits to fossil-fuel-fired plants have most LCOEs values reported between 55 and 85²⁶ USD₂₀₁₇/MWh, with the corresponding cost of CO₂ avoided reported to be between 11 and 35 USD₂₀₁₇/tCO₂, regardless if the CaL system is retrofitted into a CFPP or an NGCC

²⁶ These values were originally reported in 2018 euros, which were assumed as current values. Then, costs were changed to 2018 USD current dollars using the annual average exchange rate between the two currencies (EUROPEAN CENTRAL BANK, 2019). Next, the obtained value was converted to 2017 constant dollars using the CEPCI index (CHEMENGONLINE, 2019). This calculation procedure was used for all other cost values that appear in the text obtained from the literature.

(FENNELL, ANTHONY, 2015, HANAK, MICHALSKI, *et al.*, 2018, MICHALSKI, HANAK, *et al.*, 2019, ROLFE, HUANG, *et al.*, 2018). This economic performance is equal or superior to chemical solvent scrubbing retrofits, which has reported LCOE values between 72-100 USD₂₀₁₇/MWh and avoided costs between 39-83 USD₂₀₁₇/tCO₂ (HANAK, MICHALSKI, *et al.*, 2018, MICHALSKI, HANAK, *et al.*, 2019). Cheaper electricity and CO₂ avoided costs for CaL plants over power plants equipped with standard CCS technologies are also reported by the review conducted by FENNELL and ANTHONY (2015), though issues in the consistency of the underlying assumptions of the reviewed studies, such as taxation and cost of capital are pointed out (FENNELL, ANTHONY, 2015).

On the other hand, other recent studies estimated greater costs for the CaL system in comparison to conventional first-generation technologies. In the work by MANTRIPRAGADA, RUBIN (2017b), the LCOE for CaL post-combustion was reported to be 11% more expensive than an advanced amine with solvent FG+ and 91% more expensive than the reference plant without capture. The case studies were simulated for a 550 MW_e net power output plant with 90% capture efficiency. The main reason for the higher costs was the capital cost of the CaL system, which was more than two times the capital cost of the reference plant (MANTRIPRAGADA, RUBIN, 2017a). Similar results were found by the same authors in a previous study (MANTRIPRAGADA, RUBIN, 2014), which explained the higher costs of CaL, designed as a FOAK plant, by the assumptions made for process and project contingency costs. The values selected for process and project contingency factors, respectively, 21% and 22%, represent percentages of capital costs, and, are considered to be in accordance with the maturity of the technology (MANTRIPRAGADA, RUBIN, 2014).

Therefore, when compared to conventional post-combustion capture systems, previous studies on CaL systems economics have shown both greater (MANTRIPRAGADA, RUBIN, 2014, 2017a) and lower costs (FENNELL, ANTHONY, 2015, HANAK, ERANS, *et al.*, 2018, MICHALSKI, HANAK, *et al.*, 2019). Actually, comparing technologies with different levels of development is not a straightforward task, since the underlying methods in a particular study are often not clear²⁷ (RUBIN, 2012).

²⁷ The results presented in the technical literature reveals significant differences and inconsistencies in key technical, economic and financial assumptions, such as plant size or if it includes cost of transport and storage (RUBIN, 2012). This makes comparisons between studies more difficult.

In addition, the early estimates values for CaL might be overly optimistic, as it is common for developers of emerging technologies (METZ, DAVIDSON, *et al.*, 2005, RUBIN, 2017b). Obviously, two of the main goals of assessing advanced or second-generation capture technologies such as CaL are to improve performance (such as lower energy penalty, higher capture efficiency, and reduced lifecycle impacts²⁸) and costs (capital costs, costs of electricity, and avoided and captured CO₂ costs). Still, apparent improvements in costs for CCS technologies from a particular study could derive from the set of assumptions of a certain model, such as higher power efficiency of the reference plant, quality of the selected fuel and low fuel price, longer plant lifetime, higher capacity factor, lower discount rate and lower contingency costs (HOFFMANN, 2010, RUBIN, 2017b). In the case of CaL systems, some studies also consider the potential integration with the cement industry, seen as a potential opportunity for reducing CaL costs, as the high volumes of sorbent purge used in the plant could be reused as a saleable by-product for cement production (MANTRIPRAGADA, RUBIN, 2017a). In this work, such option is not considered.

In an economic model for CaL large-scale systems, direct capital costs are estimated essentially for carbonator, calciner, blowers, ASU, fuel and sorbent inventory, solids handling equipment, CO₂ compressors, and secondary steam cycle (including heat recovery steam generator – HRSG). Estimating each component of the direct capital costs is part of a “bottom-up” approach, which for technologies in early stages of development such as CaL may involve high uncertainty to achieve realistic performance and cost values for an Nth-of-a-kind (NOAK) large-scale plant, as some process design details for large-scale systems are still incomplete (ABANADES, ARIAS, *et al.*, 2015, RUBIN, 2017a). Yet, this work is based on the “bottom-up” costing method, as it is more useful to assess the contribution of each component to the total cost, as well as to perform sensitive analyses (or “what if” analysis) for specific components performance and cost. A “top-down” approach, on the other hand, would be based on technological experience and “learning curves” to estimate future NOAK plants as a function of accumulated installed capacity (RUBIN, 2017a). The two approaches can be used together to estimate the level of deployment needed to achieve NOAK cost goals (RUBIN, SHORT, *et al.*, 2013, RUBIN, YEH, *et al.*, 2007, RUBIN, 2017a). However, there is a lack of plant

²⁸ Compared to lifecycle impacts of amine-based systems, CaL systems have the potential to be present lower overall CO₂ emissions (HURST, COCKERILL, *et al.*, 2012).

experience with this technology to perform a consistent “top-down” approach (RUBIN, 2017a).

The capital cost of the carbonator might be estimated based on the costs of an atmospheric pressure CFB boiler for oxy-combustion plants, using the volume flow rate of the flue gas as the scaling variable along with a scaling factor (MANTRIPRAGADA, RUBIN, 2017a, MATUSZEWSKI, 2010). In this case, the CFB boiler already accounts for the integrated steam generating heat exchanger within the reactor. The capital cost of the calciner, on the other hand, might be estimated based on costs for calciners used in the cement industry (IEA, 2008, MANTRIPRAGADA, RUBIN, 2017a) or for biomass CFB gasifiers (CRAIG, MANN, 1996, MANTRIPRAGADA, RUBIN, 2014).

In ABANADES *et al.* (2015), the cost of the interconnected carbonator-calciner reactors system is assumed to be proportional to the cost of an oxy-fired CFB boiler system with the same fuel input (ABANADES, ARIAS, *et al.*, 2015). The cost value is approximated from recent existing cost studies on oxyfuel combustion plants (MATUSZEWSKI, 2010). Only the refractory combustion chamber of the calciner is calculated separately based on large-scale precalciners of cement plants (including a five-stage preheater) (IEA, 2008).

For most of the other equipment, existing cost models can be used, usually based on other scaling variables such as steam power for the steam turbine and mass flow for solids handling equipment. Costs for limestone handling equipment can be approximated to coal handling (MANTRIPRAGADA, RUBIN, 2017b). Annual costs for fuel and limestone, waste disposal, and labour costs are some of the O&M costs considered for LCOE and capture unit costs. Costs for transportation and storage of CO₂ can also be treated as O&M costs (MANTRIPRAGADA, RUBIN, 2017a).

There is also a degree of confusion in definitions such as costs of CO₂ avoided and captured, which are both reported in the same units of \$/tCO₂. The cost of CO₂ avoided is inversely proportional to the difference in CO₂ emission rates between the reference plant and the plant with the capture unit. The parameter is used as the minimum required CO₂ tax or carbon price needed to make the plant with CCS as economical as the reference plant (MANTRIPRAGADA, ZHAI, *et al.*, 2019b). The cost of CO₂ captured is inversely proportional to the amount of CO₂ captured by the capture plant and is used to assess the economic viability of a CO₂ capture system relative to a market price for CO₂

as an industrial commodity (RUBIN, 2012). To unveil the influence of CO₂ capture on the plant economics, CO₂ capture and avoidance costs for the power plants with capture are calculated (ROLFE, HUANG, *et al.*, 2018). These costs are given by the following equations:

(4-2)

$$CO_2 \text{ Capture Cost } (\$/tCO_2) = \frac{LCOE_{ccs} - LCOE_{reference}}{(tCO_2/MWh)_{captured}}$$

(4-3)

$$CO_2 \text{ Avoided Cost } (\$/tCO_2) = \frac{LCOE_{capture} - LCOE_{reference}}{(tCO_2/MWh)_{reference} - (tCO_2/MWh)_{ccs}}$$

Hence, all of the above should be taken into consideration when analysing cost estimates for CCS technologies. CCS comparative studies also commonly report costs in dollars and in constant (or real) currency terms, instead of current (or nominal), which excludes the effects of general inflation and interest rates (RUBIN, DAVISON, *et al.*, 2015). Therefore, costs in this work are reported in constant currency terms. Constant dollars in 2017 (US\$₂₀₁₇) is used as the standard currency. In the next sections, a methodology for estimating CaL costs is proposed.

4.4.1 Technology readiness level and contingency costs

The concept of technology readiness level (TRL) was presented in section 2.1.1 and is a way of ranking technologies based on their level of maturity (ZEP, 2017). TRL is a globally accepted benchmarking tool and has been used to assess the maturity of CO₂ capture technologies (BHOWN, 2014, ZEP, 2017). According to the scale proposed in the Zero Emissions Platform (ZEP, 2017), the CaL system is ranked as TRL 6, which describes a development stage of “*pilot plants in steady states at industrially relevant environments: pilots in the MW_{th} range*” (ZEP, 2017). In fact, as seen in section 2.4.3, CaL systems have rapidly developed from concept to development phase and the next step to be considered is demonstration plants in the 20-30 MW_{th} scale as suggested in (HILZ, HAAF, *et al.*, 2019). The paper by HILZ *et al.* (2019) defines the most mature CaL system as a TRL 6 technology based on the work of (ABANADES, ARIAS, *et al.*, 2015). The study by ABANADES *et al.* (2015) investigated the maturity of several CaL

systems concepts and classified CaL for post-combustion as the most mature among them (ABANADES, ARIAS, *et al.*, 2015). The conventional CaL process has a TRL higher than CLC and may become commercially available earlier than the last due to its use in retrofit applications for existent and capture-ready power plants. Additionally, the post-combustion Bio-CaL system proposed by (ALONSO, DIEGO, *et al.*, 2014) was evaluated and classified as TRL 4 (ABANADES, ARIAS, *et al.*, 2015).

The pilot plants of 1.9 MW_{th} La Pereda and 1 MW_{th} TU Darmstadt are the main reasons to consider the post-combustion CaL as TRL 6 (ARIAS, DIEGO, *et al.*, 2013, HELBIG, HILZ, *et al.*, 2017). A TRL 6 for post-combustion CaL can be also supported by the methodology proposed in (BHOWN, 2014) that ranks TRL of post-combustion technologies based on the size of the existent units, as shown in figure 4.2 (BHOWN, 2014).

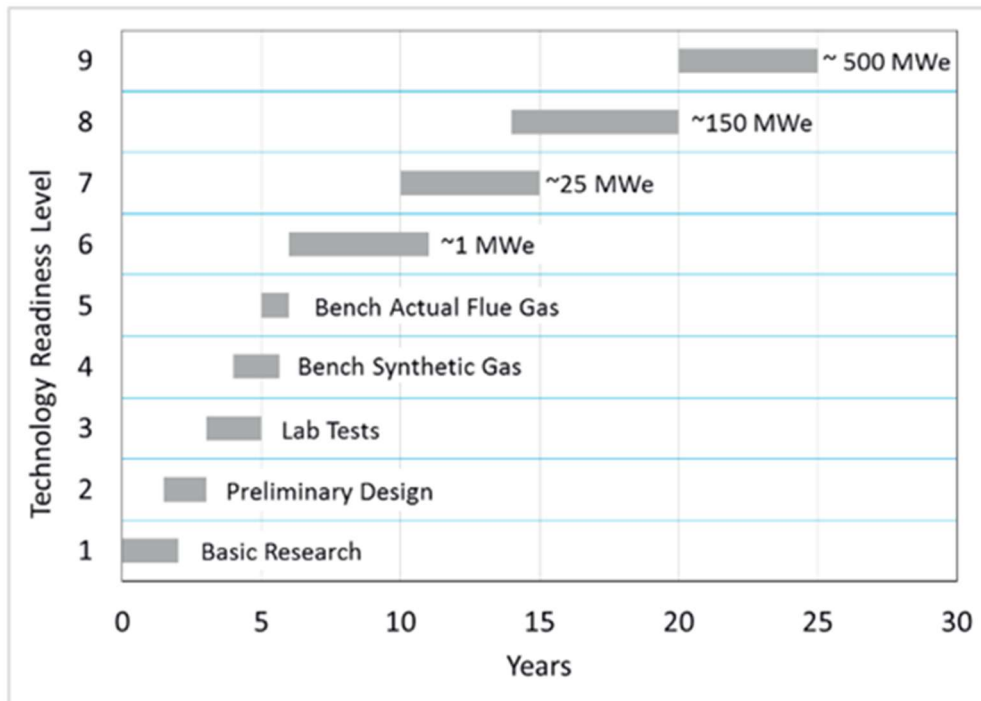


Figure 4.2. Development of Post-Combustion Capture Processes and relationship with TRL index. Obtained from (Bhown, 2014).

On the other hand, chemical absorption with amines is a mature process in the industry. It is ranked with TRL 9 due to its use in refineries for the natural gas sweetening (ABANADES, ARIAS, *et al.*, 2015). In power plants, with the experience acquired with the Boundary Dam and Petra Nova demonstrations (MANTRIPRAGADA, ZHAI, *et al.*, 2019b), the system is often considered a TRL 8 technology, but the index can vary from

7 to 9 depending on the type of amine applied (KANNICHE, LE MOULLEC, *et al.*, 2017, ZEP, 2017).

Other input parameters related to technological maturity include the process and project contingency factors often used in capital cost estimates. TRLs can be associated with the process contingency costs for different stages of development. Project contingency costs, in turn, are less related to technical maturity since even a more mature technology may have high project contingency costs in simplified and preliminary phases of a project. However, an emerging technology will hardly have a detailed estimate of project costs. Project costs are usually reported in the technical literature based on “simplified” to “detailed” estimates, as “finalized” projects data are often not available publicly (RUBIN, 2012). Process and project contingency cost adders were recommended by The Electric Power Research Institute (EPRI) for technologies at different levels of maturity and were used in works for post-combustion capture technologies (BHOWN, 2014, RUBIN, 2012, RUBIN, DAVISON, *et al.*, 2015). Therefore, a lower level of TRL may be translated as higher percentage values for contingency costs. Based on these assumptions, the following tables present the proposed values for process and project contingency costs and their respective TRL range:

Table 4.3. Process contingency costs and TRL ^a.

Technology status	Process contingency (% of associated process capital)	TRL range
New concept with limited data	40+	1-3
Concept with bench-scale data	30-70	3-5
Small pilot plant data	20-35	5-6
Full-sized modules have been operated	5-20	7-8
Process is used commercially	0-10	9

^a Elaborated by the author based on the EPRI guidelines categories (Bhown, 2014; Rubin, 2012; Rubin *et al.*, 2015).

Table 4.4. Project contingency costs and TRL^a

Design estimate effort	Project contingency (%)	TRL range
Simplified	30-50	1-9
Preliminary	15-30	4-9
Detailed	10-20	7-9
Finalized	5-10	8-9

^a Elaborated by the author based on the EPRI guidelines categories (Bhown, 2014; Rubin, 2012; Rubin et al., 2015).

According to Table 4.3, a TRL 6 technology like CaL will have high uncertainty and an upper limit for process contingency factor that increases the capital cost by 35%. This value is used to assess the cost values of a FOAK CaL plant²⁹. For a NOAK plant, a contingency factor of 10%, typical of a TRL 9 is applied. Regarding the project contingency factor of a FOAK plant, a value of 30% is selected as it represents a preliminary design effort.

Process contingency costs for the amine-based plant are presumed to be associated with a TRL 8 as full-sized modules (up to 240 MW) have been operated. In that case, the fact the flue gas comes from coal or biomass combustion is not considered relevant for contingency factor purposes. Therefore, a 10% capital cost increase factor is applied. For project contingency, a value of 20% is used as it defines a preliminary design effort. Table 4.5 summarizes the selected values for FOAK and NOAK plants.

²⁹ A TRL 4 for the bagasse-fired Bio-CaL unit is assumed, with the process contingency factor increasing the capital cost by 40%. Even though the upper limit for process contingency is 70% for this TRL, it is presumed that the large-scale Bio-CaL unit will not greatly differ from a standard CaL unit fired with coal (TRL 6), as discussed in section 2.4.4. Therefore, this process contingency factor is used to assess costs of a FOAK Bio-CaL plant.

Table 4.5. Selected values for contingency costs for the proposed carbon capture units. Elaborated by the author.

Post-Combustion Capture technology	TRL	Process contingency (%)³⁰	Project contingency (%)³¹
CaL (FOAK)	6	35	30
Amine-based (FOAK)	8	10	20
CaL (NOAK)	9	10	10
Amine-based (NOAK)	9	10	10

In IECM, contingency factors are also applied to the standard power generation equipment of the capture unit, required to produce electricity from the additional energy input to the CaL cycle. Thus, this will negatively impact the economics of CaL systems. However, due to the uncertainty of the process technology and considering a conservative analysis, no adaptation was made to the results obtained.

4.4.2 Cost structure of the post-combustion CaL system

As previously discussed, the actual cost of the post-combustion CaL system is still highly uncertain because of the inherent gaps of knowledge about the design and operational aspects of the system for application on large-scale. Accordingly, the following paragraphs refer to the cost structure of a mature CaL system, focusing on a NOAK plant assumed to be able to exploit more mature subsystems already applied in the power sector.

Within the boundaries of the CaL system, excluding the air-fired base power plant, the following main components should compose the cost structure of the capture unit:

- Carbonator
- Calciner
- Air Separation Unit (ASU)

³⁰ Applied over process facilities capital.

³¹ Applied over the sum of process facilities capital, engineering and home office fees, general facilities capital and process contingency.

- Blowers
- CO₂ Compression Unit (CCU)
- CO₂ Cryogenic Purification Unit (CPU)
- Heat Recovery Steam Generator (HRSG)
- Fuel and Ash Handling Equipment for ASU
- Solids Handling Equipment (limestone and fuel)
- Steam Turbine for Power Generation

Aside from the above equipment, added plant footprint and revamp of the cooling system should also be considered in retrofit scenarios. Regarding O&M costs, sorbent make-up, and fuel for the oxy-fired calciner have to be calculated. Limestone cost is defined as 25 \$/tonne, as used in (MANTRIPRAGADA, RUBIN, 2017a).

The carbonator capital cost is estimated based on an atmospheric CFB boiler for oxy-combustion plants. The CFB boiler is modelled as in the case S22A of the NETL baseline report on oxy-combustion plants (MATUSZEWSKI, 2010) and proposed in (MANTRIPRAGADA, RUBIN, 2017b) as follows:

(4-4)

$$C_{carb} (M\$) = C_{carb,ref} \left(\frac{F_{total,fluegas}}{F_{carb,ref}} \right)^{0.6}$$

Where $C_{carb,ref}$ is a reference value for the carbonator cost as a function of a reference molar flow rate $F_{carb,ref}$ entering the carbonator, while $F_{total,fluegas}$ is the actual molar flow rate of flue gas entering the reactor. Pressure and temperature were not considered since the CFB boiler and carbonator have similar operating conditions (MANTRIPRAGADA, RUBIN, 2017a).

The calciner cost, on the other hand, is estimated with the following equation, based on an atmospheric CFB biomass gasifier, since there are no heat exchangers inside this reactor (MANTRIPRAGADA, RUBIN, 2017a):

(4-5)

$$C_{calc} (M\$) = C_{ref} \left(\frac{F_{calc,inlet} P_{ref} T_{calc}}{F_{ref} P_{calc} T_{ref}} \right)^{0.6}$$

Where C_{ref} is a reference value for the calciner cost as a function of a reference molar flow rate F_{ref} , reference pressure P_{ref} and reference temperature T_{ref} within the reactor. $F_{calc,inlet}$ is the actual molar flow rate of oxidant from the ASU unit plus the recycle stream and P_{calc} and T_{calc} are the actual pressure and temperature values within the reactor (MANTRIPRAGADA, RUBIN, 2017a).

The costs of the other equipment follow the existing cost models in IECM. For example, the cost of the HRSG and the steam turbines are calculated based on the thermal power generated in the CaL system, calculated in section 3.1.5 (equation 3-60). Solids handling equipment is calculated using the mass flow of solids as the scaling variable. Costs for limestone handling equipment were approximated to that of coal handling (MANTRIPRAGADA, RUBIN, 2017b). Initial limestone cost is estimated based on solids inventory calculations demonstrated in section 3.2. Annual make-up cost of limestone is calculated as a function of the molar flow rate of make-up (which accounts for the loss in absorption capacity due to the sulphation reaction) and the capacity factor of the CaL plant (assumed to be the same as the base plant). Costs for transportation and geological storage of CO₂ are kept as default, which means a CO₂ product stream with 10.30 MPa after compression and transportation through pipelines with a total length of 100 km (RUBIN, 2020).

4.4.3 Summary of financial assumptions

The same financial assumptions, except for the contingency costs³², are made for all simulated cases, so they are compared on a consistent basis. The air-fired base power base plant is considered as a greenfield plant and is constructed simultaneously with the CCS system (construction period of 3 years³³ is assumed for all cases). The capital cost of a greenfield base plant and a capture-ready base plant for a CaL post-combustion

³² Discount rates may also be used to estimate costs of technologies with different levels of maturity as proposed in (MANTRIPRAGADA, RUBIN, 2014). Still, as contingency costs were already used for that aim, the discount rates were maintained equal in all cases to avoid double-count effects.

³³ In fact, construction periods of 4 years or more could be considered for power plants with CaL.

application are probably similar, since adaptations on the base plant to receive the retrofit of a CaL unit will consist of simple adjustments, such as pre-planning of the full plant layout to accommodate the CCS system. Aside from the extra physical space and optimized layout (e.g. fuel handling and feeding equipment for the base plant and future calciner are set to be located in the same place), pre-planning may encompass construction in sites where there is sufficient water source (and/or possibility for an extended water permit) to supply for an increase in water use when the CaL plant is added. This is also valid for limestone supply and it would be preferable if the source of CaOH₂ is located near the power plant.

The amine-based plants simulated are also considered to be greenfield plants. In the work by ROCHEDO (2011), the concept of capture-readiness was explored for different chemical absorption post-combustion capture configurations. The base plant configurations had different levels of capture-readiness and the capture unit was added in different years of the plant lifetime. The main motivation for the construction of capture-ready plants is to facilitate the introduction of CO₂ capture in the power generation sector in the near future, avoiding penalties and technological lock-ins, while promoting cost reduction and technological development. The work by ROCHEDO (2011) has also shown that in scenarios where capture units enter in the long term, the effect of the future value of the capture plant will be counterbalanced with the lower investment at present value, so investment decisions favour the cases without capture-ready modifications. In fact, it was proven that the perspective of investment decisions favours post-combustion, with the plant without capture-ready adjustments being dominant (a 15% discount rate was assumed) (ROCHEDO, 2011). Therefore, if CCS does not prove to be viable in the future, CaL has the advantage over other capture technologies, including amine-based systems, that its pre-investments required are minimum, and so the risk for investors of incurring in irreversible costs (or stranded assets) is lower.

The main financial assumptions proposed are summarized in Table 4.6. A discount rate of 7.1% p.a is proposed, similar to values applied in comparable studies (IEAGHG, 2014b, MICHALSKI, HANAK, *et al.*, 2019, YANG, ZHAI, *et al.*, 2010). Project lifetime is 30 years but might be lower for specific equipment in the CaL system, such as the calciner (IEA, 2010). Escalation rates were not applied (RUBIN, SHORT, *et al.*, 2013a).

Table 4.6. Summary of financial assumptions.

Parameter	Value	Unit
Year of costs reported	2017	Constant USD
Discount Rate ^a	7.1	%
Fixed Charge Factor (FCF) ^b	0.11	-
Project Lifetime	30	Years
Construction Period	3	Years

^a Based on the values proposed by (IEAGHG, 2014b, MICHALSKI, HANAK, *et al.*, 2019, YANG, ZHAI, *et al.*, 2010).

^b Calculated by IECM and derived from discount rate and project lifetime.

4.5 Case study assumptions

4.5.1 Configuration 1 – Reference plant (without CCS)

The reference case is a base plant (without CCS) with a designed gross power output of 300MW_g. It is assumed to be a new or greenfield pulverized fuel supercritical steam cycle unit, equipped with standard pollution control devices. Pollution control devices are designed to meet new source performance standards (NSPS) for air pollutants and water pollutants criteria (except CO₂ controls). The plant is modelled using the “typical new plant” configuration in IECM. Fuels considered are coal and biomass (further specified in section 4.2). A subcritical plant is also simulated for a coal application as this steam cycle type represents most of the world’s current coal-fired generation fleet (CALDECOTT, DERICKS, *et al.*, 2015, IEA, 2019g). The choice for a subcritical steam cycle for the biomass-fired case is justified by its representativity in the current Brazilian cogeneration fleet (CNA, PECEGE- USP, 2015, DANTAS, LEGEY, *et al.*, 2013, DIAS, MODESTO, *et al.*, 2011, NYKO, BRANDÃO, *et al.*, 2011).

Plant size is proposed as an intermediate value between a large-scale coal plant and a large-scale biomass plant. Also, sensitivity analyses on the full plant cost (capital and LCOE) related to size are performed with 700MW_g and 100MW_g to account for potential scale gains of the CCS technologies. The value for the capacity factor (CF) of 75% is selected based on similar studies for CaL systems (MANTRIPRAGADA, RUBIN, 2014, MANTRIPRAGADA, ZHAI, *et al.*, 2019b). Still, other studies considered a CF of 85% or higher (CRIADO, ARIAS, *et al.*, 2017). While new power plants might have to deal with more flexible operations and lower CF values, the addition of capture units might force plants to increase capacity factors to justify its capital investment (CRIADO, ARIAS, *et al.*, 2017). Therefore, sensitivity analyses are made for CF values of 40% and 85%.

As previously mentioned, the absolute cost values of the plants simulated are of less importance than the relative values between the different configurations proposed. Thus, no location factor is applied and the cost values are considered for the US Midwest region, which is the IECM default. Other important performance data on the base plant are summarized in table 4.7 below:

Table 4.7 Reference plant (no CCS) configuration parameters

Reference Plant Configuration	1	1A	1B
Fuel type	Coal	Biomass	Coal
Boiler type	Supercritical	Subcritical	Subcritical
Environment Temperature (°C)	22	22	22
Plant life (years)	30	30	30
Capacity Factor (%)	75	75	75
Steam pressure (bar)	243	164	164
Steam temperature (°C)	565	540	540
Plant gross capacity (MW)	300	300	300

Additionally, all plants configurations have the following pollutants control technologies³⁴:

- In-Furnace NOx Controls
- Hot-Side Selective Catalytic Reduction (SCR)
- Cold-Side Electrostatic Precipitator (ESP)
- Wet Flue Gas Desulfurization (FGD)

³⁴ Except from the configurations fuelled with biomass, which have only the Cold-Side Electrostatic Precipitator (ESP) as pollutant control technology, as proposed in (IEAGHG, 2011).

4.5.2 Configuration 2 - Large-scale calcium looping carbon capture unit

Configurations for a standard post-combustion CaL capture unit were extensively discussed in chapters 2 and 3. By using typical operational parameters examined in these chapters, input parameters were adjusted for the lowest LCOE possible, respecting solid looping rates limits. Figure 4.3 shows the basic diagram for the CaL system in IECM.

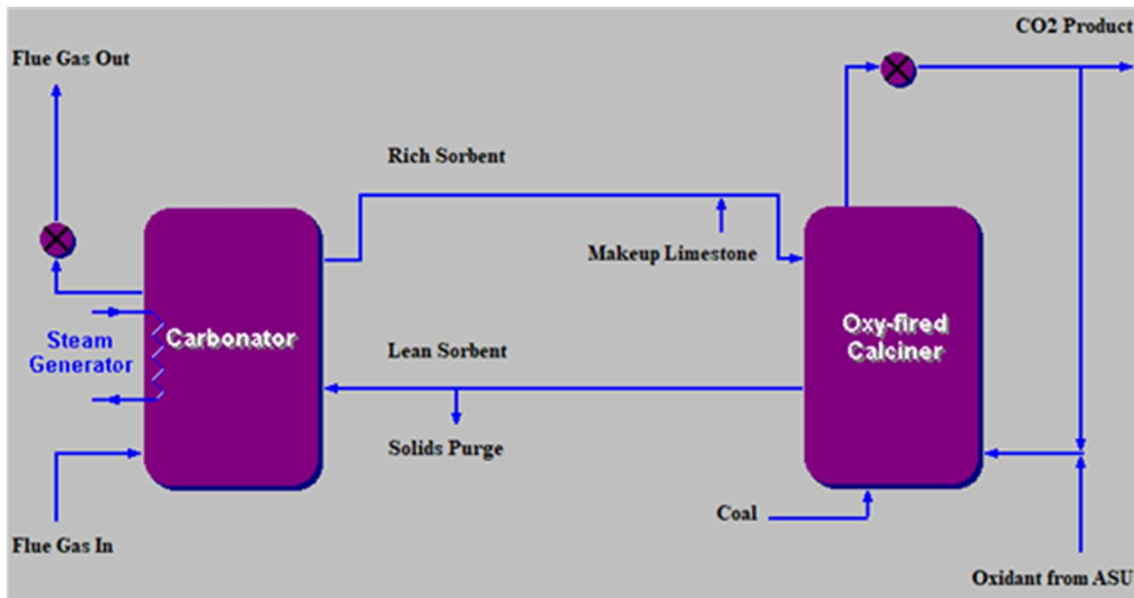


Figure 4.3 Calcium Looping Diagram for Post-combustion carbon dioxide capture. Obtained from IECM version 11.2.

The following table displays the parameters assumed for the CaL capture unit configurations. In terms of performance, these configurations can be considered both for greenfield and retrofit plants. All configurations have FGD units downstream of the process that sets SO₂ to 10 ppm (the same is done for the amine-based system models). Configuration 2 represents the capture unit for the reference plant of configuration 1. Configuration 2A represents the Bio-CaL system for the reference plant of configuration 1A and configuration 2B represents the CaL system for configuration 1B.

Table 4.8 Parameters used in the CaL carbon capture unit simulations

CaL carbon capture unit	2	2A	2B
Fuel supplied to the calciner ^a	Coal	Biomass	Coal
Capture efficiency carbonator (%)	90	80	90
Steam cycle (secondary plant) ^b	Supercritical	Subcritical	Subcritical
Make-up rate (mol/mol)	1.9	1.5	1.9
Limestone purity (%)	92.4	92.4	92.4
Carbonator Temperature (°C)	650	650	650
Degree of Carbonation (-)	0.7	0.7	0.7
Calciner Temperature (°C)	910	900	910
Degree of Calcination (-)	0.95	0.95	0.95
Fraction of Gas Recycling (fraction)	0.55	0.60	0.55
CO ₂ in flue gas at carbonator inlet (% vol) ^c	11.9	12.5	11.9

^a Same fuel properties as the fuel used in the base plant.

^b The secondary steam cycle is calculated based on the same heat rate (HR) as the primary plant, thus, conditions for steam temperature and pressure are considered to be equal to the base plant.

^c This value is an output from IECM reference plant configurations (1, 1A, and 1B).

As previously discussed, the configuration for a Bio-CaL system should be slightly different than the optimal configuration for a coal-fired CaL system, assuming plants with the same installed capacity. This is true regarding both carbonator capture efficiency and calciner nominal temperature. The capture rate in the carbonator is set to 80%, as a capture level of 90%, more usual in similar simulation studies using amine-based capture (TAGOMORI, CARVALHO, *et al.*, 2018), results in higher heat demand in the calciner, which would mean a greater supply of fuel and O₂ stream in this reactor³⁵. A carbon capture efficiency of 80% for biomass-fired calciner was also proposed by MARTÍNEZ *et al.* (2018) to reduce calciner heat demand (MARTÍNEZ, I., ARIAS, *et al.*, 2018). A lower capture level in the carbonator for biomass-fired calciner compared to coal was also suggested in (HANAK, BILİYOK, *et al.*, 2015b).

³⁵ In addition, a capture level of 90% resulted in a heat demand in the calciner out of the limits proposed by the software, which is represented by a *Calcium Looping Power Requirement* higher than 30 (% MWg) of the gross power produced by the CaL system.

4.5.3 Configuration 3 - Large-scale chemical absorption amine-based carbon capture unit

The configuration for the chemical-absorption equipped plant is based on Fig 4.4. The steam for the amine capture system is supplied from the primary steam cycle while electricity is also provided by the base power plant (with no auxiliary boiler). Other configurations for amine-based systems are proposed in (MANTRIPRAGADA, ZHAI, *et al.*, 2019b).

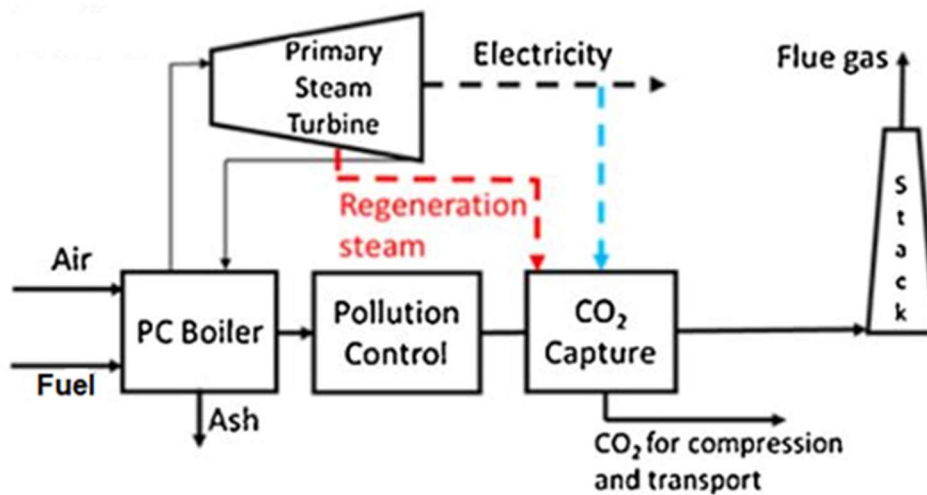


Figure 4.4 Configuration 3 proposed for amine-based post-combustion capture. Adapted from (Mantripragada *et al.*, 2019b)

Shell Cansolv is selected as the amine solvent. *Cansolv* is a tertiary amine capable of selective or sequential SO_x, NO_x, and CO₂ removal. It was used in the Boundary Dam plant, capturing CO₂ from flue gas from a 110MWe lignite-fired power plant (MANTRIPRAGADA, ZHAI, *et al.*, 2019b, ZEP, 2017). The solvent has fast kinetics and high absorption capacity compared to other conventional amines and is blended with primary amines and additives (FERON, 2016). In recent reports by the NETL on power plants with capture (CHOU, LYENGAR, *et al.*, 2015, FOUT, ZOELLE, *et al.*, 2015, TURNER, IYENGAR, *et al.*, 2019), *Cansolv* was selected as the base case both for PC and NGCC post-combustion plants. The use of newer proprietary solvents in post-combustion costs comparisons is also recommended in (RUBIN, DAVISON, *et al.*, 2015). Parameters for the amine-based process using the *Cansolv* solvent used in this work are derived from IECM software default model (with proprietary values).

Simulations were also performed using Econamine FG+, another advanced amine used in various comparable works (CLARENS, ESPÍ, *et al.*, 2016, MANTRIPRAGADA,

ZHAI, *et al.*, 2019b, ROCHEDO, 2011). This solvent was applied to the CFPP configuration with the supercritical steam cycle, as shown in table 4.9. Simulation results for cost values using Econamine FG+ in IECM are lower than *Cansolv* or conventional amine MEA (considering the same base plant). Therefore, results for the FG+ configuration are considered as the minimum cost limit for current amine-based systems. *Cansolv*, in turn, has higher absorption capacity and better thermodynamic performance than Econamine FG+, which is represented by the values of lean CO₂ loading and regenerator heat requirement, respectively, shown in table 4.10. Input parameters employed in this work for *Cansolv* and Econamine FG+ capture units are derived from IECM software or based on the works by (CLARENS, ESPÍ, *et al.*, 2016), (MANTRIPRAGADA, ZHAI, *et al.*, 2019b) and (HANAK, BILİYOK, *et al.*, 2015b).

Table 4.9 Amine-based carbon capture unit configurations

Amine-based Plant Configuration	3	3FG+	3A	3B
Fuel type (Primary plant)	Coal	Coal	Biomass	Coal
Amine system	Cansolv	Econamine FG+	Cansolv	Cansolv
Steam cycle	Supercritical	Supercritical	Subcritical	Subcritical

Table 4.10 Parameters used in the amine-based carbon capture unit simulations

Solvent Proprietary Name	Cansolv^a	Econamine FG+
Absorber CO₂ Removal Efficiency (%)^b	90	90
Sorbent Concentration (wt %)	-	30
Regenerator Heat Requirement (kJ/kg CO₂)	2559	3553
Lean CO₂ Loading (mol CO₂/mol sorb)	0.16	0.19
Sorbent Losses (kg/t CO₂)	-	3
Sorbent Recovered (kg/t CO₂)	-	1.98
Liquid-to-Gas Ratio (ratio)	-	3,9
Makeup water for wash section (% raw flue gas)	0.8	0.8

^a The values not displayed for Cansolv are proprietary and not publicly available.

^b Although config. 2A, applied for the Bio-CaL system, is designed with 80% capture efficiency in the carbonator, due to the CO₂ captured by the oxy-calcliner after the calcination step, the overall capture rate is 90% for both plants. For all other configurations, CaL systems have a higher overall capture rate than amine-based systems.

5. Results Analysis

This chapter compares and discusses the results for the configurations presented in chapter 4. Calcium looping and amine-based post-combustion carbon capture units were modelled integrated to new-built pulverized fuel power plants. Results are compared in technical and economic aspects. Results for water use and physical space requirements are also discussed. Then, key configuration parameters are modified for a sensitivity analysis.

5.1 Supercritical CFPP

5.1.1 Technical results

Configurations for the supercritical coal-fired power plants were introduced in section 4.5. A summary of technical results for the selected 300MW_g PC plants, with and without carbon capture, is presented in Table 5.1. Config. 2, or the plant with CaL, has the largest gross and net power output due to the additional power produced from the secondary steam power plant. Config. 1 and 2 have the same coal input flow rate of 84 tonnes/hr supplied to the base plant, though config. 2 has an additional coal input of 74 tonnes/hr (an 88% increase) supplied to the oxy-calcliner for the calcination process. The heat recovery associated with the CaL unit is responsible for the secondary steam cycle, which increases in 72% the net power output of the integrated plant (base plant + CaL) compared with the reference plant (config. 1).

Table 5.1. Technical evaluation summary

Parameter	Unit	1	2	3	3FG+
Gross Power Output	MW	300	300 (+289) ^a	300	300
Net Power output	MW	280	481	246	243
Auxiliary Power Consumption	MW	20	108	54	57
Fuel input flow rate	tonne/hr	84	84 (+74) ^b	98	102
Net plant efficiency	HHV (%)	38.8	35.4	29.4	27.9
Efficiency Penalty	%	-	3.3	9.4	10.8
Plant specific CO ₂ emissions	kgCO ₂ /MWh	820	50	110	114
CO ₂ Captured	tonne/hr	-	470	240	250

^a Config. 2 has additional gross power generated from the secondary steam cycle, represented in parentheses.

^b In parentheses, the fuel input rate to the calciner is displayed.

To achieve the same gross power output, the amine-based plants in configurations 3 and 3FG+ incur an increase in the fuel supply of 16% and 21%, respectively. For an existing plant, this level of fuel flow rate increase may be restrictive due to steam turbines operational limits and fuel feeding system infrastructure, among other practical and economic reasons. An auxiliary boiler could be used, but overall plant CO₂ emissions would be higher. Therefore, simulations were also performed for a variation of config. 3 and 3FG+, establishing the same fuel input value as configurations 1 and 2 while varying the gross power output. This in theory represents what would be more similar to a retrofitted³⁶ plant regarding the reference configuration. In this case, config. 3 gross output reduces to 259 MW and the net output decreases to 212 MW; a 24% de-rate compared with the 280 MW of the reference plant. Additionally, config 3FG+ had a de-rate of 28%, which indicates a better thermodynamic performance of the *Cansolv* solvent used in config. 3. Other performance parameters such as net plant efficiency and CO₂ emissions rate remained stabilized in this variation.

As shown by Figure 5.1 below, config. 2 has not only a higher net plant efficiency, but also a lower plant-specific CO₂ emission rate in comparison with the amine-based cases (config. 3 and 3FG+). The lower CO₂ emission rate of config. 2 is due to the additional power supplied by the oxy-fired calciner.

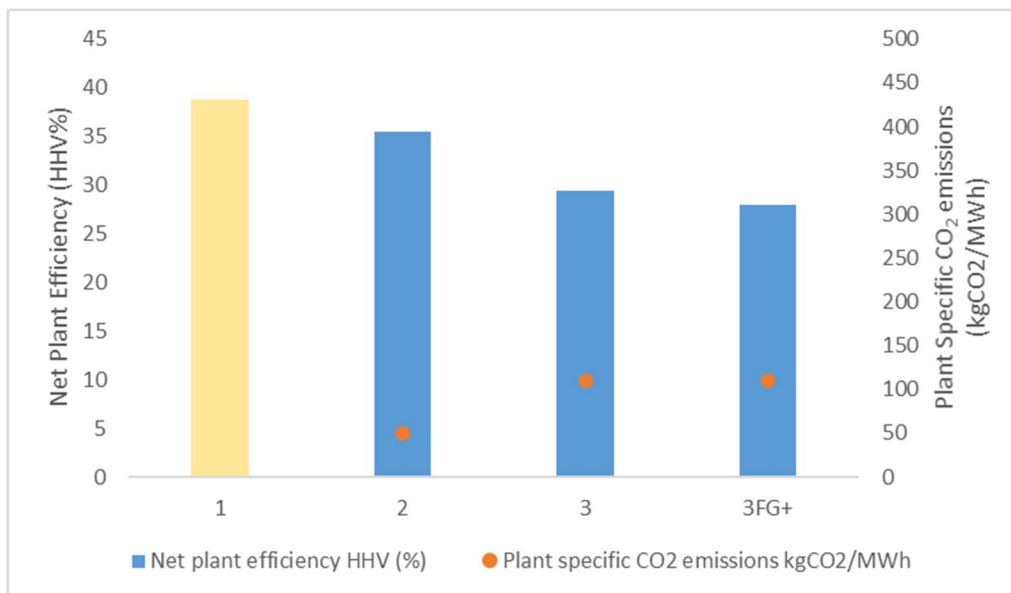


Figure 5.1. Net plant efficiency (HHV basis) on the left-axis and plant specific CO₂ emissions on the right-axis (kgCO₂/MWh)

³⁶ These models should be seen as a simplification of a retrofit simulation, since the base plants of these cases have small differences in equipment size and cost compared with the reference case in config. 1.

Thus, even if the same amount of CO₂ is being emitted by the three CCS plants in absolute terms, as a capture level of 90% from the base plant flue gas was established for all CCS cases, the CaL plant produces more energy with lower overall emission rate.

This translates as a higher plant overall capture level in config 2. (base plant and CaL unit), since almost 100% of the CO₂ present in the coal supplied to the calciner is captured. Then, carbon mass balance for config. 2 full system derives in a capture rate of 95.3%, against 90% from the amine-based system. Additionally, the extra fuel added to the calciner in config. 2 results in significantly more CO₂ captured by the power plant in absolute terms (almost the double), capturing 470 tonnes/hour in config. 2 against 240 and 250 tonnes/hour in config. 3 and 3FG+, respectively.

Also, config 2 has a low efficiency penalty of 3.3% in relation to the reference case, compared with 9.4% and 10.8% of the amine-based configurations. The net plant efficiency of config. 2 is calculated over a larger primary energy input. Thus, the energy penalty does not refer exclusively to the base plant, but the entire system. Still, auxiliary power consumption in config 2. is two times larger than in configs. 3 and 3FG+. In config. 2, almost all power consumption is due to CO₂ compression and air separation (CCU and ASU), which are responsible for about 40 MW each. In configs. 3 and 3FG+, most part of the parasitic load is due to steam extraction for solvent regeneration from the base plant cycle, followed by the CCU. Although the CCU in config. 3 compresses 49% less CO₂ (mass basis) than config 2, it consumes only 28% less energy. This indicates config. 2 is more efficient in CO₂ compression.

Finally, regarding exclusively config. 2, other technical results are displayed in table 5.2. The solids residence time in the reactors is in agreement with the literature values (between 1-3 min), with 156 seconds for the carbonator and 55 seconds for the calciner. The average carrying capacity, described in equation (3-9) and presented in chapter 3, resulted in a maximum carrying capacity of 0.2, with an actual carbonator conversion of 0.14, both typical values. This means the solid circulation molar rate of Ca-based entering the carbonator is about one order of magnitude greater than the number of moles of CO₂ coming from the flue gas. This is represented by a circulation ratio of $F_R/F_{CO_2,fluegas} = 8$, calculated with the ratio of circulating sorbent entering the carbonator over the CO₂ flue gas. Additionally, the fresh sorbent make-up rate over the flue gas rate $F_0/F_{CO_2,fluegas} = 0.13$ is also in agreement with typical circulating rates found in the

literature. These circulation rates were calculated using values from the IECM result diagram shown in Figure 5.2, which illustrates the main solid and gas flow rates of the capture plant, including sorbent make-up, sorbent purge, required oxidant and CO₂ captured. The values displayed in the result diagram are based on the mass and gas balance equations described in chapter 3. It shows the input of fresh limestone flow is in the same order of magnitude as the coal flow. In addition, it shows the flow of rich-sorbent (CaCO₃) entering the calciner is greater than the flow of lean-sorbent (CaO) leaving the calciner and entering the carbonator and entering the carbonator.

Table 5.2. Config. 2 operational results

CaL system operational results	Unit	Value
Solids residence time in the carbonator	Seconds	156
Solids residence time in the calciner	Seconds	55
Average carrying capacity X_{ave}	(fraction)	0.20
Actual CaO Conversion X_{carb}	(fraction)	0.14
$F_0/F_{CO2,fluegas}$	(mol/mol)	0.13
$F_R/F_{CO2,fluegas}$	(mol/mol)	8

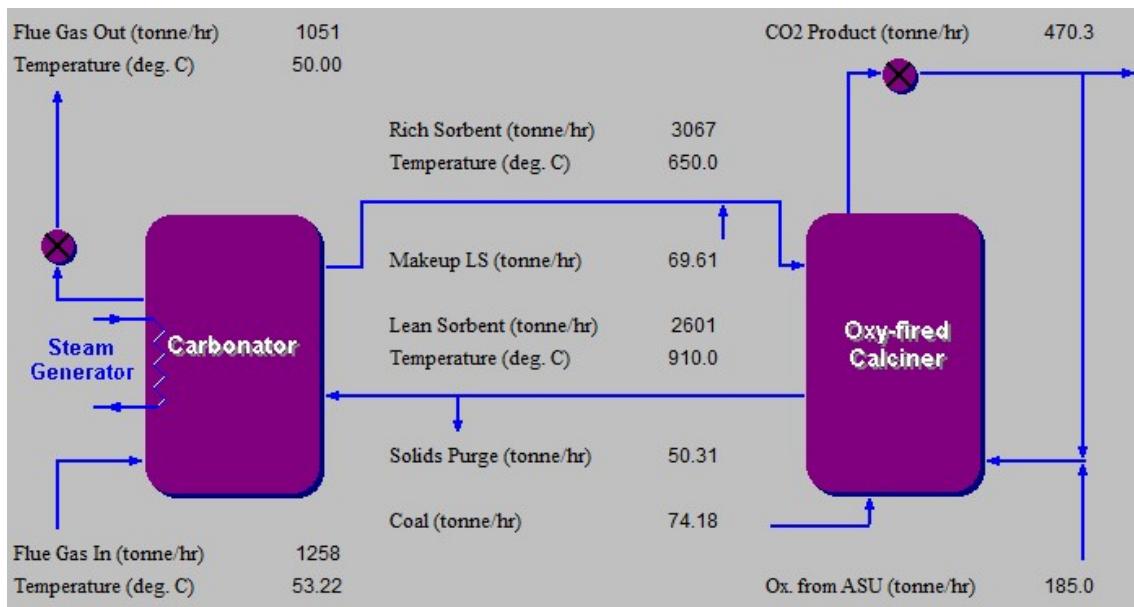


Figure 5.2 Results diagram for CaL plant added to supercritical coal plant (300 MW gross power). Obtained from IECM.

5.1.2 Economic results

Cost results for the plants simulated are summarized in Table 5.3. The plants with carbon capture are considered FOAK plants due to the contingency factors assumed, in accordance with the technologies' current maturity, as proposed in chapter 4. Plant capital cost for the CaL configuration is higher than the amine-based cases, as an additional generation plant is part of the CaL system, aside from the capture unit itself. While the total capital requirement (TCR) of config. 2 (5829 \$/kW-net) represents more than a two-fold increase compared to the reference plant (2344 \$/kW-net), config. 3FG+ is the least costly with a 78% points increase in relation to the same reference (4174 \$/kW-net). In addition, the CCS system capital cost (2120 \$M) in config. 2 is significantly higher than the amine-based configurations (415 \$M and 276 \$M). These results show CaL systems are highly intensive in capital and the contingency factors applied affected negatively the economics of these systems. Therefore, as a FOAK plant, CaL is less competitive than amine-based systems for post-combustion capture.

Table 5.3. Cost results summary (FOAK plants)

Parameter	Unit	1	2	3	3FG+
Plant capital cost³⁷	(\$M)	657	2806	1142	1016
CSS system capital cost³⁸	(\$M)	-	2120	415	276
Total Capital Requirement (TCR)	\$/kW-net	2344	5829	4639	4174
CO₂ capture capital cost	\$/kW-net	-	4404	1684	1133
Plant LCOE	\$/MWh	72.5	151.3	137.8	129.1
Plant LCOE w/o T&S	\$/MWh	-	146.4	130.4	121.5
Cost of CO₂ avoided	\$/tonne CO ₂	-	101.8	91.6	79.9
Cost of CO₂ captured	\$/tonne CO ₂	-	75.6	59.2	47.6

Regarding the LCOE of the configurations, the CaL system more than doubles the value of the reference plant and is about 10% more expensive than config. 3 and 17% more expensive than config. 3FG+. The difference in transportation and storage costs, on the other hand, favours config. 2 against the amine-based configurations, which can be

³⁷ Same as overnight cost.

³⁸ This cost does not account for adjustments in plant cooling system, SO₂ control system or any equipment or subsystem of the base plant that may need revamp to potentially accommodate a capture unit. Since the plants are considered greenfield, the cost of the cooling system, for example, is included in Plant capital cost (\$M) and is higher for the CCS configurations in comparison with config 1.

explained by the economies of scale that derive from capturing more CO₂ from one single emitting source in the case of the CaL system. Diseconomies of scale, contrarily, are likely what explains the high LCOE values that resulted from all CCS cases, above typical values reported in the literature (and discussed in section 4.4).

For costs of CO₂ avoided and captured³⁹ concerning the CaL-based plant, results are around 30% and 60% points higher in config. 2, respectively, when compared to the least costly amine-based configuration – config. 3FG+. The weight of the capture plant in total capital cost is also higher for the CaL system. The CO₂ capture capital cost in config. 2 (4404 \$/kW-net) accounts for 76% of the plant TCR, while for config 3FG+ (1133 \$/kW-net) the capture cost accounts for 27% of the TCR. A more detailed breakdown of the costs of the capture unit for the CaL configuration is presented in Figure 5.3, where the impact of the contingency costs can be better evaluated.

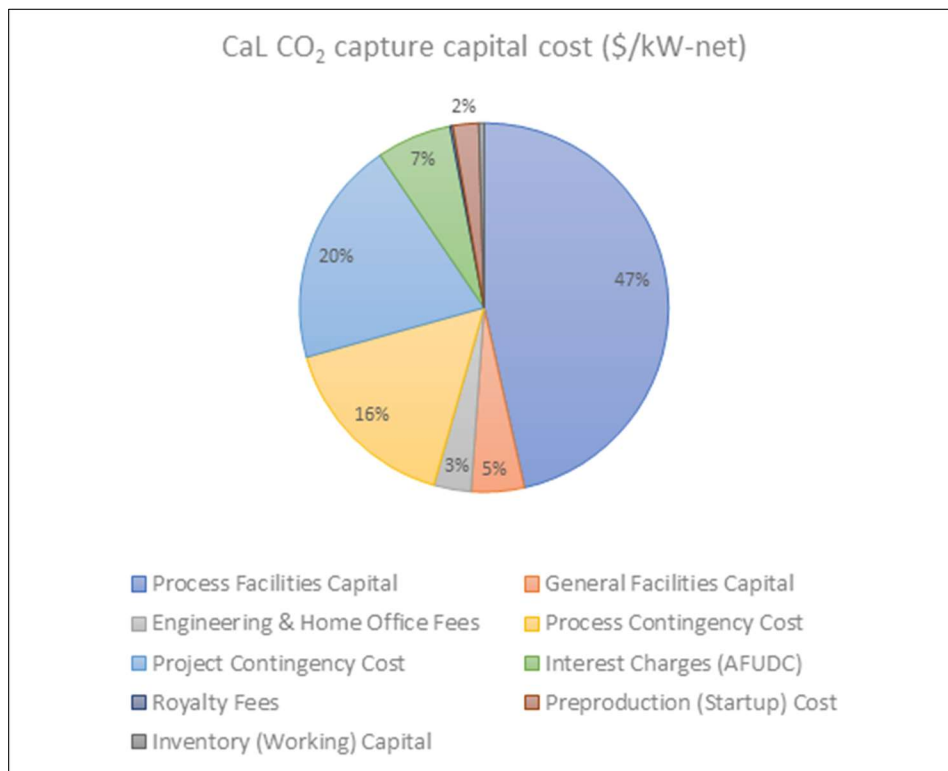


Figure 5.3 Capital cost distribution for a FOAK CaL system capture plant (\$/kW-net)

³⁹ In order to calculate costs for CO₂ captured and avoided, config. 1 was considered as the reference plant.

Figure 5.3 demonstrates process facilities capital (2047 \$/kW-net) is the main cost component, but contingency costs combined correspond to 36% of the total cost. Therefore, if contingency factors are reduced to lower values⁴⁰, the cost of CaL systems can significantly decrease. The effect of this potential reduction is further investigated in section 5.4, where both capture technologies are considered mature NOAK plants. Figure 5.3 also demonstrates other cost components have a lower influence on the overall cost of the capture unit. Still, it is worth noting that preproduction (start-up) costs of the CaL system, even if representing 2% of the capture unit capital cost (100 \$/kW-net), are more than three times the value for start-up costs of the base plant (28 \$/kW-net). On a qualitative level, this is in agreement with what was discussed in section 2.4.2.

A breakdown of costs for the CaL unit process facilities capital (2047 \$/kW-net) is exhibited in Figure 5.4. Carbonator and calciner combined represent 50% of the cost. Thus, cost reduction efforts should be aimed at these reactors. The carbonator is responsible for 33% of the costs, as it handles a greater flow rate than the calciner (resulting in a larger reactor). Other important cost components are the ASU unit (16%), the HRSG (7%), solids (limestone) handling equipment (6%), and the steam turbines (8%).

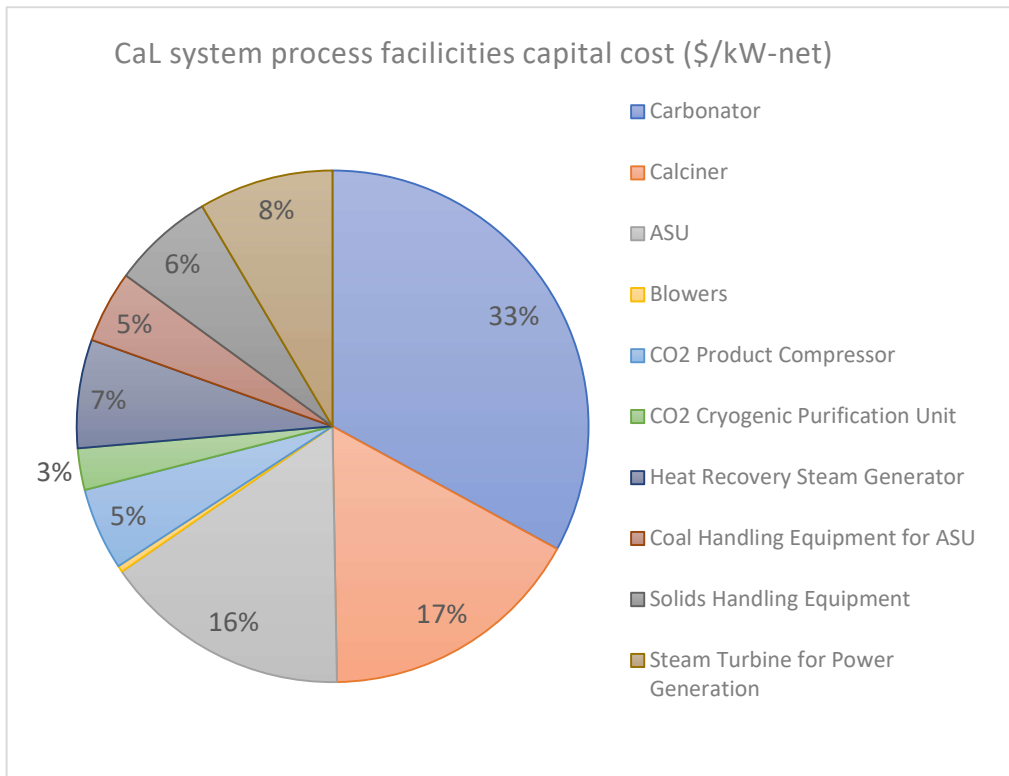


Figure 5.4 Breakdown costs of CaL capture system process facilities capital

⁴⁰ Through technology learning and/or construction of “N” plants.

5.1.3 Water use analysis

Results for water use with a wet tower cooling system are summarized in Table 5.4. Capture unit cooling duty (tH₂O/tCO₂) for CaL is significantly lower than the amine-based configurations. This translates into more efficient water use (in m³/kWh) for config. 2. Table 5.4 demonstrates that while specific water consumption for config. 2 has a 16% increase compared to config. 1, config. 3 has a 76% increase over the same reference. For specific water withdraw, config. 2 increases 2% over the reference plant, while config. 3 has a 77% increase.

Table 5.4. Water use results of power plants for wet cooling tower system*

Wet Cooling Tower	Unit	1	2	3	3FG+
Capture Cooling duty	(tH ₂ O/tCO ₂)	-	12.4	87.4	90.8
Water withdraw	m ³ /kWh (%)	2718	2779 (+2%)	4807 (+77%)	4660 (+71%)
Water consumption	m ³ /kWh (%)	1894	2192 (+16%)	3341 (+76%)	3235 (+71%)
Water withdraw	hm ³ /year (%)	5.0	8.8 (+76%)	7.8 (+55%)	7.5 (+48%)
Water consumption	hm ³ /year (%)	3.5	6.9 (+99%)	5.4 (+55%)	5.2 (+48)

* Percentage value between parenthesis indicates the percentage difference in water use in relation to the reference plant (config. 1).

Regarding water use in absolute values, the implementation of CaL doubles the volume of water consumed over the reference plant, and an increase in water withdrawal is also significant (+76% points). Likewise, the amine-based system in config. 3FG+ increases the volume withdrawal and consumed by 48% points over config. 1. Even if demand and consumption are smaller than in the CaL configuration, these are still important increments, whereas this route does not provide additional energy like CaL. Figure 5.5 illustrates the comparison in water use among all configurations. These results call attention to possible limitations to implement a CaL system, resulting from restrictions in water availability, since amine-based systems are already a concern regarding water use in Brazilian water basins (MERSCHMANN, VASQUEZ, *et al.*, 2013). Amid the amine-based systems, config. 3FG+ performs better for water use over config. 3.

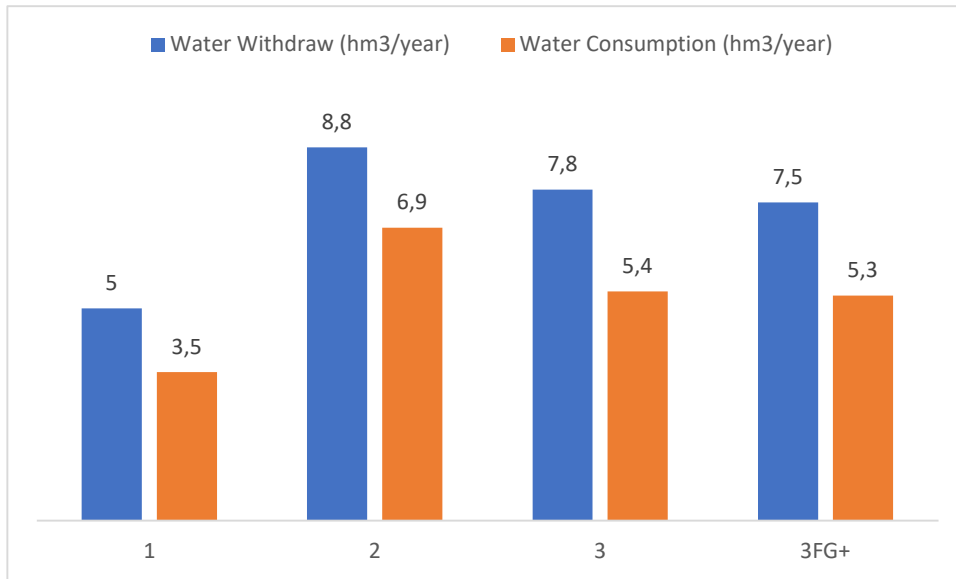


Figure 5.5 Water use analysis of carbon capture systems - wet cooling tower

Table 5.5 summarizes the results obtained when once-through systems are applied to configurations 1, 2, and 3⁴¹. Water withdraw values are greater and water consumption values are smaller compared with wet cooling systems, due to inherent characteristics of these cooling systems. For once-through systems, qualitative results obtained for the wet cooling tower systems are maintained, which means more efficient water use by the CaL system in comparison with amine-based systems. Capture unit cooling duty decreases to 8.2 tH₂O/tCO₂ in config. 2 and remains the same in config. 3.

For water-specific consumption, the result for config. 2 is even lower than in config. 1, with a decrease of 41% points over the reference plant, while the value for config. 3 is 54% points greater than config. 1. In the case of specific water withdraw, config. 2 has an increase of 24% points compared to config. 1, while config. 3 has a 120% increment. Concerning absolute values, the CaL system more than doubles the volume of water required by the plant (+115%), whereas config. 3 has an increase of 97% points. In addition, config. 2 has an increase in water absolute consumption over config. 1 of 3%, while config. 3 has an increase of +38% over the same reference.

⁴¹ Results for configuration 3FG+ are not displayed for the once-through system, since they are relatively similar to config. 3.

Table 5.5. Water use results of power plants for a once-through cooling system

Once-through	Unit	1	2	3
Capture Cooling duty	(tH ₂ O/tCO ₂)	-	8.2	87.4
Water withdraw	m ³ /kWh (%)	64840	80550 (+24%)	142300 (+120%)
Water consumption	m ³ /kWh (%)	307	182 (-41%)	471 (+54%)
Water withdraw	hm ³ /year (%)	121	259 (+115%)	237 (+97%)
Water consumption	hm ³ /year (%)	0.57	0.59 (+3%)	0.79 (+38%)

Investment costs of once-through systems are lower than other cooling alternatives. These costs are embedded in the IECM default model, and the capital costs of other cooling systems, such as the wet cooling tower, are added to a zero-base calculation. Yet, economic results for either wet cooling tower or once-through systems do not greatly change comparatively among the capture technologies. Other options for cooling systems, including an air-cooled condenser, which has a higher capital cost and minimum water use, were not considered in this work.

Therefore, results indicate the retrofit of a PC plant with CaL causes substantial impact in water use, regardless of whether the cooling system considered is a wet cooling tower or a once-through system. This is mainly due to the increase in power production, which implies in a revamp of the cooling system⁴². Comparatively to amine-based systems, however, CaL systems use water more efficiently, which can be an advantage of this capture route considering new-built power plants with CCS or future capture-ready plants.

The increase in water use is especially important considering regions already facing a critical water situation, where water scarcity could be a limiting factor for the installation of a CaL system. Particularly, the selection of a suitable location for a capture-ready plant, that intends to implement a CaL capture unit in the future, should consider the water source must be capable of supplying at least twice the original volume consumed (in the case of wet cooling tower systems) or withdrawn (in the case of once-through systems) by the base plant after the CaL unit is added.

Finally, if Brazil or other countries plan to expand their power generation fleet with thermal power plants, and later install CaL capture units as retrofits, the water

⁴² By using a wet cooling tower, the capital cost of the cooling system increases from 26 M\$ in the reference plant (config. 1) to 56 M\$ in the base plant with CaL (config 2).

balance should be considered a critical factor for selecting the sites for these plants. Regarding water constraints, results obtained in this work can be used along with past studies⁴³, which evaluated water use in power plants associated with CCS. This would make it possible to assess if existing plants would be suitable or not to receive a CaL retrofit.

5.1.4 Plant footprint analysis

For a thermal plant integration with a capture unit, the minimum requirement is the physical space at the plant site to accommodate the capture plant. The space required for carbon capture equipment depends on a range of factors, including the capture technology and some site-specific factors, which are difficult to generalize and not easily scalable. The layout of a CCS plant will also vary whether it is a retrofit of an existing plant or a capture-ready scenario⁴⁴, as the capture-ready scenario can foresee layout optimization for when the capture unit is added. Therefore, plant layouts should ultimately be considered on a case-by-case basis rather than on the basis of a minimum land footprint.

For planned capture-ready plants, the added space represents marginal capital costs, but in non-planned retrofits of CCS, there is often limited space available for expansion. Retrofit efforts then require a unique approach to utilize the space available. Additional space requirements could make a retrofit considerably more expensive to carry out (due to costly rearrangements) or, in a worst-case scenario, “*lock-in*” the plant if not previously accounted for, i.e. making the retrofit unfeasible. Thus, it is important to estimate the capture plant footprint of CaL even in a preliminary analysis.

To avoid ambiguity and facilitate comparison, land footprint estimates must specify all of the assumed equipment. For a CaL system, these would include, among others: both generation systems (steam turbines), CO₂ capture equipment (including sizing for calciner, carbonator, and the number of trains), cooling system, ASU, CO₂ dehydration, and compression (number of compressors per train), additional flue gas treatment if included, sorbent storage and handling, extra fuel (for the calciner) storage,

⁴³ For example, the work by (MERSCHMANN, VASQUEZ, *et al.*, 2013)

⁴⁴ Considering that capture-ready plants and new built CCS plants would both have the same land footprint when the capture unit is added.

handling and feeding system, CO₂ transport details, space for construction and appropriate space for health and safety. However, a detailed land footprint analysis is beyond the scope of this work and a simple estimation is conducted in the following paragraphs.

The CaL capture unit land footprint (not directly calculated by the IECM model) can be estimated based on a few simple assumptions. Equations (3-87) and (3-88), which were presented in chapter 3, can be used to calculate the cross-sections in m² of the carbonator and calciner reactors. As previously mentioned, these equations are based on the work by (LYNGFELT, LECKNER, *et al.*, 2001) for CFB boilers. The other subsystems that are part of the capture process area may be estimated based on values available in the literature for oxy-combustion capture systems. The report by FLORIN and FENNELL (2011) on pulverized coal plants, mentioned in section 2.4.2, is used as guidance to estimate plant footprint of oxy-combustion and amine-based carbon technologies.

According to FLORIN and FENNELL (2011), a typical land footprint for an amine-based system of a 300 MW_g plant would require between 8000 and 11500 m², based on linear relationships with the reported values and including area for compression (areas for the existent generation plant and FGD unit were not included). A CaL system, on the other hand, will arguably require the equivalent of an oxy-fired generation plant of 289 MW_g (equal to the added gross power output of the oxy-fired calciner in config. 2) and its associated CO₂ capture system. Thus, no possible integration with the existing plant is admitted. Also, the area for the carbonator, calciner⁴⁵, and limestone handling/storage should be accounted for. For Bio-CaL plants, these areas should be larger compared to coal-fired plants since the feedstock has lower energy density. The CCU unit of the CaL plant will also have a larger area than a typical 289 MW_g oxy-fired plant, since there is an additional amount of CO₂ captured from the carbonator.

Based on these assumptions, cross-sections areas for the carbonator and calciner for a 300 MW_g reference plant are respectively 170 m² and 70 m², using a gas superficial velocity of 5 m/s⁴⁶. In this case, one train of reactors is sufficient and the interconnected

⁴⁵ In fact, the area required for the calciner would be already accounted for in the oxy-fired unit, but the cross section is calculated to assess the number of trains required.

⁴⁶ Superficial gas velocity was previously discussed in section 3.2.3 and typical values range from 5-7 m/s.

dual CFB requires a footprint close to 500 m², considering the necessary space for interconnections, loop seals, cyclones, and equipment clearances. Based on reported values for oxy-fired systems, the CaL capture system, primary and secondary generation plants aside, results in a capture unit area of about 12 500 m². The primary generation plant alone requires about 96 000 m². Using a linear scaling factor is clearly oversimplistic and it would be more reasonable to undertake a bottom-up approach. However, as a first estimate, results show the space requirement of a CaL system could possibly be similar to an amine-based system, considering just capture unit area. This changes when the secondary power cycle is included, although CaL technologies have significant potential for utilisation of common utilities with the existing generation plant. Finally, heat rejected from capture and compression units could be exploited with tight thermal integrations if equipment is located in close proximity, which highlights the importance of space being available in critical locations. Regarding thermal plants fuelled with bagasse, which are often located in the same site as ethanol distilleries, physical space for the capture unit might present an extra challenge, since those distilleries usually have crop area around them.

5.2 Comparative analysis for subcritical BFPP

Table 5.6 shows the main performance and cost results for configurations 1A, 2A, and 3A, obtained by replacing coal with sugarcane bagasse as feedstock. Qualitatively, results do not differ from the ones using coal. Costs for the Bio-CaL system, or config. 2A, are greater than for the amine-based system, while the thermodynamic performance favours config. 2A over config. 3A. The efficiency penalty for config. 2A over the reference plant (config. 1A) is of 1.4%, while for config. 3A is of 8.9%. Comparatively to the supercritical CFPP configurations, the smaller efficiency penalty in config. 2A (1.4% against 3.3% of config. 2) is an effect of the lower capture rate assumed for the carbonator (80%). This lower capture rate impacts heat demand in the calciner, leading to a more efficient integrated system. The capture rate in the absorber of config. 3A was maintained as 90%, so both CCS configurations have a similar overall (full system) capture rate. Nevertheless, config. 2A emits more CO₂ from the flue gas than config. 3A.

Table 5.6 Performance and cost results for subcritical bagasse-fired power plants with and w/o CCS

Parameter	Unit	1A	2A	3A
Gross Power Output	MW	300	300 (+335) ^a	300
Net Power output	MW	279	508	246
Net plant efficiency	% HHV	34.6	33.2	25.7
Efficiency Penalty	% HHV	-	1.4	8.9
Total Capital Requirement (TCR)	\$/kW-net	1897	6014	4311
CO₂ capture capital cost	\$/kW-net	-	4902	1893
Plant LCOE	\$/MWh	47.5	139.1	111.4
Plant specific CO₂ emissions	kgCO ₂ /MWh	976	107	131
Cost of CO₂ avoided	\$/tonne CO ₂	-	105.4	75.6
Cost of CO₂ captured	\$/tonne CO ₂	-	78.0	47.1
Water withdraw (WTC)	m ³ /kWh (%)	2776	3169 (+14%) ^b	5451 (+96%)
Water consumption (WTC)	m ³ /kWh (%)	1895	2356 (+24%)	3827 (+102%)
Water withdraw (WTC)	hm ³ /year (%)	5.1	10.5 (+108%)	8.8 (+73%)
Water consumption (WTC)	hm ³ /year (%)	3.5	7.9 (+126%)	6.2 (+78%)

^a Config. 2A has additional gross power generated from the secondary steam cycle, represented in parenthesis.

^b Percentage value between parenthesis indicates the percentage difference in water use in relation to the reference plant (config. 1A).

Regarding economics, LCOE in config 1A has a 34% decrease in relation to config. 1. This is likely caused by the lower fuel price of bagasse in comparison to coal, the absence of pollution control technologies that are present in the coal-fired plant, and the fact the biomass-fired plant represents a subcritical steam cycle (opposed to a supercritical steam cycle, with greater capital cost, in config. 1). In the CCS configurations, however, these effects are partially compensated by the capital cost impact of larger equipment⁴⁷, which is required to handle twice the amount of fuel on a mass basis⁴⁸. Then, LCOE in config. 2A is reduced by 8% points over config. 2, while in config. 3A the decrease is of 19% in comparison with config. 3. Thus, the difference in LCOE between CCS configurations is larger for the biomass-fired plant. More specifically, LCOE in config 2A is 25% points more expensive than 3A, while the difference is 10% points between config. 2 and config. 3. Therefore, the use of biomass favoured the amine-based system over the Bio-CaL system. Results for water use remained similar to what was found for supercritical CFPP configurations, but the impact in water use increment due to the CCS configurations was greater for the BFPP configurations.

During simulation modelling, when high temperatures (above 900 °C) were applied for the biomass-fired calciner, the residence time of solids in the reactor was lower⁴⁹ compared to a coal-fired calciner using the same temperature, which could impact designed calcination efficiency. To avoid this, the calciner temperature was set to 900 °C. The lower residence time for biomass feedstock compared to coal is likely due to higher material reactivity of the former, as suggested in (ALONSO, DIEGO, *et al.*, 2014).

Table 5.7 displays Bio-CaL operational results for reactors' residence time and circulation rates through the interconnected system. These parameters change from config. 2 due to differences in the fuel composition. Residence time in the carbonator in config 2A. is shorter than in config. 2, while in the calciner is longer in config. 2A.

⁴⁷ Additionally, the process contingency factor assumed for the Bio-CaL plant was greater than for the CFPP FOAK plant, while for the amine-based system the same factor was applied. Although Bio-CaL has not been tested at the same size as coal-fired CaL, previous discussions in this work point out that the technology learning accumulated for CaL could be, in some level, used for Bio-CaL. Therefore, even though Bio-CaL was ranked as TRL 4, the difference between process contingency costs applied for CaL and Bio-CaL is small.

⁴⁸ As the heating value of bagasse is almost half of coal.

⁴⁹ The value for residence time of solids was below 1 min, which is below the limit suggested by the literature and the software. Furthermore, low reaction time could impact the designed calcination efficiency.

Overall, bagasse reacted faster than coal in the CaL system. Circulation rates, in turn, are lower for the bagasse-fired system, but results remain within the limits suggested by the literature for CFB systems.

Finally, results indicate that, with few adaptations, the model proposed can be used to assess a Bio-CaL system. Further investigation on system modifications and possible cost differences, particularly in pre-treatment stages and feeding, handling and storage systems, is recommended.

Table 5.7 Operational results for config. 2A (Bio-CaL)

Bio-CaL system operational results	Unit	Value
Solids residence time in the carbonator	Seconds	80
Solids residence time in the calciner	Seconds	63
$F_0/F_{CO2,fluegas}$	(mol/mol)	0.10
$F_R/F_{CO2,fluegas}$	(mol/mol)	7

5.3 Comparative analysis for subcritical CFPP

Considering most of the current global generation fleet is composed of subcritical coal-fired plants (CALDECOTT, DERICKS, *et al.*, 2015), simulations were also conducted for this type of steam cycle. In general terms, results are similar to supercritical plants. Table 5.8 demonstrates that the CaL system (config. 2B) outperforms the amine-based system (config. 3B) in thermodynamics and plant emissions rate. Still, economic parameters of config. 2B are not competitive with config. 3B, with the first presenting the higher costs for FOAK plants.

In addition, the subcritical cycle is less efficient in water use compared with the supercritical cycle, though, results for water use increment⁵⁰, both in specific and absolute terms, are proportional to the ones obtained for the supercritical steam cycle. Comparatively to the supercritical configuration, the impact of CaL in the reference plant cost is higher, with an LCOE increase of 120% over config. 1B, against a 108% increase among the correspondent supercritical system. While LCOE in config. 2B is 13% points higher than in config. 3B, the increase is 10% points for the supercritical configurations. Similar results are found for TCR costs, favouring CaL supercritical configuration. Also, the difference in efficient penalty between the CaL and amine-based capture is greater for the supercritical plants. Therefore, it can be concluded that amid supercritical and subcritical plants, the first is more suitable for the implementation of CaL systems.

Table 5.8 Performance and cost results for subcritical coal-fired power plants with and w/o CCS

Parameter	Unit	1B	2B	3B
Gross Power Output	MW	300	300 (+289) ^a	300
Net Power output	MW	279	474	243
Net plant efficiency	% HHV	36.4	33.0	27.3
Efficiency Penalty	% HHV	-	3.4	9.1
Total Capital Requirement (TCR)	\$/kW-net	2173	5944	4539
CO₂ capture capital cost	\$/kW-net	-	4602	1772
Plant LCOE	\$/MWh	70.4	155.8	138.2
Plant specific CO₂ emissions	kgCO ₂ /MWh	870	50	120
Cost of CO₂ avoided	\$/tonne CO ₂	-	103.7	89.5
Cost of CO₂ captured	\$/tonne CO ₂	-	76.5	57.2

⁵⁰ Water use increment caused by the addition of capture units and considering config. 1B as the reference plant.

Water withdraw (WTC)	m3/kWh (%)	2984	3105 (+4%) ^b	5277 (+77%)
Water consumption (WTC)	m3/kWh (%)	2096	2447 (+17%)	3690 (+76%)
Water withdraw (WTC)	m3/year (%)	5.5	9.7 (+77%)	8.4 (+54%)
Water consumption (WTC)	m3/year (%)	3.8	7.6 (+99%)	5.9 (+54%)

^a Config. 2B has additional gross power generated from the secondary steam cycle, represented in parenthesis.

^b Percentage value between parenthesis indicates the percentage difference in water use in relation to the reference plant (config. 1B).

5.4 Sensitivity analysis

The previous sections indicated that the CaL-based configurations have better thermodynamic performances (higher net plant efficiency and power output) but worse economic ones (higher capital cost, LCOE, and costs of CO₂ captured and avoided). In this section, a sensitivity analysis was conducted to assess the effect of key variables – fuel price, plant size, capacity factor, and contingency costs – on the costs of the compared supercritical CFPP configurations – see Table 5.9.

Table 5.9 Parameters and values assumed for sensitivity analysis

Parameter	Sensitivity values
Coal price	\$40 and 80\$/tonne
Plant size (MW _g)	100, 300 and 700
Capacity factor	40%, 75% and 85%
Contingency costs ⁵¹	FOAK and NOAK plants

5.4.1 Fuel price

Fuel price is investigated to assess if variations on market conditions have a different impact on CaL systems economics relative to amine-based systems, as the first uses an additional amount of fuel to supply the oxy-fired calciner, but has a higher capital cost. Table 5.10 summarizes the main cost results for configurations 2 and 3. Cost values for TCR and CO₂ captured show small variations between the two coal prices (in TCR, variations are caused by differences in fuel inventory for pre-production costs) while LCOE, as it includes O&M costs, is more affected.

Table 5.10 Cost sensitivity analysis for fuel price

Low Fuel Price \$40/tonne	Unit	Config. 2	Config. 3
Total Capital Requirement (TCR)	\$/kW	5827	4634
Plant LCOE	\$/MWh	148.1	133.9
Cost of CO ₂ captured	\$/tonne CO ₂	75.3	58.2
High Fuel Price \$80/tonne	Unit	Config. 2	Config. 3
Total Capital Requirement (TCR)	\$/kW	5833	4647
Plant LCOE	\$/MWh	161.4	149.9
Cost of CO ₂ captured	\$/tonne CO ₂	76.5	62.14

⁵¹ Contingency costs were varied based on the values presented in Table 4.5, in chapter 4.

The effect of fuel price on plant LCOE is more significant for the amine-based plant compared to the CaL-based plant, as illustrated in Figure 5.6. The graph demonstrates that while the LCOE in config. 2 has an increase of 9% points from low to high fuel price, increase in config. 3 is of 12% points. This is due to the higher capital cost of CaL and the lower influence of its O&M costs in LCOE.

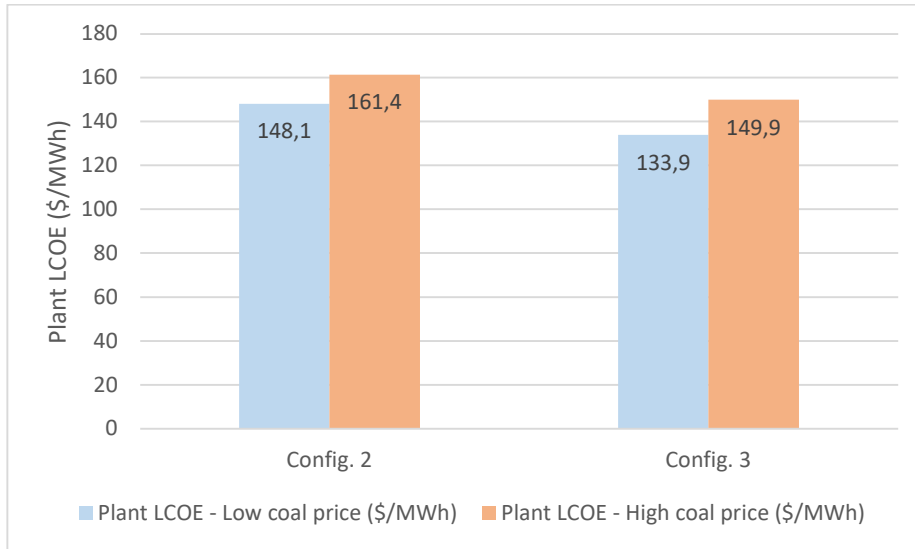


Figure 5.6 Effect of fuel price on plant LCOE

5.4.2 Size

Plant size influence in costs - TCR and LCOE - is investigated for plants with 100 MW and 700 MW gross power output, aside from original configurations with 300 MW_g. Results are shown in Table 5.11 and Fig 5.7. The 100 MW_g plant is coal-fired but represents the typical size of a large-scale biomass-fired power plant.

Table 5.11 Cost sensitivity analysis for plant size

Plant size – 700 MW _g	Unit	1	2	3
Total Capital Requirement (TCR)	\$/kW	1875	4658	3803
Plant LCOE	\$/MWh	58.6	123.3	112.1
Plant size – 100 MW _g	Unit	1	2	3
Total Capital Requirement (TCR)	\$/kW	3246	8480	6129
Plant LCOE	\$/MWh	106.2	219.7	197.6

Both technologies are affected by economies of scale, although config. 3 remains more economical. Still, results indicate larger plants tend to favour TCR of CaO-based

over amine-based systems, as for 100 MW config. 2 is 38% more expensive than config. 3, while for 700 MW config. 2 is 22% more expensive than config. 3. LCOE values, in turn, remained proportionally stable for all plant sizes, with config. 2 around 10% more expensive than config. 3. Also, the LCOE percentage increment for CCS configurations in relation to the reference plants remained almost equal for all plant sizes. Config. 2 is about 110% more expensive than config. 1, while config. 3 has an increase of around 90% over the same reference

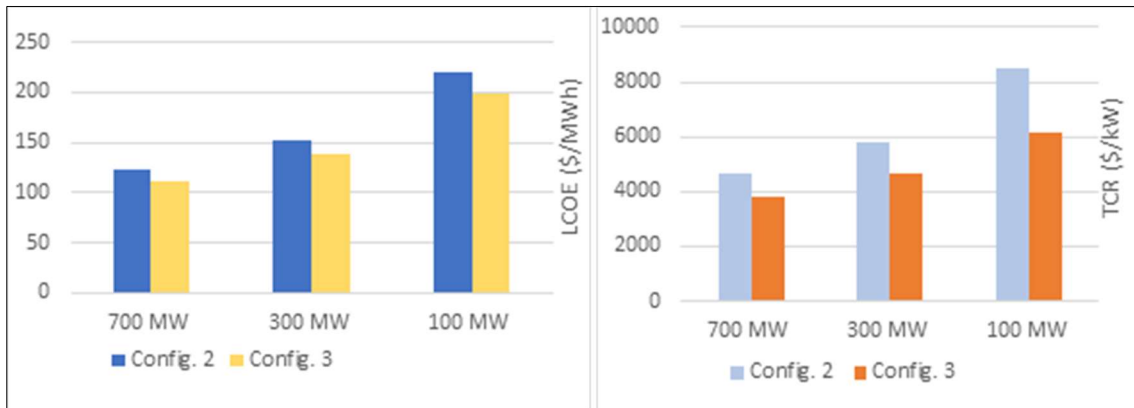


Figure 5.7 (Left) LCOE for different plant sizes for config. 2 and 3. (Right) Total capital requirement with different plant sizes for config. 2 and 3.

5.4.3 Capacity factor

Capacity factor affects LCOE in particular, since capital costs are maintained and revenue and operational costs vary. Results for LCOE in config. 1, 2, and 3 when capacity factors of 40% and 85% are applied, are summarized in Table 5.12. It can be noticed that LCOE almost doubles from CF of 40% to CF of 80% for config. 2, and the increase in cost is similar for config 3. Therefore, CF does not seem to favour any specific technology in terms of LCOE. Indirectly, this neutrality regarding cost can favour CaL systems, as the technology supposedly deals with greater ease with more flexible plants (from an operational perspective), while amine-based systems may incur increased forced downtime if operated with different CF values throughout the year.

Table 5.12 Cost sensitivity analysis for capacity factor

CF – 40%	Unit	1	2	3
Plant LCOE	\$/MWh	120.5	261.3	234.2
CF – 85%	Unit	1	2	3
Plant LCOE	\$/MWh	66.1	136.6	124.9

5.4.4 Contingency factor

As seen in section 5.12, due to the current high uncertainty associated with the CaL technology, an important cost component of these systems is the contingency cost (process and project). Thus, it is also worth comparing costs of CaL and amine-based configurations assuming both technologies have reached high technology maturity (TRL 9), with “N” plants constructed. If the cost of CaL systems remains significantly greater than amine-based systems under these conditions, one can interpret as a strong sign the technology will remain non-competitive compared with amine-based systems, regardless of their level of maturity.

Table 5.13 displays LCOE, TCR, and costs of CO₂ captured and avoided for config. 2, 3, and 3FG+ considering equal contingency factors, equivalent to TRL 9. CaL system has the lowest LCOE value among the simulated capture technologies. Regarding TCR, config. 2 remains more expensive, but the difference decreases from 26% points to a negligible 1% point plus compared with config. 3, and from 40% to 12% points plus compared with config. 3FG+. For the cost of CO₂ captured, config. 2 has an intermediate value between the amine-based systems, while for CO₂ avoided config. 2 has the lowest cost among CCS configurations. Therefore, compared with the amine-based system, the CaL process demonstrates advantages in LCOE and cost of CO₂ avoided, and benefits such as better thermodynamic performance, the larger amount of CO₂ captured in the plant location, lower plant-specific CO₂ emission, and potential to re-power and operate an existing plant with greater ease and flexibility.

Table 5.13 Cost results for NOAK CCS plants

NOAK Plant	Unit	2	3	3FG+
Total Capital Requirement (TCR)	\$/kW	4570	4509	4085
Plant LCOE	\$/MWh	125.8	135.1	127.3
Cost of CO₂ captured	\$/tonne CO ₂	49.5	56.3	45.8
Cost of CO₂ avoided	\$/tonne CO ₂	68.9	87.7	77.4

Finally, results above indicate that continuous effort in R&D and CaL demonstration and FOAK plants could help the technology to become economically feasible against benchmark post-combustion capture technologies in the long-term, as long as technology developers and investors pay present costs (currently higher for FOAK plants) to build the necessary “N” plants that could bring costs down. Still, even for a potential CaL NOAK plant, LCOE increased by 74% compared with a reference plant without capture. Therefore, continuous effort to reduce the costs of CaL below the expected values is paramount and involves more innovations and operational experience with its two major capital cost components: the carbonator and the calciner.

6. Conclusions

This work aimed to evaluate technical and economic aspects of the emerging capture technology known as calcium looping when applied for post-combustion CO₂ capture in solid fuel combustion power plants, as well as its feasibility compared to more conventional capture routes. Particularly, comparison analyses were conducted with the state-of-the-art amine-based CO₂ capture process, considered the benchmark capture technology in post-combustion capture. Knowledge gaps in potential cost reduction due to technology learning, water use, and space requirements, were recognized by reviewing previous comparative studies with the calcium looping technology applied in large-scale thermal power plants. The work objectives were then set to assess these gaps, plus the applicability of the technology to capture-ready and/or existent plants. The feedstocks selected were coal and sugarcane bagasse. From the author's knowledge, this is the first detailed study on CaL for carbon capture developed in Brazil, including also the evaluation of bagasse as a fuel.

Prior to the comparative analysis, however, a brief discussion in chapter 2 was made over CCS demand, its general global status, and the main technologies for energy generation and CO₂ capture. In addition, technological maturity and suitability of the capture routes to existent, new and capture-ready power plants were discussed, followed by characterization of high-temperature solid looping cycles, chemical looping technologies, and, finally, calcium looping technology. It was concluded that calcium looping or CaL systems can be used as a post-combustion capture route and is a technology suitable for retrofitting an existent power plant.

Also in chapter 2, a literature review of the calcium looping technology was made describing the technical process for post-combustion, its main challenges and potential advantages. Other promising applications of CaL and end uses for the purged sorbent were briefly introduced. Regarding potential benefits, the possibility of re-powering a power plant was highlighted as a unique feature among available capture technologies. In addition, advantages from the use of subsystems that compose the CaL system and are in a superior technology development stage, such as the ASU or CFB boilers, were addressed, as these components have their own technology development path, apart from the CaL technology. This can facilitate the scale-up of CaL systems.

Possible operational difficulties regarding the use of large scale solid-gas processing plants with solids transportation between reactors were pointed out, as well as potential challenges related to plant availability and sorbent attrition. However, absolutely restrictive technical bottlenecks were not identified. Also, the integration with a base plant was found to be potentially less complex than amine-based systems, which can enable the steam cycles and capture plant to operate more independently and with greater flexibility. Also, the current pilot plant experience was detailed to help to define the maturity level of the technology, which was set as TRL 6, when applied to post-combustion, as of today. Finally, relevant feedstock properties related to the operation of a CaL system were discussed. The use of biomass as feedstock for CaL, though still with limited data and only a few experimental tests on bench-scale (lower TRL than coal), was investigated foreseeing the need for technologies with net negative emissions.

In chapter 3, mathematical modelling of the standard CaL system for post-combustion was described, on the basis of experimentally validated performance models published in other studies. The calculation procedure adopted by the Integrated Environmental Control Model (IECM) software guided the model description, as this software was used to conduct simulations for power plants with and without capture. Mass and energy balance of the system were detailed, accounting for possible heat integration using the CaL cycle heat streams and a secondary steam power cycle. Then, reactors' design was discussed for carbonator and calciner based on semi-empirical equations, pilot plant experience, and experience with CFB systems. The chapter also discussed optimal operational and design parameters of a standard CaL plant, such as the CO₂ rich gas recirculation rate in the calciner (to reach a desired oxygen concentration in the reactor), the optimal temperature in the reactors, superficial gas velocity in the reactor, maximum cross-section area of reactors, the reaction kinetics of calcination and carbonation and the expected sorbent carrying activity. The permanent equilibrium analyses allowed the use of the simulator, by helping to define the appropriate inputs. From the estimation of mass flows, they also allowed the evaluation of the plants' footprints. Hence, the proposed models proved to be suitable for the aims of this study.

Chapter 4 presented the methodology and data applied for the comparative analyses. Two feedstocks were selected for the cases modelled: bituminous coal and sugarcane bagasse. The criteria behind the selection of these feedstocks involved the dominant and wide use of coal in power plants, and particular aspects of the Brazilian

energy mix, which has sugarcane bagasse as an important energy vector for thermal power plants. It was also shown that bagasse has further advantages over other biomasses due to its inherent properties, which would likely allow its use in high calcination temperatures and advanced steam cycles without negatively affecting the CaL system operation with bed agglomeration, fouling, and ash fusion. The IECM broad use in carbon capture comparative studies and its capabilities to evaluate CaL systems were then introduced to justify its utilization for the plant simulations. The chapter also briefly reviewed economic models for CaL systems and developed a cost method to estimate cost uncertainty in emerging capture technologies, and, by doing so, differentiate costs for FOAK and NOAK plants. The method consisted of applying appropriate contingency factors to the capital cost of the capture unit, so that the uncertainty was in line with the Technology Readiness Level of the evaluated post-combustion capture technology. Finally, base configurations were defined to represent a reference plant and power plants with CaL and amine-based CO₂ capture. The simulations were conducted for supercritical and subcritical CFPPs, as well as subcritical BFPPs. Sensitivity analyses were also performed regarding fuel price, plant size, plant capacity factor, and contingency costs.

Technical results in chapter 5 were in agreement with literature values and revealed the better thermodynamic performance of the CaL system. Not only the CaL plant had a lower efficiency penalty - 3.3% in relation to the reference case, compared with 9.4% and 10.8% of the amine-based configurations - but it has also shown a lower specific emissions rate compared to the amine-based systems when the same capture rate of 90% is applied to the flue gas. Furthermore, the additional generation capacity in the base power plant with the retrofit of a CaL system was substantial, reaching a 72% increase compared with the reference plant without capture in the simulation for a supercritical CFPP. At the same time, the increase in required fuel input was 88% points.

Regarding economic results, it was seen that the CaL system is still highly intensive in capital, not competing with amine-based systems when the current maturity of the two technologies is considered (FOAK plants). Nevertheless, when the contingency factors were low for both technologies (typical of NOAK plants), LCOE and cost of CO₂ avoided favoured the CaL system technology. Among the other parameters varied in the sensitivity analysis, plant size had the biggest influence in reducing CaL costs, which indicates economies of scale. However, the costs increase in LCOE varied between 90% and 120% compared with the reference plant with no capture. Even for a potential CaL

NOAK plant, LCOE increased by 74% points compared with a reference plant without capture, which indicates the need for innovations and operational experience, particularly in CaL systems' two major capital cost components: the carbonator and the calciner. Results for subcritical BFPP and CFPP were similar to what was obtained with the supercritical CFPP. For the biomass-fired plant, the model worked properly and small differences in solid circulation rates and solids residence time in reactors did not compromise the operational parameters of the plant, that remained within reasonable values. The cost analysis for the Bio-CaL adopted a process contingency factor greater than for the CFPP cases, assuming biomass use in CaL systems is more incipient and some of the equipment might need adaptations to receive biomass instead of coal.

Regarding water use, analyses were conducted in chapter 5 for withdrawal and consumption parameters considering two typical water-cooling systems: once-through and wet cooling tower. For both cooling systems, the addition of the CaL unit represented a substantial increase in water use absolute values compared with the reference plant (in some cases, more than twice the original value) and the amine-based systems. However, the specific water use in m^3/kWh was lower for the CaL system in all cases simulated. Thus, a greater water use efficiency of the CaL system compared to amine-based systems was demonstrated. This implies that if the addition of the capture unit is a retrofit to an existent plant, - i.e. constructed without planning or preparing for the retrofit - the water availability could be a restrictive aspect for CaL installation, even more than already is for amine-based systems. On the other hand, if the plant is newly built or capture-ready, and already accounts for the addition of a CO_2 capture system in the present or sometime in the future, the option for the CaL system could be preferable as it produces more energy using less water.

For space requirements, it was seen that the CaL plant occupies a larger land footprint due to the secondary steam cycle, but integration with the base plant could be more flexible regarding the need for capture unit proximity, since there is no steam-extraction from the primary steam cycle as in the amine-based system. In the CaL system, the only integration with the base plant is the flue gas diverted from the stack. Besides, some of the equipment required for the secondary steam cycle could be shared with existing equipment of the primary cycle, so there is probably room for layout optimization when applying CaL systems, and actual space requirements should be addressed in a case-by-case basis.

Furthermore, the applicability of the CaL system cannot be discarded either for greenfield, capture-ready, or brownfield scenarios (existent and without any pre-modification to receive the capture plant). Nevertheless, it can be considered more suitable for greenfield and/or capture-ready plants, as these can previously account for the requirements regarding water, space, and additional fuel, which could be impeditive for a brownfield plant.

Therefore, even though it is not possible to predict if calcium looping systems will sometime in the near future become a disruptive capture technology, capable of outperforming current state-of-the-art amine-based systems, there are clear advantages in using these systems, markedly the lower efficiency penalty associated with additional power generation. If capital costs of CaL are reduced, through sustained R&D and technological learning, policy framework for investments, plant operation experience, and scale-up, CaL systems could get closer to current advanced amine-based systems regarding economic feasibility. Technically, the system is already feasible by using relatively mature CFB power plant technology, even if there are operational challenges to be faced.

Still, to enable more quantitative and precise cost and performance assessments and confirm process advantages, it is important that this technology scales-up and reaches a pilot or demonstration scale testing at a TRL 7 or higher, which could be a “dead valley” for this emerging technology, as it will require large investments to build plants of tens of MW_{th}. Also, the demonstration of these technologies for biomass and other fuels needs to be advanced to higher TRL.

For future work, the following subjects are recommended:

- A study with a focus on developing learning rate curves for CaL systems, accounting for the learning rate of individual components such as the carbonator and the calciner;
- A more detailed thermodynamic analysis, evaluating the minimal work of separation of this technology based on the second law of thermodynamics;
- Evaluation of chemical looping combustion (CLC) and other calcium looping concepts such as calcination using pure oxygen or applied to pre-combustion capture;

- A study focused on industrial applications of CaL, such as cement and steel production plants (possible integration with the industry sector and use of the purged sorbent as a sealable product);
- Project lifetime of power plants could be longer than certain equipment of the CaL system, such as the calciner. The impact of a reduced lifetime of equipment in CaL systems have not been assessed so far;
- Operational plant commission, start-up, and shut-down procedures have not been fully addressed in the literature;
- A sensibility analysis focused on determining potential limitations for CaL systems application regarding coal quality for high sulphur and ash content;
- A comparative multicriteria analysis of the carbon capture technologies assessed in this work with a focus on the 12 principles of Green Chemistry;
- Comparison and determination of policies to enable emerging capture technologies such as CaL against conventional capture and other low carbon technologies;
- Plant flexibility with CaL has only been addressed in a few preliminary studies. These studies have pointed out possible advantages of the CaL system compared with the amine-based system. However, much has to be learned about how flexibility requirements will impact the efficiency and cost prospects of CaL. Combinations with energy storage concepts also need to be investigated.

References

ABANADES, J. C., ARIAS, B., LYNGFELT, A., *et al.* "Emerging CO₂ capture systems", **International Journal of Greenhouse Gas Control**, v. 40, p. 126–166, 2015. DOI: 10.1016/j.ijggc.2015.04.018. .

ACKIEWICZ, M., LITYNSKI, J., KEMPER, J., *et al.* "Technical Summary of Bioenergy Carbon Capture and Storage (BECCS)", **Carbon Sequestration Leadership Forum**, p. 1–76, 2018. Disponível em: https://www.cslforum.org/cslf/sites/default/files/documents/Publications/BECCS_Task_Force_Report_2018-04-04.pdf.

ALONSO, M., DIEGO, M. E., PÉREZ, C., *et al.* "Biomass combustion with in situ CO₂ capture by CaO in a 300kWth circulating fluidized bed facility", **International Journal of Greenhouse Gas Control**, v. 29, p. 142–152, 2014. DOI: 10.1016/j.ijggc.2014.08.002. Disponível em: <http://dx.doi.org/10.1016/j.ijggc.2014.08.002>.

ALONSO, M., RODRÍGUEZ, N., GRASA, G., *et al.* "Modelling of a fluidized bed carbonator reactor to capture CO₂ from a combustion flue gas", **Chemical Engineering Science**, v. 64, n. 5, p. 883–891, 2009. DOI: 10.1016/j.ces.2008.10.044. .

ALONSO, Mónica, ARIAS, B., FERNÁNDEZ, J. R., *et al.* "Measuring attrition properties of calcium looping materials in a 30 kW pilot plant", **Powder Technology**, v. 336, p. 273–281, 2018. DOI: 10.1016/j.powtec.2018.06.011. Disponível em: <https://doi.org/10.1016/j.powtec.2018.06.011>.

AMEC FOSTER WHEELER ENERGIA OY. "Advanced Utility Cfb Technology for Challenging New Solid Biomass Fuels", **PowerGen Europe**, p. 1–15, 2015.

ANEEL. **BIG - Banco de Informações de Geração**. 2020. Disponível em: <http://www2.aneel.gov.br/aplicacoes/capacidadebrasil/OperacaoCapacidadeBrasil.cfm>. Acesso em: 2 mar. 2020.

ARIAS, B., CRIADO, Y. A., SANCHEZ-BIEZMA, A., *et al.* "Oxy-fired fluidized bed combustors with a flexible power output using circulating solids for thermal energy storage", **Applied Energy**, v. 132, p. 127–136, 2014. DOI: 10.1016/j.apenergy.2014.06.074. Disponível em:

<http://dx.doi.org/10.1016/j.apenergy.2014.06.074>.

ARIAS, B., DIEGO, M. E., ABANADES, J. C., *et al.* "Demonstration of steady state CO₂ capture in a 1.7MWth calcium looping pilot", **International Journal of Greenhouse Gas Control**, v. 18, p. 237–245, 2013. DOI: 10.1016/j.ijggc.2013.07.014. Disponível em: <http://dx.doi.org/10.1016/j.ijggc.2013.07.014>.

ARIAS, Borja, ALONSO, M., ABANADES, C. "CO₂ Capture by Calcium Looping at Relevant Conditions for Cement Plants: Experimental Testing in a 30 kW th Pilot Plant", **Industrial and Engineering Chemistry Research**, v. 56, n. 10, p. 2634–2640, 2017. DOI: 10.1021/acs.iecr.6b04617. .

ARIAS, Borja, DIEGO, M. E., MÉNDEZ, A., *et al.* "Operating Experience in la Pereda 1.7 MWth Calcium Looping Pilot", **Energy Procedia**, v. 114, p. 149–157, 2017. DOI: 10.1016/j.egypro.2017.03.1157. .

ARJUNWADKAR, A., BASU, P., ACHARYA, B. "A review of some operation and maintenance issues of CFBC boilers", **Applied Thermal Engineering**, v. 102, p. 672–694, 2016. DOI: 10.1016/j.applthermaleng.2016.04.008. Disponível em: <http://dx.doi.org/10.1016/j.applthermaleng.2016.04.008>.

ASTOLFI, M., DE LENA, E., ROMANO, M. C. "Improved flexibility and economics of Calcium Looping power plants by thermochemical energy storage", **International Journal of Greenhouse Gas Control**, v. 83, n. October 2018, p. 140–155, 2019. DOI: 10.1016/j.ijggc.2019.01.023. Disponível em: <https://doi.org/10.1016/j.ijggc.2019.01.023>.

ÁVILA, I., MORTARI, A., SANTOS, A. M., *et al.* "the Calcium Looping Cycle Study for Capturing Carbon Dioxide Applied To the Energy Generation", **Revista de Engenharia Térmica**, v. 12, n. 2, p. 28, 2013. DOI: 10.5380/reterm.v12i2.62041. .

AZZI, M., WHITE, S. **Emissions from amine-based post-combustion CO₂ capture plants**. [S.l.], Elsevier Ltd, 2016. Disponível em: <http://dx.doi.org/10.1016/B978-0-08-100514-9.00020-2>.

BAHADORI, A., ZAHEDI, G., ZENDEHBOUDI, S., *et al.* "Estimation of the effect of biomass moisture content on the direct combustion of sugarcane bagasse in boilers", **International Journal of Sustainable Energy**, v. 33, n. 2, p. 349–356, 2014. DOI: 10.1080/14786451.2012.748766.

BARKER, R. "The Reversibility of the Reaction CaCO_3 to $\text{CaO} + \text{CO}_2$ ", **J. appl. Biotechnol.**, v. 223, n. August, p. 733--742--, 1973.

BASTOS, J. B. V. **Avaliação de Mecanismos de Incentivo à Cogeração de Energia a partir do Bagaço da Cana de Açúcar em uma Planta Química Brasileira de Soda-Cloro**. 2011. 180 f. UFRJ, 2011.

BASU, P. **Circulating fluidized bed boilers: Design, operation and maintenance**. [S.l: s.n.], 2015.

BASU, P. **Combustion and Gasification in Fluidized Beds**. [S.l.], CRC Press, 2006.

BEN ANTHONY, E. "Carbon Capture and Storage and Carbon Capture, Utilisation and Storage", **Issues in Environmental Science and Technology**, v. 2018-Janua, n. 45, p. 198–215, 2018. DOI: 10.1039/9781788010115-00198. Disponível em: <https://www.iea.org/topics/carbon-capture-and-storage/>. Acesso em: 27 nov. 2019.

BENNETT, S., STANLEY, T. "Commentary : US budget bill may help carbon capture get back on track", n. March 2018, p. 1–8, 2019. Disponível em: <https://www.iea.org/newsroom/news/2018/march/commentary-us-budget-bill-may-help-carbon-capture-get-back-on-track.html>. Acesso em: 3 dez. 2019.

BERGMAN, P. C. A., BOERRIGTER, H., COMANS, R. N. J., *et al.* "CONTRIBUTIONS ECN BIOMASS TO THE "12th EUROPEAN CONFERENCE AND TECHNOLOGY EXHIBITION ON BIOMASS FOR ENERGY, INDUSTRY AND CLIMATE PROTECTION", ... **ECN BIOMASS TO THE "12th ...**, n. June, 2002. Disponível em: <http://www.ecn.nl/docs/library/report/2002/rx02014.pdf#page=23>.

BERSTAD, D., ANANTHARAMAN, R., JORDAL, K. "Post-combustion CO_2 capture from a natural gas combined cycle by CaO/CaCO_3 looping", **International Journal of Greenhouse Gas Control**, v. 11, p. 25–33, 2012. DOI: 10.1016/j.ijggc.2012.07.021. Disponível em: <http://dx.doi.org/10.1016/j.ijggc.2012.07.021>.

BHOWN, A. S. "Status and analysis of next generation post-combustion CO_2 capture technologies", **Energy Procedia**, v. 63, n. 650, p. 542–549, 2014. DOI: 10.1016/j.egypro.2014.11.059. Disponível em: <http://dx.doi.org/10.1016/j.egypro.2014.11.059>.

BP. **BP Statistical Review of World Energy Statistical Review of World. The Editor**

BP Statistical Review of World Energy. [S.l: s.n.], 2019. Disponível em: <https://www.bp.com/content/dam/bp/business-sites/en/global/corporate/pdfs/energy-economics/statistical-review/bp-stats-review-2019-full-report.pdf>.

BUI, M., DOWELL, N. Mac. **Carbon Capture and Storage.** Cambridge, Royal Society of Chemistry, 2019. Disponível em: <http://ebook.rsc.org/?DOI=10.1039/9781788012744>. Acesso em: 30 jan. 2020. (Energy and Environment Series).

BUI, M., FAJARDY, M., DOWELL, N. Mac. "Thermodynamic Evaluation of Carbon Negative Power Generation: Bio-energy CCS (BECCS)", **Energy Procedia**, v. 114, p. 6010–6020, 1 jul. 2017. DOI: 10.1016/j.egypro.2017.03.1736. Disponível em: <https://www.sciencedirect.com/science/article/pii/S1876610217319380>. Acesso em: 4 dez. 2018.

BUTLER, J. **Limestone as a sorbent for CO₂ capture and its application in enhanced biomass gasification.** 2014. 279 f. 2014. Disponível em: <http://circle.ubc.ca/handle/2429/45680>.

CALDECOTT, B., DERICKS, G., MITCHELL, J. **Stranded Assets and Subcritical Coal: The Risk to Companies and Investors.** [S.l: s.n.], 2015. Disponível em: https://ora.ox.ac.uk/objects/uuid:30c2bc1b-2ee4-4b04-9fa2-767842a64805/download_file?file_format=pdf&safe_filename=2015.03.13_SA_and_S C.pdf&type_of_work=Report.

CAO, Y., PAN, W. P. "Investigation of chemical looping combustion by solid fuels. 1. Process analysis", **Energy and Fuels**, v. 20, n. 5, p. 1836–1844, 2006. DOI: 10.1021/ef050228d. .

CARBO, M. C., ABELHA, P. M. R., CIEPLIK, M. K., *et al.* "Fuel pre-processing, pre-treatment and storage for co-firing of biomass and coal", **Fuel Flexible Energy Generation: Solid, Liquid and Gaseous Fuels**, p. 121–143, 2016. DOI: 10.1016/B978-1-78242-378-2.00005-5. .

CASTELO BRANCO, D. A., MOURA, M. C. P., SZKLO, A., *et al.* "Emissions reduction potential from CO₂ capture: A life-cycle assessment of a Brazilian coal-fired power plant", **Energy Policy**, v. 61, p. 1221–1235, 2013. DOI: 10.1016/j.enpol.2013.06.043. Disponível em: <http://dx.doi.org/10.1016/j.enpol.2013.06.043>.

CENTENO-GONZÁLEZ, F. O., SILVA LORA, E. E., VILLA NOVA, H. F., *et al.* "CFD modeling of combustion of sugarcane bagasse in an industrial boiler", **Fuel**, v. 193, p. 31–38, 2017. DOI: 10.1016/j.fuel.2016.11.105. .

CHANG, M. H., CHEN, W. C., HUANG, C. M., *et al.* "Design and Experimental Testing of a 1.9MW th Calcium Looping Pilot Plant", **Energy Procedia**, v. 63, p. 2100–2108, 2014a. DOI: 10.1016/j.egypro.2014.11.226. Disponível em: <http://dx.doi.org/10.1016/j.egypro.2014.11.226>.

CHANG, M. H., CHEN, W. C., HUANG, C. M., *et al.* "Design and Experimental Testing of a 1.9MWth Calcium Looping Pilot Plant", **Energy Procedia**, v. 63, p. 2100–2108, 2014b. DOI: 10.1016/j.egypro.2014.11.226. Disponível em: <http://dx.doi.org/10.1016/j.egypro.2014.11.226>.

CHEMENGONLINE. **Chemical Engineering Plant Cost Index: 2018 Annual Value - Chemical Engineering | Page 1**. 2019. Disponível em: <https://www.chemengonline.com/2019-cepci-updates-january-prelim-and-december-2018-final/>. Acesso em: 7 mar. 2020.

CHENG, Z., QIN, L., FAN, J. A., *et al.* "New Insight into the Development of Oxygen Carrier Materials for Chemical Looping Systems", **Engineering**, v. 4, n. 3, p. 343–351, 2018. DOI: 10.1016/j.eng.2018.05.002. Disponível em: <https://doi.org/10.1016/j.eng.2018.05.002>.

CHOU, V., LYENGAR, A., SHAH, V., *et al.* "Cost and Performance Baseline for Fossil Energy Plants Supplement: Sensitivity to CO₂ capture Rate in Coal-Fired Power Plants", p. 26, 2015.

CLARENS, F., ESPÍ, J. J., GIRALDI, M. R., *et al.* "Life cycle assessment of CaO looping versus amine-based absorption for capturing CO₂ in a subcritical coal power plant", **International Journal of Greenhouse Gas Control**, v. 46, p. 18–27, 2016. DOI: 10.1016/j.ijggc.2015.12.031. Disponível em: <http://dx.doi.org/10.1016/j.ijggc.2015.12.031>.

CMU EPP. **Integrated Environmental Control Model (IECM)**. 2012. Disponível em: <https://www.cmu.edu/epp/iecm/index.html>. Acesso em: 10 fev. 2019.

CNA, PECEGE- USP. **Custos de Produção de Cana-de-Açúcar, Açúcar, Etanol e Bioeletricidade no Brasil**. . [S.l: s.n.], 2015.

COELHO JUNIOR, L. M., DA SILVA SEGUNDO, V. B., DOS SANTOS, N. A., *et al.* "Carbon footprint of the generation of bioelectricity from sugarcane bagasse in a sugar and ethanol industry", **International Journal of Global Warming**, v. 17, n. 3, p. 235, 2019. DOI: 10.1504/ijgw.2019.10020020.

CONSOLI, C. "Bioenergy and CCS 2019 Perspective", **Global CCS Institute**, n. c, p. 1–14, 2019.

COPPOLA, A., MONTAGNARO, F., SALATINO, P., *et al.* "Attrition of limestone during fluidized bed calcium looping cycles for CO₂ capture", **Combustion Science and Technology**, v. 184, n. 7–8, p. 929–941, 2012. DOI: 10.1080/00102202.2012.663986.

CORMOS, A. M., CORMOS, C. C. "Investigation of hydrogen and power co-generation based on direct coal chemical looping systems", **International Journal of Hydrogen Energy**, v. 39, n. 5, p. 2067–2077, 2014. DOI: 10.1016/j.ijhydene.2013.11.123. Disponível em: <http://dx.doi.org/10.1016/j.ijhydene.2013.11.123>.

CORMOS, A. M., SIMON, A. "Assessment of CO₂ capture by calcium looping (CaL) process in a flexible power plant operation scenario", **Applied Thermal Engineering**, v. 80, p. 319–327, 2015. DOI: 10.1016/j.applthermaleng.2015.01.059. Disponível em: <http://dx.doi.org/10.1016/j.applthermaleng.2015.01.059>.

CORMOS, A. M., SIMON, A. "Dynamic modelling of CO₂ capture by calcium-looping cycle", **Chemical Engineering Transactions**, v. 35, p. 421–426, 2013. DOI: 10.3303/CET1335070. .

CORMOS, C. C., PETRESCU, L. "Evaluation of calcium looping as carbon capture option for combustion and gasification power plants", **Energy Procedia**, v. 51, p. 154–160, 2014. DOI: 10.1016/j.egypro.2014.07.017. Disponível em: <http://dx.doi.org/10.1016/j.egypro.2014.07.017>.

CRAIG, K. R., MANN, M. K. "Cost and Performance Analysis of Biomass-Based Integrated Gasification Combined-Cycle (BIGCC) Power Systems Cost and Performance Analysis of Biomass-Based Integrated Gasification Combined-Cycle (BIGCC) Power Systems", **Biomass**, n. October, p. 1–70, 1996.

CRIADO, Y. A., ARIAS, B., ABANADES, J. C. "Calcium looping CO₂ capture system for back-up power plants", **Energy and Environmental Science**, v. 10, n. 9, p. 1994–2004, 2017. DOI: 10.1039/c7ee01505d. .

CUI, H., ZHAO, T., WU, R. "An investment feasibility analysis of ccs retrofit based on a two-stage compound real options model", **Energies**, v. 11, n. 7, 2018. DOI: 10.3390/en11071711. .

DA SILVA, F. T. F., CARVALHO, F. M., CORRÊA, J. L. G., *et al.* "CO₂ capture in ethanol distilleries in Brazil: Designing the optimum carbon transportation network by integrating hubs, pipelines and trucks", **International Journal of Greenhouse Gas Control**, v. 71, n. January, p. 168–183, 2018. DOI: 10.1016/j.ijggc.2018.02.018. .

DAI, J., SOKHANSANJ, S., GRACE, J. R., *et al.* "Overview and some issues related to co-firing biomass and coal", **Canadian Journal of Chemical Engineering**, v. 86, n. 3, p. 367–386, 2008. DOI: 10.1002/cjce.20052. .

DANTAS, G. A., LEGEY, L. F. L., MAZZONE, A. "Energy from sugarcane bagasse in Brazil: An assessment of the productivity and cost of different technological routes", **Renewable and Sustainable Energy Reviews**, v. 21, p. 356–364, 2013. DOI: 10.1016/j.rser.2012.11.080. Disponível em: <http://dx.doi.org/10.1016/j.rser.2012.11.080>.

DEAN, C. C., BLAMEY, J., FLORIN, N. H., *et al.* "The calcium looping cycle for CO₂ capture from power generation, cement manufacture and hydrogen production", **Chemical Engineering Research and Design**, v. 89, n. 6, p. 836–855, 2011. DOI: 10.1016/j.cherd.2010.10.013. .

DIAS, M. O. S., MODESTO, M., ENSINAS, A. V., *et al.* "Improving bioethanol production from sugarcane: Evaluation of distillation, thermal integration and cogeneration systems", **Energy**, v. 36, n. 6, p. 3691–3703, 2011. DOI: 10.1016/j.energy.2010.09.024. Disponível em: <http://dx.doi.org/10.1016/j.energy.2010.09.024>.

DIEGO, M. E., ARIAS, B., ABANADES, J. C. "Evolution of the CO₂ carrying capacity of CaO particles in a large calcium looping pilot plant", **International Journal of Greenhouse Gas Control**, v. 62, n. April, p. 69–75, 2017. DOI: 10.1016/j.ijggc.2017.04.005. Disponível em: <http://dx.doi.org/10.1016/j.ijggc.2017.04.005>.

DIEGO, M. Elena, ARIAS, B., ALONSO, M., *et al.* "The impact of calcium sulfate and inert solids accumulation in post-combustion calcium looping systems", **Fuel**, v. 109, p. 184–190, 2013. DOI: 10.1016/j.fuel.2012.11.062. Disponível em:

<http://dx.doi.org/10.1016/j.fuel.2012.11.062>.

DIEGO, M. Elena, ARIAS, B., GRASA, G., *et al.* "Design of a novel fluidized bed reactor to enhance sorbent performance in CO₂ capture systems using CaO", **Industrial and Engineering Chemistry Research**, v. 53, n. 24, p. 10059–10071, 2014. DOI: 10.1021/ie500630p. .

DIEGO, M.E., MARTÍNEZ, I., ALONSO, M., *et al.* **Calcium looping reactor design for fluidized-bed systems**. [S.l.], Elsevier, 2015. Disponível em: <http://dx.doi.org/10.1016/B978-0-85709-243-4.00006-9>.

DIETER, H, HAWTHORNE, C., BIDWE, A. R., *et al.* "The 200 kWth dual fluidized bed calcium looping pilot plant for efficient CO₂ capture: plant operating experiences and results". 1, 2012. **Anais [...]** [S.l: s.n.], 2012. p. 397–404. Disponível em: https://www.researchgate.net/publication/284813961_The_200_kWth_dual_fluidized_bed_calcium_looping_pilot_plant_for_efficient_CO2_capture_Plant_operating_experiences_and_results. Acesso em: 20 fev. 2020.

DIETER, Heiko, BIDWE, A. R., VARELA-DUELLI, G., *et al.* "Development of the calcium looping CO₂ capture technology from lab to pilot scale at IFK, University of Stuttgart", **Fuel**, v. 127, p. 23–37, 2014. DOI: 10.1016/j.fuel.2014.01.063. Disponível em: <http://dx.doi.org/10.1016/j.fuel.2014.01.063>.

ECN. **Phyllis2 - Database for biomass and waste**. 2013. Web Database. Disponível em: <https://www.ecn.nl/phyllis2/>. Acesso em: 14 fev. 2019.

ENDESA. "CaOling project. Final publishable summary report", 2013. .

EPE. "Balanço energético nacional: Ano base 2018", **EPE - Empresa de Pesquisa Energética**, p. 67, 2019. .

EPE. **Empresa de Pesquisa Energética - Thermal Power Energy: Natural Gas, Biomass, Coal, Nuclear (In Portuguese)**. [S.l: s.n.], 2017. Disponível em: <http://www.epe.gov.br/Documents/Energia Termelétrica - Online 13maio2016.pdf>.

ERANS, M., JEREMIAS, M., MANOVIC, V., *et al.* "Operation of a 25 KWth calcium looping pilot-plant with high oxygen concentrations in the calciner", **Journal of Visualized Experiments**, v. 2017, n. 128, p. 1–10, 2017. DOI: 10.3791/56112. .

ETC. **Mission Possible: Reaching Net-Zero Carbon Emissions from the Hard-to-**

Abate Sectors by Mid-Century. . [S.l: s.n.], 2019. Disponível em: http://www.energy-transitions.org/sites/default/files/ETC_MissionPossible_FullReport.pdf. Acesso em: 20 out. 2019.

EUROPEAN CENTRAL BANK. **ECB euro reference exchange rate: US dollar (USD).** 2019. ECB/ Eurosystem policy and exchange rates. Disponível em: https://www.ecb.europa.eu/stats/policy_and_exchange_rates/euro_reference_exchange_rates/html/eurofxref-graph-usd.en.html. Acesso em: 7 mar. 2020.

EUROPEAN COMMISSION. **Calcium looping CO2 capture technology with extreme oxy- coal conditions in the calciner.** . [S.l: s.n.], 2019.

FAN, F., LI, Z. S., CAI, N. S. "Experiment and modeling of CO2 capture from flue gases at high temperature in a fluidized bed reactor with ca-based sorbents", **Energy and Fuels**, v. 23, n. 1, p. 207–216, 2009. DOI: 10.1021/ef800474n. .

FAN, L., LI, F., RAMKUMAR, S. "Utilization of chemical looping strategy in coal gasification processes", **Particuology**, v. 6, n. 3, p. 131–142, 2008. DOI: 10.1016/j.partic.2008.03.005. .

FAN, L. S. **Chemical Looping Systems for Fossil Energy Conversions.** [S.l: s.n.], 2010. Disponível em: <https://www.wiley.com/en-us/Chemical+Looping+Systems+for+Fossil+Energy+Conversions-p-9780470872529>.

FAN, L. S., ZENG, L., WANG, W., *et al.* "Chemical looping processes for CO2 capture and carbonaceous fuel conversion – prospect and opportunity", **Energy and Environmental Science**, v. 5, n. 6, p. 7254–7280, 2012. DOI: 10.1039/c2ee03198a. .

FENNELL, P. S., ANTHONY, E. J. **Calcium and Chemical Looping Technology for Power Generation and Carbon Dioxide (CO2) Capture.** [S.l.], Woodhead, 2015. Disponível em: <https://www.sciencedirect.com/book/9780857092434/calcium-and-chemical-looping-technology-for-power-generation-and-carbon-dioxide-co2-capture>. Acesso em: 1 set. 2019.

FERON, P. H. M. **Absorption-Based Post-combustion Capture of Carbon Dioxide.** [S.l: s.n.], 2016. Disponível em: <https://books.google.com.br/books?id=X5PBCQAAQBAJ&pg=PA765&lpg=PA765&dq=cansolv+kinetics&source=bl&ots=ZS3pPSED7&sig=ACfU3U220A-Y9fEpjJN-pQlj4Gmxhwet9w&hl=pt->

BR&sa=X&ved=2ahUKEwjy6tXGuszmaAhUqGrkGHfQWBIUQ6AEwCHoECAoQAQ#v=onepage&q=cansolv kinetics&f=false. Acesso em: 4 jan. 2020.

FLORIN, N., FENNELL, P. **CCR Land Footprint Review, IC 26.** . [S.l: s.n.], 2011. Disponível em: https://www.gov.uk/government/uploads/system/uploads/attachment_data/file/43615/CCR_guidance_-_Imperial_College_review.pdf.

FOUT, T., ZOELLE, A., KEAIRNS, D., *et al.* **Cost and Performance Baseline for Fossil Energy Plants Volume 1a: Bituminous Coal (PC) and Natural Gas to Electricity Revision 3. National Energy Technology Laboratory (NETL).** [S.l: s.n.], 2015. Disponível em: http://www.netl.doe.gov/File_Library/Research/Energy_Analysis/Publications/Rev3Vol1aPC_NGCC_final.pdf.

FREEMAN, B. C., BHOWN, A. S. "Assessment of the technology readiness of post-combustion CO₂ capture technologies", **Energy Procedia**, v. 4, p. 1791–1796, 2011. DOI: 10.1016/j.egypro.2011.02.055. Disponível em: <http://dx.doi.org/10.1016/j.egypro.2011.02.055>.

GARDARSDOTTIR, S. O., DE LENA, E., ROMANO, M., *et al.* "Comparison of technologies for CO₂ capture from cement production—Part 2: Cost analysis", **Energies**, v. 12, n. 3, 2019. DOI: 10.3390/en12030542. .

GLOBAL CCS INSTITUTE. **Facilities - Global CCS Institute Database.** 2020. Disponível em: <https://co2re.co/FacilityData>. Acesso em: 4 set. 2020.

GLOBAL CCS INSTITUTE. **Global CCS Institute Fact Sheet Capturing CO₂.** . [S.l: s.n.], 2018a. Disponível em: https://www.globalccsinstitute.com/wp-content/uploads/2018/12/Global-CCS-Institute-Fact-Sheet_Capturing-CO2.pdf. Acesso em: 1 set. 2019.

GLOBAL CCS INSTITUTE. "The Global Status of CCS: 2017", p. 43, 2017. Disponível em: http://www.globalccsinstitute.com/sites/www.globalccsinstitute.com/files/uploads/global-status/1-0_4529_CCS_Global_Status_Book_layout-WAW_spreads.pdf.

GLOBAL CCS INSTITUTE. "The Global Status os CCS 2018", p. 84, 2018b. Disponível em: www.globalccsinstitute.com.

GLOBAL CCS INSTITUTE. "Water use in Thermal power Plants equipped with CO₂ capture systems", p. 51, 2016. .

GRACE, J. R., CHAOUKI, J., PUGSLEY, T. **Fluidized bed reactor**. [S.l: s.n.], 2016.

GRASA, G. S., ABANADES, J. C. "CO₂ capture capacity of CaO in long series of carbonation/calcination cycles", **Industrial and Engineering Chemistry Research**, v. 45, n. 26, p. 8846–8851, 2006. DOI: 10.1021/ie0606946. .

HAAF, M., STROH, A., HILZ, J., *et al.* "Process Modelling of the Calcium Looping Process and Validation Against 1 MWth Pilot Testing", **Energy Procedia**, v. 114, n. November 2016, p. 167–178, 2017. DOI: 10.1016/j.egypro.2017.03.1159. Disponível em: <http://dx.doi.org/10.1016/j.egypro.2017.03.1159>.

HAAF, Martin, HILZ, J., HELBIG, M., *et al.* "Assessment of the operability of a 20 MWth calcium looping demonstration plant by advanced process modelling", **International Journal of Greenhouse Gas Control**, v. 75, n. May, p. 224–234, 2018. DOI: 10.1016/j.ijggc.2018.05.014. Disponível em: <https://doi.org/10.1016/j.ijggc.2018.05.014>.

HANAK, D., MANOVIC, V. "Calcium looping for decarbonisation of coal-fired power plants Calcium looping for decarbonisation of coal-fired power plants Dawid P. Hanak *, Vasilije Manovic Combustion and CCS Centre, Cranfield University," n. November 2016.

HANAK, Dawid P., ANTHONY, E. J., MANOVIC, V. "A review of developments in pilot-plant testing and modelling of calcium looping process for CO₂ capture from power generation systems", **Energy and Environmental Science**, v. 8, n. 8, p. 2199–2249, 2015. DOI: 10.1039/c5ee01228g. .

HANAK, Dawid P., BILYOK, C., ANTHONY, E., *et al.* "Evaluation of a calcium looping CO₂ capture plant retrofit to a coal-fired power plant". 38, 2016. **Anais [...]** [S.l.], Elsevier Masson SAS, 2016. p. 2115–2120. DOI: 10.1016/B978-0-444-63428-3.50357-X. Disponível em: <http://dx.doi.org/10.1016/B978-0-444-63428-3.50357-X>.

HANAK, Dawid P., BILYOK, C., ANTHONY, E. J., *et al.* "A study of integration of calcium looping CO₂ capture plant and coal-fired power plant", 2015a. .

HANAK, Dawid P., BILYOK, C., ANTHONY, E. J., *et al.* "Modelling and comparison

of calcium looping and chemical solvent scrubbing retrofits for CO₂ capture from coal-fired power plant", **International Journal of Greenhouse Gas Control**, v. 42, p. 226–236, 2015b. DOI: 10.1016/j.ijggc.2015.08.003. Disponível em: <http://dx.doi.org/10.1016/j.ijggc.2015.08.003>.

HANAK, Dawid P., BILYOK, C., MANOVIC, V. "Calcium looping with inherent energy storage for decarbonisation of coal-fired power plant", **Energy and Environmental Science**, v. 9, n. 3, p. 971–983, 2016. DOI: 10.1039/c5ee02950c. .

HANAK, Dawid P., ERANS, M., NABAVI, S. A., *et al.* "Technical and economic feasibility evaluation of calcium looping with no CO₂ recirculation", **Chemical Engineering Journal**, v. 335, p. 763–773, 2018. DOI: 10.1016/j.cej.2017.11.022. Disponível em: <https://doi.org/10.1016/j.cej.2017.11.022>.

HANAK, Dawid P., MANOVIC, V. "Calcium looping combustion for high-efficiency low-emission power generation", **Journal of Cleaner Production**, v. 161, p. 245–255, 2017. DOI: 10.1016/j.jclepro.2017.05.080. Disponível em: <http://dx.doi.org/10.1016/j.jclepro.2017.05.080>.

HANAK, Dawid P., MICHALSKI, S., MANOVIC, V. "From post-combustion carbon capture to sorption-enhanced hydrogen production: A state-of-the-art review of carbonate looping process feasibility", **Energy Conversion and Management**, v. 177, n. April, p. 428–452, 2018. DOI: 10.1016/j.enconman.2018.09.058. Disponível em: <https://doi.org/10.1016/j.enconman.2018.09.058>.

HANAK, Dawid Piotr, MANOVIC, V., ANTHONY, E. J. "The future of Ca looping – A review of developments", n. November, 2014. DOI: 10.13140/2.1.3638.8162. .

HE, D., QIN, C., MANOVIC, V., *et al.* "Study on the interaction between CaO-based sorbents and coal ash in calcium looping process", **Fuel Processing Technology**, v. 156, p. 339–347, 2017. DOI: 10.1016/j.fuproc.2016.09.017. Disponível em: <http://dx.doi.org/10.1016/j.fuproc.2016.09.017>.

HELBIG, M., HILZ, J., HAAF, M., *et al.* "Long-term Carbonate Looping Testing in a 1 MW th Pilot Plant with Hard Coal and Lignite", **Energy Procedia**, v. 114, n. November 2016, p. 179–190, 2017. DOI: 10.1016/j.egypro.2017.03.1160. Disponível em: <http://dx.doi.org/10.1016/j.egypro.2017.03.1160>.

HEPBURN, C., ADLEN, E., BEDDINGTON, J., *et al.* "The technological and economic

prospects for CO₂ utilization and removal", **Nature**, v. 575, n. 7781, p. 87–97, 2019. DOI: 10.1038/s41586-019-1681-6. Disponível em: <http://dx.doi.org/10.1038/s41586-019-1681-6>.

HETLAND, J., YOWARGANA, P., LEDUC, S., *et al.* "Carbon-negative emissions: Systemic impacts of biomass conversion. A case study on CO₂ capture and storage options", **International Journal of Greenhouse Gas Control**, v. 49, p. 330–342, 2016. DOI: 10.1016/j.ijggc.2016.03.017. Disponível em: <http://dx.doi.org/10.1016/j.ijggc.2016.03.017>.

HILLS, T. P., SCEATS, M. G., FENNELL, P. S., "Chapter 10: Applications of CCS in the cement industry". **RSC Energy and Environment Series**, [S.l.], Royal Society of Chemistry, 2020. v. 2020-Janua. p. 315–352. DOI: 10.1039/9781788012744-00315.

HILZ, J., HAAF, M., HELBIG, M., *et al.* "Scale-up of the carbonate looping process to a 20 MWth pilot plant based on long-term pilot tests", **International Journal of Greenhouse Gas Control**, v. 88, n. April, p. 332–341, 2019. DOI: 10.1016/j.ijggc.2019.04.026. Disponível em: <https://doi.org/10.1016/j.ijggc.2019.04.026>.

HIRAMA, T., HOSODA, H., KITANO, K., *et al.* **Method of separating carbon dioxide from carbon dioxide containing gas and combustion apparatus having function to separate carbon dioxide from the combustion gas.** . [S.l: s.n.]. , 1994

HOFFMANN, B. S. **O ciclo combinado com gaseificação integrada e a captura de CO₂: Uma solução para mitigar as emissões de CO₂ em termelétricas a carvão em larga escala no curto prazo?** 2010. 0–128 f. UFRJ, 2010.

HOFFMANN, B. S., SZKLO, A., SCHAEFFER, R. "Limits to co-combustion of coal and eucalyptus due to water availability in the state of Rio Grande do Sul, Brazil", **Energy Conversion and Management**, v. 87, p. 1239–1247, 2014. DOI: 10.1016/j.enconman.2014.01.062. Disponível em: <http://dx.doi.org/10.1016/j.enconman.2014.01.062>.

HORNBERGER, M., SPÖRL, R., SCHEFFKNECHT, G. "Calcium Looping for CO₂ Capture in Cement Plants - Pilot Scale Test", **Energy Procedia**, v. 114, n. November 2016, p. 6171–6174, 2017. DOI: 10.1016/j.egypro.2017.03.1754. Disponível em: <http://dx.doi.org/10.1016/j.egypro.2017.03.1754>.

HU, J., GALVITA, V. V., POELMAN, H., *et al.* "Advanced chemical looping materials for CO₂ utilization: A review", **Materials**, v. 11, n. 7, 2018. DOI: 10.3390/ma11071187.

HUMBIRD, D., DAVIS, R., TAO, L., *et al.* "Process design and economics for conversion of lignocellulosic biomass to ethanol", **NREL technical report NREL/TP-5100-51400**, v. 303, n. May 2011, p. 275–3000, 2011. Disponível em: <http://www.nrel.gov/docs/fy11osti/51400.pdf>⁵Cnpapers2://publication/uuid/49A5007E-9A58-4E2B-AB4E-4A4428F6EA66.

HURST, T. F., COCKERILL, T. T., FLORIN, N. H. "Life cycle greenhouse gas assessment of a coal-fired power station with calcium looping CO₂ capture and offshore geological storage", **Energy and Environmental Science**, v. 5, n. 5, p. 7132–7150, 2012. DOI: 10.1039/c2ee21204h. .

IEA. **20 Years of Carbon Capture and Storage. 20 Years of Carbon Capture and Storage**. [S.l: s.n.], 2016.

IEA. **Carbon capture, utilisation and storage - A critical tool in the climate energy toolbox**. 2019a. Disponível em: <https://www.iea.org/topics/carbon-capture-and-storage/>. Acesso em: 28 nov. 2019.

IEA. "Cement production", **IEA ETSAP - Technology Brief**, n. June, p. 138–139, 2010. DOI: 10.18356/78df6b88-en-fr. .

IEA. **Coal explained Coal prices and outlook**. 2019b. Disponível em: <https://www.eia.gov/energyexplained/coal/prices-and-outlook.php>. Acesso em: 4 mar. 2020.

IEA. **Five keys to unlock CCS investment**. . [S.l: s.n.], 2017a. Disponível em: <https://www.iea.org/media/topics/ccs/5KeysUnlockCCS.PDF>⁰A<http://www.iea.org/media/topics/ccs/5KeysUnlockCCS.PDF>.

IEA. **Five keys to unlock CCS investment**. . [S.l: s.n.], 2017b. Disponível em: <https://www.iea.org/media/topics/ccs/5KeysUnlockCCS.PDF>.

IEA. **Gaps: CCS applied to cement manufacturing**. 2019c. Disponível em: <https://www.iea.org/topics/innovation/industry/gaps/ccs-applied-to-cement-manufacturing-2.html>. Acesso em: 22 out. 2019.

IEA. **Gaps: Reduce the energy penalty and cost of CCUS capture**. 2019d. Disponível em: <https://www.iea.org/topics/innovation/power/gaps/reduce-the-energy-penalty-and-cost-of-ccus-capture.html>. Acesso em: 20 out. 2019.

IEA. **Geco 2019**. 2019e. International Energy Agency Website. Disponível em: <https://www.iea.org/geco/>. Acesso em: 1 set. 2019.

IEA. **Power**. 2019f. Disponível em: <https://www.iea.org/topics/innovation/power/>. Acesso em: 15 out. 2019.

IEA. **Tracking Power, IEA, Paris**. 2019g. Disponível em: <https://www.iea.org/reports/tracking-power-2019/coal-fired-power>. Acesso em: 9 mar. 2020.

IEAGHG. **ASSESSMENT OF EMERGING CO₂ CAPTURE TECHNOLOGIES AND THEIR POTENTIAL TO Report : 2014 / TR4 December 2014**. . [S.l: s.n.], 2014a.

IEAGHG. **Assessment of Emerging CO₂ Capture Technologies and Their Potential**. . [S.l: s.n.], 2014b. Disponível em: https://ieaghg.org/docs/General_Docs/Reports/2014-TR4.pdf. Acesso em: 20 out. 2019.

IEAGHG. **Potential for Biomass and Carbon Dioxide Capture and Storage**. **ieaghg**. [S.l: s.n.], 2011. Disponível em: www.ieaghg.org.

INTERCEPT. **The Environmental Left Is Softening on Carbon Capture Tech**. 2019. Disponível em: <https://theintercept.com/2019/09/20/carbon-capture-technology-unions-labor/>. Acesso em: 15 out. 2019.

INTERNATIONAL ENERGY AGENCY. "Carbon Dioxide Capture in the Cement Industry", n. July, p. 1–180, 2008. Disponível em: <http://hub.globalccsinstitute.com/sites/default/files/publications/95751/co2-capture-cement-industrypdf.pdf>.

IPCC. **2. Mitigation Pathways. Global Warming of 1.5°C**. [S.l: s.n.], 2018a.

IPCC. **Special Report on the impacts of global warming of 1.5°C - Summary for Policymakers**. . [S.l: s.n.], 2018b. Disponível em: <https://www.ipcc.ch/sr15/chapter/summary-for-policy-makers/>.

IPCC. **Summary for Policymakers - Global warming of 1.5oC, an IPCC special report.** [S.l: s.n.], 2019. Disponível em:

https://www.researchgate.net/publication/329866816_Summary_for_Policymakers_In_Global_warming_of_15C_An_IPCC_Special_Report%0Ahttps://www.ipcc.ch/sr15/cha-pter/spm/.

JANTTI, T. "Advanced CFB technology for large scale biomass firing power plants.", **Bioenergy from Forest**, 2012. .

JENKINS, S. **CEPCI Updates: January 2018 (prelim.) and December 2017 (final) - Chemical Engineering | Page 1.** 2018. Chemengonline. Disponível em: <https://www.chemengonline.com/cepci-updates-january-2018-prelim-and-december-2017-final/?printmode=1>. Acesso em: 16 fev. 2020.

JUNK, M., KREMER, J., STRÖHLE, J., *et al.* "Design of a 20 MWth carbonate looping pilot plant for CO₂-capture of coal fired power plants by means of limestone", **Energy Procedia**, v. 63, p. 2178–2189, 2014. DOI: 10.1016/j.egypro.2014.11.237. Disponível em: <http://dx.doi.org/10.1016/j.egypro.2014.11.237>.

KANNICHE, M., LE MOULLEC, Y., AUTHIER, O., *et al.* "Up-to-date CO₂ Capture in Thermal Power Plants", **Energy Procedia**, v. 114, n. July, p. 95–103, 2017. DOI: 10.1016/j.egypro.2017.03.1152. Disponível em: <http://dx.doi.org/10.1016/j.egypro.2017.03.1152>.

KEITH, D. W., REINELT, S. "Carbon Capture Retrofits and the Cost of Regulatory Uncertainty", **Energy Journal**, v. 28, n. 4, p. 101–127, 2009. .

KHAN, A. A., DE JONG, W., JANSSENS, P. J., *et al.* "Biomass combustion in fluidized bed boilers: Potential problems and remedies", **Fuel Processing Technology**, v. 90, n. 1, p. 21–50, 2009. DOI: 10.1016/j.fuproc.2008.07.012. Disponível em: <http://dx.doi.org/10.1016/j.fuproc.2008.07.012>.

KHATIWADA, D., LEDUC, S., SILVEIRA, S., *et al.* "Optimizing ethanol and bioelectricity production in sugarcane biorefineries in Brazil", **Renewable Energy**, v. 85, p. 371–386, 2016. DOI: 10.1016/j.renene.2015.06.009. Disponível em: <http://dx.doi.org/10.1016/j.renene.2015.06.009>.

KNOWLTON, T. M. "Tools and Techniques for Diagnosing and Solving Operating Problems in Fluidized Bed Systems", **Oil and Gas Science and Technology**, v. 55, n. 2,

p. 209–217, 2000. DOI: 10.2516/ogst:2000013. .

KRZEMIENI, A., WIĘCKOL-RYK, A., DUDA, A., *et al.* "Risk Assessment of a Post-Combustion and Amine-Based CO₂ Capture Ready Process", **Journal of Sustainable Mining**, v. 12, n. 4, p. 18–23, 2013. DOI: 10.7424/jsm130404. .

KUNII, D., LEVENSPIEL, O. "Circulating fluidized-bed reactors", **Chemical Engineering Science**, v. 52, n. 15, p. 2471–2482, 1997. DOI: 10.1016/S0009-2509(97)00066-3. .

KURSUN, B., RAMKUMAR, S., BAKSHI, B. R., *et al.* "Life cycle comparison of coal gasification by conventional versus calcium looping processes", **Industrial and Engineering Chemistry Research**, v. 53, n. 49, p. 18910–18919, 2014. DOI: 10.1021/ie404436a. .

LARA, Y., ROMEO, L. M. "On the Flexibility of Coal-fired Power Plants with Integrated Ca-looping CO₂ Capture Process", **Energy Procedia**, v. 114, n. July, p. 6552–6562, 2017. DOI: 10.1016/j.egypro.2017.03.1791. Disponível em: <http://dx.doi.org/10.1016/j.egypro.2017.03.1791>.

LASHERAS, A., STRÖHLE, J., GALLOY, A., *et al.* "Carbonate looping process simulation using a 1D fluidized bed model for the carbonator", **International Journal of Greenhouse Gas Control**, v. 5, n. 4, p. 686–693, 2011. DOI: 10.1016/j.ijggc.2011.01.005. Disponível em: <http://dx.doi.org/10.1016/j.ijggc.2011.01.005>.

LI, F., ZENG, L., FAN, L. S. "Biomass direct chemical looping process: Process simulation", **Fuel**, v. 89, n. 12, p. 3773–3784, 2010. DOI: 10.1016/j.fuel.2010.07.018. Disponível em: <http://dx.doi.org/10.1016/j.fuel.2010.07.018>.

LI, Z. S., CAI, N. S., CROISSET, E. "Process analysis of CO₂ capture from flue gas using carbonation/calcination cycles", **AIChE Journal**, v. 54, n. 7, p. 1912–1925, 2008. DOI: 10.1002/aic.11486. .

LIVINGSTON, W., MIDDLEKAMP, J., WILLEBOER, W., *et al.* "The status of large scale biomass firing", p. 1–88, 2016. Disponível em: http://www.ieabcc.nl/publications/IEA_Bioenergy_T32_cofiring_2016.pdf.

LUIS, P. "Use of monoethanolamine (MEA) for CO₂ capture in a global scenario:

Consequences and alternatives", **Desalination**, v. 380, p. 93–99, 2016. DOI: 10.1016/j.desal.2015.08.004. Disponível em: <http://dx.doi.org/10.1016/j.desal.2015.08.004>.

LYNGFELT, A., LECKNER, B. "A 1000 MWth boiler for chemical-looping combustion of solid fuels – Discussion of design and costs", **Applied Energy**, v. 157, p. 475–487, 2015. DOI: 10.1016/j.apenergy.2015.04.057. Disponível em: <http://dx.doi.org/10.1016/j.apenergy.2015.04.057>.

LYNGFELT, A., LECKNER, B., MATTISSON, T. "A fluidized-bed combustion process with inherent CO₂ separation; Application of chemical-looping combustion", **Chemical Engineering Science**, v. 56, n. 10, p. 3101–3113, 2001. DOI: 10.1016/S0009-2509(01)00007-0. .

LYNGFELT, A., LINDERHOLM, C. "Chemical-Looping Combustion of Solid Fuels - Status and Recent Progress", **Energy Procedia**, v. 114, n. November 2016, p. 371–386, 2017. DOI: 10.1016/j.egypro.2017.03.1179. Disponível em: <http://dx.doi.org/10.1016/j.egypro.2017.03.1179>.

MACIEJEWSKA, A., VERINGA, H., SANDERS, J., *et al.* **Co-Firing of Biomass With Coal: Constraints and Role of Biomass Pre-Treatment**. Institute for Energy. [S.l.: s.n.], 2006.

MANTRIPRAGADA, H. C., RUBIN, E. S. "Calcium looping cycle for CO₂ capture: Performance, cost and feasibility analysis", **Energy Procedia**, v. 63, p. 2199–2206, 2014. DOI: 10.1016/j.egypro.2014.11.239. Disponível em: <http://dx.doi.org/10.1016/j.egypro.2014.11.239>.

MANTRIPRAGADA, H. C., RUBIN, E. S. "Chemical Looping Combustion for Pre-combustion CO₂ Capture", n. September, p. 58, 2012. Disponível em: [http://www.cmu.edu/epp/iecm/documentation/IECM CLC Tech Report - 09_27_2012.pdf](http://www.cmu.edu/epp/iecm/documentation/IECM_CLC_Tech_Report_09_27_2012.pdf).

MANTRIPRAGADA, H. C., RUBIN, E. S. "Chemical Looping for Pre-combustion and Post-combustion CO₂ Capture", **Energy Procedia**, v. 114, n. November 2016, p. 6403–6410, 2017a. DOI: 10.1016/j.egypro.2017.03.1776. Disponível em: <http://dx.doi.org/10.1016/j.egypro.2017.03.1776>.

MANTRIPRAGADA, H. C., RUBIN, E. S. "IECM Technical Documentation: Calcium

Looping Cycle for Post-Combustion CO₂ Capture", n. November, 2017b. .

MANTRIPRAGADA, H. C., ZHAI, H., RUBIN, E. S. "Boundary Dam or Petra Nova – Which is a better model for CCS energy supply?", **International Journal of Greenhouse Gas Control**, v. 82, n. December 2018, p. 59–68, 2019a. DOI: 10.1016/j.ijggc.2019.01.004. Disponível em: <https://doi.org/10.1016/j.ijggc.2019.01.004>.

MANTRIPRAGADA, H. C., ZHAI, H., RUBIN, E. S. "Boundary Dam or Petra Nova – Which is a better model for CCS energy supply?", **International Journal of Greenhouse Gas Control**, v. 82, n. October 2018, p. 59–68, 2019b. DOI: 10.1016/j.ijggc.2019.01.004. Disponível em: <https://doi.org/10.1016/j.ijggc.2019.01.004>.

MARÍA ERANS MORENO. "Enhanced Sorbents for the Calcium Looping Cycle and Effects of High Oxygen Concentrations in the Calciner", **Cranfield University**, n. May 2017, p. 2017–2018, 2017. .

MARQUES, F. **Bagasse is the target** | **Revista Pesquisa Fapesp**. 2011. Pesquisa FAPESP. Disponível em: <https://revistapesquisa.fapesp.br/en/2011/04/20/bagasse-is-the-target-2/>. Acesso em: 14 fev. 2020.

MARTÍNEZ, I., ARIAS, B., GRASA, G. S., *et al.* "CO₂ capture in existing power plants using second generation Ca-Looping systems firing biomass in the calciner", **Journal of Cleaner Production**, v. 187, p. 638–649, 2018. DOI: 10.1016/j.jclepro.2018.03.189. .

MARTÍNEZ, I., GRASA, G., MURILLO, R., *et al.* "Modelling the continuous calcination of CaCO₃ in a Ca-looping system", **Chemical Engineering Journal**, v. 215–216, p. 174–181, 2013. DOI: 10.1016/j.cej.2012.09.134. .

MARTÍNEZ, I., MURILLO, R., GRASA, G., *et al.* "Integration of a Ca-looping system for CO₂ capture in an existing power plant", **Energy Procedia**, v. 4, p. 1699–1706, 2011a. DOI: 10.1016/j.egypro.2011.02.043. .

MARTÍNEZ, I., MURILLO, R., GRASA, G., *et al.* "Integration of a Ca-looping system for CO₂ capture in an existing power plant", **Energy Procedia**, v. 4, p. 1699–1706, 2011b. DOI: 10.1016/j.egypro.2011.02.043. Disponível em: <http://dx.doi.org/10.1016/j.egypro.2011.02.043>.

MARTÍNEZ, Isabel, GRASA, G., PARKKINEN, J., *et al.* "Review and research needs

of Ca-Looping systems modelling for post-combustion CO₂ capture applications", **International Journal of Greenhouse Gas Control**, v. 50, p. 271–304, 2016. DOI: 10.1016/j.ijggc.2016.04.002. Disponível em: <http://dx.doi.org/10.1016/j.ijggc.2016.04.002>.

MARX-SCHUBACH, T., SCHMITZ, G. "Modeling and simulation of the start-up process of coal fired power plants with post-combustion CO₂ capture", **International Journal of Greenhouse Gas Control**, v. 87, n. April, p. 44–57, 2019. DOI: 10.1016/j.ijggc.2019.05.003. Disponível em: <https://doi.org/10.1016/j.ijggc.2019.05.003>.

MATUSZEWSKI, M. **Cost and Performance for Low-Rank Pulverized Coal Oxycombustion Energy Plants**. . [S.l: s.n.], 2010.

MERROW, E. "Linking R&D to problems experienced in solids processing", 1984. Disponível em: <https://apps.dtic.mil/docs/citations/ADA154238>. Acesso em: 19 fev. 2020.

MERSCHMANN, VASQUEZ, E., SZKLO, A. S., *et al.* "Modeling water use demands for thermoelectric power plants with CCS in selected Brazilian water basins", **International Journal of Greenhouse Gas Control**, v. 13, p. 87–101, 2013. DOI: 10.1016/j.ijggc.2012.12.019. Disponível em: <http://dx.doi.org/10.1016/j.ijggc.2012.12.019>.

MERSCHMANN, SZKLO, SCHAEFFER, "Technical potential and abatement costs associated with the use of process emissions from sugarcane ethanol distilleries for EOR in offshore fields in Brazil", **International Journal of Greenhouse Gas Control**, v. 52, p. 270–292, 2016. DOI: 10.1016/j.ijggc.2016.07.007. Disponível em: <http://dx.doi.org/10.1016/j.ijggc.2016.07.007>.

METZ, DAVIDSON, O., LOOS, M., *et al.* **The IPCC special report on carbon dioxide capture and storage**. [S.l: s.n.], 2005.

MICHALSKI, S., HANAK, D. P., MANOVIC, V. "Techno-economic feasibility assessment of calcium looping combustion using commercial technology appraisal tools", **Journal of Cleaner Production**, v. 219, p. 540–551, 2019. DOI: 10.1016/j.jclepro.2019.02.049. Disponível em: <https://doi.org/10.1016/j.jclepro.2019.02.049>.

MIT. **Carbon Capture and Sequestration Technologies Database**. 2009. Disponível em: http://sequestration.mit.edu/tools/projects/wa_parish.html. Acesso em: 23 out. 2019.

MOGHTADERI, B. "Review of the recent chemical looping process developments for novel energy and fuel applications", **Energy and Fuels**, v. 26, n. 1, p. 15–40, 2012. DOI: 10.1021/ef201303d. .

MONTAGNARO, F., SALATINO, P., SCALA, F. "The influence of temperature on limestone sulfation and attrition under fluidized bed combustion conditions", **Experimental Thermal and Fluid Science**, v. 34, n. 3, p. 352–358, 2010. DOI: 10.1016/j.expthermflusci.2009.10.013. Disponível em: <http://dx.doi.org/10.1016/j.expthermflusci.2009.10.013>.

MOORE, C. C. S., KULAY, L. "Effect of the implementation of carbon capture systems on the environmental, energy and economic performance of the Brazilian electricity matrix", **Energies**, v. 12, n. 2, 2019. DOI: 10.3390/en12020331. .

MOREIRA, J. R., ROMEIRO, V., FUSS, S., *et al.* "BECCS potential in Brazil: Achieving negative emissions in ethanol and electricity production based on sugar cane bagasse and other residues", **Applied Energy**, v. 179, p. 55–63, 1 out. 2016. DOI: 10.1016/j.apenergy.2016.06.044. Disponível em: <https://www.sciencedirect.com/science/article/pii/S0306261916308194>. Acesso em: 9 dez. 2018.

MUKHERJEE, S., KUMAR, P., YANG, A., *et al.* "Energy and exergy analysis of chemical looping combustion technology and comparison with pre-combustion and oxy-fuel combustion technologies for CO₂ capture", **Journal of Environmental Chemical Engineering**, v. 3, n. 3, p. 2104–2114, 2015. DOI: 10.1016/j.jece.2015.07.018. Disponível em: <http://dx.doi.org/10.1016/j.jece.2015.07.018>.

NIU, Y., TAN, H., HUI, S. "Ash-related issues during biomass combustion: Alkali-induced slagging, silicate melt-induced slagging (ash fusion), agglomeration, corrosion, ash utilization, and related countermeasures", **Progress in Energy and Combustion Science**, v. 52, p. 1–61, 2016. DOI: 10.1016/j.pecs.2015.09.003. Disponível em: <http://dx.doi.org/10.1016/j.pecs.2015.09.003>.

NUORTIMO, K., ERIKSSON, T., NEVALAINEN, T. "Large scale utility CFB technology in worlds largest greenfield 100% biomass power plant", **European Biomass**

Conference and Exhibition Proceedings, v. 2017, n. 25thEUBCE, p. 1920–1925, 2017.

NYKO, D., BRANDÃO, R., FARIA, A. Y., *et al.* "Determinantes do baixo aproveitamento do potencial elétrico do setor sucroenergético : uma pesquisa de campo", **BNDES Setorial**, v. 33, p. 18, 2011. .

OLHOFF, A. "Emissions Gap Report 2018 Key Messages". 2018. **Anais [...]** [S.l: s.n.], 2018. p. 1–20. Disponível em: http://wedocs.unep.org/bitstream/handle/20.500.11822/26896/EGR-KEYMESSAGES_2018.pdf?sequence=1&isAllowed=y. Acesso em: 1 set. 2019.

ORTIZ, C., CHACARTEGUI, R., VALVERDE, J. M., *et al.* "A new model of the carbonator reactor in the calcium looping technology for post-combustion CO₂ capture", **Fuel**, v. 160, p. 328–338, 2015. DOI: 10.1016/j.fuel.2015.07.095. Disponível em: <http://dx.doi.org/10.1016/j.fuel.2015.07.095>.

OZCAN, D. C., BOCCIARDO, D., FERRARI, M. C., *et al.* "Comparison of various carbon capture technologies to reduce CO₂ emissions from a cement plant", **CO₂ Capture 2013 - Topical Conference at the 2013 AIChE Annual Meeting: Global Challenges for Engineering a Sustainable Future**, n. November, p. 133, 2013. .

OZCAN, Dursun Can. "Techno-Economic Study for the Calcium Looping Process for CO₂ Capture from Cement and Biomass Power Plants", **PhD Thesis, School of Engineering, The University of Edinburgh**, n. November, 2014. DOI: 10.1016/j.enconman.2015.01.060. Disponível em: <http://dx.doi.org/10.1016/j.wasman.2011.12.015>
<http://www.scopus.com/inward/record.url?eid=2-s2.0-79954467269&partnerID=40&md5=5efec8df756a4f4a00a90a8de29bd559>
<http://petd.up.ac.za/thesis/available/etd-07022009-133535/unrestricted/dissertation.pdf>.

OZCAN, ALONSO, AHN, *et al.* "Process and cost analysis of a biomass power plant with in situ calcium looping CO₂ capture process", **Industrial and Engineering Chemistry Research**, v. 53, n. 26, p. 10721–10733, 2014. DOI: 10.1021/ie500606v. .

OZCAN, BOCCIARDO, FERRARI, *et al.* "Comparison of various carbon capture technologies to reduce CO₂ emissions from a cement plant". 2013. **Anais [...]** [S.l: s.n.], 2013. p. 133.

PARKKINEN, J., MYÖHÄNEN, K., ABANADES, J. C., *et al.* "Modelling a Calciner with High Inlet Oxygen Concentration for a Calcium Looping Process", **Energy Procedia**, v. 114, n. November 2016, p. 242–249, 2017. DOI: 10.1016/j.egypro.2017.03.1166. Disponível em: <http://dx.doi.org/10.1016/j.egypro.2017.03.1166>.

PAWLAK-KRUCZEK, H., BARANOWSKI, M. "Effectiveness of CO₂ Capture by Calcium Looping with Regenerated Calcium Sorbents - Last Step Calcination", **Energy Procedia**, v. 105, p. 4499–4512, 2017. DOI: 10.1016/j.egypro.2017.03.962. Disponível em: <http://dx.doi.org/10.1016/j.egypro.2017.03.962>.

PELLEGRINI, L. F., DE OLIVEIRA JÚNIOR, S., BURBANO, J. C. "Supercritical steam cycles and biomass integrated gasification combined cycles for sugarcane mills", **Energy**, v. 35, n. 2, p. 1172–1180, 2010. DOI: 10.1016/j.energy.2009.06.011. .

PEREJÓN, A., ROMEO, L. M., LARA, Y., *et al.* "The Calcium-Looping technology for CO₂ capture: On the important roles of energy integration and sorbent behavior", **Applied Energy**, v. 162, p. 787–807, 2016. DOI: 10.1016/j.apenergy.2015.10.121. .

PILLAI, B. B. K., SURYWANSHI, G. D., PATNAIKUNI, V. S., *et al.* "Performance analysis of a double calcium looping-integrated biomass-fired power plant: Exploring a carbon reduction opportunity", **International Journal of Energy Research**, n. December 2018, p. 5301–5318, 2019. DOI: 10.1002/er.4520. .

RENTIZELAS, A. A. **Biomass storage**. [S.l.], Elsevier Ltd, 2016. Disponível em: <http://dx.doi.org/10.1016/B978-1-78242-366-9.00006-X>.

RITTER, B. C. **Projeto Conceitual de uma termelétrica a biomassa com captura de carbono**. 2019. 2019. Disponível em: <http://monografias.poli.ufrj.br/monografias/monopoli10028333.pdf>.

ROCHEDO, Pedro R.R., COSTA, I. V. L., IMPÉRIO, M., *et al.* "Carbon capture potential and costs in Brazil", **Journal of Cleaner Production**, v. 131, p. 280–295, 2016. DOI: 10.1016/j.jclepro.2016.05.033. .

ROCHEDO, Pedro Rua Rodriguez. **Análise Econômica Sob Incerteza Da Captura De Carbono Em Termoelétricas a Carvão: Retrofitting E Capture-Ready**. 2011. 362 f. UFRJ, 2011.

RODRIGUEZ, ALONSO, M., ABANADES, J. C. "Experimental Investigation of a Circulating Fluidized-Bed Reactor to Capture CO₂ with CaO", **AICHE Journal**, v. 57, p. 1356–1366, 2011. DOI: 10.1002/aic.12337. .

RODRIGUEZ, N., ALONSO, M., ABANADES, J. C., *et al.* "Comparison of experimental results from three dual fluidized bed test facilities capturing CO₂ with CaO", **Energy Procedia**, v. 4, p. 393–401, 2011. DOI: 10.1016/j.egypro.2011.01.067. .

RODRÍGUEZ, N., ALONSO, M., ABANADES, J. C. "Average activity of CaO particles in a calcium looping system", **Chemical Engineering Journal**, v. 156, n. 2, p. 388–394, 2010. DOI: 10.1016/j.cej.2009.10.055. .

ROLFE, A., HUANG, Y., HAAF, M., *et al.* "Integration of the calcium carbonate looping process into an existing pulverized coal-fired power plant for CO₂ capture: Techno-economic and environmental evaluation", **Applied Energy**, v. 222, n. January, p. 169–179, 2018. DOI: 10.1016/j.apenergy.2018.03.160. Disponible em: <https://doi.org/10.1016/j.apenergy.2018.03.160>.

ROLFE, A., HUANG, Y., HAAF, M., *et al.* "Techno-economic and Environmental Analysis of Calcium Carbonate Looping for CO₂ Capture from a Pulverised Coal-Fired Power Plant", **Energy Procedia**, v. 142, p. 3447–3453, 2017. DOI: 10.1016/j.egypro.2017.12.228. Disponible em: <https://doi.org/10.1016/j.egypro.2017.12.228>.

ROMANO, M. C. "Modeling the carbonator of a Ca-looping process for CO₂ capture from power plant flue gas", **Chemical Engineering Science**, v. 69, n. 1, p. 257–269, 2012. DOI: 10.1016/j.ces.2011.10.041. Disponible em: <http://dx.doi.org/10.1016/j.ces.2011.10.041>.

ROMANO, M. C., MARTÍNEZ, I., MURILLO, R., *et al.* "Process simulation of Ca-looping processes: Review and guidelines", **Energy Procedia**, v. 37, n. i, p. 142–150, 2013. DOI: 10.1016/j.egypro.2013.05.095. Disponible em: <http://dx.doi.org/10.1016/j.egypro.2013.05.095>.

ROMANO, M., MARTÍNEZ, I., MURILLO, R., *et al.* **Guidelines for modeling and simulation of Ca-looping processes. Prepared for the European Energy Research Alliance.** Sintef.No. [S.l: s.n.], 2012. Disponible em: <http://www.sintef.no/project/EERA-CCS/EERA - Ca-looping simulation guidelines.pdf>.

ROMEO, L. M., ABANADES, J. C., ESCOSA, J. M., *et al.* "Oxyfuel carbonation/calcination cycle for low cost CO₂ capture in existing power plants", **Energy Conversion and Management**, v. 49, n. 10, p. 2809–2814, 2008. DOI: 10.1016/j.enconman.2008.03.022. .

RUBIN, E.S. **Integrated Environmental Control Model**. 2020. Center for Energy and Environmental Studies. Disponível em: <https://www.cmu.edu/epp/iecm/>. Acesso em: 4 mar. 2020.

RUBIN, Edward S. "Understanding the pitfalls of CCS cost estimates", **International Journal of Greenhouse Gas Control**, v. 10, p. 181–190, 2012. DOI: 10.1016/j.ijggc.2012.06.004. Disponível em: <http://dx.doi.org/10.1016/j.ijggc.2012.06.004>.

RUBIN, Edward S., DAVISON, J. E., HERZOG, H. J. "The cost of CO₂ capture and storage", **International Journal of Greenhouse Gas Control**, v. 40, p. 378–400, 2015. DOI: 10.1016/j.ijggc.2015.05.018. Disponível em: <http://dx.doi.org/10.1016/j.ijggc.2015.05.018>.

RUBIN, Edward S., SHORT, C., BOORAS, G., *et al.* "A proposed methodology for CO₂ capture and storage cost estimates", **International Journal of Greenhouse Gas Control**, v. 17, p. 488–503, 2013a. DOI: 10.1016/j.ijggc.2013.06.004. Disponível em: <http://dx.doi.org/10.1016/j.ijggc.2013.06.004>.

RUBIN, Edward S., SHORT, C., BOORAS, G., *et al.* "A proposed methodology for CO₂ capture and storage cost estimates", **International Journal of Greenhouse Gas Control**, v. 17, n. September 2013, p. 488–503, 2013b. DOI: 10.1016/j.ijggc.2013.06.004. .

RUBIN, Edward S., YEH, S., ANTES, M., *et al.* "Use of experience curves to estimate the future cost of power plants with CO₂ capture", **International Journal of Greenhouse Gas Control**, v. 1, n. 2, p. 188–197, 2007. DOI: 10.1016/S1750-5836(07)00016-3. .

RUBIN, Edward S. "Status and Outlook for CO₂ Capture Systems Outline of Talk Resources for the Future Many Ways to Capture CO₂ Amine-Based CO₂ Capture at a Natural Gas Processing Plant Power Plant Option 1 : Post-Combustion CO₂ Capture Post-Combustion Capture at the Bo", p. 1–8, 2017a. .

RUBIN, Edward S. "The Outlook for Lower-Cost Carbon Capture and Storage for Climate Change Mitigation Outline of Talk Schematic of a CCS System Leading

Candidates for CCS Motivation for CCS Without CCS ...", p. 1–13, 2017b. .

RYDÉN, M., LYNGFELT, A., LANGØRGEN, O., *et al.* "Negative CO₂ Emissions with Chemical-Looping Combustion of Biomass - A Nordic Energy Research Flagship Project", **Energy Procedia**, v. 114, p. 6074–6082, 2017. DOI: 10.1016/j.egypro.2017.03.1744. .

RYDÉN, M., MOLDENHAUER, P., MATTISSON, T., *et al.* "Chemical-looping combustion with liquid fuels", **Energy Procedia**, v. 37, p. 654–661, 2013. DOI: 10.1016/j.egypro.2013.05.153. Disponível em: <http://dx.doi.org/10.1016/j.egypro.2013.05.153>.

SACRISTÁN, M. A. S.-B. **Final Report Summary - CAOLING (Development of postcombustion CO₂ capture with CaO in a large testing facility: “CaOling”)**. 2014. Disponível em: <https://cordis.europa.eu/project/id/241302>. Acesso em: 21 fev. 2020.

SAI, G. V. S. N., PUNDLIK, R. C., VENKATESWARA RAO, P., *et al.* "Chemical looping combustion of biomass for renewable and non- CO₂ emissions energy - status and review", **International Journal of Engineering and Technology(UAE)**, v. 7, n. 2, p. 6–10, 2018. DOI: 10.14419/ijet.v7i2.1.9872. .

SAIKAEW, T., SUPUDOMMAK, P., MEKASUT, L., *et al.* "Emission of NO_x and N₂O from co-combustion of coal and biomasses in CFB combustor", **International Journal of Greenhouse Gas Control**, v. 10, n. x, p. 26–32, 2012. DOI: 10.1016/j.ijggc.2012.05.014. Disponível em: <http://dx.doi.org/10.1016/j.ijggc.2012.05.014>.

SÁNCHEZ-BIEZMA, A., BALLESTEROS, J. C., DIAZ, L., *et al.* "Postcombustion CO₂ capture with CaO. Status of the technology and next steps towards large scale demonstration". 4, 2011. **Anais** [...] [S.l.], Elsevier Ltd, 2011. p. 852–859. DOI: 10.1016/j.egypro.2011.01.129.

SÁNCHEZ-BIEZMA, A., PANIAGUA, J., DIAZ, L., *et al.* "Testing postcombustion CO₂ capture with CaO in a 1.7 MW t pilot facility", **Energy Procedia**, v. 37, p. 1–8, 2013. DOI: 10.1016/j.egypro.2013.05.078. .

SCALA, F., CHIRONE, R., SALATINO, P. **Attrition phenomena relevant to fluidized bed combustion and gasification systems**. [S.l: s.n.], 2013.

SCHOLARSARCHIVE, B., LIN BAXTER, L., LIN, L. "Biomass-coal Co-combustion: Opportunity for Affordable Renewable Energy BYU ScholarsArchive Citation", **Original Publication Citation Fuel**, v. 84, p. 1295–1302, 2005. Disponível em: <https://scholarsarchive.byu.edu/facpubcoalCo-combustion:OpportunityforAffordableRenewableEnergy%22>.

SEKAR, R. C., PARSONS, J. E., HERZOG, H. J., *et al.* "Future carbon regulations and current investments in alternative coal-fired power plant technologies", **Energy Policy**, v. 35, n. 2, p. 1064–1074, fev. 2007. DOI: 10.1016/j.enpol.2006.01.020. Disponível em: <https://linkinghub.elsevier.com/retrieve/pii/S0301421506000759>. Acesso em: 3 ago. 2019.

SHIMIZU, T., HIRAMA, T., HOSODA, H., *et al.* "A twin fluid-bed reactor for removal of CO₂ from combustion processes", **Chemical Engineering Research and Design**, v. 77, n. 1, p. 62–68, 1999. DOI: 10.1205/026387699525882. .

SILVA, A. J. G. da. **Avaliação Da Rota Termoquímica De Produção De Etanol E Alcoóis Superiores**. 2013. 1–223 f. UFRJ, 2013. Disponível em: <http://www.ppe.ufrj.br/pppe/production/tesis/gerbasi.pdf>.

SILVA, J. A. da, CHIMENTÃO, R. J., SANTOS, J. B. O. dos. **Impactos das Tecnologias na Engenharia Química - Capítulo 25 - CAPTURA DE CO₂ UTILIZANDO O PROCESSO CALCIUM-LOOPING**. [S.l: s.n.], 2019.

SPINELLI, M., MARTÍNEZ, I., DE LENA, E., *et al.* "Integration of Ca-Looping Systems for CO₂ Capture in Cement Plants", **Energy Procedia**, v. 114, n. November 2016, p. 6206–6214, 2017. DOI: 10.1016/j.egypro.2017.03.1758. Disponível em: <http://dx.doi.org/10.1016/j.egypro.2017.03.1758>.

STRÖHLE, J., JUNK, M., KREMER, J., *et al.* "Carbonate looping experiments in a 1 MWth pilot plant and model validation", **Fuel**, v. 127, p. 13–22, 2014. DOI: 10.1016/j.fuel.2013.12.043. .

STRÖHLE, J., LASHERAS, A., GALLOY, A., *et al.* "Simulation of the carbonate looping process for post-combustion CO₂ capture from a coal-fired power plant", **Chemical Engineering and Technology**, v. 32, n. 3, p. 435–442, 2009. DOI: 10.1002/ceat.200800569. .

TAGOMORI, I. S., CARVALHO, F. M., DA SILVA, F. T. F., *et al.* "Designing an

optimum carbon capture and transportation network by integrating ethanol distilleries with fossil-fuel processing plants in Brazil", **International Journal of Greenhouse Gas Control**, v. 68, n. October 2017, p. 112–127, 2018. DOI: 10.1016/j.ijggc.2017.10.013. .

TAMARYN, N., HILLS, T., SOLTANI, S. M., *et al.* **A survey of key technological innovations for the low-carbon economy. Grantham Institute - Climate Change and Environment.** [S.l: s.n.], 2017. Disponível em: <http://www.oecd.org/environment/cc/g20-climate/collapsecontents/Imperial-College-London-innovation-for-the-low-carbon-economy.pdf>. Acesso em: 20 out. 2019.

THE ECONOMIST. "Should the world pay more attention to adapting to climate change than to efforts to mitigate it? |". 2019. Disponível em: <https://www.economist.com/what-the-world-thinks/should-world-pay-more-attention-adapting-climate-change-than-efforts-mitigate-it?page=3>. Acesso em: 20 out. 2019.

THITAKAMOL, B., VEAWAB, A., AROONWILAS, A. "Environmental impacts of absorption-based CO₂ capture unit for post-combustion treatment of flue gas from coal-fired power plant", **International Journal of Greenhouse Gas Control**, v. 1, n. 3, p. 318–342, 2007. DOI: 10.1016/S1750-5836(07)00042-4. .

TIAN, X., NIU, P., MA, Y., *et al.* "Chemical-looping gasification of biomass: Part II. Tar yields and distributions", **Biomass and Bioenergy**, v. 108, n. November 2017, p. 178–189, 2018. DOI: 10.1016/j.biombioe.2017.11.007. .

TURNER, M., IYENGAR, A., WOODS, M. **COST AND PERFORMANCE BASELINE FOR FOSSIL ENERGY PLANTS SUPPLEMENT: SENSITIVITY TO CO₂ CAPTURE RATE IN COAL-FIRED POWER PLANTS.** . [S.l: s.n.], 2019. Disponível em: [http://netl.doe.gov/File Library/Research/Energy Analysis/OE/BitBase_FinRep_Rev2a-3_20130919_1.pdf](http://netl.doe.gov/File%20Library/Research/Energy%20Analysis/OE/BitBase_FinRep_Rev2a-3_20130919_1.pdf).

U.S. DEPARTMENT OF ENERGY/NETL. **Carbon Capture and Storage Database | netl.doe.gov.** 2019a. Disponível em: <https://www.netl.doe.gov/coal/carbon-storage/worldwide-ccs-database>. Acesso em: 1 set. 2019.

U.S. DEPARTMENT OF ENERGY/NETL. "DOE/NETL Capture Program R&D: Compendium of Carbon Capture Technology", n. April, 2018. Disponível em: <https://www.netl.doe.gov/research/coal/carbon-storage/research-and-development/precombustion>.

U.S. DEPARTMENT OF ENERGY/NETL. **Post-Combustion CO₂ Capture** | netl.doe.gov. 2019b. Disponível em: <https://netl.doe.gov/coal/carbon-capture/post-combustion>. Acesso em: 20 out. 2019.

UNICA. **União da Indústria de Cana-de-Açúcar. Boletim/Unica: a bioeletricidade em números – setembro/2018**. . [S.l: s.n.], 2018. Disponível em: www.unica.com.br/documentos/documentos/.

VALIX, M., KATYAL, S., CHEUNG, W. H. "Combustion of Thermochemically Torrefied Sugar Cane Bagasse", **Bioresource Technology**, v. 223, n. June, p. 202–209, 2017. DOI: 10.1016/j.biortech.2016.10.053. .

VALVERDE, J. M., SANCHEZ-JIMENEZ, P. E., PEREZ-MAQUEDA, L. A. "Ca-looping for postcombustion CO₂ capture: A comparative analysis on the performances of dolomite and limestone", **Applied Energy**, v. 138, p. 202–215, 2015. DOI: 10.1016/j.apenergy.2014.10.087. .

VAN VUUREN, D. P., STEHFEST, E., GERNAAT, D. E. H. J., *et al.* "Alternative pathways to the 1.5 °c target reduce the need for negative emission technologies", **Nature Climate Change**, v. 8, n. 5, p. 391–397, 2018. DOI: 10.1038/s41558-018-0119-8. .

VERSTEEG, P., RUBIN, E. S. "IECM Technical Documentation : Amine-based Post-Combustion CO₂ Capture", n. September, p. 59, 2019. .

VERSTEEG, P., RUBIN, E. S. "IECM Technical Documentation: Ammonia-Based Post-Combustion CO₂ Capture. Prepared for: National Energy Technology Laboratory", n. September, p. 59, 2012. Disponível em: [http://www.cmu.edu/epp/iecm/documentation/IECM Ammonia System - September 2012.pdf](http://www.cmu.edu/epp/iecm/documentation/IECM%20Ammonia%20System%20-%20September%202012.pdf). Acesso em: 8 dez. 2018.

VOLDSUND, M., GARDARSDOTTIR, S. O., DE LENA, E., *et al.* "Comparison of technologies for CO₂ capture from cement production—Part 1: Technical evaluation", **Energies**, v. 12, n. 3, 2019. DOI: 10.3390/en12030559. .

WANG, M., LAWAL, A., STEPHENSON, P., *et al.* "Post-combustion CO₂ capture with chemical absorption: A state-of-the-art review", **Chemical Engineering Research and Design**, v. 89, n. 9, p. 1609–1624, 2011a. DOI: 10.1016/j.cherd.2010.11.005. Disponível em: <http://dx.doi.org/10.1016/j.cherd.2010.11.005>.

WANG, M., LAWAL, A., STEPHENSON, P., *et al.* "Post-combustion CO₂ capture with chemical absorption: A state-of-the-art review", **Chemical Engineering Research and Design**, v. 89, n. 9, p. 1609–1624, 1 set. 2011b. DOI: 10.1016/j.cherd.2010.11.005. Disponível em: <https://www.sciencedirect.com/science/article/pii/S0263876210003345>. Acesso em: 4 dez. 2018.

WOOLF, D., LEHMANN, J., LEE, D. R. "Optimal bioenergy power generation for climate change mitigation with or without carbon sequestration", **Nature Communications**, v. 7, n. 1, p. 13160, 21 dez. 2016. DOI: 10.1038/ncomms13160. Disponível em: <http://www.nature.com/articles/ncomms13160>. Acesso em: 3 dez. 2018.

XU, Y., YANG, K., ZHOU, J., *et al.* "Coal-Biomass Co-Firing Power Generation Technology: Current Status, Challenges and Policy Implications", **Sustainability**, v. 12, n. 9, p. 3692, 2020. DOI: 10.3390/su12093692. .

YANG, Y., ZHAI, R., DUAN, L., *et al.* "Integration and evaluation of a power plant with a CaO-based CO₂ capture system", **International Journal of Greenhouse Gas Control**, v. 4, n. 4, p. 603–612, 2010. DOI: 10.1016/j.ijggc.2010.01.004. Disponível em: <http://dx.doi.org/10.1016/j.ijggc.2010.01.004>.

YLÄTALO, J., PARKKINEN, J., RITVANEN, J., *et al.* "Modeling of the oxy-combustion calciner in the post-combustion calcium looping process", **Fuel**, v. 113, n. Figure 1, p. 770–779, 2013. DOI: 10.1016/j.fuel.2012.11.041. .

ZEP. **Future CCS technologies, Zero Emission Platform**. . [S.l: s.n.], 2017. Disponível em: https://ec.europa.eu/clima/policies/ets/reform/index_en.htm. Acesso em: 20 out. 2019.

ZHAI, H., RUBIN, E. S. "Carbon capture effects on water use at pulverized coal power plants", **Energy Procedia**, v. 4, n. October, p. 2238–2244, 2011. DOI: 10.1016/j.egypro.2011.02.112. .

ZHAI, H., RUBIN, E. S., VERSTEEG, P. L. "Water Use at Pulverized Coal Power Plants with Postcombustion Carbon Capture and Storage", **Environmental Science & Technology**, v. 45, n. 6, p. 2479–2485, 15 mar. 2011. DOI: 10.1021/es1034443. Disponível em: <https://pubs.acs.org/doi/10.1021/es1034443>.

ZHANG, X., SONG, P. "Performance Assessment of Coal Fired Power Plant Integrated with Calcium Looping CO₂ Capture Process", **Energy Sources, Part A: Recovery**,

Utilization and Environmental Effects, v. 00, n. 00, p. 1–22, 2019. DOI: 10.1080/15567036.2019.1673510. Disponível em: <https://doi.org/10.1080/15567036.2019.1673510>.

ZHAO, X., ZHOU, H., SIKARWAR, V. S., *et al.* "Biomass-based chemical looping technologies: The good, the bad and the future", **Energy and Environmental Science**, v. 10, n. 9, p. 1885–1910, 2017. DOI: 10.1039/c6ee03718f. .

ZHENG, L., YAN, J. **Thermal coal utilization**. [S.l.], Woodhead Publishing Limited, 2013. v. 2. Disponível em: <http://dx.doi.org/10.1533/9781782421177.3.237>.